AD NUMBER
AD489696
LIMITATION CHANGES
TO: **Approved for public release; distribution is unlimited.**
FROM: **Distribution authorized to U.S. Gov't. agencies and their contractors; Critical Technology; AUG 1966. Other requests shall be referred to Rome Air Development Center, EMASP Griffiss AFB, NY 13440. This document contains export-controlled technical data.**
AUTHORITY
RADC USAF ltr, 17 Sep 1971

RADC-TR-66-215
Interim Report

AD No. 489696
DDC FILE COPY

RADAR TARGET SCATTER SITE (RAT SCAT) VHF MEASUREMENT FEASIBILITY INVESTIGATION

C. C. Freeny
D. O. Cisco
General Dynamics

TECHNICAL REPORT NO. RADC-TR-66-215
August, 1966

This document is subject to special export controls and each transmittal to foreign governments or foreign nationals may be made only with prior approval of RADC (EMLI) GAFB, N Y 13440.

Rome Air Development Center
Research and Technology Division
Air Force Systems Command
Griffiss Air Force Base, New York

(19)

(18) RADC-TR-66-215

(6) RADAR TARGET SCATTER SITE (RAT SCAT) VHF MEASUREMENT FEASIBILITY INVESTIGATION.

(9) Interim rept. on Phase 1,

(10) C.C. Freeny
D.O. Cisco
General Dynamics

(15) AF30(602)-3815

(16) AF-6503

(17) 650301

This document is subject to special export controls and each transmittal to foreign governments or foreign nationals may be made only with prior approval of RADC (EMLI) GAFB, N Y 13440.

(11) Aug 66

(12) 201p.

(14) FZE-528

MAINLINE ENGINEERING MAPLE SHADE, N.J.
9/23/66 177

mk

147 800

1473
ecf

FOREWORD

This report was prepared by Mr. C.C. Freeny and Mr. D.O. Cisco of General Dynamics, Fort Worth, Texas under Contract AF30(602)-3815, Project 6503, Task 650301.

The RADC project engineers were Mr. Donald M. Montana, EMASP and Major J. Fogarty.

The General Dynamics Report Number is FZE-528.

This report is a documentation of the first phase of a two phase program designed to investigate the feasibility of making Radar Cross Section Measurements at RATSCAT. A second and final report will cover the second phase of the program.

Release of subject report to the general public is prohibited by the Strategic Trade Control Program, Mutual Defense Assistance Control List (revised 6 January 1965), published by the Department of State.

This technical report has been reviewed and is approved.

Donald M. Montana

Approved: DONALD M. MONTANA
Program Directors' Office
Space Surveillance and
Instrumentation Branch

for Vincent J. Coyne

Approved: JOSEPH FALLIK
Chief, Space Surveillance
and Instrumentation Branch
Surveillance and Control Division

ABSTRACT

The material presented in this report is a result of an investigation of the feasibility of making radar cross section measurements in the VHF region at the Radar Target Scatter Site, White Sands Missile Range (RAT SCAT). Included herein are the results of an experimental and analytical investigation which was conducted in the 30- to 180-megahertz region for the purpose of (1) determining the feasibility of making measurements at RAT SCAT and (2) defining the range condition(s) and measurement technique(s) for use in a feasibility demonstration program to be conducted at RAT SCAT.

A study was made of the properties of RAT SCAT soil since a ground plane cross section measurement technique was under consideration. The electrical properties of the soil, in terms of the complex permittivity and associated loss tangent, were measured as a function of moisture, temperature, and sample location. The results of the soil investigation were used in conjunction with a ground plane model programmed on a CDC 1604 to investigate the RF field patterns to be expected at RAT SCAT. These fields were studied as a function of frequency, range, soil conditions, antenna height, and target height. A VHF radar system from the Fort Worth Division of General Dynamics was taken to RAT SCAT to obtain information with which to validate the results of the computer study and obtain additional information on the feasibility of operating VHF equipment at the RAT SCAT site. The results of the study and measurements are analyzed and a dual range and measurement technique is described; this technique is considered a feasible approach to measuring targets up to 70 feet in length.

TABLE OF CONTENTS

TABLE OF CONTENTS

TABLE OF CONTENTS

LIST OF ILLUSTRATIONS

LIST OF ILLUSTRATIONS

LIST OF ILLUSTRATIONS

LIST OF ILLUSTRATIONS

LIST OF ILLUSTRATIONS

LIST OF ILLUSTRATIONS

LIST OF ILLUSTRATIONS

LIST OF ILLUSTRATIONS

LIST OF ILLUSTRATIONS

LIST OF TABLES

SECTION 1

INTRODUCTION

The information presented in this report is a direct result of the basic programs designated to investigate the feasibility and method of making cross section measurements at the Radar Target Scattering Site (RAT SCAT) in the VHF (30- to 180-megahertz) region. On the basis of the results reported herein, equipment will be fabricated and tests will be performed at RAT SCAT to demonstrate the feasibility of obtaining high quality cross section data in the VHF region. The results of the demonstration of feasibility will be reported in a second and final report.

The basic study and measurement programs reported in this document were primarily undertaken to determine the feasibility and the related values of range geometry parameters which could be used to make cross section measurements at RAT SCAT on the basis of the ground plane technique. In addition, cross section measurements were made at RAT SCAT by utilizing a long pulse (50-microsecond) cancelled electronic system to obtain information on the basic capabilities of such a system.

In addition to the normal considerations associated with obtaining valid cross section data (reference RADC-TDR-64-397), measurements in the VHF region result in problems which are considered negligible in the case of measurements at the higher frequencies. The objectives set for the phase of the program reported in this document were (1) the methodical investigation of these problem areas, and (2) on the basis of the results obtained define the most feasible operational parameters for use in a VHF cross section measurement system.

In the case of a ground plane range, potential problems arising in the VHF region are (1) measurement field gradients and stability as function of soil characteristics, frequency, antenna and target height, polarization, and range, (2) soil characteristics as function of the climatic parameters, moisture and temperature, (3) target-ground coupling, and (4) versatility of use of polarization. The major problem associated with the capability of a measurement system in the VHF region is that of achieving sufficient antenna isolation. In addition, the amount of RFI present in the VHF region limits the system bandwidth. The majority of the reported material is related to the four areas enumerated above. However, information related to the aforementioned measurement system problems was also obtained and utilized in conjunction with the other study results to arrive at feasible range designs which will be evaluated during the demonstration phase of the program.

Because of the number of parameters which influence the measurement fields over a ground plane range in the VHF region, a mathematical model was considered a necessity for effective study of the problem. Such a model of a ground plane was programmed on a CDC 1604 computer at RADC. A large number of measurements made on RAT SCAT soil at RAT SCAT and at the Fort Worth Division of General Dynamics were to obtain information to demonstrate the validity of this ground plane model. The ground plane model was demonstrated to be quite accurate; consequently, it was utilized to generate vertical field probe data for a number of conditions which were impractical to undertake in a measurement program. Approximately twelve hundred computer runs were made during the investigation in order to assess the effects of variations in the parameters, antenna height, target height, range, frequency, polarization, and soil characteristics. The computer study and selected results are described in Section 3.

Section 2 contains a description of the study and measurement program devoted to obtaining RAT SCAT soil electrical characteristics. It was necessary to undertake this study before the computer study because of the field sensitivity in the VHF region to the value of the soil complex permittivity. The soil study was designed (1) to investigate the homogeneity of RAT SCAT soil as a function of depth and location and (2) to evaluate the complex permittivity as a function of frequency, moisture, and temperature. The results of the study indicated that the soil is homogeneous in both location and depth. Also, the moisture content of the soil remains quite stable at a fairly high level (approximately 15 percent).

In Section 4, the study of the fields near the surface at RAT SCAT and the measurement results are presented. The results of this study provided information as to the validity of the ground plane model and the sensitivity of the surface field amplitude to grazing angle.

Section 5 contains a description of the measurement program conducted at RAT SCAT to obtain (1) field probe information, (2) target-ground coupling, and (3) cross section data. In the discussion of the results, it is shown that the field probe information compared quite favorably with the computed data. Results of the target-ground coupling experiments demonstrated that errors caused by coupling need to be considered in the 30- to 180-megahertz region in the case of large targets (greater than 10 feet) even at 30- to 65-foot target heights. However, in the case of the smaller targets, target heights between 10 and 30 feet appear satisfactory. Cross section data was obtained at 30 and 60 megahertz and compared with scale model data. The results of the experiments indicated accurate cross section data can be obtained in this frequency range although such effects as tilt angle and bistatic angle were noticeable in the case of the larger targets at the range geometries at which the measurements were made.

In Section 6, a summary of the basic study results is presented along with a review of other considerations associated with range geometry design. The recommended range design involves a range with dual capability. A short range (200 to 400 feet) used in conjunction with a cancelled pulse system can be used to measure relatively small targets (less than 10 feet) by target heights in the 10- to 30-foot region. This range design is considered feasible on the basis of the results obtained by operating this type of system at RAT SCAT in this range interval. In addition, a long-range capability is considered feasible (1000 to 2000 feet) on the basis of the results of the computer study and the long-range measurements made at RAT SCAT. It is proposed to operate the same electronic system at these ranges by using the range gate to achieve isolation and the cancellation capability to cancel the target support return. Use of this range design will allow measurements in the 30- to 200-megahertz frequency region and will minimize the effects of bistatic and tilt angle, $2D^2/\lambda$ near-field errors in the case of large targets (up to 72 feet in length), radial gradient near-field errors in the case of large targets, and field ellipticity in vertical polarization. In addition, use of these range lengths enable the following:

1. Target heights sufficient to minimize coupling effects of these larger targets

2. Antenna heights and separation sufficient to utilize the ground plane effect to achieve better isolation

3. The capability to operate a range-gated system with a relatively narrow bandwidth.

SECTION 2

RAT SCAT SOIL INVESTIGATIONS

2.1 General

At the beginning of the VHF program an extensive measurement program was conducted in order to evaluate the electrical properties of the soil at RAT SCAT. Knowledge of the soil electrical properties as a function of representative climatic variations was considered necessary because of the known dependence of the field patterns to these properties in the VHF region. The objective of the investigation was to (1) determine the homogeneity of the soil at RAT SCAT, (2) determine the material constants ϵ_r, σ and $\tan\delta_\epsilon$ in terms of moisture, and temperature, and (3) determine the soil moisture content and variations to be expected at RAT SCAT.

In coordination with personnel at RAT SCAT, the area tentatively selected for the VHF range was defined as being approximately along a line N45^{o}E from Target Pit Number 3 and starting 20 feet northeast of the Bistatic Road. This area is indicated in Figure 1.

To obtain a representative cross section of the soil electrical characteristics in this area, 15 samples were taken at depths varying from 0 to 2 feet under the surface. Of these samples, a total of 10 were taken from five specific points on a line extending 1200 feet N45^{o}E along the site location; the remaining 5 were taken from points east and west of this line. From the 15 samples taken, 12 were used in a preliminary investigation of the electrical properties and moisture content of the soil.

To determine the possibility that the average moisture content, and thus the electrical characteristics, might change over an extended period of time, the moisture content was determined for soil samples taken on July 15, November 2, and December 1, 1965. Results of the individual averages showed the moisture content to be approximately 16 percent, with a ± 2 percent variation, independent of sample location or sample depth. Also noted was the fact that the average was constant over the 5-month period (see Figure 2). Shown in Figure 3 is the time rate at which the moisture content decreases to its average value after a moderate rainfall. On the basis of the tests for homogeneity and moisture content variation, two surface samples and two subsurface samples were chosen for the temperature-controlled measurements.

2.2 Measurement Technique

The measurement technique used to obtain the material constants was to measure the admittance of a coaxial wave guide in which samples of soil were placed. Admittance values obtained from these measurements were then used to evaluate the electrical constants ϵ_r, σ and $\tan\delta_\epsilon$ of the soil. Because the soil was very lossy (except for the dry condition) special attention to factors such as sample length, meter corrections, and evaporation was necessary in order to obtain data which was sufficiently accurate. Even with the special care taken to eliminate variations caused by the above mentioned factors, it was still necessary to make repeated measurements and determine the expected value of the electrical constants via statistical techniques.

The test system used to obtain the admittance measurements is shown in Figure 4. The bridge is a General Radio 1602-A, the input to which is a 400-cps modulated RF signal supplied from the Hewlett Packard 608 RF generator. To determine the bridge balanced condition, a Neims Clark communications receiver was used to pass the 400-cps signal for audio null detection. This particular method of detection was chosen because it eliminated the need for a local oscillator and IF mixer.

2.2.1 <u>Basic Principles</u>

To obtain the soil electrical parameters ϵ_r, $\tan\delta_\epsilon$, and σ, the measured input admittance of a circular waveguide filled with the soil may be related to the desired quantities through the use of transmission line equations. The measured input admittance is determined by: the length of line between the point of measurement and the soil sample, the characteristic admittance of this line, the characteristic admittance of the section of line containing the soil sample, the length of the soil test sample, and the test section terminating admittance (see Figure 4). These parameters along with the corrections for the stray capacitance of the admittance meter and the open circuit termination can be related to the electrical parameters by the relationships presented in Appendix A.

In Figure 5 the effective increase in length of the open circuit termination plane caused by stray capacitance is illustrated. The two most important sources of meter error were found to be the mutual couplings between the different branches of the admittance bridge and the inductance of the sections of line between the junction of the bridge arms and the center of the meter measuring coils. Corrections for the errors produced by cross-coupling were made by using Equations A-14 and A-15 which were obtained from Reference 1.

2.2.2 Special Considerations

Investigation of the equations relating the material constants to the measured quantities (Equations A-9 through A-13) revealed the necessity of optimizing the length of the air-filled guide and the length of the test section if the computational errors were to be minimized. From preliminary results, it was found that the length of the air-filled guide should be as small as possible. Optimizing the length of the test section was more difficult in that it had to "best satisfy" two opposing requirements. The first requirement was that it be long enough to provide sufficient attenuation of an input signal to give an accurate admittance measurement. The second requirement was that it had to be short enough to keep the magnitudes of the measured admittance in a range compatible with the measurement technique used. In many cases, the optimum test sample length had to be found by trial and error since the input admittance was greatly affected by the moisture content of the soil, the frequency at which the measurements were being made, and (to some degree) the temperature of the soil under consideration. Depending on the values of these factors, the sample lengths used to optimize the accuracy of the measurements ranged between 80 centimeters and .35 centimeters.

Because of the short soil sample lengths required at the higher moisture conditions (.35 to 2 centimeters) the effects of evaporation had to be considered. The effects of evaporation were minimized by sealing the soil test section with an epoxy. This technique was also used at the 32°F and 120°F temperature conditions.

2.3 Measurements

To determine whether or not the average moisture content, and the related electrical properties, would change over an extended period of time, a total of 34 soil samples were taken over a period of 5 months for the evaluation of the moisture content.

Preparation of the samples for the measurements to be made consisted of determining their moisture content as received. The samples were first weighed, moisture was then driven out at a controlled temperature, and the samples were then weighed again. The differences in weighings were then used to establish the moisture content as a percentage of dry weight.

After the "received" moisture content of the samples was determined, measurements were taken for the cases of seven surface locations and five subsurface locations at the "received" moisture content and 80°F. The resulting electrical parameters indicated that the surface and subsurface soils were essentially homogeneous over the proposed VHF site; only a slight difference was found between surface and subsurface conductivities. As a validity check for homogeneity, four surface locations and four subsurface locations were selected and used for zero moisture content measurements. In all, 210 preliminary measurements were made on 12 samples; 160 were made to confirm soil homogeneity, and more than 50 other measurements were made to define system error, reproducibility of measurements, and the effect of temperature on the equipment. In all, over 1100 measurements were made to determine the electrical characteristics of the RAT SCAT soil in the VHF region.

To obtain the data necessary for calculating ϵ_r, $\tan\delta_\epsilon$, and σ at 120°F, four sections of air-guide were first sealed with an epoxy to eliminate evaporation of moisture at this temperature. To heat the sections, a commercial Glocoil was adapted to permit insertion of the samples into its heating coils, the temperature being maintained at $120^\circ \pm 2^\circ$F by adjusting the voltage input to the Glocoil. The chosen sample lengths varied from 0.35 to 1.8 centimeter, the shortest length being used as the highest moisture content. Controlling the temperature at 32°F was accomplished by surrounding the test section with an ice jacket which served as a constant temperature reservoir for the time required to make measurements at four frequencies. Sample lengths chosen for this temperature varied from 0.35 to 30.0 centimeters.

2.4 Results

The measurement results revealed that the relative dielectric constant, ϵ_r, did not vary appreciably with temperature or with sample location when data from samples of the same moisture content were compared. The mean values of ϵ_r obtained from measurements are shown in Figure 6 as a function of moisture content. In an attempt to relate (1) the percentage of moisture content, (2) ϵ_r of the dry soil, and (3) ϵ_r of water with values calculated from measured data, it was found that the mean values from calculations were in very good agreement with either of two classic equations for the relative dielectric constant of a homogeneous mixture of two substances. The graphs of these equations are also presented in Figure 6.

On the basis of the statistical error analysis conducted and discussed in Appendix A, it is felt that the differences between the theoretical ϵ_r (Figure 6, Curve 2) and those values obtained by measurements are sufficiently accounted for in terms of the measurement limitations of the test system.

From the theoretical values of ϵ_r in Figure 6, an empirical equation was formulated to express the conductivity as a function of moisture content and temperature. The empirical equation which was found to express the subsurface conductivity is shown below:

$$\sigma = \epsilon_r^2 \sigma_0 \left[0.1 + 5(\%)\right] \left[1 + 8(\%)^2\right] e^{(.041T)}$$

where

ϵ_r = $\epsilon_{rd}(1-\%) + \% \, \epsilon_{rw}$
ϵ_{rd} = relative dielectric constant of the dry soil
ϵ_{rw} = relative dielectric constant of water
T = temperature in degrees centigrade
% = moisture content in percent of dry weight
σ_0 = the "base" conductivity of the dry subsurface soil referred to zero degrees centigrade.

Numerically, σ_0 is given as 0.00138 mhos per meter at 0^oC, and ϵ_{rd} is given as 3.95 independent of temperature. The surface conductivity of any given temperature is related to the subsurface conductivity at that temperature by 1.30.

The mean values of the surface and subsurface conductivity as calculated from measured data, and the empirical equation found to describe them may be found plotted in Figures 7 and 8, respectively, for the case of T = 80^oF. Results of calculations of the conductivities at T = 120^oF and T = 32^oF may be found in Figures 9 through 12. To obtain a representation of the loss tangent, extreme values of ϵ_r and σ were calculated by assuming that known errors existing in the system measurements, temperature, the moisture content of a given sample, and the sample length. From these extreme values, an average loss tangent was calculated. Shown in Figures 13 and 14 are the mean values of the loss tangent from subsurface measurement data taken at T = 80^oF and the calculated average loss tangent. Similar results on the surface soil may be found in Figures 15 and 16. Figures 17 through 24 show the various loss tangents for temperatures of 120^oF and 32^oF.

To obtain a representative description of the soil electrical parameters at a fixed temperature and moisture content, it was found necessary to repeat measurements by using different lengths of test section so that a statistical average could be found. This was necessary even though any set of data could be reproduced to within ± 5 percent of the first set obtained under similar "environmental" conditions. Also noted was an increase in the standard deviation of ϵ_r, σ, and $\tan \delta_\epsilon$ as the moisture content was increased; consequently, it was highly desirable to obtain a larger volume of measured data at the higher moisture contents. The standard deviation of ϵ_r as a function of moisture content is illustrative of this increase (Figure 25) as well as the standard deviation of the subsurface conductivity as a function of moisture content (Figure 26).

To relate the statistical variation of the results with measurement errors and "environment" fluctuation, small changes in the temperature, moisture content, soil test section length, and recorded values of admittance were analytically introduced to simulate the effect of combined system error. The specific errors assumed were $\pm 2^{\circ}$F in the temperature, ± 1 percent in the moisture content, ± 5 percent in the ability to define the test section length, Ls, and ± 5 percent in the measured input admittance. This analysis is discussed in subsection A.3 of the Appendix.

On the basis of the above mentioned statistical error analysis, it is doubtful that the difference between surface and subsurface conductivity could be accurately defined by using the present results in that the extreme variations of one overlap those of the other. If such a distinction were found necessary, confidence would have to be placed strictly in the statistical averages obtained from a larger volume of measured data. From the calculations made, the surface conductivity was found to be approximately 30 percent higher than that of the subsurface when the moisture content was 15 percent or greater. Although this relationship appeared to be slightly different below 15 percent, the analytical expression used to describe the conductivity is rather insensitive to changes in moisture content below 10 percent.

SECTION 3

COMPUTER STUDY

3.1 General

The most extensive computational study associated with the VHF program was that of computing the RF field patterns over a ground plane range. The study was undertaken in order to generate information to help in the selection of an optimum range geometry for cross section measurements in the VHF region. Field patterns were computed as a function of the "noncontrollable" parameters, soil constants, polarization, and frequency, along with the "controllable" parameters, antenna height, target height, and range. The soil constants used in the computations were those obtained from the RAT SCAT soil measurement program. Six frequencies between 30 and 180 megahertz were selected as representative, and computations were made at both vertical and horizontal polarizations. The antenna heights were varied between $\lambda/4$ and 49 feet (antenna heights of 66 and 85 feet were used at several ranges); the target heights were plotted between ground level and 72 feet. Amplitude and phase data were generated for the above conditions at ranges between 20 and 800 meters and for $\lambda/4$ antenna heights out to 1200 meters.

Selected results of this study are presented in this section to demonstrate the effects of both the noncontrollable and controllable parameters on the field patterns. In the summary (Section 6), range geometries are selected which can be used to minimize the undesirable effects of the noncontrollable parameters and/or allow cross section measurements to be performed by proper selection of the controllable parameters.

3.2 Study Program

The computer study was based on the ground plane mathematical model developed by Norton (Reference 2). All of the computations were made on a CDC 1604 at RADC. This model can be used to describe the total field above a homogeneous ground plane of complex permittivity (ϵ^*) produced by a dipole located a specific distance (h_a) above the ground plane. The computer program had been used to predict field patterns in the 1- to 10-gigahertz region at RAT SCAT and good correlation was obtained. However, above the 1-gigahertz region, the field patterns are quite insensitive to soil parameters, and the patterns can be computed by using a simpler ground plane mathematical model, such as that described in Reference 3. Hence, the results of this study yielded information on the validity of the Norton model in the VHF region at relatively short ranges (information is readily available for longer ranges, Reference 4).

Before the results of the computations are presented, a mathematical description of the computerized ground plane model is given, and this description is followed by a discussion of the input parameters used in the study.

3.2.1 Computer Program

The computer program was based on the mathematical description of the radiation problem depicted in Figure 27. As indicated in this figure, there are two types of fields which can be used to describe the total field: the surface field and the space field. At the higher frequencies or in the case of horizontal polarization, the surface field is usually considered negligible, and the total field is the space field composed of the direct and reflected wave.

The expression for the space wave in the case of vertical polarization is given in Equation 1:

$$E_S^V = E_{SV}^V + E_{SR}^V \tag{1}$$

where

E_{SV}^V = Vertical component of space wave

E_{SR}^V = Radial component of space wave

$$E_{SV}^V = A_h \left(\cos^2\psi'' \frac{e^{ikr_1}}{r_1} + \rho_V \cos^2\psi' \frac{e^{ikr_2}}{r_2}\right)$$

$$E_{SR}^V = -A_h \left(\sin\psi'' \cos\psi'' \frac{e^{ikr_1}}{r_1} + \rho_V \sin\psi' \cos\psi' \frac{e^{ikr_2}}{r_2}\right)$$

A_h = Gain of dipole

$$\rho_V = \frac{\sin\psi' - u\,(1 - u^2\cos^2\psi')^{\frac{1}{2}}}{\sin\psi' + u\,(1 - u^2\cos^2\psi')^{\frac{1}{2}}}$$ (reflection factor for vertical polarization)

$u = 1/(\epsilon' - j\,\epsilon'')^{\frac{1}{2}}$

ϵ' = relative dielectric constant

$\epsilon'' = \sigma/\omega\epsilon_o$

σ = Conductivity in mhos per meter

ω = radian frequency

ϵ_o = free space permittivity $10^{-9}/36\pi$ farads per meter.

The corresponding expression for the surface wave is given in Equation 2:

$$E^{V}_{SWV} = E^{V}_{SWV} + E^{V}_{SWR} \qquad (2)$$

where

$$E^{V}_{SWV} = A_h(1-\rho_V)\,(1 - u^2 + u^4\cos^2\psi')\;F\frac{e^{ikr_2}}{r_2}$$

$$E^{V}_{SWR} = A_h\cos\psi'\,(1-\rho_V)\,u\sqrt{1 - u^2\cos^2\psi'}\;\left(1 - u^2\left|1 - u^2\cos^2\psi'\right|/2 + (\sin^2\psi')/2\right)F\frac{e^{ikr_2}}{r_2}$$

$$F = 1 + i(\pi w)^{\frac{1}{2}}\,e^{-w}\,\mathrm{erfc}(-i(\pi w)^{\frac{1}{2}})$$

$$w = 4P/(1 - \rho_V)^2$$

$$P = ikr_2\,u^2(1 - u^2\cos^2\psi')/2$$

The computer program is such that the surface wave field (Equation 2), along with the corresponding vertical and radial components, are printed out in amplitude and phase which is referenced to the source. In addition, Equation 1 and 2 are summed to give the total field, along with the corresponding vertical and radial components. Computations are made as a function of height above the ground plane, and the data are recorded on digital printout and automatic plotter magnetic tape.

Computations similar to those described for the vertical polarization case are also made for the case of horizontal polarization with the exception that the surface field is considered negligible. The expression used for the horizontal polarization case is given in Equation 3.

$$E^H = A_h \left(e^{ikr_1}/r_1 - \rho_H \; e^{ikr_2}/r_2 \right) \tag{3}$$

where

$$\rho_H = \frac{(1 - u^2 \cos^2 \psi')^{\frac{1}{2}} - u \sin \psi'}{(1 - u^2 \cos^2 \psi')^{\frac{1}{2}} + u \sin \psi'}$$ (reflection factor for horizontal polarization)

In the case of horizontal polarization, the computer output is the amplitude and phase (referenced to the source) as a function of height.

In addition to the output data described above, the values of the reflection factors and the "tilt" angle for vertical polarization can be printed out. The tilt angle is the angle that the major axis of the vertically polarized field ellipse makes with the normal to the ground plane.

Although the fundamental equations, i.e., Equations 1 through 3 are based on a dipole, a larger aperture can be synthesized by using superposition. The computer program is presently designed to handle a 20-dipole aperture. The number and the separation of probe heights can be specified, but in its present form is limited to 50 points. Other limitations of the program in its present form are the following: (1) frequency must not be less than 30 megahertz, (2) $\sigma > 0$, and (3) $\epsilon' > 2$.

Presented in Table 1 are portions of the computer printout of the various parameters discussed above. In Figures 50 and 51 are typical amplitude and phase plots produced by use of the RADC automatic plotter in conjunction with the program automatic plotter magnetic tape output.

3.2.2 Computer Study Parameters

The parameters used in the computer study were selected so as to obtain a representative simulation of the possible conditions which would exist and/or would be operationally feasible. The material constants associated with the RAT SCAT soil were those determined under the soil measurement program. The primary cause of variations in material constants was found to

Table 1. Computer Print Out Format

NUMBER OF RANGE POINTS	3
RANGE INCREMENT	524.96
CENTER RANGE POINT	1574.80
NUMBER OF HEIGHT POINTS	49
HEIGHT INCREMENT	1.50
CENTER HEIGHT POINT	36.00
NUMBER OF DIPOLES	1
DISTANCE BETWEEN DIPOLES	0
HEIGHT OF CENTER DIPOLE	85.00
INTENSITY OF DIPOLE NO. 1 FROM BOTTOM	1.00
RELATIVE PERMITTIVITY OF EARTH	14.48
CONDUCTIVITY OF EARTH IN MHOS PER METER	.61
FREQUENCY IN MEGACYCLES	180.00
CALCULATE SURFACE WAVE (1). SET TO ZERO (0).	1
PRINT THE REFLECTION COEFFIENTS (1). DO NOT PRINT (0)	1
CALL SUB. FOR INTERPOLATION (1). DO NOT CALL (0).	0

TOTAL WAVE FOR VERTICAL POLARIZATION. RANGE 1049.840 FEET

HEIGHT	COMPONENTS ALONG THE MAJOR AXIS			VERTICAL COMPONENT		RADIAL COMPONENT	
(FEET)	INTENSITY DB	PHASE DEGREES	TILT DEG.	INTENSITY DB	PHASE DEG.	INTENSITY DB	PHASE DEG.
0	-4.263	300.913	9.737	-4.307	301.358	-22.264	263.474
1.500	-5.401	289.699	7.978	-5.471	290.213	-22.091	259.026
3.000	-6.411	275.590	9.628	-6.519	276.131	-21.929	255.078

SURFACE WAVE FOR VERTICAL POLARIZATION. RANGE 1049.840 FEET

HEIGHT	COMPONENTS ALONG THE MAJOR AXIS			VERTICAL COMPONENT		RADIAL COMPONENT	
(FEET)	INTENSITY DB	PHASE DEGREES	TILT DEG.	INTENSITY DB	PHASE DEG.	INTENSITY DB	PHASE DEG.
0	-33.291	35.596	-5.695	-33.334	36.039	-51.306	177.737
1.500	-33.474	43.181	-5.695	-33.516	43.624	-51.488	185.322
3.000	-33.655	50.911	-5.695	-33.698	51.354	-51.669	193.052

TOTAL WAVE FOR HORIZONTAL POLARIZATION. RANGE 1049.840 FEET

HEIGHT	INTENSITY	PHASE
FEET	DB	DEG
0	-36.395	237.693
1.500	-13.324	189.743
3.000	-7.595	188.411

REFLECTION COEFFIENTS. RANGE 1049.84 FEET

HEIGHT (FEET)	ANGLE OF INCIDENCE (DEGREES)	VERTICAL MAGNITUDE (NUMERIC)	VERTICAL PHASE (DEGREES)	HORIZONTAL MAGNITUDE (NUMERIC)	HORIZONTAL PHASE (DEGREES)
0	4.63	.41	126.[illegible]	.98	.73
1.5	4.71	.40	125.75	.98	.75
3.0	4.79	.40	124.89	.[illegible]	.76

be moisture rather than temperature or nonhomogeneity. For this reason, the range of material constants was selected on the basis of moisture variations. However, most of the data was generated by using material constants associated with 10 percent or greater moisture conditions. These conditions were considered appropriate since the normal moisture condition at RAT SCAT appears to be near 15 percent (Figure 2).

The parameter values associated with range, antenna height, and frequency are listed in Table 2. The total number of conditions used in the simulation of the potential operating conditions was 1192.

3.3 Study Results

The number of parameters and the range of their values which were used in the ground plane simulation study enabled the generation of information on the effects produced on the RF fields as a function of anticipated conditions and/or potential operating conditions.

The properties of the vertical fields which are considered important in the type of study under discussion are (1) field gradients (amplitude and phase) as a function of RAT SCAT soil conditions, (2) field gradients of typical RAT SCAT soil conditions as a function of antenna heights, target heights, range, frequency and polarization, (3)tilt angle and field ellipticity (vertical polarization) as a function of range, frequency, and target height, and (4) polarization capability as a function of range, frequency, and target height (i.e., conditions which allow arbitrary polarizations to be obtained by using the same antenna height for the horizontally and vertically polarized antennas). In the following paragraphs, the effects of the various parameters on the above mentioned aspects of the vertical fields are demonstrated.

In Section 4, the results of the computer study on the surface wave are presented. In Section 5 measured versus computed data is presented for the case of selected operating conditions, and in Section 6 a further discussion of the computer results is presented in conjunction with a discussion of feasible range geometries.

3.3.1 Field Patterns as a Function of Soil Parameters

Listed in Table 2 are the material constants used in generating information on the field pattern versus the soil condition. The material constants listed in this table are those associated with dry, 5-, 10-, 15-, 20-, and 25-percent soil moisture conditions at ambient temperature. The dry and 5-percent data was only used in computations involving antenna heights of $\lambda/4$ for subsequent use in the surface field study (Section 4) since measurements indicate that, at RAT SCAT, the soil moisture remains at the 15-or-above-percent level.

Amplitude and phase changes are presented in Figures 28 through 39 as a function of moisture variations between 10 and 25 percent. The data was obtained for frequencies of 30-, 60-, and 120-megahertz, 60-, 160-, and 480-meter range lengths, and antenna heights of 16.5 and 33 feet.

The data is referenced to the 15 percent moisture condition (normal conditions) and indicates the maximum changes occurring in a six-foot vertical region centered about the target height which would be used for the case being considered. Amplitude and phase plots are presented in Figures 40 through 47 for the 60-megahertz, 16.5 foot antenna height, 160-meter range length case.

The data is Figures 28 through 39 indicates that, in general, the influence of soil moisture variation decreases at (1) the larger percent soil moisture conditions, (2) the frequencies below 60 megahertz, and (3) horizontal polarization. These considerations are used in Section 6 when discussing cancellation levels and stability.

3.3.2 Field Patterns for Normal Soil Conditions

In order to choose a feasible range geometry or geometries for making cross section measurements at RAT SCAT in the VHF region, vertical field patterns were computed under normal soil conditions by using realizable parameter values for antenna height, target height, and range. The complete ranges of the above variables are listed in Table 2 along with the frequencies and other soil conditions on which the computations were based.

RANGE (FEET)	ANT HT (FT) 30 MHz	45	60	90	120	180	%	ϵ_r	σ
65.62 524.96 131.24 1049.92 196.86 1574.88 262.48 2099.84 328.10 2624.8	8.2	5.44	4.1	2.72	2.05	1.36	0 5	3.95 6.26	0.002 0.03
65.62 524.96 131.24 1049.92 196.86 1574.88 262.48 2099.84 328.10 2624.8	16.4 32.8 49	16.4 32.8 49	16.4 32.8 49	8.2 16.4 32.8 49	8.2 16.4 32.8 49	4.1 8.2 16.4 32.8 49	10 15 20 25	12.53 14.49 23.47 24.97	0.25 0.61 1.2 1.6
1049.2 1574.88 2099.84	66 85	66 85	66 85	66 85	66 85	66 85	15	14.49	0.61
3927.2	8.2	5.44	4.1	2.72	2.05	1.36	0 5 10 15 20 25	3.95 6.26 12.53 14.49 23.47 24.97	0.002 0.03 0.25 0.61 1.2 1.6

Table 2 RANGE GEOMETRY AND SOIL PARAMETERS USED COMPUTER STUDY

The data generated by using normal soil conditions was examined in relation to the amplitude and phase gradients which existed over vertical target regions of different sizes. The center of each target region was selected at a height corresponding to the maximum of the first lobe (unless the first lobe maximum was at ground level) and in this latter case, the second lobe maximum was used. In the cases where the maximum of the lobe was higher than 72 feet, the best gradient position was used. Target heights below 10 feet were not considered. The antenna heights used to generate the data under this study were in the range of 16.5 to 49 feet at 60 megahertz and below and 8.25 to 49 feet above 60 megahertz.

Operating regions are presented in Figures 48 and 49 in terms of range, frequency, and polarization as a function of target region size. The field gradient criteria used to generate the regions were (1) a 2-db-or-less, two-way amplitude gradient and (2) a 45-degree-or-less, two-way phase gradient. The operating regions are shown for the cases of a 6- and 8-foot target region.

Presented in Figures 50 through 61 are selected amplitude and phase plots at each of the six frequencies from which the operating regions shown in Figures 48 and 49 were obtained. The plots in Figures 50 through 61 are a part of the more than 2000 plots made by the RADC automatic plotter.

3.3.3 Tilt Angle and Field Ellipticity

In the VHF region, the target heights necessary to reduce ground interference (Section 5) and the target sizes of interest make it impractical to consider tilting the target support to compensate for the wave tilt (angle between Poynting vector and ground plane) produced by the ground plane. In addition, for the case of vertical polarization, the ellipticity of the wave in the vertical plane (the vertical plane through the target and antenna) needs to be considered in the case of short ranges and relatively large target heights (Figure 62).

In the case of horizontal polarization, only the tilt angle must be considered since the field is linearly polarized in the vertical plane through the radar and target. The tilt of this linear vector is given by the geometrical tilt angle as indicated in Figure 62 and is therefore independent of frequency. However, in the vertical polarization case, the tilt angle is a function of frequency, antenna height, soil parameters, and range. The tilt angle for the case of vertical polarization corresponds to the angle of the major axis of the elliptical field relative to the vertical to the ground plane (Figure 62). This tilt angle is a computer output parameter; consequently, it is available for all of the conditions studied. The horizontal tilt angle is easily computed as a function of range and target height.

Tilt angle data are presented in Figures 63 and 64 as a function of range and frequency for two target heights. In the case of vertical polarization the tilt angle was obtained from the computed data which was based on antenna heights commensurate with the target heights used in the study (30 and 60 feet).

The data in Figures 63 and 64 demonstrates that, at the lower frequencies, the tilt angles related to vertical and horizontal polarization noticeably differ, but that this difference decreases as frequency and/or range increases.

Axial ratio data are presented in Figures 65 through 67 as a function of range for the case of 30-, 60-, and 120-megahertz frequencies. The axial ratio is shown for a 30- and 60-foot target height. The antenna heights used in obtaining the data shown in Figures 65 through 67 were those necessary to achieve acceptable field patterns at the target heights used in the study.

On the basis of the data shown in Figures 65 through 67, a range greater than 400 feet is necessary to maintain the axial ratio of a value greater than 20 db in the case of a 60-foot target height in the 30- to 100-megahertz frequency region. In the case of a 30-foot target height, the 20-db axial ratio criterion can still be met with a decrease in range to 200 feet.

3.3.4 Polarization Capability

Polarization capability refers to the ability to establish an arbitrary polarization over a target region of selected size. On a ground plane range, this type of operation can be accomplished under certain conditions even though the vertical and horizontal ground reflection factors are different. A necessary and sufficient property of the horizontally and vertically polarized fields is that they exhibit the same amplitude and phase gradients over the selected target region. In general, these conditions cannot be met by using the same antenna height, as illustrated by the data in Figure 42. In such cases, either two sets of two antennas ("transmit and receive") could be used, or possibly the scattering matrix could be recorded by changing antenna heights for the two polarizations. Both of these approaches are undesirable from a cost and/or operational viewpoint. For this reason, the computer results were examined to see if such operating conditions existed that arbitrary polarization could be achieved by using the same antenna height for both polarizations.

Presented in Figure 68 is a graphic representation of operating conditions which allow arbitrary polarization to be achieved by using the same antenna heights. The operating conditions are plotted in terms of range regions as a function of frequency. The operating regions were determined for a 6- and 8-foot vertical target region at two heights (the horizontal plane region match should not be a problem at the frequencies and ranges being considered). This work was based on meeting criteria to the effect that the two-way amplitude and phase gradient were 1db and 20 degrees, respectively. These criteria represent quite good conditions of orthogonality as determined by the cross section dynamic range σ_D recorded from a test sphere measured in the region of interest. The expression for this dynamic range is given by Equation 4 in terms of an amplitude gradient error of α^4 and a phase gradient error of $2\Delta\phi$.

$$\sigma_D = \frac{1 + \alpha^4 + 2\,\alpha^2 \cos 2\Delta\phi}{1 + \alpha^4 - 2\,\alpha^2 \cos 2\Delta\phi} \qquad (4)$$

Using values of 1-db and 20-degrees (in Equation 4) results in a dynamic range of 23 db. (This value is based on the assumption that the gradient errors all occur in the region of the test sphere - a conservative assumption.)

The operating regions indicated in Figure 68 are such that the polarization capability can be achieved at reasonable ranges at frequencies above 30 megahertz if a 60-foot target height is used. The cut off frequency for the 30-foot target height (or less) is between 60 and 90 megahertz.

SECTION 4

SURFACE FIELD INVESTIGATION

4.1 General

In the VHF region, the field patterns are noticeably a function of ground conditions, frequency, range, antenna height, and polarization. The effect of these parameters are especially noticeable in the case of vertical polarization as indicated by the mathematical model presented in Section 3. When vertical polarization is used, the field at the surface of the ground can become greater than the field over the target region. This condition is undesirable from the standpoint of the target support background levels that will be encountered in the operation of a cross section measurement facility. For this reason, an investigation of the surface fields at RAT SCAT was undertaken. The study program included a measurement phase and an analytical phase in which use was made of the ground plane model presented in Section 3. In this section, a technical description of the study is presented along with selected results obtained during the investigation.

4.2 Analytical and Measurement Programs

The analytical and measurement programs were so conducted that not only were the surface field conditions at RAT SCAT examined, but additional information was also provided on the validity of the ground plane model. This additional information was generated by making surface field measurements as a function of range and frequency and comparing the resultant data with computed data.

The analytical study consisted of making computations by use of the computer program described in Section 3. The computations were made for the case of a half-wave dipole whose center was located $\lambda/4$ above the ground plane. The use of this condition afforded a small grazing angle which is conducive to producing a large surface field. Computations were made for the ranges and frequencies indicated in Table 2 in terms of each of the moisture contents indicated.

Measurements were made at the RAT SCAT site at $\lambda/4$ antenna heights at the frequencies and ranges listed in Table 3 for the case of vertical polarization. The measurements were obtained by using a Manson Labs frequency synthesizer generator which exhibits a frequency stability of 1 part in 10^8 per day. The receiver used was an NF-105 and the associated half-wave dipoles whose antenna factor is known. The path losses of the feed cables were measured, and the mismatch factor between the antennas and the feed cable was taken to be that between 50 and 72 ohms. During the measurements, the temperature was recorded and soil samples were taken in order to obtain the moisture content. The power output of the generator was monitored to ensure that it did not deviate more than 1/4 db.

4.3 Program Results

The data obtained from measurements at RAT SCAT is presented in Table 3. The transmitter power and receiver power refer to the power delivered to and received at the antenna terminals. To compare the measured data with that computed, both types of data were plotted as a function of range referenced to the closest range. These plots are shown in Figures 69 through 74. The soil conditions indicated at the time of measurement was that of 15 percent moisture and ambient temperature. Hence the computer curves of Figures 69 through 74 are based on these conditions.

In order to verify the necessity of using the correct soil moisture conditions between 0 and 25 percent to obtain the degree of correlation indicated in Figures 69 through 74, similar curves were plotted for the case of each of the soil conditions used in the computations. This data is presented in Figures 75 through 77 for the cases of 30-, 60-, and 120-megahertz frequencies. The measured data are also plotted in these curves, and it can be readily seen that, in order to obtain the degree of correlation achieved in Figures 69 through 74, the selected soil constants were necessary. These results provided information as to the validity of the ground plane model in a region (near the surface) where reliable field probe information is normally difficult to obtain.

Another investigation which was conducted with the aid of the computer results was the investigation of the amount of surface wave contribution versus space wave contribution to the total surface field as a function of grazing angle. Presented in Figure 78 is a plot of the ratio of space wave to surface wave as a function of range for two frequencies between 30 and 100 megahertz.

Table 3 SURFACE FIELD MEASUREMENT CONDITIONS AND RESULTS
(sheet 1 of 2)

Date Time	Range Meters	Frequency MHz	Power At Xmitter Antenna	Power At Receiver Antenna	Temp. °F	Wind Knots
7/15/65						
4:40 AM	20	180	-3 dbm	-45.5 dbm	90	0 - 5
4:47	20	120	-3 dbm	-42 dbm	90	0 - 5
4:55	20	90	-1 dbm	-40 dbm	90	0 - 5
5:00	20	60	0 dbm	-37 dbm	90	0 - 5
5:05	20	45	0 dbm	-36 dbm	90	0 - 5
10/17/65						
1:10 PM	20	30	0 dbm	-34 dbm	80	5 - 6
7/15/65						
2:55 PM	40	180	-2 dbm	-50.5 dbm	96	10 - 15
2:43	40	120	-2 dbw	-18 dbw	96	15 - 20
2:22	40	90	0 dbw	-19 dbw	94	15 - 20
2:18	40	60	0 dbw	-15 dbw	99	0 - 5
2:13	40	45	0 dbw	-13 dbw	99	0 - 5
10/17/65						
1:20 PM	40	30	0 dbm	-40 dbm	80	5 - 6
7/15/65						
1:30 PM	80	180	-3 dbw	-29.5 dbw	98	0 - 3
1:36	80	120	-2 dbw	-25 dbw	98	0 - 3
1:42	80	90	0 dbw	-21 dbw	99	0 - 3
1:47	80	60	0 dbw	-20.5 dbw	100	0 - 3
1:55	80	45	0 dbw	-18.5 dbw	94	0 - 3
10/17/65						
1:30 PM	80	30	0 dbm	-46 dbm	80	5 - 6
7/15/65						
12:10 PM	160	180	-2 dbw	-41.5 dbw	96	0 - 5
12:02	160	120	-2 dbw	-33 dbw	96	0 - 5
11:58	160	90	0 dbw	-29 dbw	96	0 - 5
11:53	160	60	0 dbw	-28.5 dbw	96	0 - 5
11:48	160	45	0 dbw	-22.5 dbw		0 - 5
10/17/65						
1:40 PM	160	30	0 dbm	-52 dbm	80	5 - 6

Table 3 SURFACE FIELD MEASUREMENT CONDITIONS AND RESULTS
(Sheet 2 of 2)

Date Time	Range Meters	Frequency MHz	Power At Xmitter Antenna	Power At Receiver Antenna	Temp. °F	Wind Knots
7/15/65						
10:10 AM	320	180	-2 dbw	-63 dbw	90	5 - 10
10:15	320	120	-2 dbw	-50 dbw	91	5 - 10
10:20	320	90	0 dbw	-40 dbw	93	5 - 10
10:25	320	60	0 dbw	-36 dbw	94	5 - 10
10:30	320	45	0 dbw	-31 dbw	95	5 - 10
10/17/65						
2:00 PM	320	30	0 dbm	-59 dbm	80	5 - 6
7/15/65						
10:00 AM	640	180	-2 dbw	-73.5 dbw	86	5 - 10
9:54	640	120	-2 dbw	-65 dbw	86	5 - 10
9:50	640	90	0 dbw	-54.5 dbw	85	5 - 10
9:44	640	60	0 dbw	-44 dbw	84	5 - 10
9:40	640	45	0 dbw	-37 dbw	87	5 - 10
10/17/65						
2:20 PM	640	30	0 dbm	-77 dbm	80	5 - 6
7/14/65						
5:15 PM	1200	180	-6 dbw	-87.5 dbw	98	5 - 10
4:35	1200	120	-5 dbw	-80.5 dbw	99	5 - 10
5:30	1200	90	-2 dbw	-72 dbw	94	5 - 10
5:45	1200	60	0 dbw	-50.5 dbw	91	5 - 10
6:00	1200	45	0 dbw	-47 dbw	92	5 - 10
10/17/65						
2:50 PM	1200	30	0 dbm	-74 dbm	80	5 - 6

The grazing angle is denoted on each of the curves, and it is apparent that the ratio of surface wave to space wave is a function of the grazing angle and is rather independent of frequency.

Although antenna heights very near the ground were considered in the surface field measurement and validation program, surface fields are still present at antenna heights which are practical for an operational backscatter range. However, just as in the case of the lower antenna heights, the amount of surface field relative to the space field (or total field in the target region) is dependent on range, frequency, and soil conditions. In Section 6, data is presented for practical antenna heights to indicate the decay of the surface field relative to the field in the target region as a function of range and frequency.

SECTION 5

INDUCTION FIELD AND VALIDATION TESTS

5.1 General

A measurement program was conducted at RAT SCAT during this initial study phase of the VHF program to obtain (1) data on coupling errors which are introduced by target-ground induction field interaction, (2) further information on the validity of the ground plane computer model, and (3) cross section measurements of full-scale targets in the VHF region for comparison with data obtained under free space conditions.

The induction field data was obtained by making measurements on cylindrical objects of different sizes as a function of frequency, polarization, and target height. The $\lambda/4$ cyclic variation of the field occurring as a function of height was then analyzed in terms of the parameters indicated above.

Field probe validation data was obtained by making one-way field probes at antenna heights, frequencies, and ranges used in the computer study. The soil moisture and the temperature were noted during the measurements, and the measured data was compared with the computer data generated by using the soil constants nearest in value to those indicated by the moisture and temperature readings.

The cross section measurements were made at frequencies of 30 and 60 megahertz on targets for which comparative data was available from scaled model measurements.

5.2 Induction Field Program

To obtain information representative of the effects of the mutual coupling between the target and the ground on cross section accuracy, a measurement program was conducted at RAT SCAT. The parameters varied during the measurement program were (1) frequency, (2) target size, (3) polarization, and (4) target height. The measurement system used was the GD/FW VHF electronic system and a target support constructed for the VHF program. The measurements were made by using a range of 350 feet (except for the case of 120- and 180-megahertz vertical polarization, refer to Table 4) and a dual-antenna system for which the transmitting and receiving antennas were separated between 85 and 150 feet (Figure 79). The electronic system (Figure 80) was operated essentially CW and the achievable background levels were obtained by cancelling the extraneous signals received without a target. RFI was maintained below the cancellation levels by using a relatively narrow bandwidth IF system (2 megahertz) and RF filters.

The target height was varied continuously be means of a pulley system supported on the 36-inch-diameter fiberglass tube used for a target support (Figure 81). The wall thickness of the fiberglass tube was 3/8 inch, and the tube was adjustable from 36 to 65 feet in height. The column was extended to 65 feet for measurements at 30 and 60 megahertz while a 37-foot height was used to obtain data at 120 and 180 megahertz. Cross section and height were correlated by driving the recorder from a height servo connected to the target.

Although measurements were made on dipoles, loops, and spheres, these were primarily taken for calibration purposes. The primary targets used to investigate coupling were cylindrical objects constructed by welding 2-foot diameter oil drums end-to-end (Figure 82). This technique was used to construct cylindrical targets of 40-, 20-, and 10-foot lengths.

5.2.1 Induction Field Measurement Results

Table 4 contains a list of the conditions under which the induction field measurements were made. Except for the vertical polarization cases (especially at 120 and 180 megahertz), the background levels were sufficiently below the target return (for maximum return position) that errors caused by background interference did not greatly degrade the coupling experiments. However, in almost all cases (especially at the higher frequencies), background interference and/or target motion was noticeable as evidenced by differences between plots obtained by repeating the measurement. The isolation, cancellation and background levels indicated in Table 4 are representative values obtained from repeated measurements made at the indicated range geometries. These values will not necessarily correspond to any of the values noted with the data selected for presentation in this report.

(Induction Field and Coupling Tests):

Polarization	Freq. (MHz)	Range (Feet)	Xmitter Antenna Height (Feet)	Receiver Antenna Height (Feet)	Antenna Separation (Feet)	Max. Target Height (Feet)	Antenna Isolation (db)	Cancellation (db)	Background (dbsm)
Horizontal	30	350	43	18	85	60	-55	-47	-30
Vertical	30	350	12	18	150	60	-60	-43	-30
Horizontal	60	350	43	18	85	50	-60	-45	-20
Vertical	60	350	12	18	150	50	-60	-47	-15
Horizontal	120	350	18	18	150	35	-69	-40	-25
Vertical	120	225	18	18	150	35	-66	-40	-12
Horizontal	180	350	18	18	150	35	-70	-40	-45
Vertical	180	225	18	18	150	35	-66	-40	-15

(Validation Tests):

Polarization	Freq. (MHz)	Range (Feet)	Xmitter Antenna Height (Feet)	Receiver Antenna Height (Feet)	Antenna Separation (Feet)	Max. Target Height (Feet)	Antenna Isolation (db)	Cancellation (db)	Background (dbsm)
Horizontal	30	350	43	18	85	65	-55	-47	-30
Vertical	30	350	12	18	150	38.5	-60	-43	-30
Horizontal	60	350	43	18	85	38.5	-60	-45	-20
Vertical	60	350	12	18	150	38.5	-60	-47	-15

Table 4 MEASUREMENT PROGRAM CONDITIONS

Typical plots obtained from the measurement program are shown in Figures 83 through 88 for the cases of 30, 60, 120 and 180 megahertz. In all cases associated with the cylinders, the horizontal polarization measurements exhibited the largest evidence of coupling. However, this result should be expected if a simple scattering model based on far-field type scattering is considered. In other words, in a simple far-field scattering model, the coupling error is a function of the bistatic cross section level (σ_b) and monostatic cross section level (σ_m) in the form (σ_b^2/σ_m). Hence, if the monostatic and bistatic cross sections kept the same relative differences but each was much smaller in one polarization than in another, the coupling error should reflect this change.

The measured data was reduced to a more useful form by plotting the coupling error as a function of target height, target size, frequency, and polarization. This data is presented in Figures 89 through 92. The data was obtained by taking the deviation in db from the mean drawn through the cyclic field probe and referring to this deviation as the error produced by the coupling. There is quite good correlation between the height positions where maximum and minimum deviations occur and the multiples of $\lambda/4$. In the vertical polarization cases in which no coupling error could be detected data is not shown. Even in the case where vertical polarization data are plotted (30 megahertz), the non-periodic variations indicate the anomalies were caused by target motion and/or background interference except near ground level.

One of the important parameters of interest during this study was the decay rate of the ground-reflected energy as a function of height. Analyses of the data indicate that the reflected power appears to decay proportional to $R^{-X}, 1 \leq X \leq 2$. This finding indicates that the decay rate is much slower than that predicted by use of a simple far-field model. However, it is not too difficult to construct a near-field model which can be used to predict decay rates such as those observed (namely, a model in which consideration is given to the increase in gain of the effective ground aperture as a function of height). Hence the ground reflected energy height decay rates indicated by the measurements should be considered typical when considering a target support system.

Another fact which is supported by the measured data is that, in the region below 60 megahertz, it is quite easy to choose a target height so that the ground-reflected energy has a null effect on the measured cross section. These heights are the odd multiples of $\lambda/8$. At these heights (theoretically the exact heights are slightly different from these odd multiples of $\lambda/8$), the cross section of the interacting component adds incoherently, and the error introduced practically vanishes. Although this phenomenon occurs at all frequencies, only below the 60-megahertz region (and as a function of target size) does it become practical to place a target in an $\lambda/8$ height position. Use of this technique in the 30-megahertz region would allow target heights to be used at which there would be a noticeable coupling error at $\pm\ \lambda/8$ distances from the target position.

The coupling results presented above indicate that coupling must be taken into consideration in the choice of a feasible range configuration. In Section 6, the range geometries are selected based on a consideration of target heights and sizes which should produce insignificant coupling errors; these heights are based on the data generated during the investigation of the induction field.

5.3 Validation Program

The validation program was undertaken in order to obtain information on the validity of the ground plane model and to obtain cross section measurements at range geometries selected on the basis of results obtained from the computer study and induction field measurements. Further, the results obtained from this program were to be used in defining a more optimum configuration, if necessary, for making final measurements to demonstrate feasibility of making cross section measurements in the VHF region.

Information as to the validity of the ground plane model was obtained in the form of field probe data. Data was taken at two ranges, a short range (328 feet) and a long range (1575 feet) at four frequencies and both polarizations. All of the parameters used in the measurements were such that computer data was available for these conditions (except possibly the soil parameters). The soil parameters were estimated by noting the temperature and soil moisture condition during the measurement. The computer data generated on the basis of soil conditions most similar to those noted during the measurements were used for comparison purposes.

The measurements obtained at the short ranges were obtained at the lower frequencies (30 and 60 megahertz) by using a yagi transmitting antenna and a dipole for receiver and two dipoles at the higher frequencies (120 and 180 megahertz). The data was recorded by using the GD/FW cross section measurement system discussed in subsection 5.2 by running a coaxial cable from the target region back to the receiver. At the longer range, this technique was not feasible, and use was made of a technique similar to that described in Section 4 for obtaining surface field data. Also, at the longer range, information on absolute path loss was obtained.

In the cross section measurement program, the targets measured at 30 and 60 megahertz were those for which cross section data was obtained from scaled models of the targets. The scaled data was obtained at RAT SCAT from measurements made at 1320 megahertz. The targets used in the measurements were those described in subsection 5.2, i.e., cylindrical targets constructed from oil drums (Figure 82). The scaled models of the cylindrical objects are depicted in Figure 93. The scale factors used to obtain the models were 1/44 in the case of 30 megahertz and 1/22 in the case of 60 megahertz. Physical measurements of the actual scaled models showed that the model scaled for the 30-megahertz full-scale target of 41.5 feet actually represented a target 43 feet in length (3.6 percent error) with the same diameter as the actual target. The remaining models represented full-scale targets within .5 percent of the dimensions of the actual targets.

The primary difference between the scaled data and full-scale data appeared to be caused by the difference in the bistatic angles used in the two measurements. The bistatic angle used to obtain the scaled data was less than .5 degree, whereas in the full-scale measurements, bistatic angles of 12 and 22 degrees were used in the case of horizontal and vertical polarizations, respectively. These bistatic angles were necessary in order to achieve the amount of stable isolation required to maintain a stable background level sufficiently below the target cross section to give negligible background interference. At the beginning of the measurement program, it was found that spatial antenna separation was necessary to achieve the required amount of stable isolation. At first a RAT SCAT mobile target shelter was used to isolate one of the antennas from the other. This technique is illustrated in Figure 94. Although a RAT SCAT mobile shelter is not ideally suited for an antenna housing (Figure 95 shows the vertical field for an antenna inside and outside of the mobile shelter), results obtained at GD/FW by using an antenna housing constructed for the purpose of isolation indicated cancellation instability problems not as severe but similar to those experienced at RAT SCAT in the use of the mobile shelter.

The problems encountered and results obtained during this phase of the validation program have lead to considering different range geometry configurations than those used for the reported measurement. In other words, the range, antenna heights, and target lengths used to obtain the cross section data were based primarily on (1) acceptable field gradients in the target region, (2) target heights sufficient to minimize coupling, and (3) a range which allowed a sufficiently low level of measurement sensitivity with the available electronic system. In Section 4, range configurations are discussed in terms of the above factors, but in addition, consideration is given to isolation by antenna separation (bistatic angle) and to other undesirable features, such as tilt angle, which were present in the cross section measurements being reported.

5.3.1 Validation Measurement Results

The results obtained from the vertical field measurement program are presented in Figures 96 through 99. The 328-foot range data are presented in Figures 96 and 97 along with the computed data. The 1575-foot range data are presented in Figures 98 and 99. The computed data was normalized to the measured data by equating the maximum relative amplitudes of both sets of data over the height range for which both types of data were available. The degree of correlation achieved between measured and computed data was in general quite good, and in the few cases close to the ground level where substantial differences were noted these were attributed to interaction between the probe and the target support as well as possible field anomalies caused by the 20-foot diameter pit located under the probe region.

In the case of the 1575-foot range measurements, absolute path loss information was obtained in addition to the field gradient information. The path loss data was obtained by measuring the antenna feed cable losses and maintaining the output of a calibrated HP 608 generator constant during the measurements. The calibrated dipole antennas used in these measurements produced a mismatch between feed line and antenna of 1.7 db. The measured data is presented in Table 5.

Table 5 FIELD PROBE AND PATH LOSS DATA

Field Probe Data

(Temperature - 70°F)

Probe Height (Feet)	30 MHz H	30 MHz V	60 MHz H	60 MHz V	120 MHz H	120 MHz V	180 MHz H	180 MHz V
0	0	—	0	—	0	6	-16	-5
3	8	—	7	26	1	3.5	-6	-4.5
6	13.5	—	14	26	5	2	-2	-3.5
9	15.5	39.5	18.5	26.5	9.5	4	0	-2.5
12	18.1	40	20	25.8	11.4	5	1.5	-1
15	20.5	39.5	22	26	11.4	6	2.8	0.5
18	22.3	39.2	24.5	25.6	13.5	8.5	3.8	1.4
21	23.8	39.1	25	24.7	14.8	9	4.8	1.7
24	24.5	39.1	26.5	24	15.8	10.5	4.8	2.5
27	25.2	38.8	27.8	23.7	16	11.2	6.1	3
30	26.2	38.7	28	23.7	16.4	12.1	6.6	3.9
33	27.3	38.6	29	23.7	17.4	12.8	7.2	4.8
36	28.2	38.5	29.8	23.5	18.3	13.5	7.2	5
39	28.7	38.3	30	23.5	18.8	14	7.2	5
42	29.3	38.4	30.8	24	19.6	14.5	7.2	5
45	29.9	38.3	31.3	24	19.7	15	6.9	5.3
48	30.5	38.0	31.7	24.3	20	15.5	6.3	5.5
51	31.1	37.9	32.8	24.3	20.4	16	6	5.4
54	31.5	37.7	32.8	24.3	20.5	16.3	5.7	5
57	31.8	37.4	33	24.8	20.75	16.7	5.6	4.5
60	32	—	33.5	25	21	17.2	5.4	4.5
63	32.5	—	33.5	—	22	—	4	—
Line Loss	10.9 db		14.4 db		19.4 db		23.4 db	
Reference	99		100		99		98	

Path Loss Data

Frequency (MHz)	Computed (db)	Measured (db)
30	55	57
60	63.6	64
120	75.4	77
180	83.4	90

A comparison between measured path loss and that computed by using the standard one-way transmission equation (Reference 3) was made for the case of horizontal polarization in order to check the validity of using the standard radar equation along with the ground plane computations for predicting measurement sensitivities of other range geometries. The ground plane effect was included into the one-way, free-space equation by adding 6 db to the computed data minus the amount the computed data indicated the maximum value was from the ideal ground plane maximum (for -1 reflection factor, this ideal value would be 6 db above the antenna free space maximum). The computed versus measured path loss information is also presented in Table 5. Except for the case of 180 megahertz, the correlation between computed and measured was within 2 db. At 180 megahertz, the large difference (6 db) was partially attributed to a change in IF gain on the NF-105 receiver which was made for the 180-megahertz measurement to increase the measurement sensitivity beyond the 100-db calibrated scale, and the maintenance of proper orientation of the dipoles.

The measured path loss data was used in conjunction with the radar equation and computer study results to obtain an estimate of the measurement sensitivity as a function of range and frequency. Path loss information was extended to other ranges by using the relationship given in Equation 5 ; this data is presented in Figures 100 and 101 for the cases of horizontal and vertical polarizations at frequencies of 30, 60, 120 and 180 megahertz.

$$\sigma = 4 \pi R^2 P_r/M \; (480/R)^2 \; G_R^2 \; P_R^2 \; L \qquad (5)$$

where

M = Measured path loss without cable loss at 1575 feet referenced to correct position for selected antenna heights and target height

R = Range in meters

G_R = Antenna gain relative to a dipole (2 db)

P_r = Receiver sensitivity (dbm)

P_R = Transmitter power (dbm)

L = Cable and filter losses

The value of M in the above equation was adjusted from that measured at 1575 feet by using the amount predicted on the basis of the computer results. This amount in general depends upon the target height, antenna heights, frequency, and soil conditions. The soil parameters used were those associated with 15-percent moisture conditions (normal conditions); the antenna heights used were those values which give acceptable field patterns at target heights in the 30- to 65-foot region.

The transmitter power used to arrive at the sensitivity curves was 200 watts and the antenna gains were 10 db and 15 db over a dipole at 30 and 60 megahertz and 120 and 180 megahertz respectively. The cable and filter loss was assumed to be 5 db at frequencies of 30 and 60 megahertz and 8 db at 120 and 180 megahertz. The receiver sensitivity (including the noise figure) was taken as -105 dbm.

The data presented in Figures 100 and 101 were used as the basis for establishing the potential measurement capabilities associated with the range geometries discussed in Section 6.

5.3.2 Cross Section Measurement Results

The full-scale cross section measurements were obtained under the range geometry conditions presented in Table 4. The measured data is presented in Figures 102 through 105.

In the vertical polarization case, the target height (38 feet) and range (350 feet) were such that a tilt angle of ≈ 5 and ≈ 4 degrees were present in the case of 30 and 60 megahertz, respectively. In the case of horizontal polarization, the tilt angles were 11 and 6 degrees for the cases of 30 and 60 megahertz, respectively. The bistatic angles associated with each of the measurement conditions were 12 degrees for horizontal polarization and 22 degrees for vertical polarization. The heights selected for the measurements were such that coupling errors should be minimized except in the case of horizontal polarization at 30 megahertz. Except for this case, the target heights were approximately odd multiples of $\lambda/8$. In the 30-megahertz horizontal polarization case, the target was placed at the maximum height attainable which was a position of 2λ (66 feet). Consequently, an additive error of the magnitude predicted from the induction field measurements was anticipated for the broadside condition. Comparison of the model data with full-scale data for this case indicates an error very close to the predicted amount.

The full-scale cross section measurements were made by using a half-wave dipole to calibrate the system. The background levels were in all cases better than 20 db lower than the maximum cross section, and in the case of horizontal polarization, the background was 40 db lower than the maximum cross section of the cylinders. Background data is presented in Figures 106 and 107 for the case of 60-megahertz frequencies at horizontal and vertical polarization.

Scale model cross section data corresponding to the full-scale target geometries are presented in Figures 108 through 111 for the case of zero tilt angle and essentially zero bistatic angle. The background levels associated with these scaled model measurements are presented in Figures 112 and 113. The vertical polarization measurements were made with a background between 15 and 30 db below the maximum return. Hence in some cases a comparison between full-scale and model data except at the maximum values has little meaning. The worst case is the 14-barrel model (Figure 109) where the model background was at most 15 db below the model return.

To compare cross section levels between the full-scale and model data, 32.9 db should be added to the 14-barrel model data scale and 26.9 db to the 7-barrel model data scale. In Table 6, the values of several scattering characteristics are listed for both full-scale and model cases; these data serve to summarize the degree of correlation achieved between the two measurement series. The broadside cross section values agreed to within 2 db in all cases; the worst case was that of 30-megahertz horizontal polarization. However, on the basis of the induction field tests and the 2λ height used in the measurement (see Figure 89), a 1 db error should be present.

Hence, if this error is accounted for, the agreement of the broadside values is within 1.5 db in all cases. The most noticeable differences between the two sets of data are the side lobe levels and the angular distances between nulls and the end-on cross section differences in the cases of vertical and horizontal polarizations. These characteristics are those most affected by the difference in the bistatic and tilt angle between the two sets of measurements. For example, in comparing the two sets of 14-barrel data in the case of horizontal polarization, it is seen that in the full-scale case the side lobe levels are less (even if coupling error is subtracted) than the main lobe, whereas in the model data they are

Table 6 COMPARISON OF FULL SCALE AND MODEL SCATTERING CHARACTERISTICS

(30 MHz, 14 Barrel Measurements):

Measurement Conditions / Scattering Characteristics	MODEL		FULL SCALE	
	Horizontal Polarization	Vertical Polarization	Horizontal Polarization	Vertical Polarization
Main Lobe Value (dbsm)	16.5	1.7*	18.5	3.25
Side Lobe Value (dbsm)	17.5	-9.43**	15.8	***
Main Lobe Null Width (degrees)	40	47	46	61

(60 MHz, 7 Barrel Measurements):

Main Lobe Value (dbsm)	14.5	7.1	16	8.25
Side Lobe Value (dbsm)	12.6	-5.4	13.1	-2.75**
Main Lobe Null Width (degrees)	40	45	42	47

* Background Levels such that 1-2 db errors possible

** Background Levels such that 2-4 db errors possible

*** No Side Lobes on Full Scale data

larger. Also, the distance between nulls in the full-scale case is 46 degrees and only 40 degrees in the model data. Although some of the angular separation can be accounted for ($\approx$ 2 degrees) because the model data represents a full-scale target 3.6 percent longer than the actual full-scale target, most of the difference is due to the angles mentioned above. To demonstrate this fact, the 14-barrel model was measured at the tilt angles for which the full-scale measurements were made (Figures 114H and 114V). Although the data should still not be related isomorphically because the bistatic angles are different, the data obtained with the same tilt angles used in the full-scale model is approaching the full-scale data in the right manner. In the horizontal polarization case (Figure 114H), the null separation has decreased 2 degrees, and the side lobes relative to the main lobe have decreased (there was a slight wobble in the column rotation which causes the asymmetry of the side lobes).

The largest discrepancy in the measured data is that of the end-on cross section values between horizontal and vertical polarizations in the case of 30 megahertz. The cross section for each of the polarizations in this case should be the same as indicated by the data in Figures 108 and 109 (the 2 db difference is attributed to the background levels as shown in Figures 112 and 113). The difference between the cross sections in the full-scale case was 9 db. However, this difference can be accounted for by noting that azimuth variation in the vertical polarization case is equivalent to tilt angle in the horizontal case and vice versa (true for end-on only and neglecting bistatic angle). Also it is noted that in the vertical polarization case the cross section is insensitive to azimuth change about end-on, but not so in the horizontal polarization case. Hence, if the difference between end-on and 5 to 6 degrees from end-on in the horizontal case with zero bistatic (Figure 108) is examined most of the discrepancy (8 db) in the full scale data can be explained. Furthermore, the scale model tests conducted with and without the full scale tilt angles shows the same 9 db difference exhibited by the full scale data. Also, the same reasoning can be used to obtain correlation in the 60 megahertz data although the differences were not as great at this frequency.

In the vertical polarization case another substantial change appears to be produced by that angle. The data obtained by using a 5-degree tilt angle (Figure 114V) did not exhibit side lobes, just as in the case of the full-scale data. Also, the main lobe null width increased to approximately 55 degrees in comparison to 47 degrees for the zero tilt angle model data and 61 degrees in the case of the full-scale data. Although the background level which was present in the case of the 5-degree tilt model data was such that the recorded levels in the side lobe and nose-on regions are not considered accurate, the trend of the data to converge to that recorded in the full-scale case is apparent. The tilt angle conditions for the 7-barrel data were used to obtain new model data also, but these angles were 6 degrees or less, and although the same trends were noted as discussed above, the measured results were so similar to the zero tilt angle data that the plots are not presented.

The information obtained from the cross section measurement program provided evidence that the bistatic angles and tilt angles associated with the range configurations used in the recorded measurements produce detectable errors in the cross section data. Also the data indicated that, if these angles were reduced to the less-than-4-and 2-degree regions, respectively, incurred errors should become negligible. This type of criterion is used in Section 6 in selecting range geometries.

SECTION 6

SUMMARY

6.1 General

In the preceding sections, the results of several specific study and measurement programs have been reported. These individual programs were undertaken to obtain information with which to design a VHF cross section measurement system to demonstrate the feasibility of making VHF cross section measurements at RAT SCAT.

Before such a system is designed, consideration should be given to the integrated effects of the factors discussed separately in the preceding sections, as well as those of other factors normally associated with a cross section measurement system. In other words, an effort should be made to consider simultaneously the pertinent factors influencing the performance of a VHF cross section system, as well as the available hardware and the operational problems associated with potential designs.

In this section the results of such an integrated effort are presented after the individual factors germane to a feasible range design are reviewed. From these, an approach is recommended for implementation and demonstration of a dual measurement capability at RAT SCAT (by use of the same electronic system). In making this recommendation, consideration is given to the fact that in the present program it is planned to demonstrate, via measurements at RAT SCAT, feasibility only in the 30- to 100-megahertz frequency region. However, the frequency region (30 to 180 megahertz) has been considered from a performance viewpoint, and even though the demonstration equipment can only be operated in the 30- to 100-megahertz region, the recommended range design and chosen measurement techniques will be feasible up to 180 megahertz.

Along the same lines, there are several factors considered in the forthcoming paragraphs which are not feasibility requirements for the present program (e.g., polarization capability); however, even though these factors are not used to rule out potential range designs, as evidenced by the short-range recommendation, they are considered as representative of the advantages in choosing one range design rather than another. In other words, an effort has been made to select a measurement approach which can be used to demonstrate not only measurement feasibility in terms of the current program goals but also to show measurement feasibility in terms of a more general set of capability requirements.

6.2 Study Summary

The results of the investigations reported in Section 2 through 5 are summarized in terms of factors which should be considered in a range design study. In the case of the soil measurement programs, these factors are considered to be (1) soil homogeneity, (2) the variation of soil electrical characteristics with frequency, moisture, and temperature, and (3) the electrical variations expected as a result of RAT SCAT climatic conditions.

In the case of the computer study, the factors are considered to be (1) the RF field gradients over the vertical target region as a function of frequency, range, and antenna heights for normal soil characteristics, (2) the field gradient changes caused by expected variations in soil electrical parameters, (3) the surface field versus the space field as a function of frequency, range, target and antenna height, (4) vertical polarization field ellipticity and polarization versatility, and (5) tilt angle versus target height and range.

In the case of the induction field and validation measurement program, the important factors are (1) coupling error versus target size, height, frequency and polarization, (2) the influence of range geometry parameters, tilt angle, and bistatic angle on cross section data and the performance of the target support, (3) the achievable cancellation levels (and associated background levels) and stability as a function of frequency and polarization, (4) antenna isolation, and (5) long-range field probes and path loss data.

6.2.1 RAT SCAT Soil Characteristics

Samples of RAT SCAT soil were selected on a statistical basis as indicated in Section 2. On the basis of soil samples selected, the RAT SCAT soil appears to be electrically homogeneous. This conclusion was supported by the results of the validation experiments conducted at RAT SCAT since much of the field probe data was obtained at locations different from those from which soil samples were obtained to measure the electrical constants. Nevertheless, the measured field probe data was closely correlated to the computer results obtained by using the measured electrical constants of the soil samples.

The soil electrical parameters exhibited the greatest variation as a function of moisture content rather than temperature. The data in Figures 6, 7, and 8 shows the expected value of the dielectric constant and conductivity as a function of moisture at ambient temperature conditions. The expected value of moisture content at RAT SCAT appears to be 15 to 16 percent on the basis of the determination of soil sample moisture over a five-month period (Figure 2). On the basis of this percent moisture, the data in the above indicated figures shows the dielectric constant will normally be in the range of 14 to 16 and the conductivity in the range .4 to 8 mhos per meter. The data in Figures 9 and 10 for temperature conditions at 32°F and 120°F shows that the variation in conductivity as a function of temperature is well within the range of moisture variations of ±5 percent from the 15 percent value established for ambient temperature. Hence the primary source of field variation resulting from soil changes should be caused by moisture changes between 15-percent (normal dry conditions) to 25-percent conditions which would prevail during rainy periods.

6.2.2 Computer Study

The ground plane model programmed on the computer was used to investigate the effect of the major range geometry parameters on the RF fields at RAT SCAT. The computed data was based upon the results of the soil measurement study in which results representative of a number of conditions were compared with measured data and found to be in close agreement.

One of the first factors investigated with the aid of the computer results was that of the field gradients over the target region. Operating regions are shown in Figures 48 and 49 in terms of range and frequency where acceptable vertical field gradients over a six-foot target are achievable. These operating regions were determined by using a two-way, 2-db amplitude and 45-degree phase gradient, or less, as acceptable and allowing the antenna and target heights to be adjustable within wide limits and dependent upon polarization and frequency. On the basis of the data in these figures, acceptable vertical fields are achieved (for targets up to six feet in vertical extent) between 200 and 2100 feet at frequencies between 30 and 120 megahertz at both vertical and horizontal polarization. Hence vertical field gradients, considered separate from other factors, are not fundamental limitations on VHF operation.

After the field gradients were examined in terms of normal soil conditions, they were examined as a function of soil moisture conditions. Typical results from this study are presented in Figures 28 through 39. Results indicated that, in the case of horizontal polarization, field changes were almost negligible at all frequencies and ranges. In the case of vertical polarization, the field changes ranged between 1 db in amplitude and 15 degrees in phase, depending on frequency, antenna height, and range. However, the greatest sensitivity was exhibited in the frequency region above 60 megahertz. Although the above gradients were primarily caused from moisture changes between 10 and 20 percent and would probably not be detected in field probe measurements, they are of concern in considering a cancellation system. This is the case even if the gradient changes between 15 and 20 percent are divided by 5 to approximate the effects of daily temperature and moisture variations. For example, in a case where the phase change is 5 degrees (one way) for 5-percent moisture change and 20 is used as a division in order to approximate a moderate hourly change rate caused by temperature and moisture, the amount of cancellation would be upper-bounded by 47 db because of the phase drift caused by soil changes. After a rain the drift problem caused by soil parameter changes is potentially even more severe as indicated by the data presented in Figure 3. However, upon examination of the field gradient caused by moisture change, it appears safe to assume that 45 to 55 db of cancellation could be maintained in the VHF region over long periods of time and that this cancellation would not be affected by soil conditions (except possibly during and immediately following a rain).

In addition to examining the field gradients as a function of vertical regions and soil parameter changes, the computer results were used to investigate the surface field relative to the field in the target region as a function of range and frequency. The investigation was conducted only for the case of vertical polarization since in the horizontal case the surface field is negligible in comparison to the field in the target region. The results of this investigation are presented in Figure 115. The data in this figure was obtained by using antenna and target heights in the 10- to 66-foot region which would provide acceptable measurement fields. The results of the investigation indicated that, in the frequency region above 90-megahertz, the ratio of the field in the target region to that on the surface (pit rotator region) can be increased substantially by operating in the 1000- to 2000-foot range region rather than the 200- to 400-foot range region. Therefore, in order to reduce the cross section of the rotator and target support in vertical polarization, a longer range is preferable.

Two other factors associated with operating in the VHF region on a ground plane range are field ellipticity and polarization versatility. These factors were investigated by using the computer data and results presented in Figures 62 and 68. Results of the investigation indicated that field ellipticity would not be a problem at ranges greater than 400 feet and target heights up to

60 feet, or ranges greater than 200 feet for target heights up to 30 feet. As a result of the study, it was also indicated that high-quality polarization versatility could be achieved by use of a single antenna system at ranges above 1000 feet and frequencies above 30-megahertz, but could not be achieved by use of a single antenna system at the shorter ranges, and lower frequencies.

Another factor which should be considered at the shorter ranges is that of tilt angle. Presented in Figures 63 and 64 is tilt angle information relative to the parameters of range, frequency, and target height at horizontal and vertical polarization, respectively. Horizontal polarization presents the greatest problem, but in both polarization cases the tilt angle is reduced to less than 5 degrees for 30-foot target heights at a range of 400 feet and less than 4 degrees for 65-foot target heights at a 1000-foot range.

6.2.3 Induction Field and Validation Program

The induction field measurement program results are presented in Figures 89 through 92 in terms of expected coupling error. These results indicate that, in the case of horizontal polarization and relatively large cylindrical-type targets (40 feet), significant coupling errors (1 to 2 db) can be obtained up to heights of 66 feet at 30 megahertz and 37 feet at 180 megahertz. However, these errors occur at predictable heights in the lower frequency range (below 60 megahertz) and can therefore be minimized by proper selection of target height. In the case of smaller targets (less than 10 feet, the coupling error was confined to a region of less than 1 db when target heights were above 20 feet. In the case of vertical polarization, coupling effects were almost insignificant for all cylinder sizes and target heights tested. On the basis of the results obtained from this program, it appears that a capability of using target heights up to 70 feet would provide the necessary versatility to keep coupling errors below the 1-db level, even in the case of relatively large targets and frequencies between 30 and 180 megahertz. When relatively small targets (< 10 feet) are considered, a capability of using target heights up to 30 feet appears to be sufficient to keep coupling errors below the 1-db level at frequencies between 30 and 180 megahertz.

The cross section data obtained by using frequencies of 30- and 60-megahertz and cylindrical type targets compared quite favorably with the scaled model data. When the known differences between the two sets of measurements were considered, the correlation between the full-scale and model data (except for background interference regions) was within 1.5 db. The differences between the two sets of measurements which appeared to influence the cross section were produced by the bistatic and tilt angles used to obtain the full scale data. These angles altered primarily the angular separation between null widths except for the end-on condition in the case of vertical polarization where significant cross section errors can occur because of tilt angle.

The cross section of the telescoping fiberglass target support used during the validation tests exhibited a sufficiently low cross section and/or the support was sufficiently stable to remain cancelled at the measurement frequency of 30 megahertz so that it could not be detected when it was rotated. Also, the cancelled background level was below the recorder lower limit of -25 dbsm at this frequency for the case of both polarizations. In the case of the 60-megahertz measurements, the target support system contributed to the observable background level in both polarizations as indicated in Figures 106 and 107. However, only in the case of horizontal polarization, when the effects of the target fiberglass saddle are quite evident near broadside, is there substantial evidence that the fiberglass target support system was being observed rather than the pit and rotator. In the case of 60-megahertz measurements, the cancelled background levels were in the range of -25 (horizontal polarization) to -15 dbsm (vertical polarization) during target support rotation. However, the fiberglass target support was telescoped during these measurements (and 30-megahertz vertical polarization measurement); consequently, the wall thickness was twice that obtained when the support was extended.

When the support was fully extended to a height of 65 feet, its load bearing capability was not taxed by target weights up to 800 pounds (i.e., the 42-foot cylinder measured during this program). However, this result was expected since the design capability of the fully extended support was 2000 pounds.

Background levels representative of those achieved during the induction field and validation tests are indicated in Table 4 for each of the frequencies of 30, 60, 120, and 180 megahertz and polarizations at which the measurements were made. These background levels represent the levels at which the system would remain cancelled over a period of time sufficient to allow measurements to be made. These time periods were noticeably a function of frequency and wind conditions, and in general, as the frequency increased, the time periods decreased. At 30 and 60 megahertz, the system would typically remain cancelled for several hours when the winds were less than 10 knots. The amount of cancellation maintained during these time periods was typically 40 to 50 db with the larger cancellation levels occurring at the lower frequencies. Consideration of the frequency stability of the generator used (1 part in 10^5), along with the difference in cancellation path length and the path length of the signal to be cancelled (300 to 700 feet), this amount of stable cancellation is all that should be expected in view of the frequency-induced phase drift. Except for the case of 120- and 180-megahertz vertical polarization, this amount of cancellation resulted in stable backgrounds better than -25 dbsm (neglecting changes produced by target support rotation). For these two cases, the loss of gain caused by the ground plane (15 to 20 db) and the inability to maintain more than 40 db of cancellation increased the background levels to the-10 to -15 dbsm region. On the basis of the results of the induction field and validation tests, along with the factors which limit the amount of cancellation that can be maintained at RAT SCAT, such as wind, frequency stability, soil parameter variations, and temperature effects on equipment, 40 db of cancellation should be considered as the expected operational cancellation capability by the use of a 1 part in 10^7 or better frequency source and a highly stabilized antenna cancellation system. However, with such a system, up to 60 db of cancellation could possibly be obtained for sufficient periods of time to allow the measurement of relatively small targets.

The amount of cancellation capability, along with the amount of achievable antenna isolation, determines the lower limit measurement capability of a cancelled system. Listed in Table 4 are the amounts of antenna isolation achieved with the antenna configurations used during the induction field and validation measurements. The amount of antenna isolation ranged between 50 and 70 db for the four frequencies and both polarizations. This amount of isolation was obtained by using spatial separations between 100 and 150 feet with and without the mobile target shelter between the antennas (Figure 79). At first, the mobile shelter was used to house one of the antennas, but the instability of the isolation was such that a sufficient amount of cancellation could not be maintained. In addition, the vertical field probe of the shelter-housed antenna was very distorted (Figure 95). A method of increasing the amount of antenna isolation has been investigated by using the results of the computer study. This technique is based on utilizing the ground plane effect by proper antenna spacing and height adjustment; however, physical demonstration of the technique has not been undertaken. Table 7 contains a list of the expected increases in isolation over free space isolation based on the computer results for frequencies of 30, 45, 60 and 90 megahertz and use of an antenna separation of 131 feet. The antenna heights of the transmitter and receiver are also noted. The data in Table 7 indicates a potential increase of 10 to 30 db, depending upon the frequency and polarization. Hence it is expected that, if use is made of a spatially separated antenna system whose height is adjustable, at least 60 to 80 db of antenna isolation can be achieved in the 30- to 180 megahertz region by using an antenna separation of no more than 150 feet and antenna heights of no more than 60 feet.

A number of considerations investigated in the computer study and noted during the validation measurement program indicated that a longer range would be desirable if feasible. The computer results indicated that rather ideal RF field conditions could be obtained in the 1000- to 2000-foot range region. Hence a range geometry was selected at a 1575-foot range for obtaining field probe data and path loss information. The data resulting from both of these measurement studies are presented in Figures 98 and 99 and Table 5.

The results of this investigation verified the accuracy of the fields predicted on the basis of the computer results. Also, the path loss information was used in conjunction with the computer results to estimate the lower bound measurement capability (Figures 100 and 101) at these longer ranges as a function of frequency. This estimate of capability was based on the use of a 200-watt transmitter and realistic values of antenna gain, receiver sensitivity, and line loss. The data in Figures 100 and 101 indicates that, if the full capability of the system can be realized, sensitivities between -50 and -40 dbsm can be obtained at a 1500-foot range for frequencies between 30 and 180 megahertz at both polarizations.

An investigation of the longer range geometry was made as a result of the feasibility indicated by the path loss information and initial computer results. The RF fields at 1050, 1575 and 2100 feet of range for antenna heights in the range which give optimum field conditions are presented in Figures 116 through 129. On the basis of the results presented in these figures, operation at a 1000-foot range enables the use of target heights between 20 and 50 feet in conjunction with an antenna height of 66 feet, or if a fixed target height of 50 feet is used, the 30- to 180-megahertz frequency region can be covered by using antenna heights between 33 and 66 feet. The amount of necessary variation in antenna height and/or target height to cover the frequency range of interest

Table 7 EXPECTED ISOLATION INCREASE VS FREQUENCY AND POLARIZATION

Frequency Megahertz	Transmit Antenna Height (Feet)		Receive Antenna Height (Feet)		Isolation Increase Over Free Space (db)	
	Vertical Polarization	Horizontal Polarization	Vertical Polarization	Horizontal Polarization	Vertical Polarization	Horizontal Polarization
30	33	49	33	49	12	22
45	49	33	49	49	10	28
60	35	33	49	35	10	32
90	33	49	33	49	10	24
Above 90	Very little limitation on heights or differences between horizontal and vertical.				>10	>25

decreases as the range is increased to 1575 feet; and on the basis of the data in Figure 126, at 2100 feet only one target height (65 feet) and one antenna height (50 feet) is needed to cover the 30- to 180-megahertz frequency. Even at the 1050 foot range, a 30-megahertz bandwidth can be covered by the use of a single antenna and target height for both polarizations. In the case of the 1575- and 2100-foot ranges, data on an 85 foot-antenna height is presented in Figures 125 and 129. On the basis of this information, the ability to achieve polarization versatility is lost as a result of the increased differences in the vertical field amplitude gradients between vertical and horizontal polarization. However, scattering matrix measurements would still be practical since the same target height and antenna heights could be used for both vertical and horizontal polarizations. Also the advantages gained in using an 85-foot antenna height rather than a 66-foot height are rather small in terms of decreased target height, and the surface field in comparison to the space field is less advantageous with the 85-foot antenna height than the 49- or 66-foot heights. Presented in Figures 117 through 127 are data at 20-percent soil moisture for each of the three longer ranges. On the basis of the data in these figures, the field changes are of the same order of magnitude as indicated in the data obtained under the field gradient versus soil moisture study (Figures 28 through 39) and hence present no major difficulties.

6.2.4 Other Range Design Considerations

In addition to the factors discussed in the preceding paragraphs, other considerations associated with a cross section range design should be examined. The major factors not discussed in the preceding paragraphs are (1) near-field errors caused by horizontal phase curvature ($2D^2/\lambda$ criteria) and (2) near-field errors caused by the radial field gradient. These factors are discussed below with respect to range, frequency, and target size.

6.2.4.1 Near-Field Errors Caused by Phase Curvature. Because of the relatively longer wave lengths involved, phase curvature in the VHF region is not a problem of the magnitude that it is at the higher frequencies, such as the 1- to 10-gigahertz region. However, if consideration is given to a short range, limitations on target size must be considered. In Figure 130, target size versus range is plotted for 30, 60, 120 and 180 megahertz. By inspection of Figure 130, it can be seen that 10-foot targets can be measured down to a range of 40 feet for frequencies up to 200 megahertz. Also, 50-foot targets can be measured down to a range of 1000 feet for frequencies up to 200 megahertz. Hence, in the case of relatively small targets (less than 10 feet), no horizontal phase gradient problems are encountered at any of the ranges considered in this program. In the case of relatively large targets (40 to 70 feet), ranges between 1000 and 2000 feet can be used.

6.2.4.2 Near-Field Error Caused by the Range Amplitude Gradient. The consideration of measurement errors caused by the amplitude gradient, which results from the 1/R field intensity decay, can provide a more severe restriction on the relationship of target size versus range than the phase curvature restrictions. However, the range gradient is not frequency dependent as it was in the former case. To relate target size and range, an error model is required. The chosen error model, which appears to be quite conservative, involves the consideration of the cross section dynamic range of two equal scatterers separated in range, that is, the ratio of the maximum return to the minimum return as a function of range and scatter separation. This ratio is expressed in Equation 6:

$$\gamma = 20 \text{ Log } \frac{1}{2} \left(\frac{1}{\alpha} + \alpha\right) \tag{6}$$

where

α = D/2R

D = Scatterer separation

R = Range to first scatterer plus D/2

In Figure 131a, Equation 6 is plotted in terms of values between 1/8 and 1/256. In Figure 131b, target size versus range are presented in terms of values of α representing 20-, 30-, and 40-db nulls. If it is assumed, for example, that a minimum of 30-db nulls are desired in measuring the cross section of two equal scatters separated a distance of 10 feet, the data in Figure 131b indicates that a range greater than 320 feet is necessary. If the null depth criterion is relaxed to 25 db, the range can be decreased to 160 feet. In the case of larger targets (40 to 70 feet), the criteria used above indicate range operation in the 1000- to 2000-foot range.

6.2.5 Study and Measurement Program Summary

The results obtained from the individual study and measurement program indicate that cross section measurements at RAT SCAT are feasible in the 30- to 180-megahertz region by using a cancelled system and operating in the 200- to 400-foot range region. Operation in this region would allow measurement of relatively small targets (less than 10 to 12 feet) which could be measured by the use of target heights in the 10- to 30-foot region and adjustment of antenna and target height as a function of frequency and polarization. The effects of field ellipticity, the bistatic angle, and the tilt angle would be quite small if the above mentioned target dimension were not exceeded. The background levels achievable in this range region by use of a cancelled system would be in the region of -20 to -60 dbsm, depending, of course, on polarization, frequency, range, and climatic conditions. For example, in the 30 to 100 megahertz region at a 300 foot range -30 to -50 dbsm background levels appear quite feasible using a 20 to 30 foot target support.

In addition to the validation of the shorter range cancelled system technique, investigations and measurements obtained during the first phase of the VHF program indicate the feasibility of operation at a longer range (1000 to 2000 feet) by using antenna heights in the 30- to 70-foot region and target heights in the 30- to 65-foot region. The primary advantages of such a range are (1) small tilt and bistatic angles can be used, (2) horizontal and vertical polarization measurements can be made at the same antenna and target height, (3) a relatively large frequency range can be covered without having to change antenna or target height, (4) targets up to 70 feet in length can be measured and still satisfy near-field criteria, (5) a capability of polarization versatility is provided, and (6) measurement sensitivities in the region of -60 to -20 dbsm are possible if a range-gated system can be utilized (no recovery time limitations). In this longer range design, the same electronic system can be used as that used in the shorter range design if a pulse width capability down to .5 microsecond (250 feet) is provided (assuming the system will recover in 4 times the pulsewidth which would allow operation at 1000 feet). This system could still be operated with a bandwidth system of approximately 2 megahertz so that significant RFI problems could be reduced.

REFERENCES

1. Operating Instructions for Type 1702-A Admittance Meter, General Radio Company, March 1963.

2. Norton, K. A., The Propagation of Radio Waves Over the Surface of the Earth and in the Upper Atmosphere, Part II, Proceedings of the Institute of Radio Engineers, Volume 25, Number 9, September 1937

3. Kerr, D. E., Propagation of Short Radio Waves, Radiation Laboratory Series, Volume 13, McGraw-Hill, Inc., 1951

4. Jordan, E. C., Electromagnetic Waves and Radiating Systems, Prentice-Hall, Inc., New York, May 1955

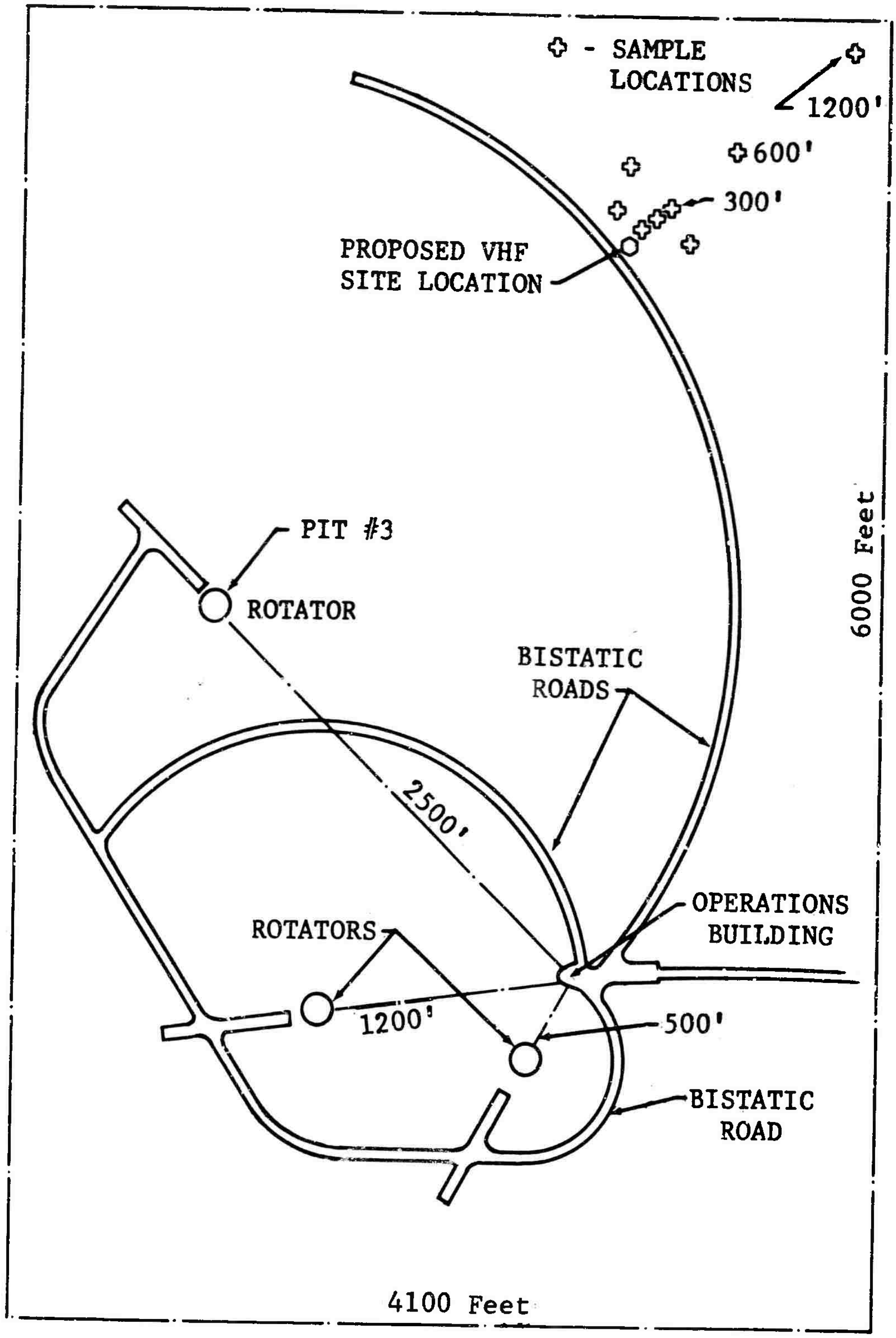

Fig. 1 RAT SCAT RANGE SOIL SAMPLE LOCATIONS

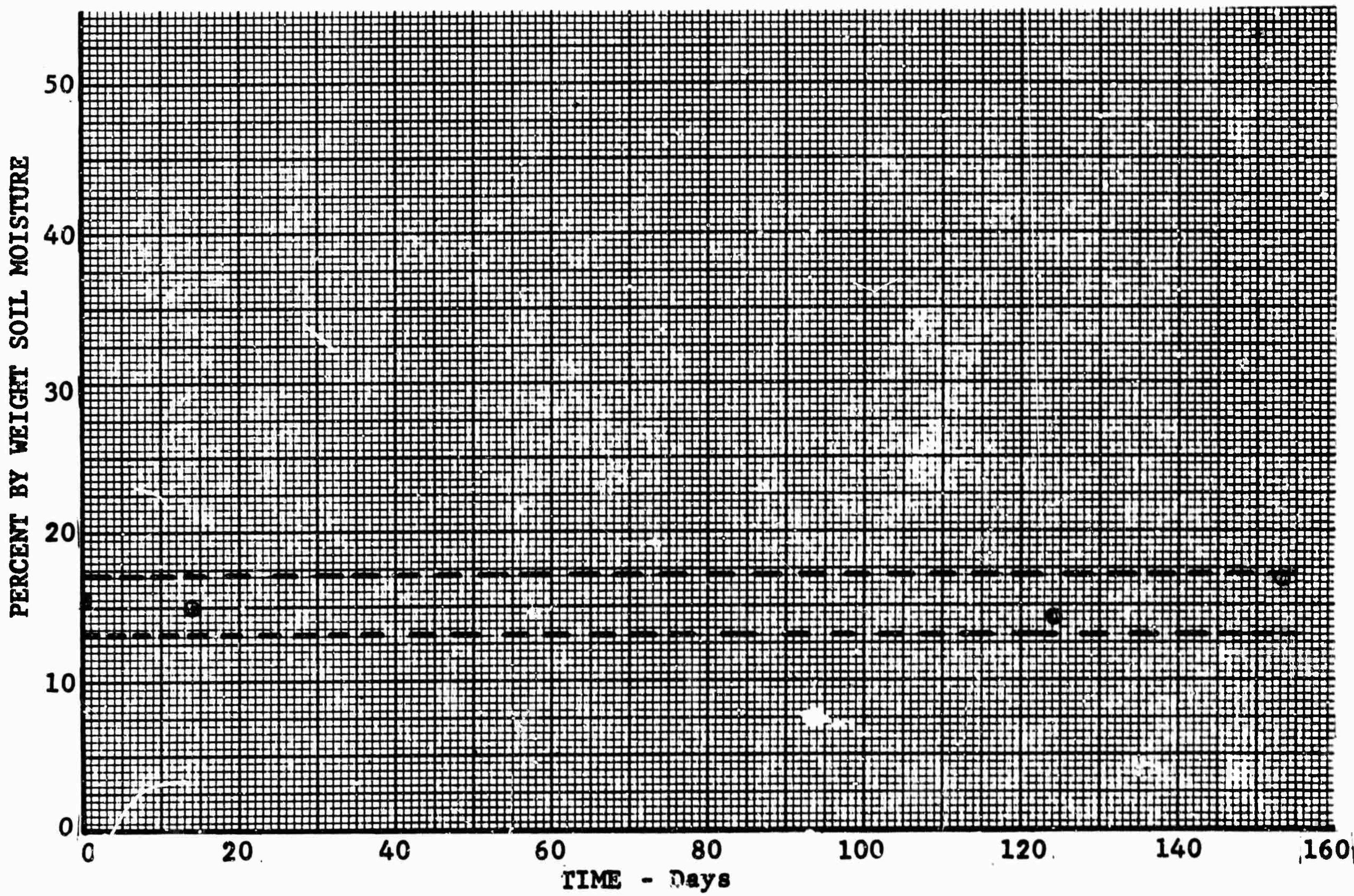

Fig. 2 NORMAL RAT SCAT SOIL MOISTURE VERSUS TIME

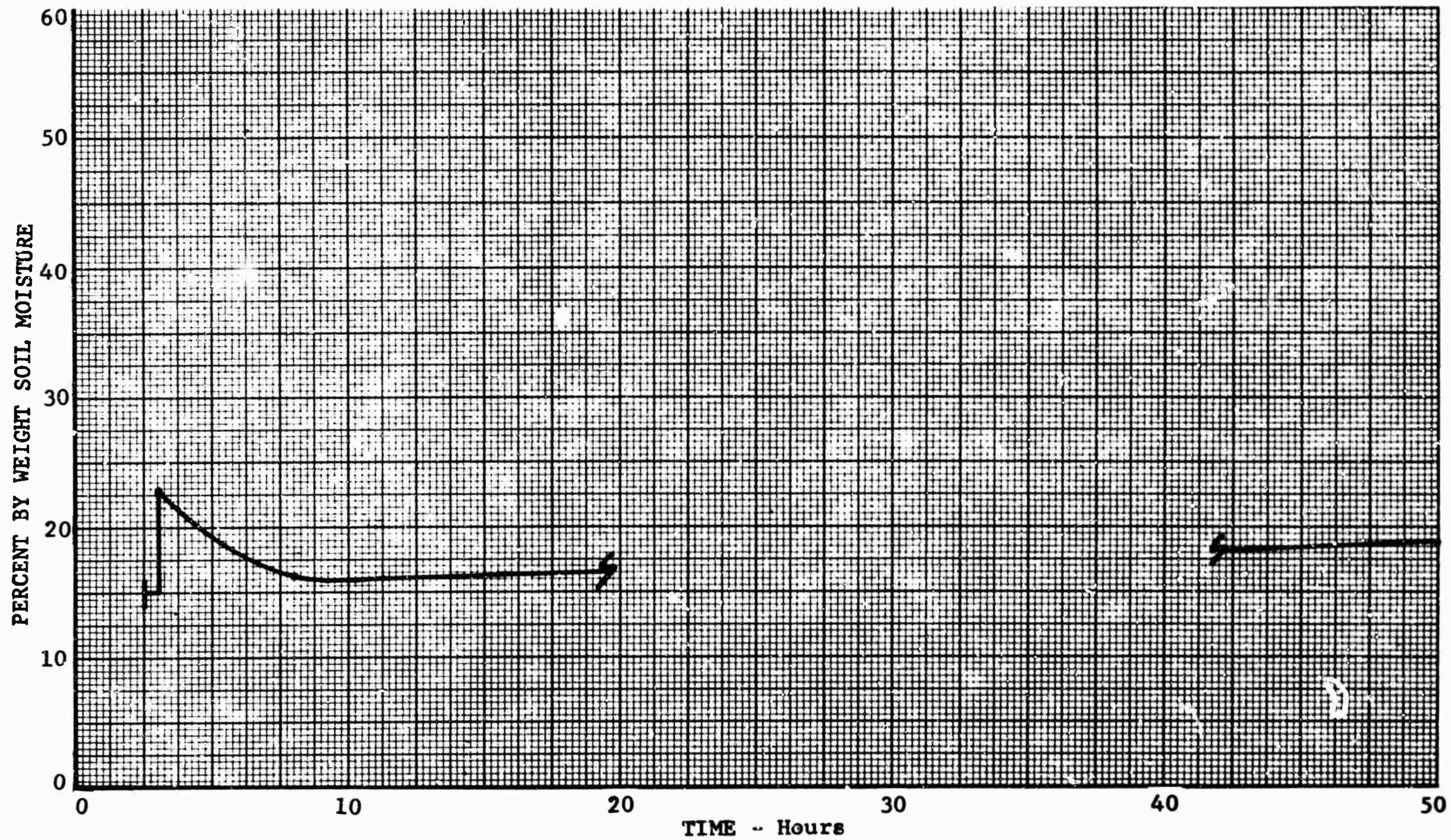

Fig. 3 TIME RATE OF DECREASE OF MOISTURE CONTENT FOLLOWING RAINFALL

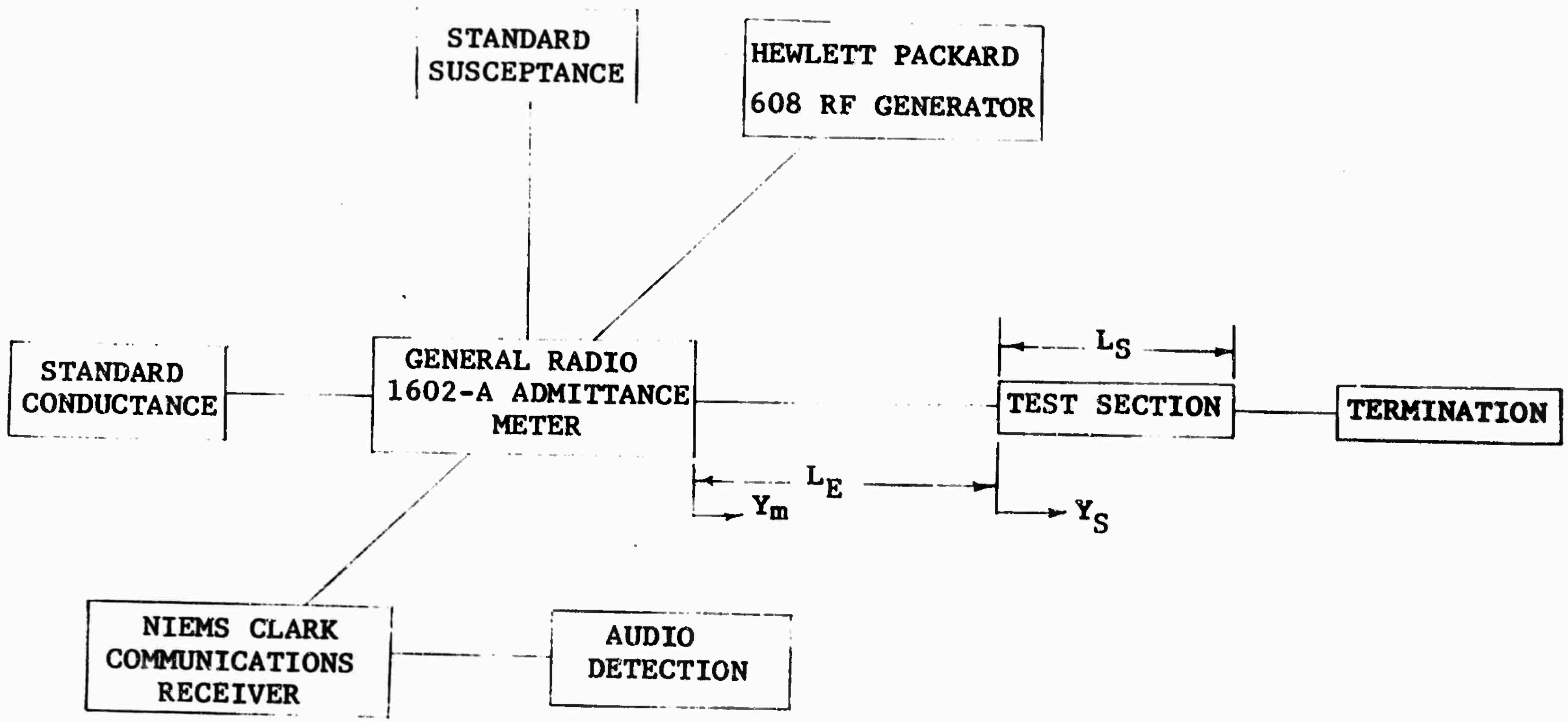

Fig. 4 SOIL MEASUREMENT TEST SYSTEM

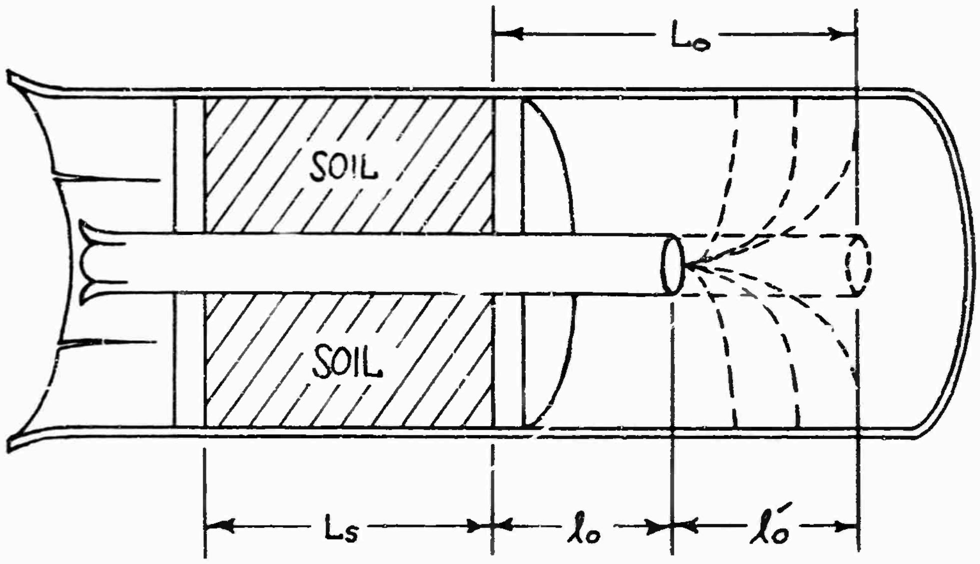

L_s = length of test section

l_o = length of remaining air filled guide and dielectric bead

l_o' = effective length necessary to describe imperfect open-circuit

Fig. 5 LENGTH RELATIONSHIPS FOR SHORT TEST SECTIONS

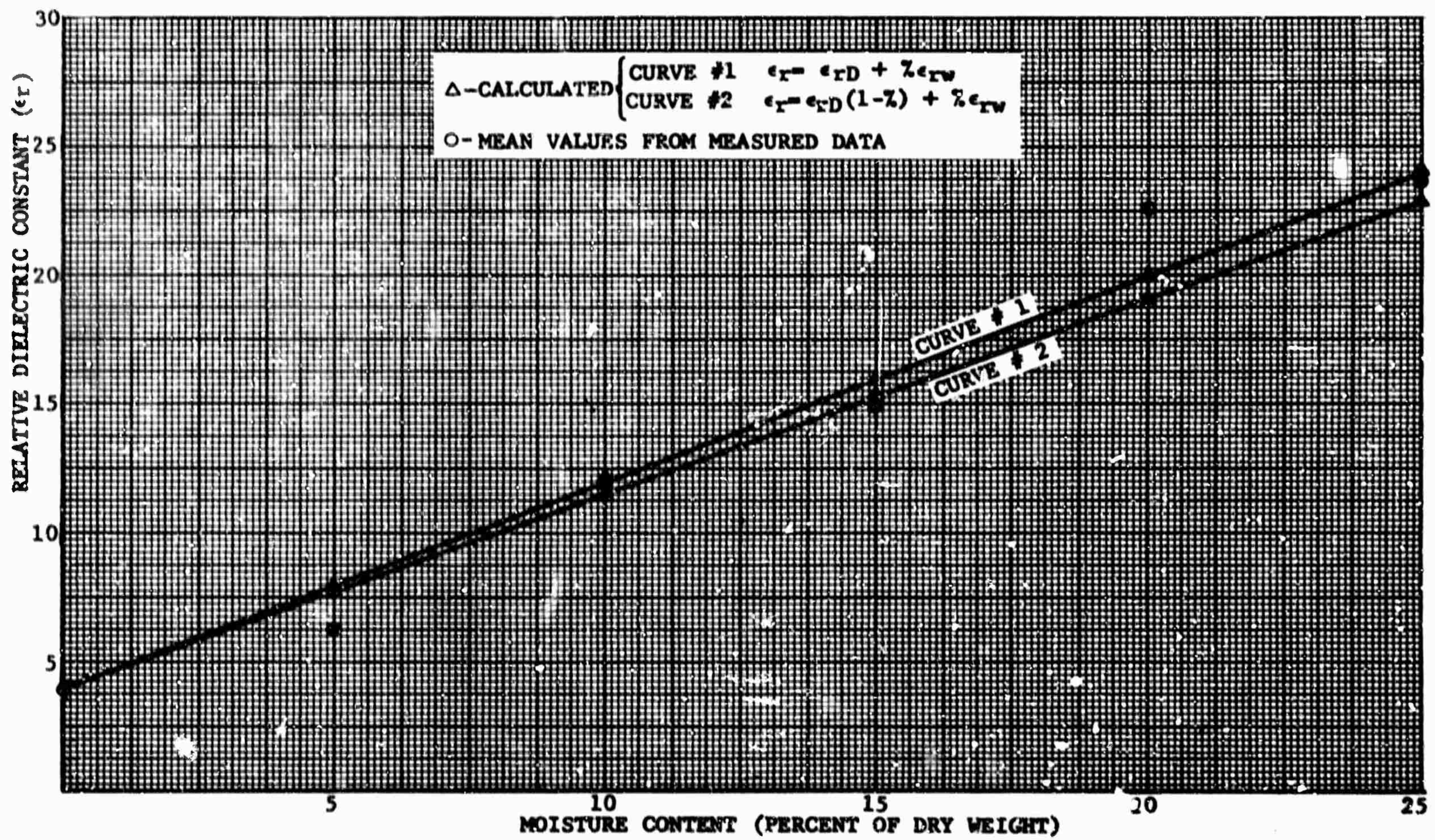

Fig. 6 DIELECTRIC CONSTANT

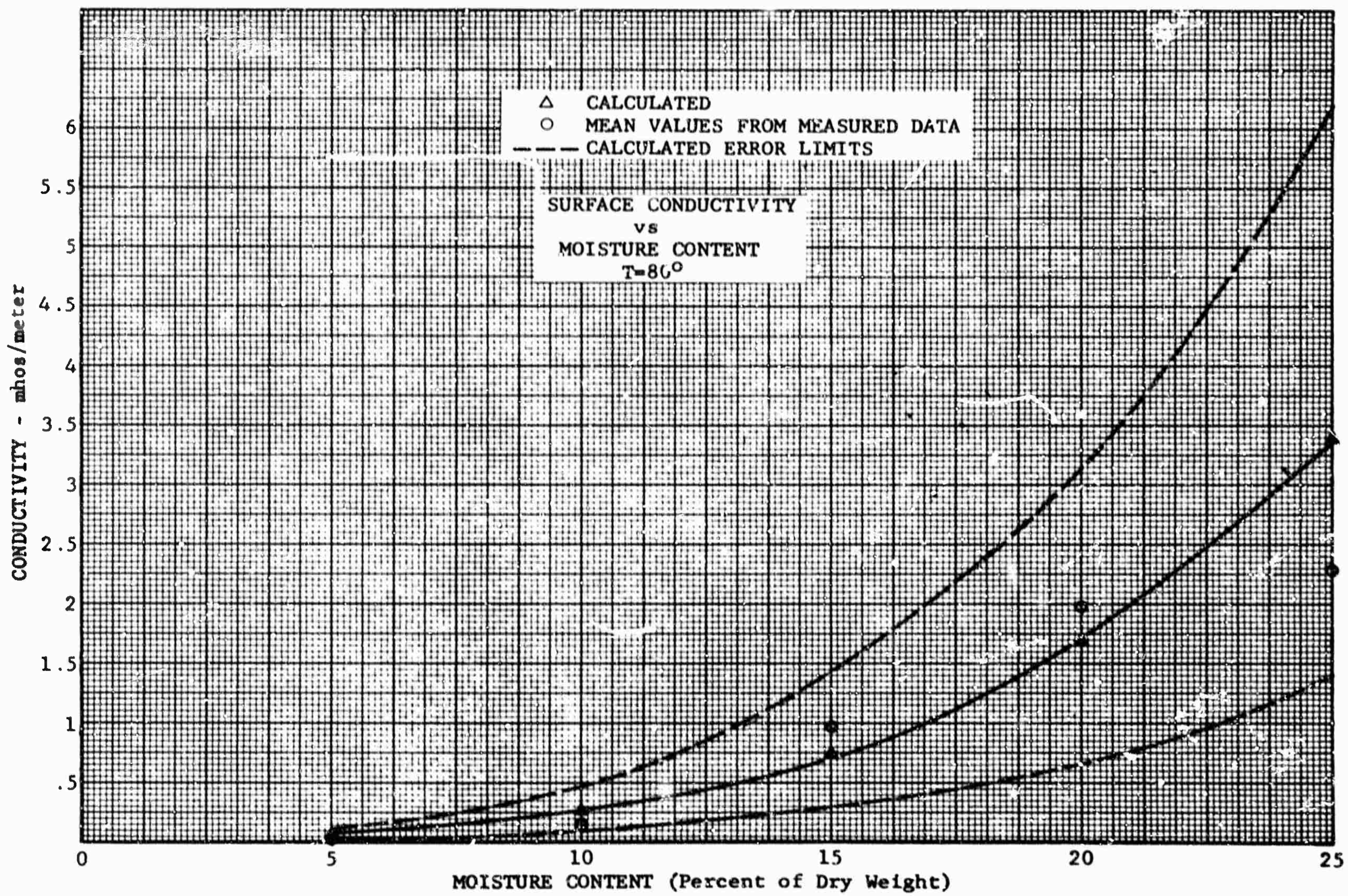

Fig. 7 CONDUCTIVITY OF SURFACE SOIL (T = 80°F)

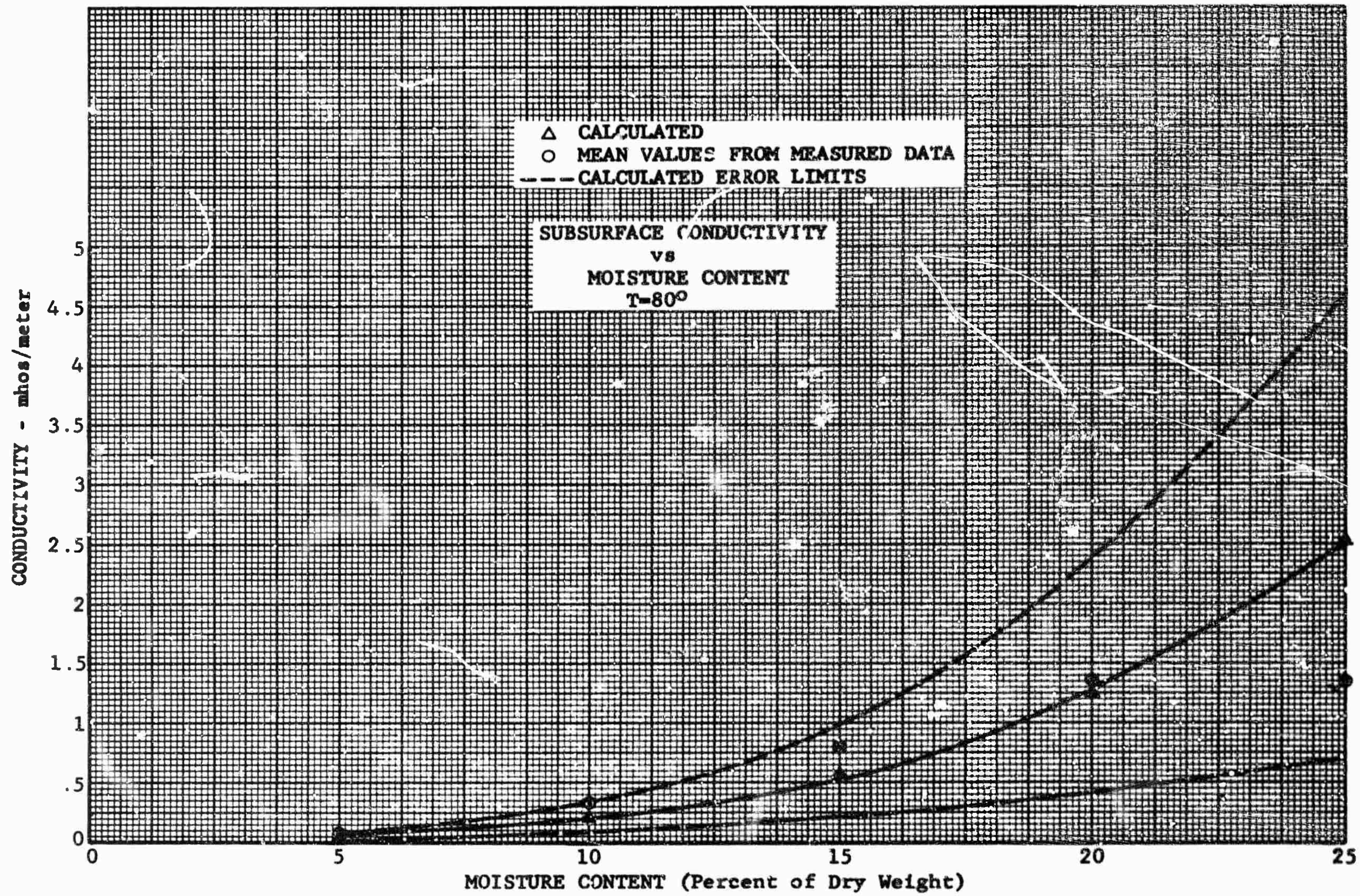

Fig. 8 CONDUCTIVITY OF SUBSURFACE SOIL (T = 80°F)

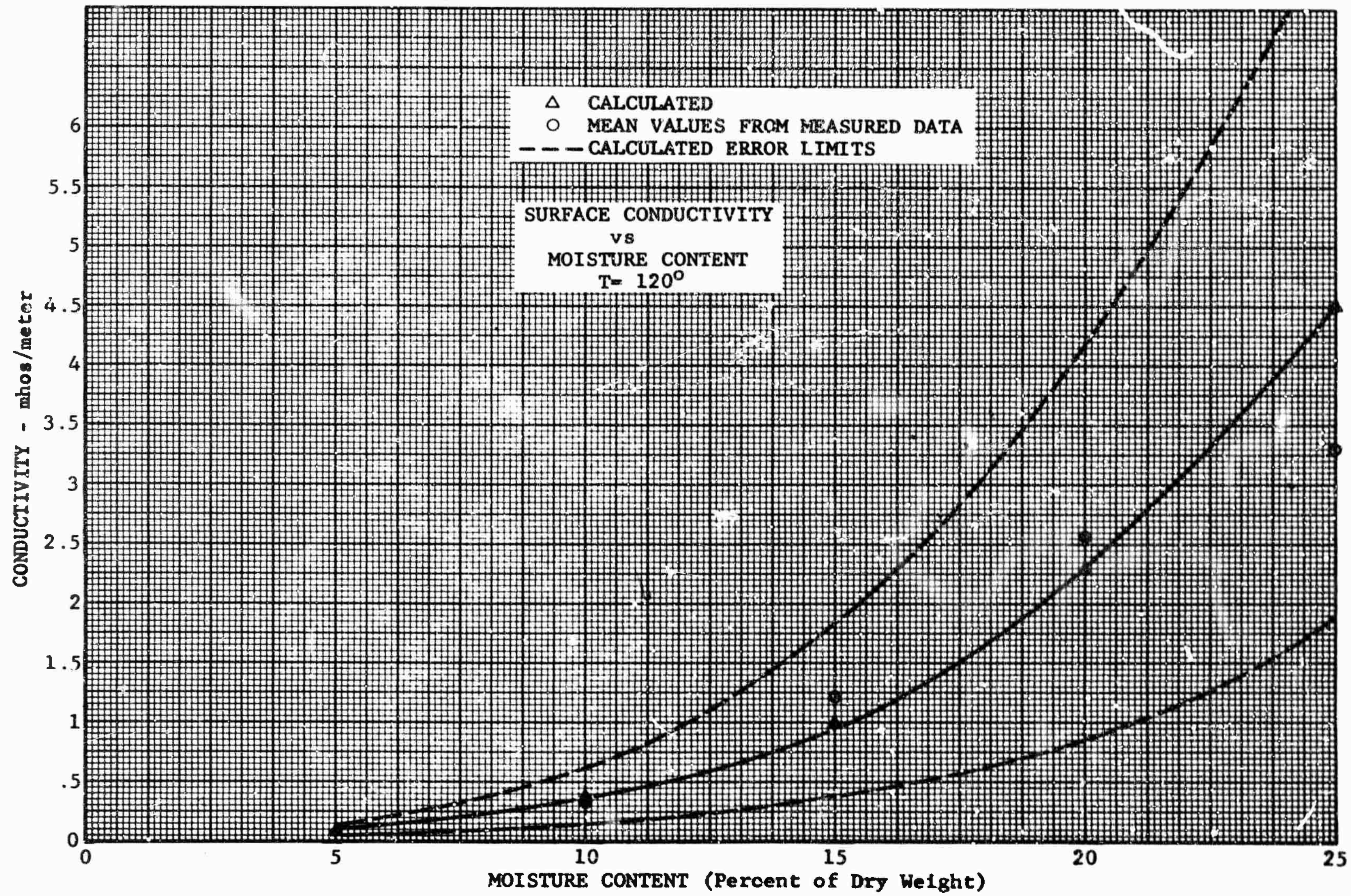

Fig. 9 CONDUCTIVITY OF SURFACE SOIL (T = 120°F)

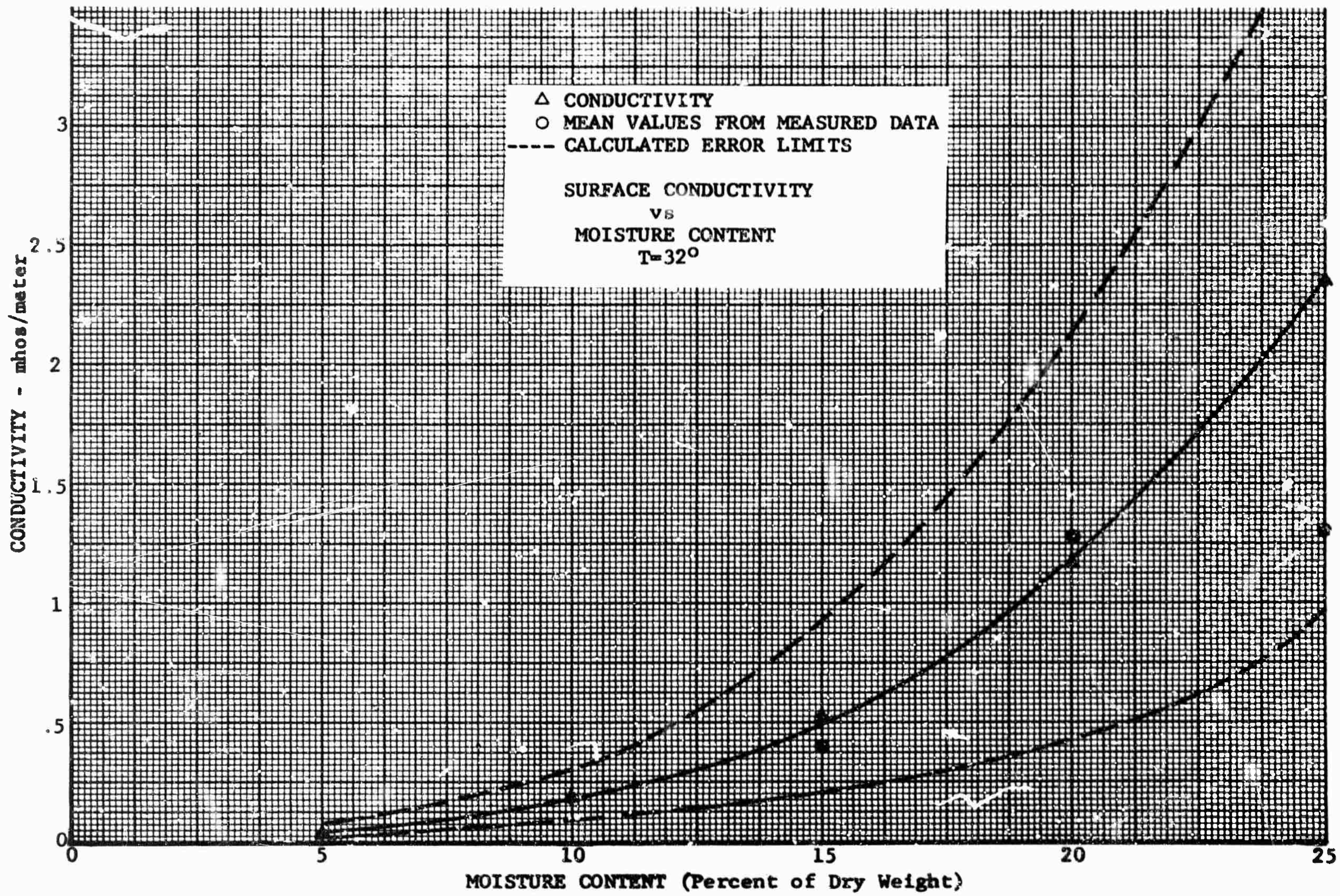

Fig. 10 CONDUCTIVITY OF SURFACE SOIL (T = 32°F)

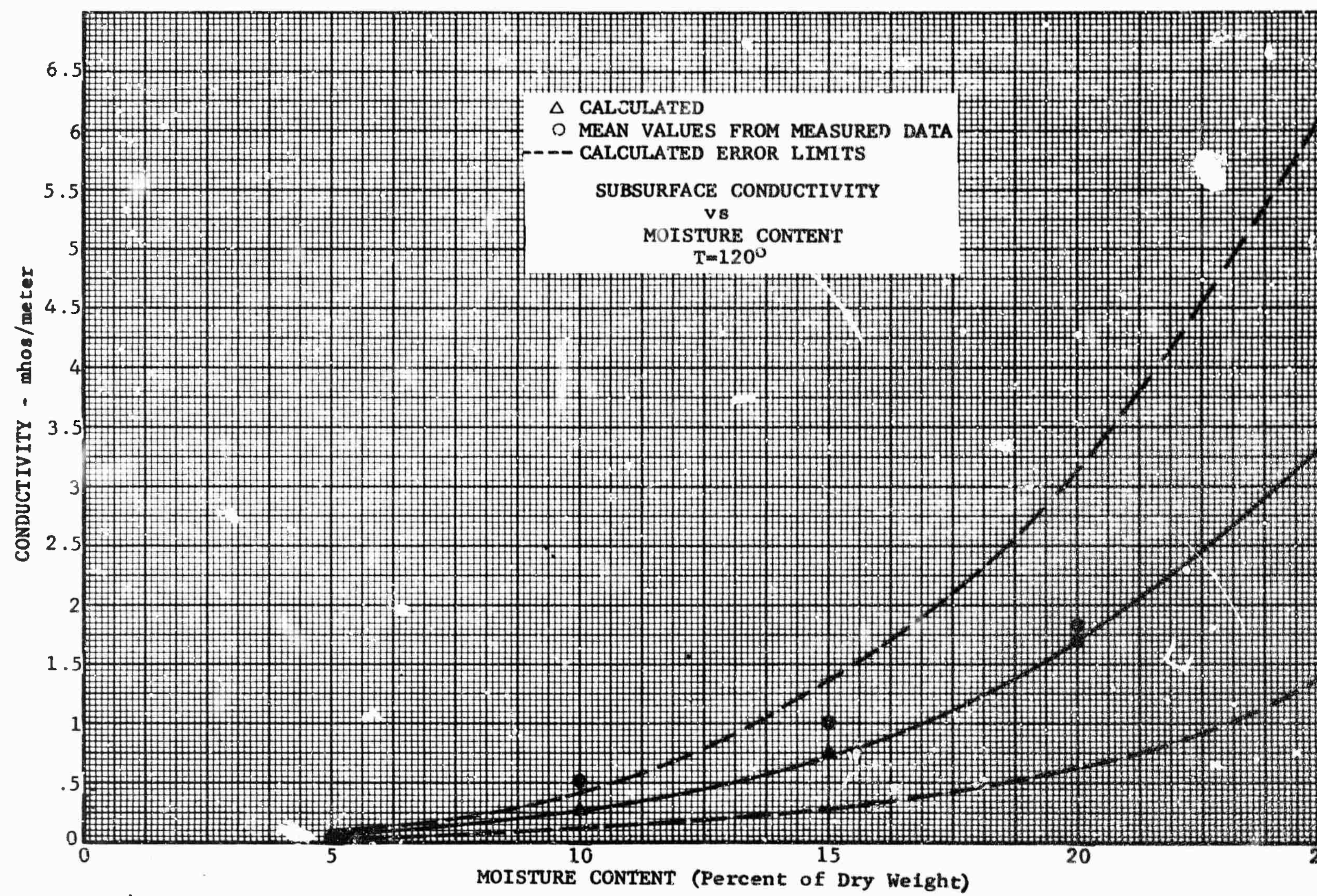

Fig. 11 CONDUCTIVITY OF SUBSURFACE SOIL (T = 120°F)

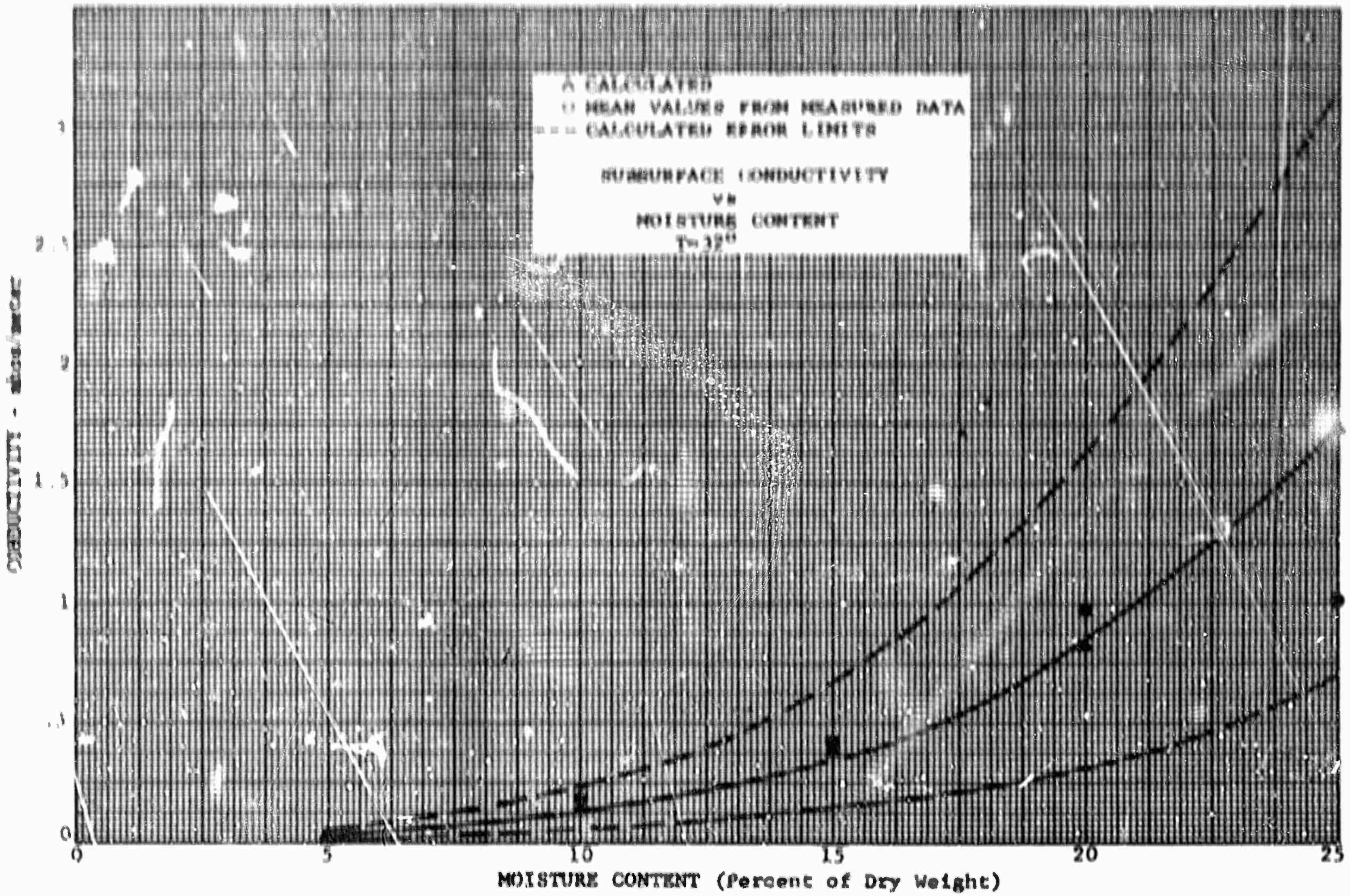

Fig. 12 CONDUCTIVITY OF SUBSURFACE SOIL (T - 32°F)

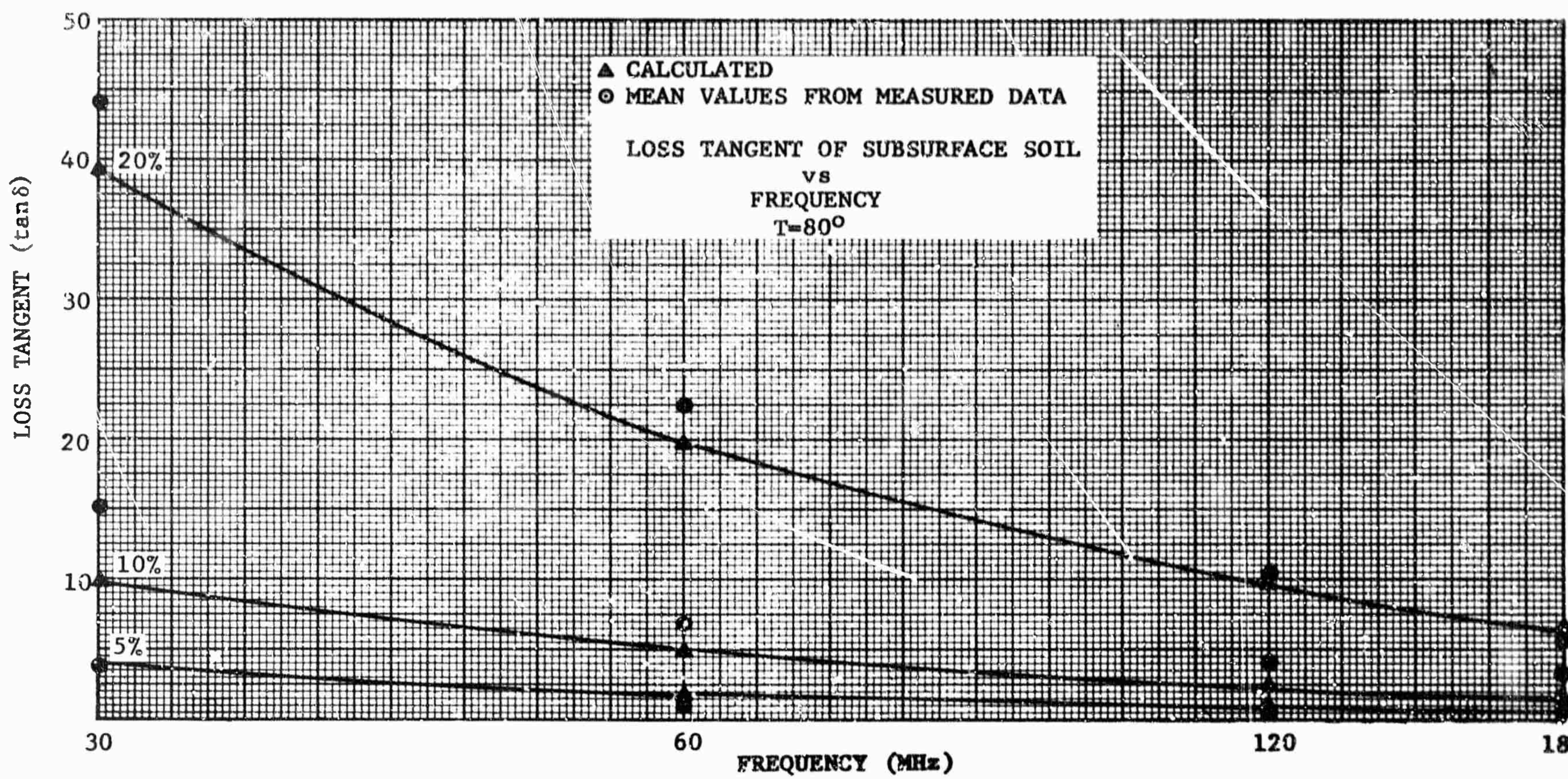

Fig. 13 LOSS TANGENT OF SUBSURFACE SOIL (T = 80°F) 5, 10, AND 20 PERCENT

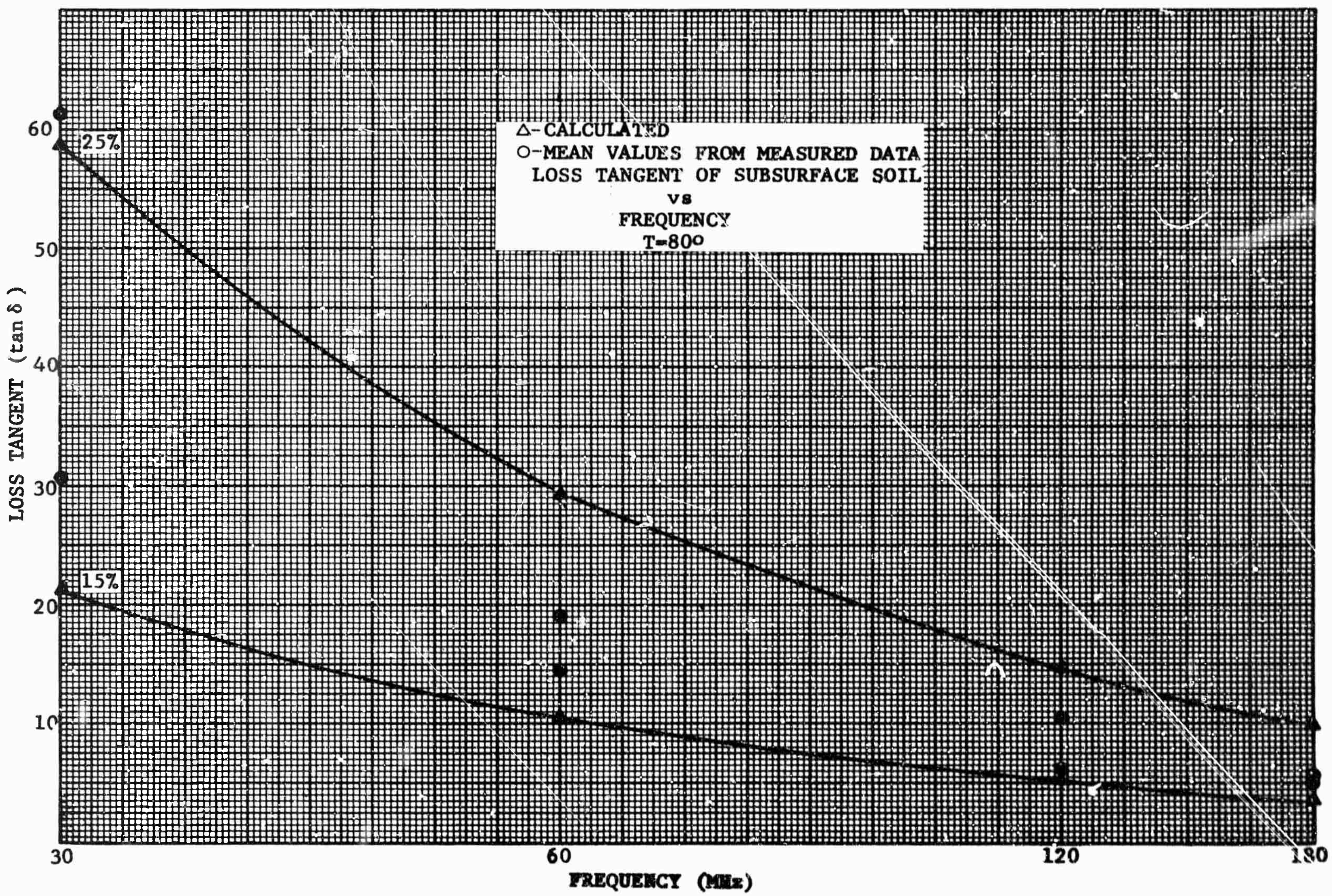

Fig. 14 LOSS TANGENT OF SUBSURFACE SOIL (T = 80°F) 15 AND 25 PERCENT

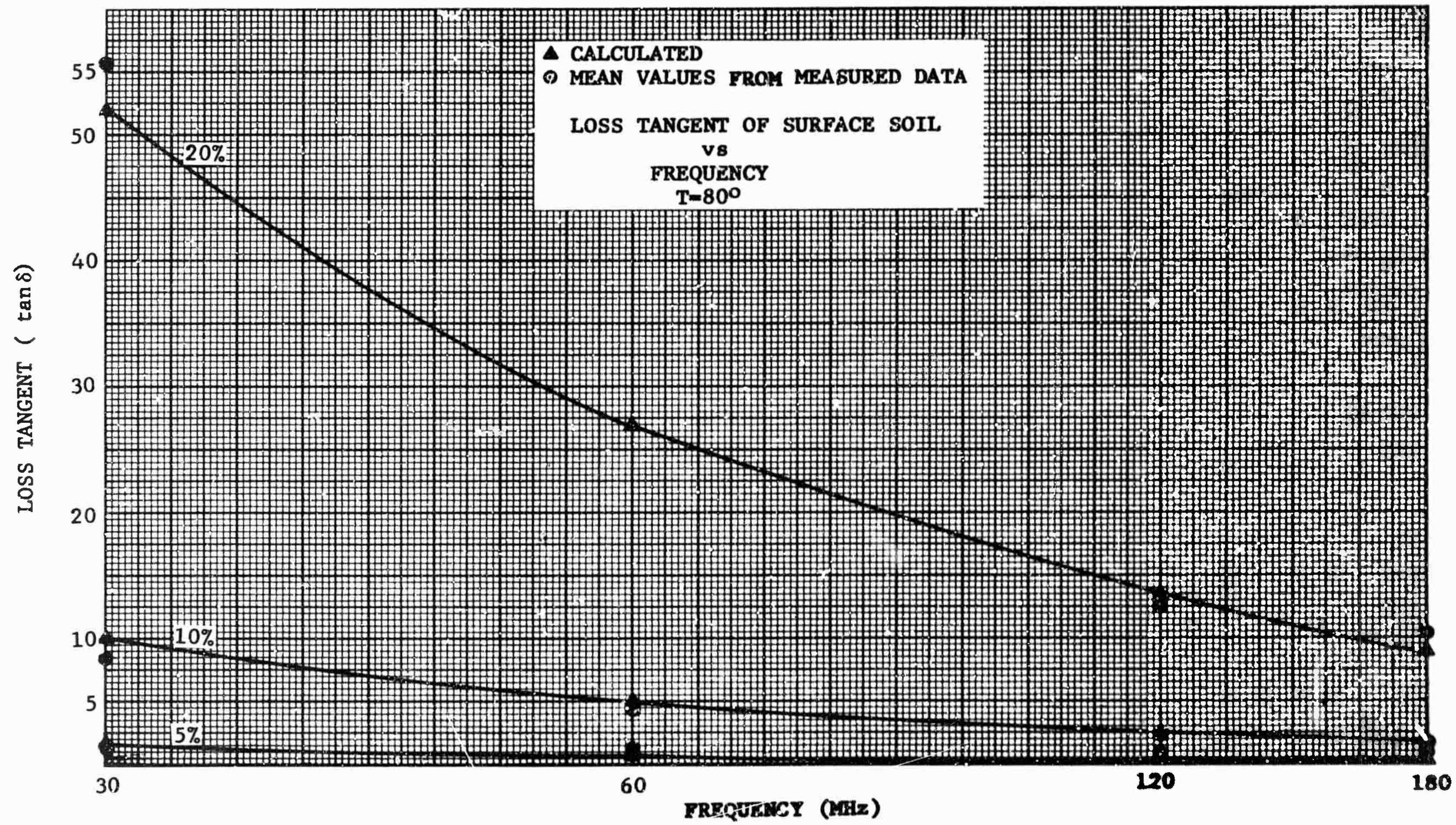

Fig. 15 LOSS TANGENT OF SURFACE SOIL (T = 80°F) 5, 10, AND 20 PERCENT

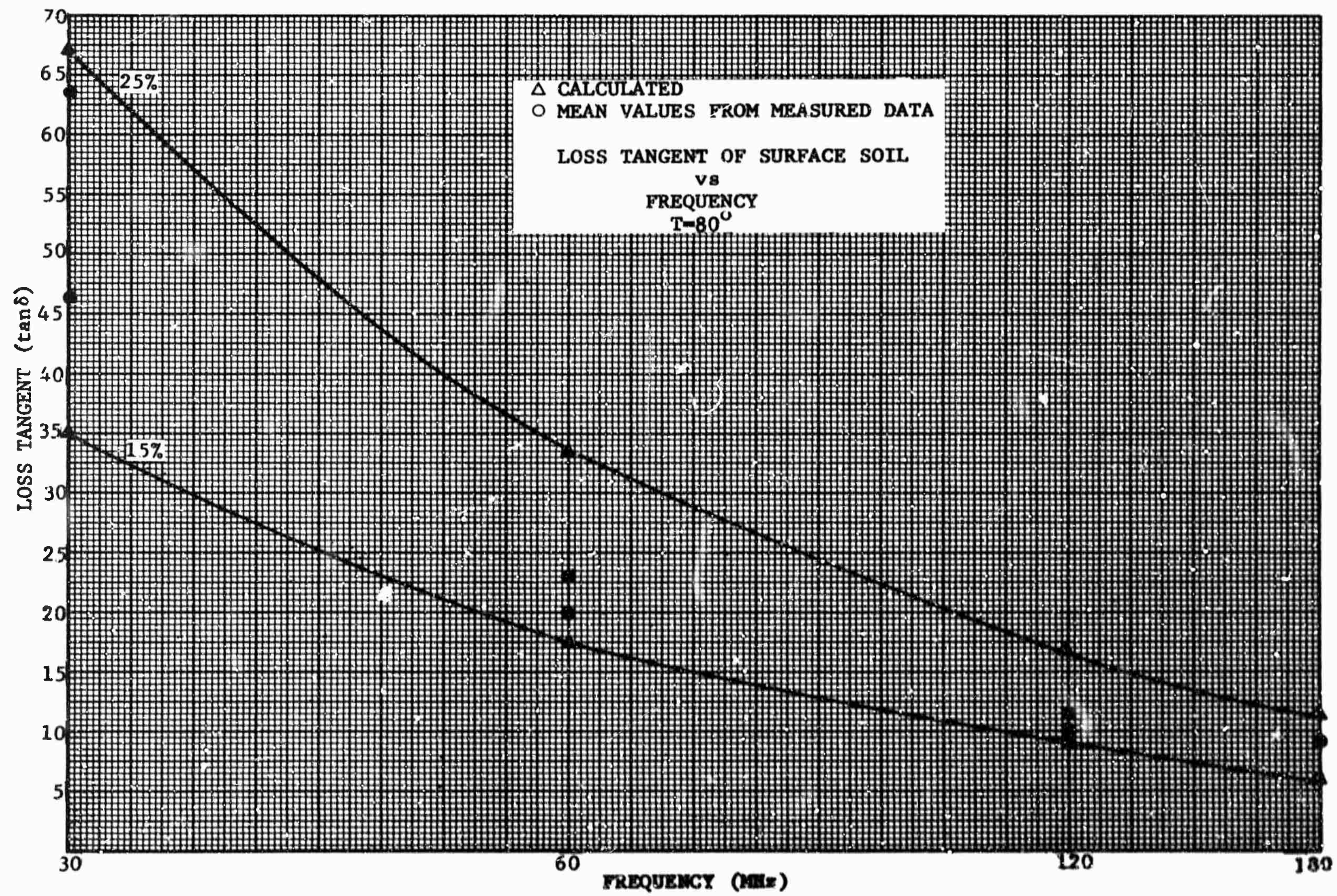

Fig. 16 LOSS TANGENT OF SURFACE SOIL (T = 80°F) 15 AND 25 PERCENT

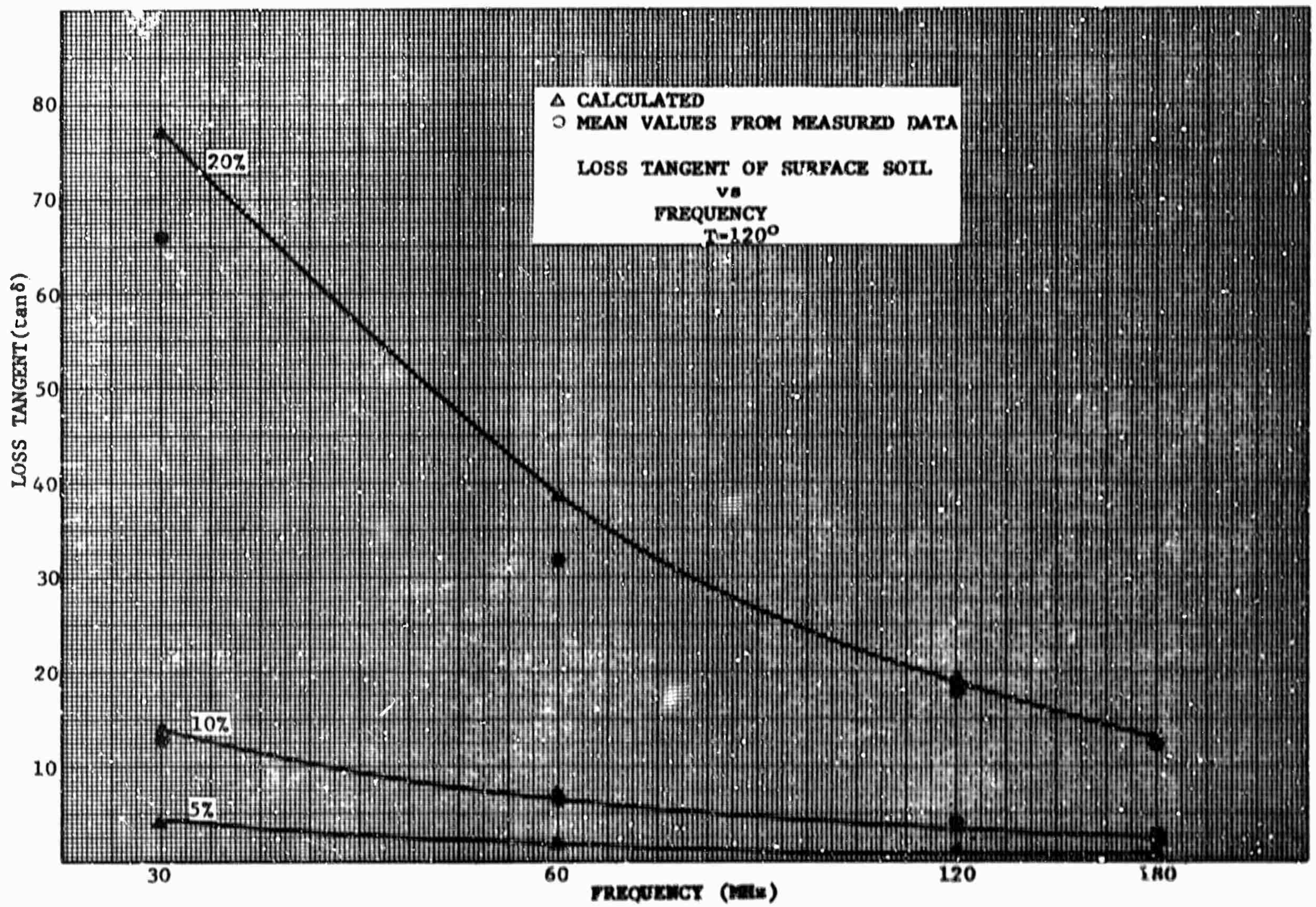

Fig. 17 LOSS TANGENT OF SURFACE SOIL (T = 120°F) 5, 10, AND 20 PERCENT

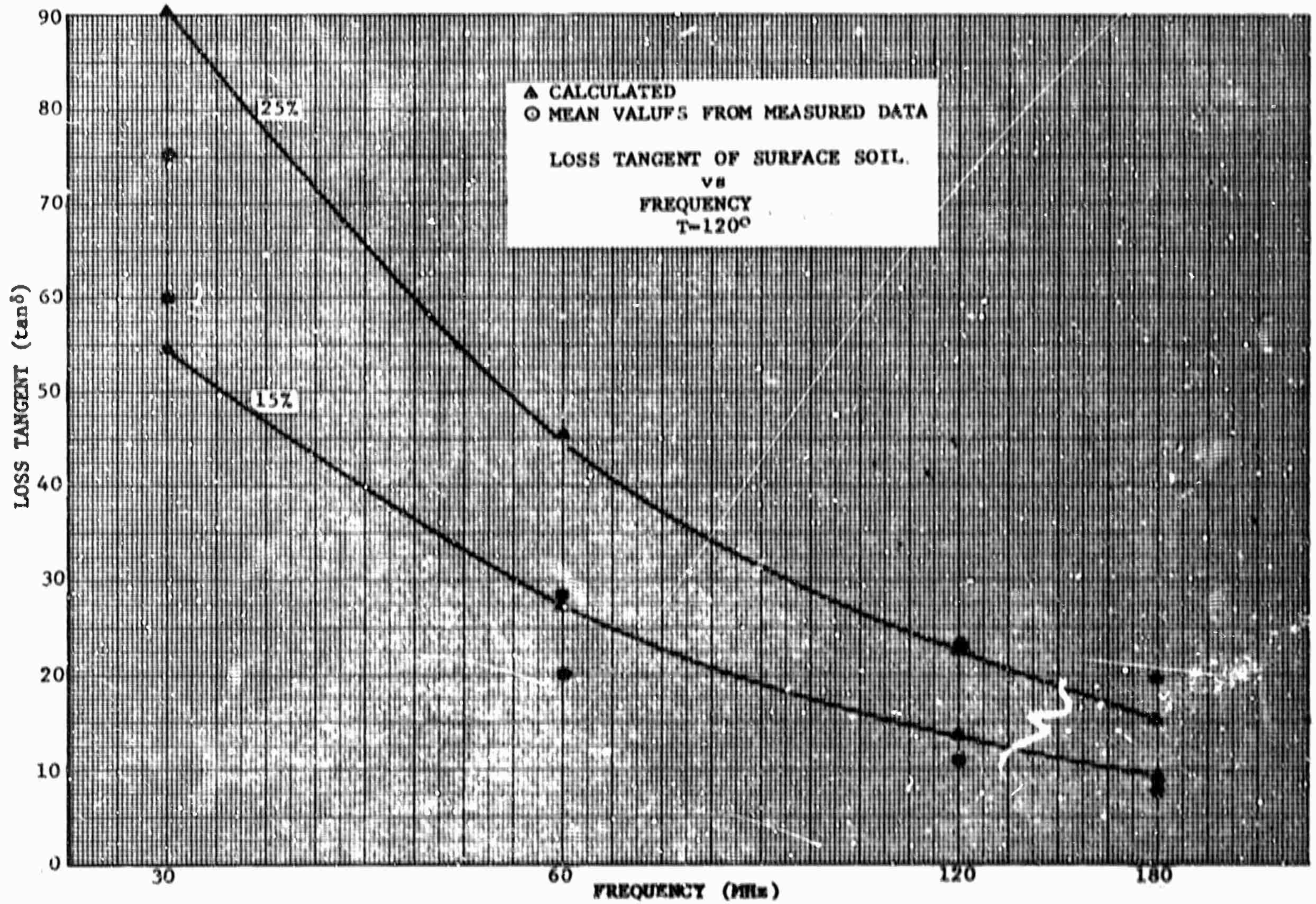

Fig. 18 LOSS TANGENT OF SURFACE SOIL (T - 120°F) 15 AND 25 PERCENT

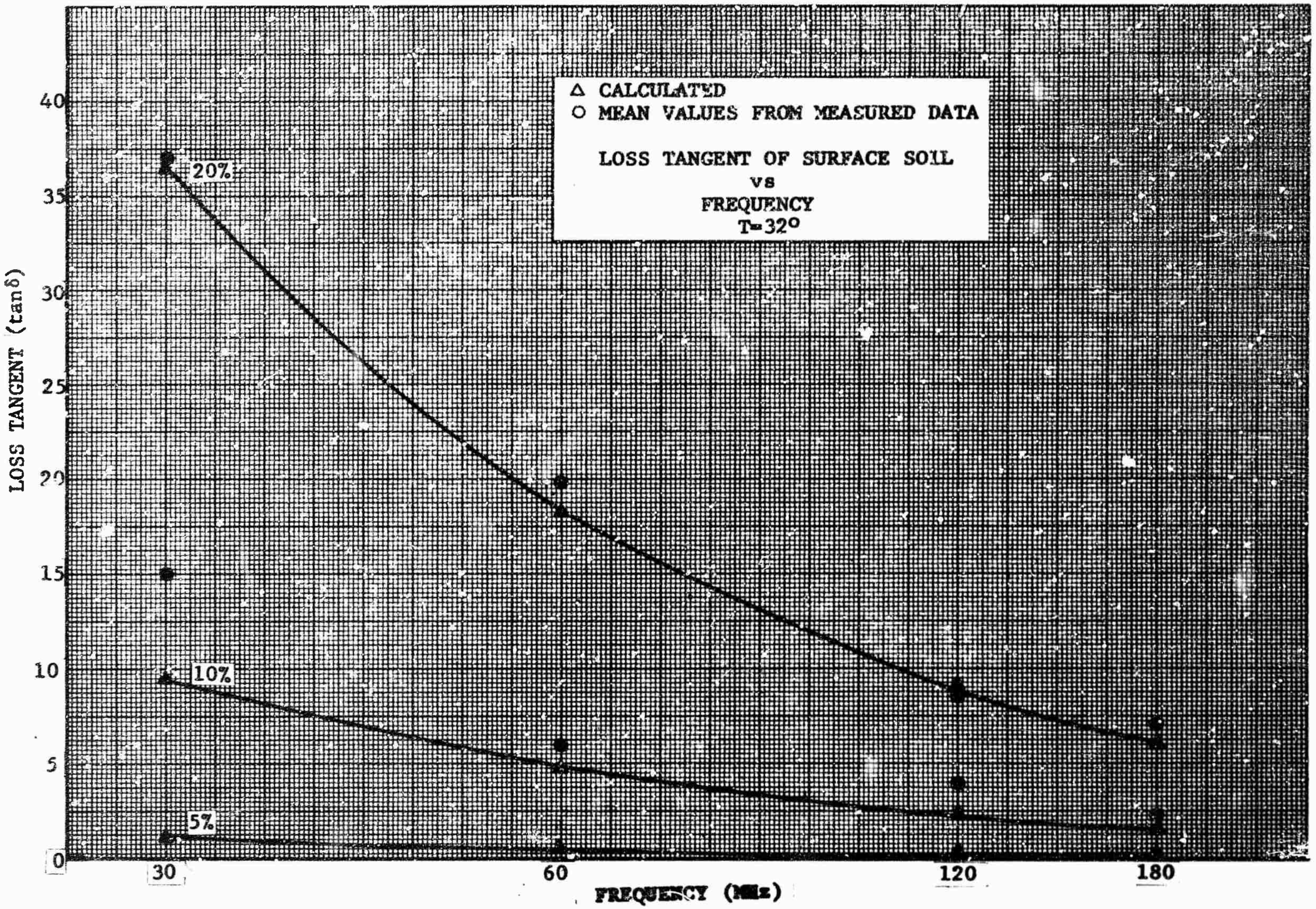

Fig. 19 LOSS TANGENT OF SURFACE SOIL (T = 32°F) 5, 10, AND 20 PERCENT

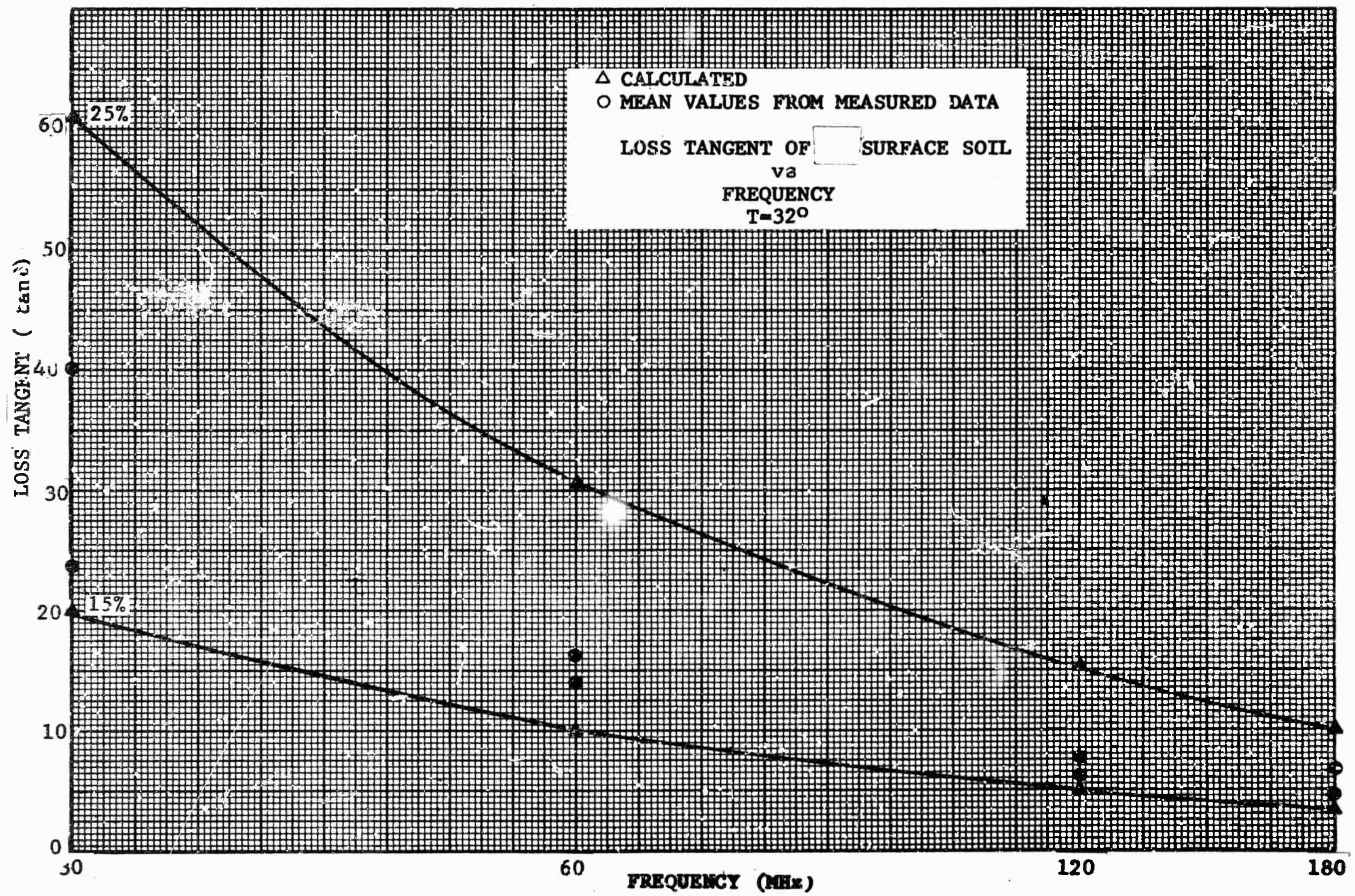

Fig. 20 LOSS TANGENT OF SURFACE SOIL (T = 32°F) 15 AND 25 PERCENT

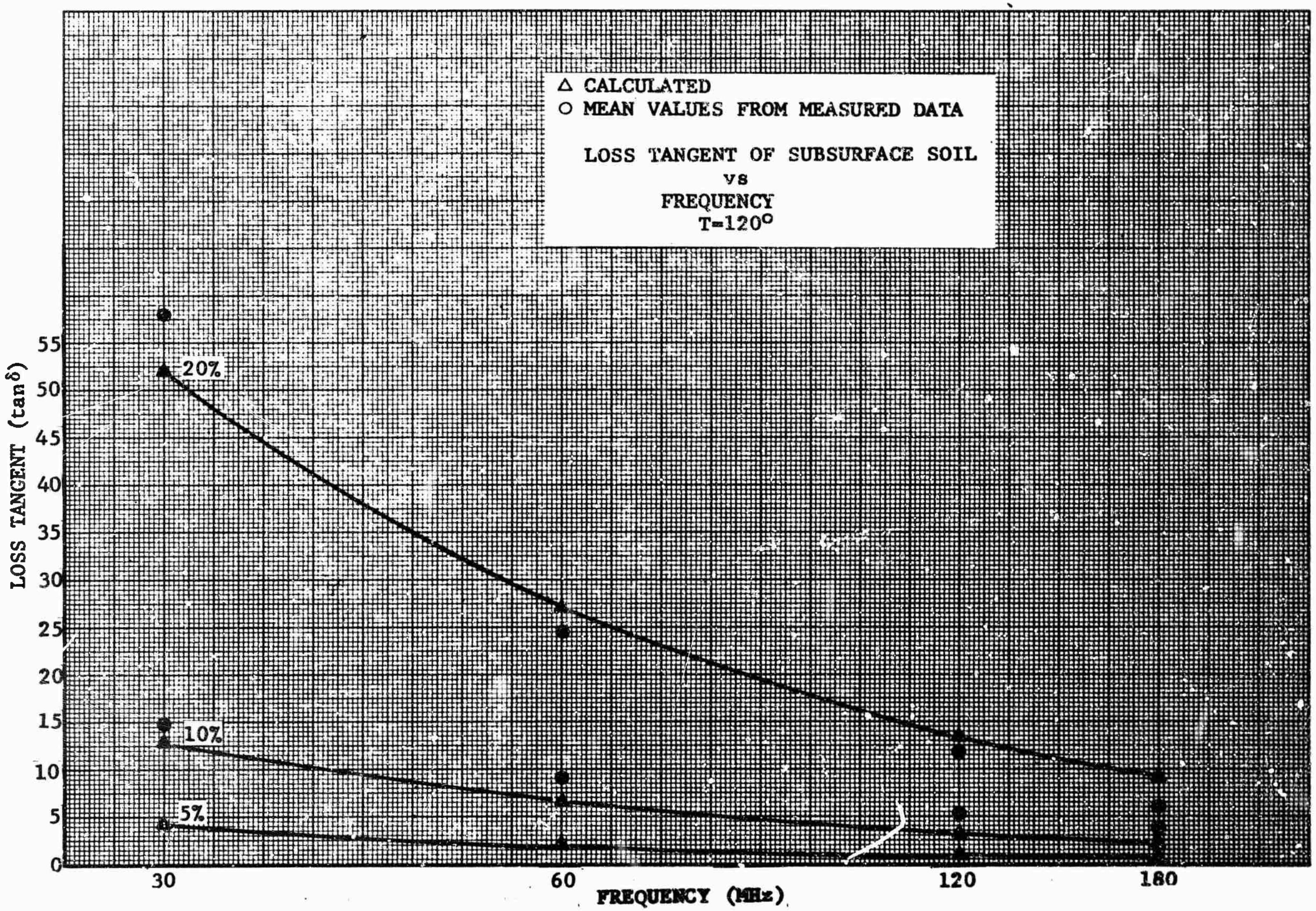

Fig. 21 LOSS TANGENT OF SURSURFACE SOIL (T = 120°F) 5, 10, AND 20 PERCENT

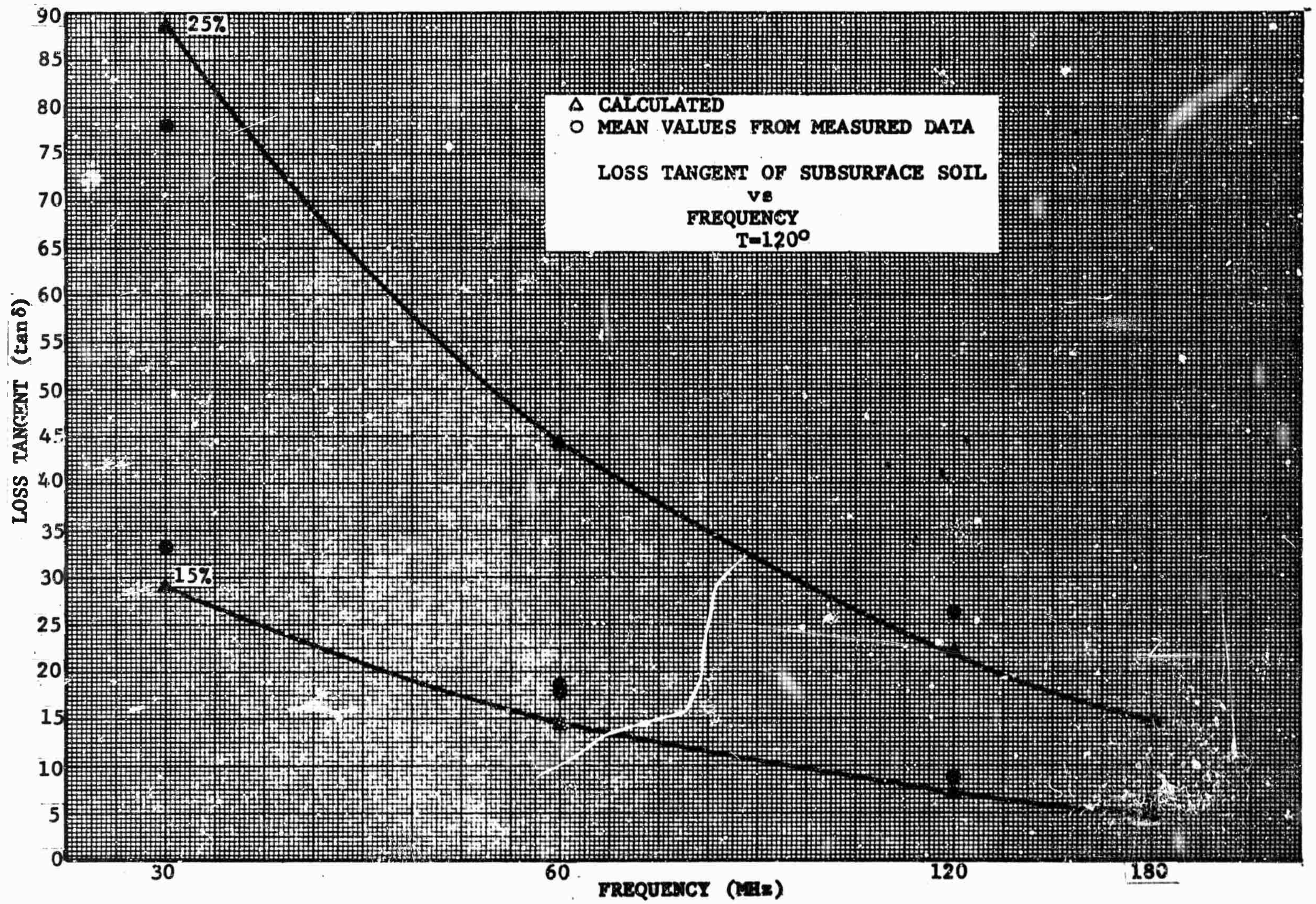

Fig. 22 LOSS TANGENT OF SUBSURFACE SOIL (T = 120°F) 15 AND 25 PERCENT

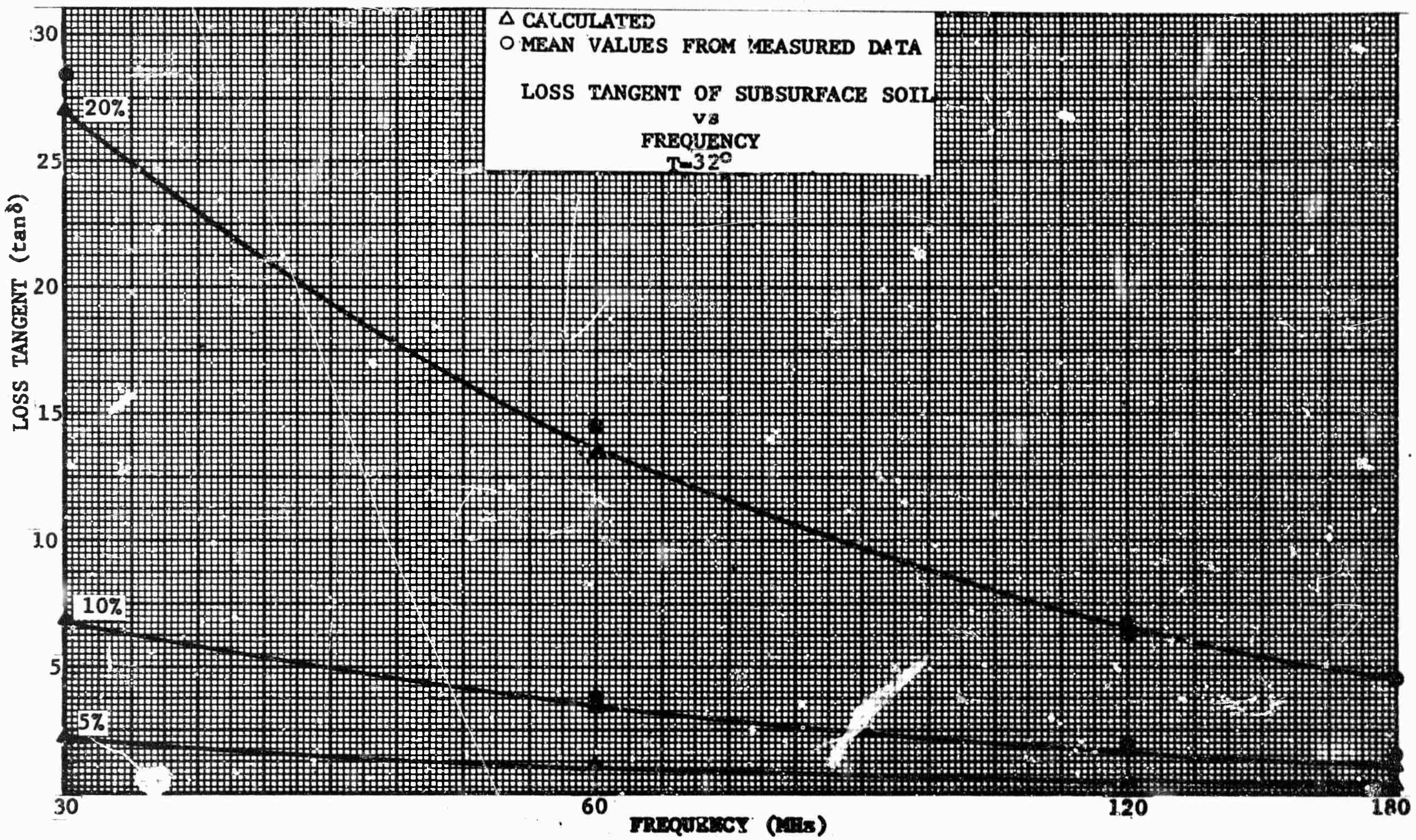

Fig. 23 LOSS TANGENT OF SUBSURFACE SOIL (T = 32°F) 5, 10, AND 20 PERCENT

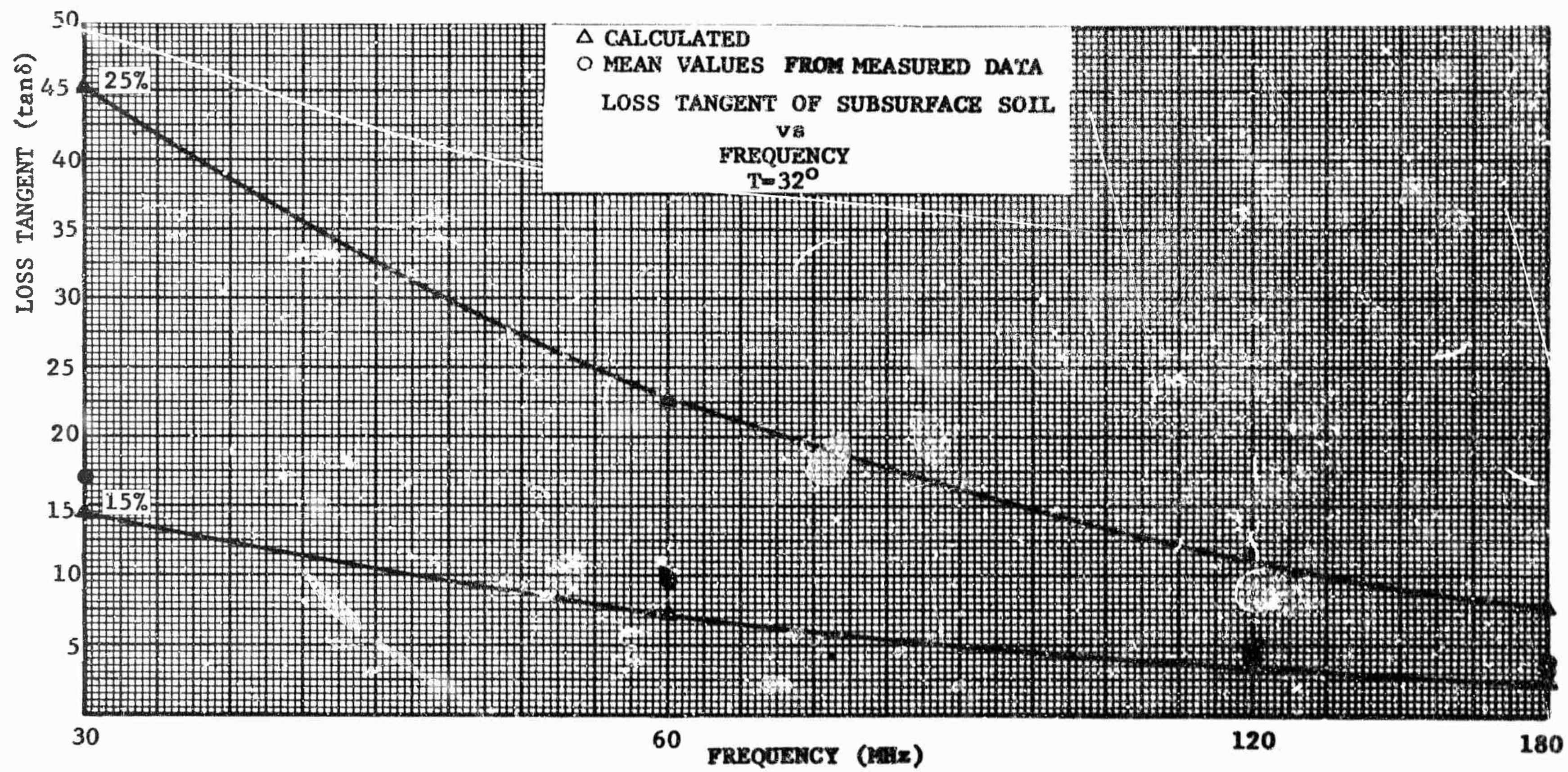

Fig. 24 LOSS TANGENT OF SUBSURFACE SOIL (T = 32°F) 15 AND 25 PERCENT

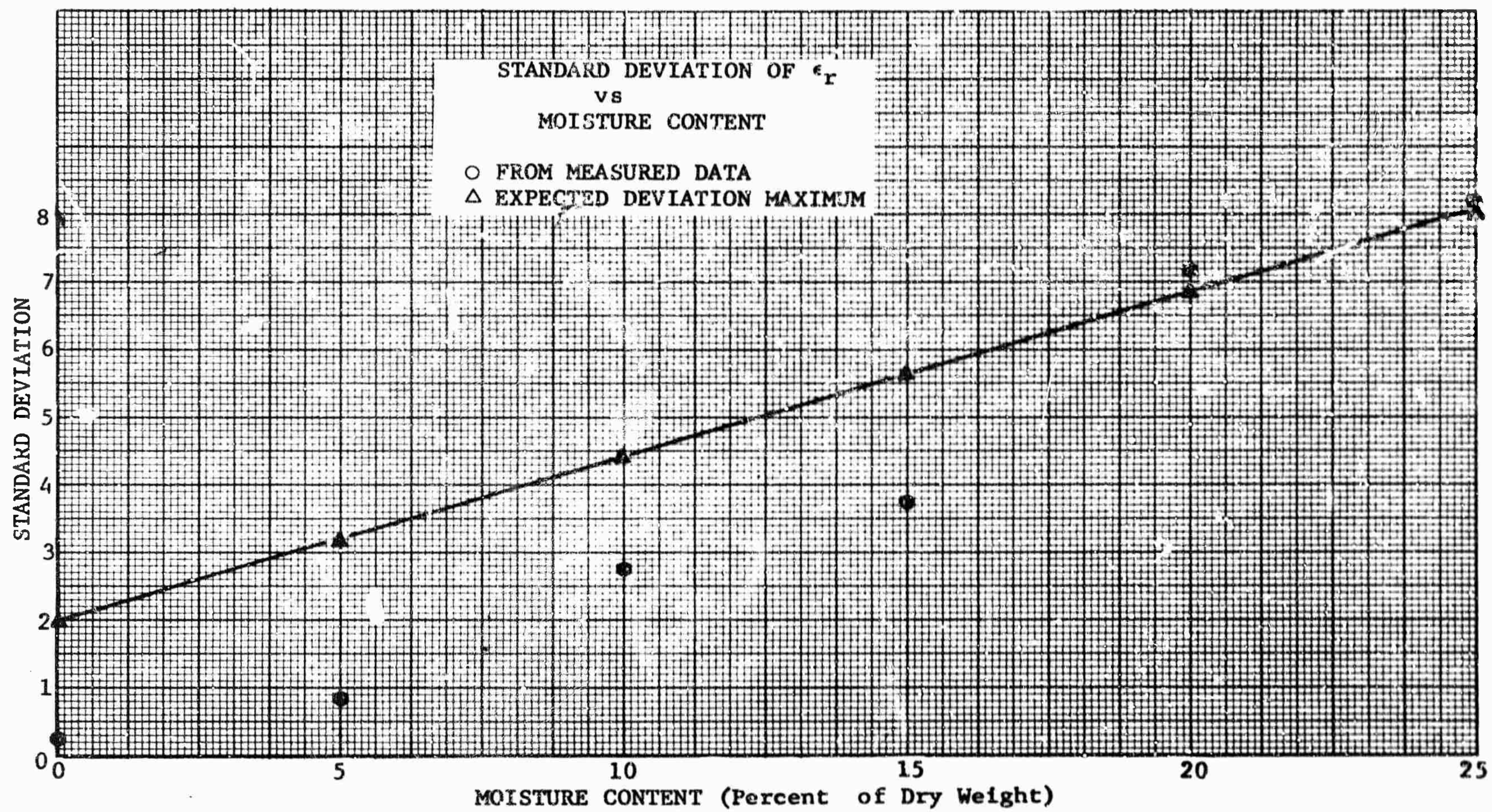

Fig. 25 STANDARD DEVIATION OF THE RELATIVE DIELECTRIC CONSTANT AS A FUNCTION OF MOISTURE CONTENT

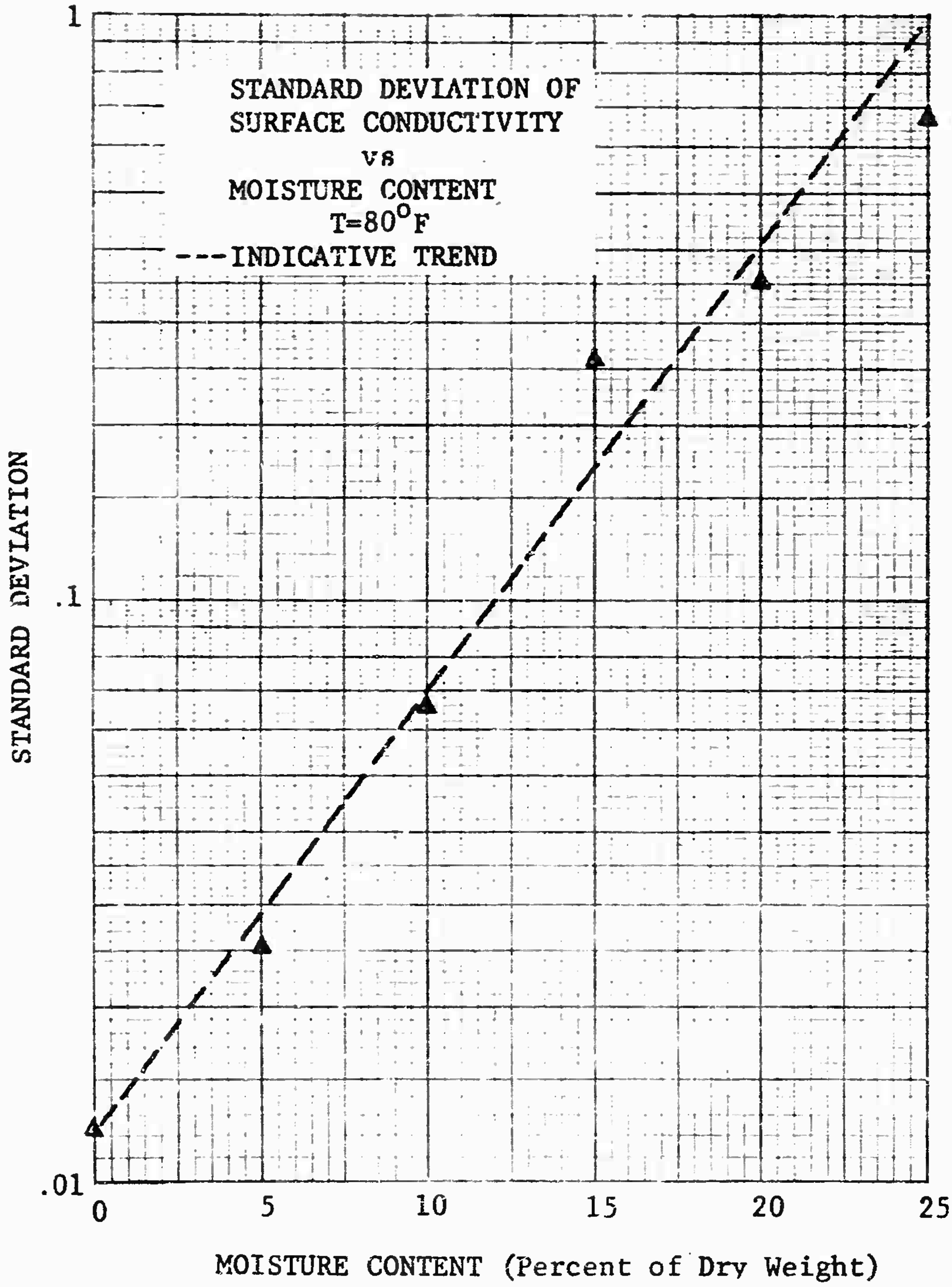

Fig. 26 STANDARD DEVIATION OF THE CONDUCTIVITY AS A FUNCTION OF MOISTURE CONTENT

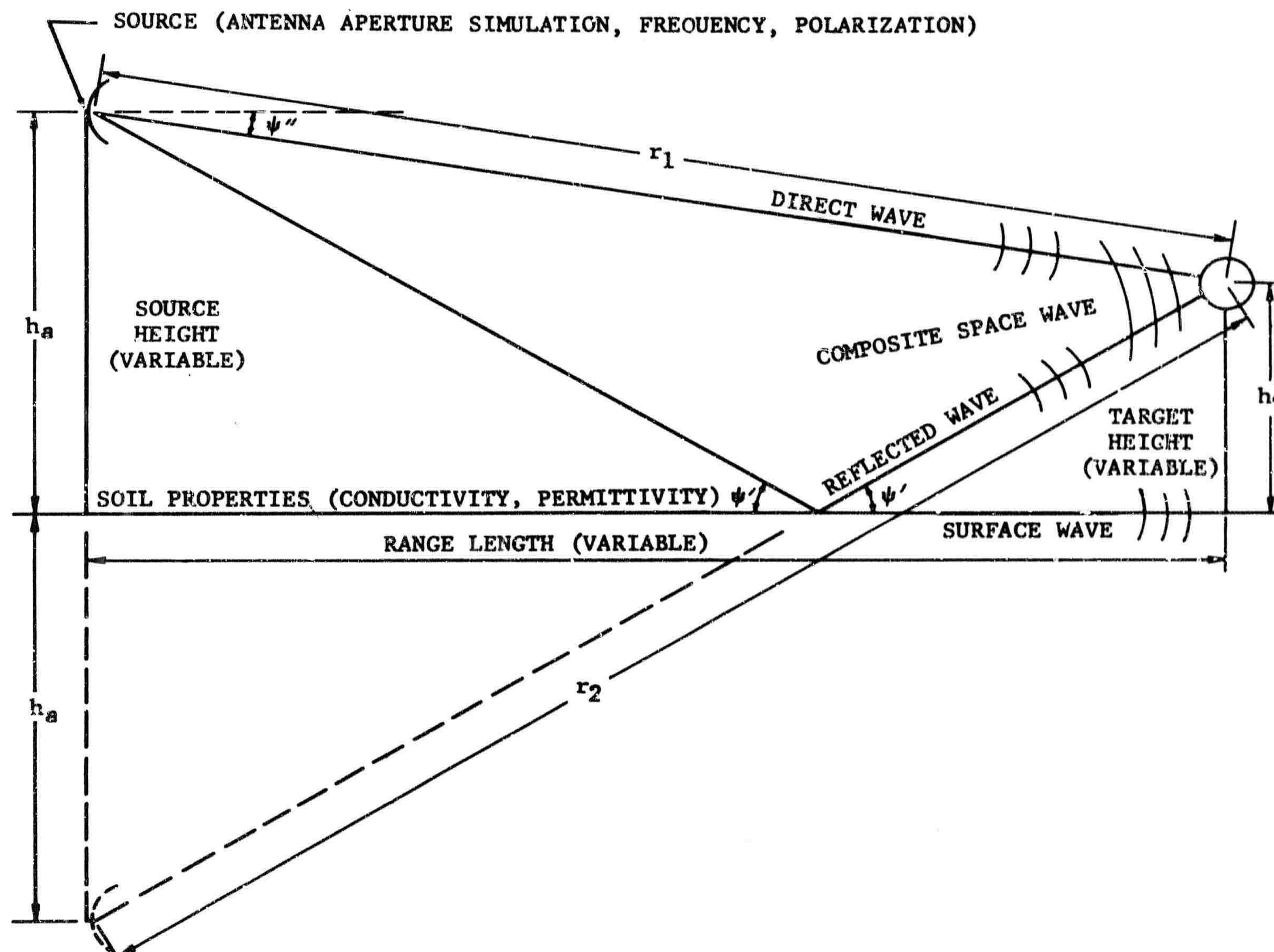

Fig. 27 GROUND PLANE RADAR GEOMETRY AND OPERATING PARAMETERS

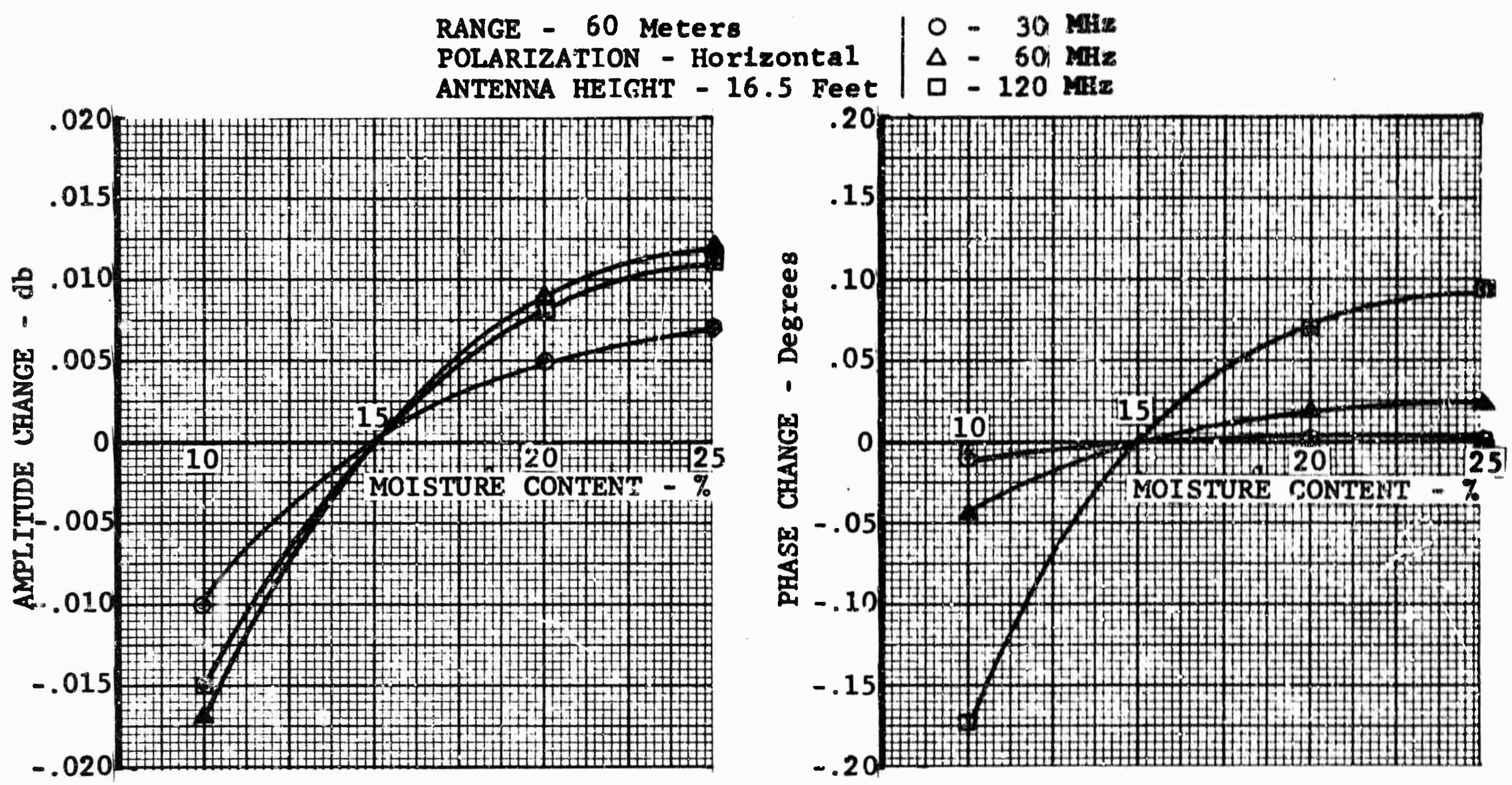

Fig. 28 FIELD GRADIENTS PRODUCED BY SOIL MOISTURE CHANGE
(16.5-FOOT ANTENNA HEIGHT, HORIZONTAL, 60-METER RANGE)

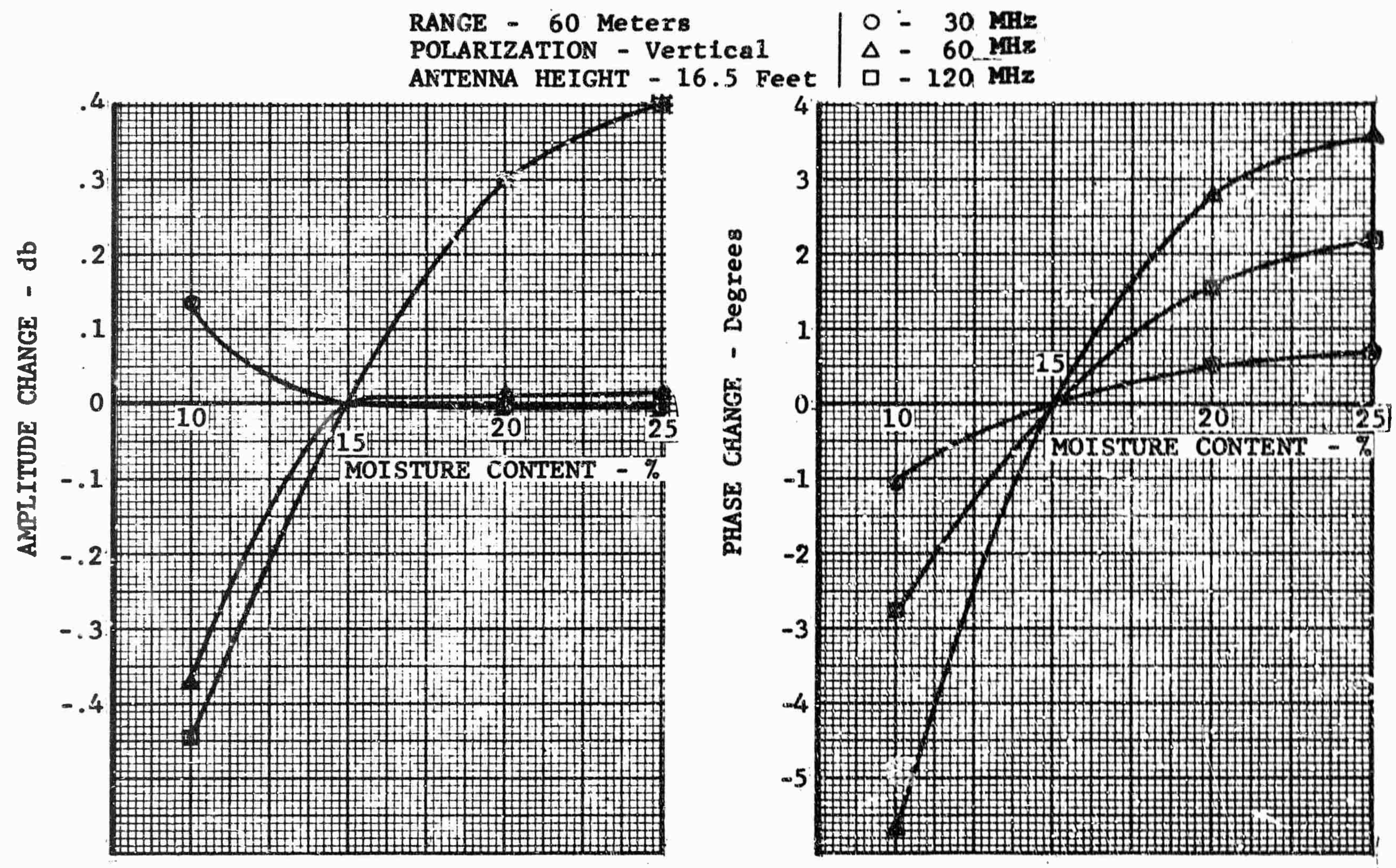

Fig. 29 FIELD GRADIENTS PRODUCED BY SOIL MOISTURE CHANGE (16.5-FOOT ANTENNA HEIGHT, VERTICAL, 60-METER RANGE)

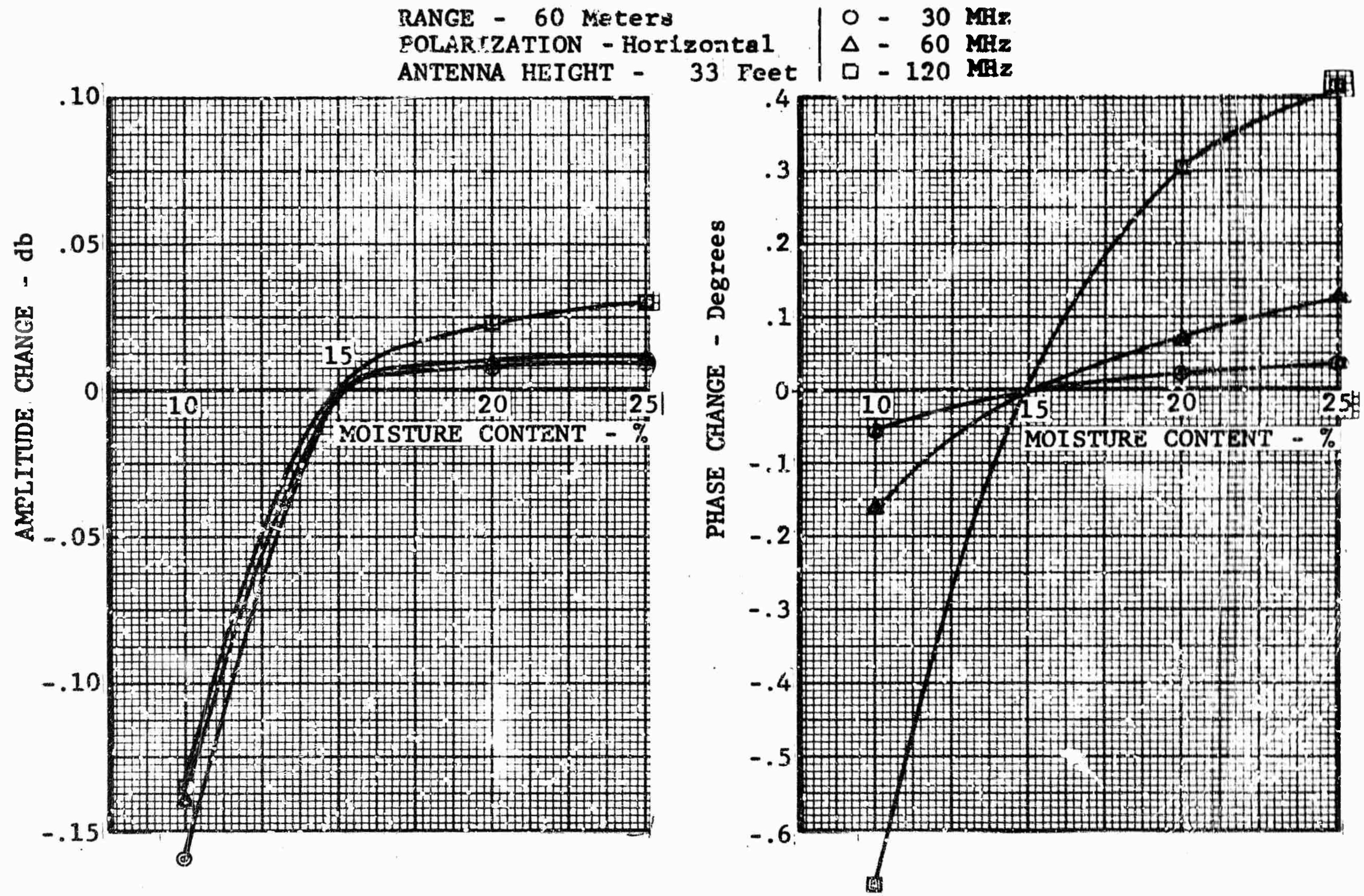

Fig. 30 FIELD GRADIENTS PRODUCED BY SOIL MOISTURE CHANGE (33-FOOT ANTENNA HEIGHT, HORIZONTAL, 60-METER RANGE)

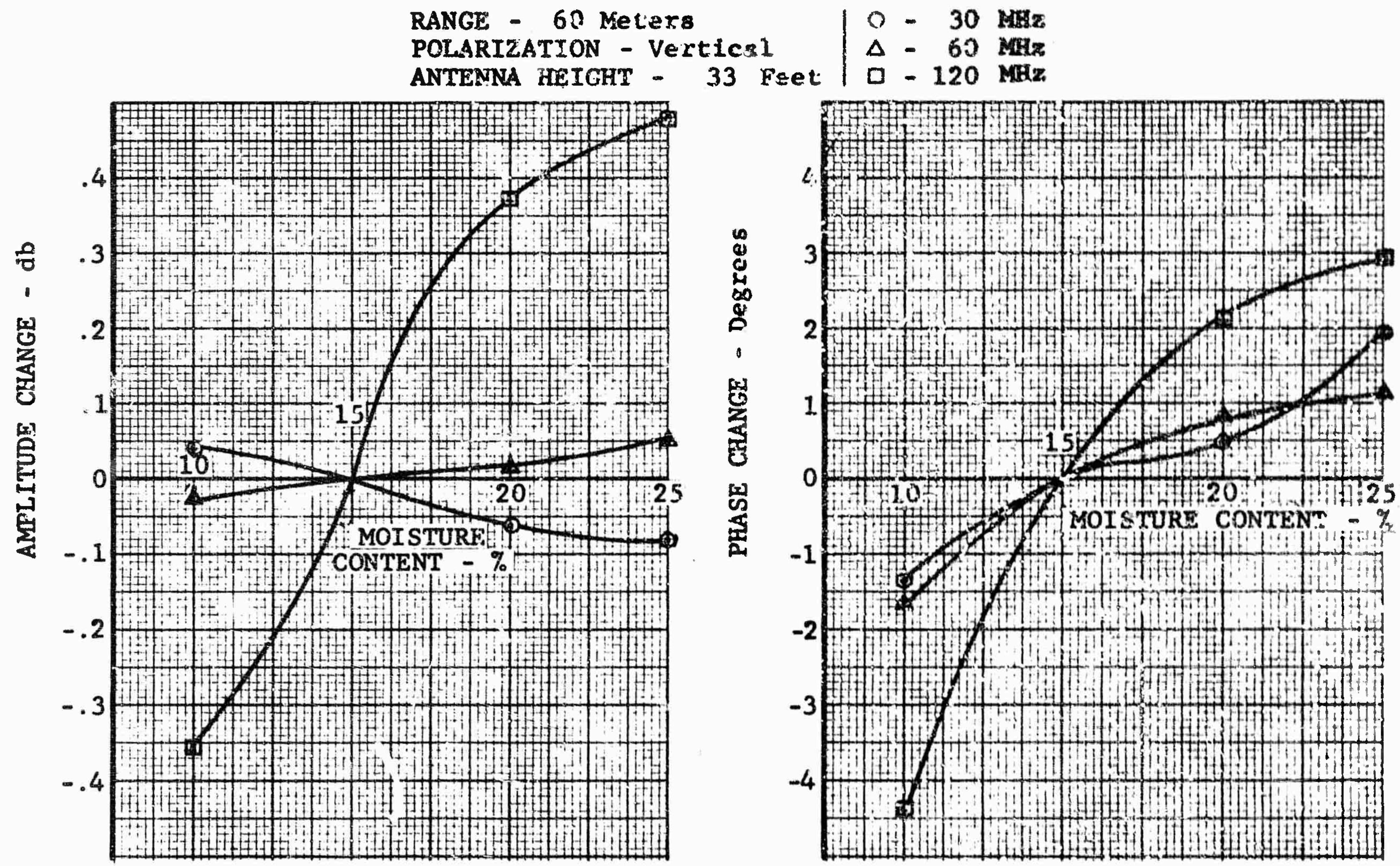

Fig. 31 FIELD GRADIENTS PRODUCED BY SOIL MOISTURE CHANGE (33-FOOT ANTENNA HEIGHT, VERTICAL, 60-METER RANGE)

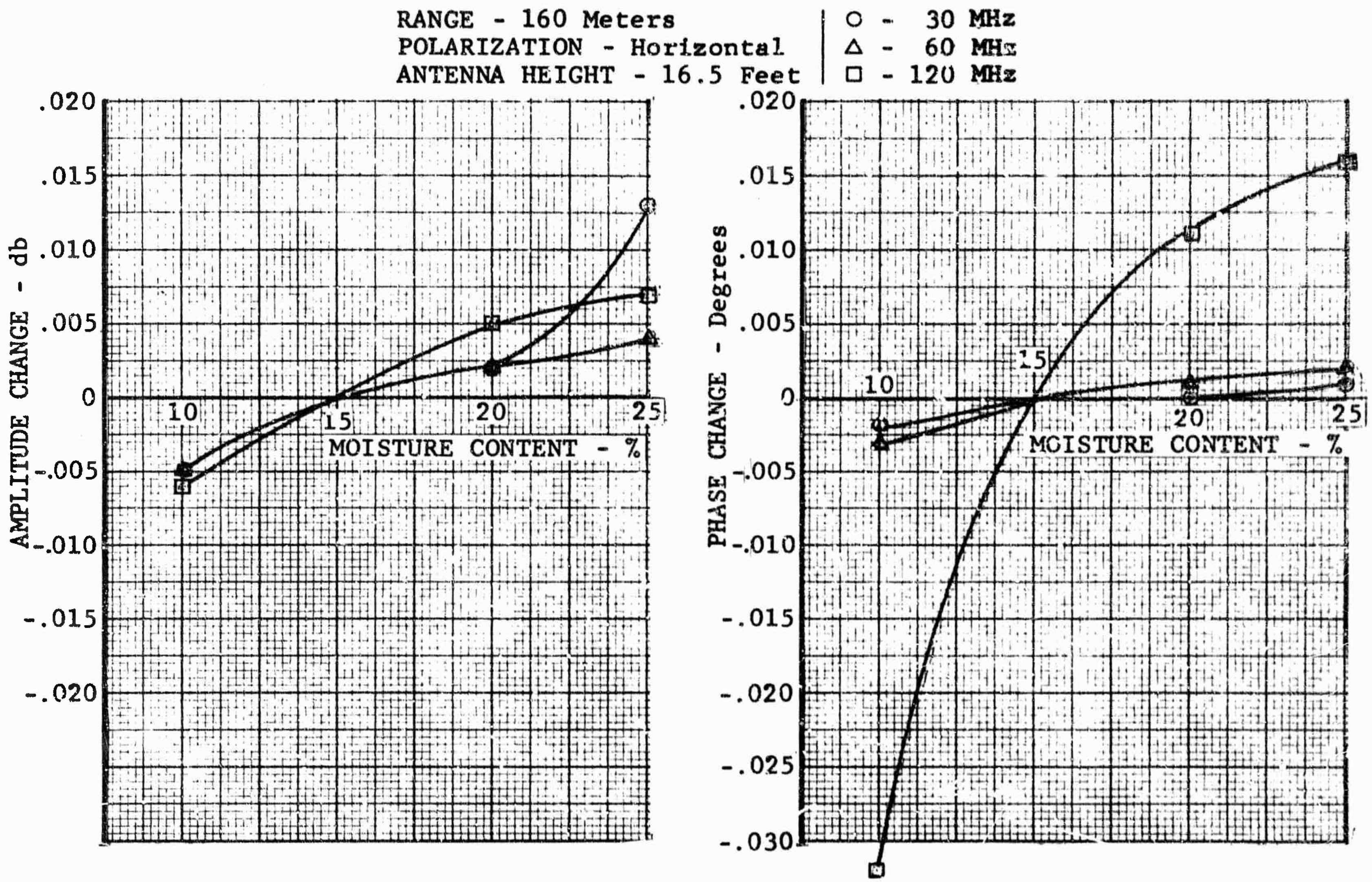

Fig. 32 FIELD GRADIENTS PRODUCED BY SOIL MOISTURE CHANGE (16.5-FOOT ANTENNA HEIGHT, HORIZONTAL, 160-METER RANGE)

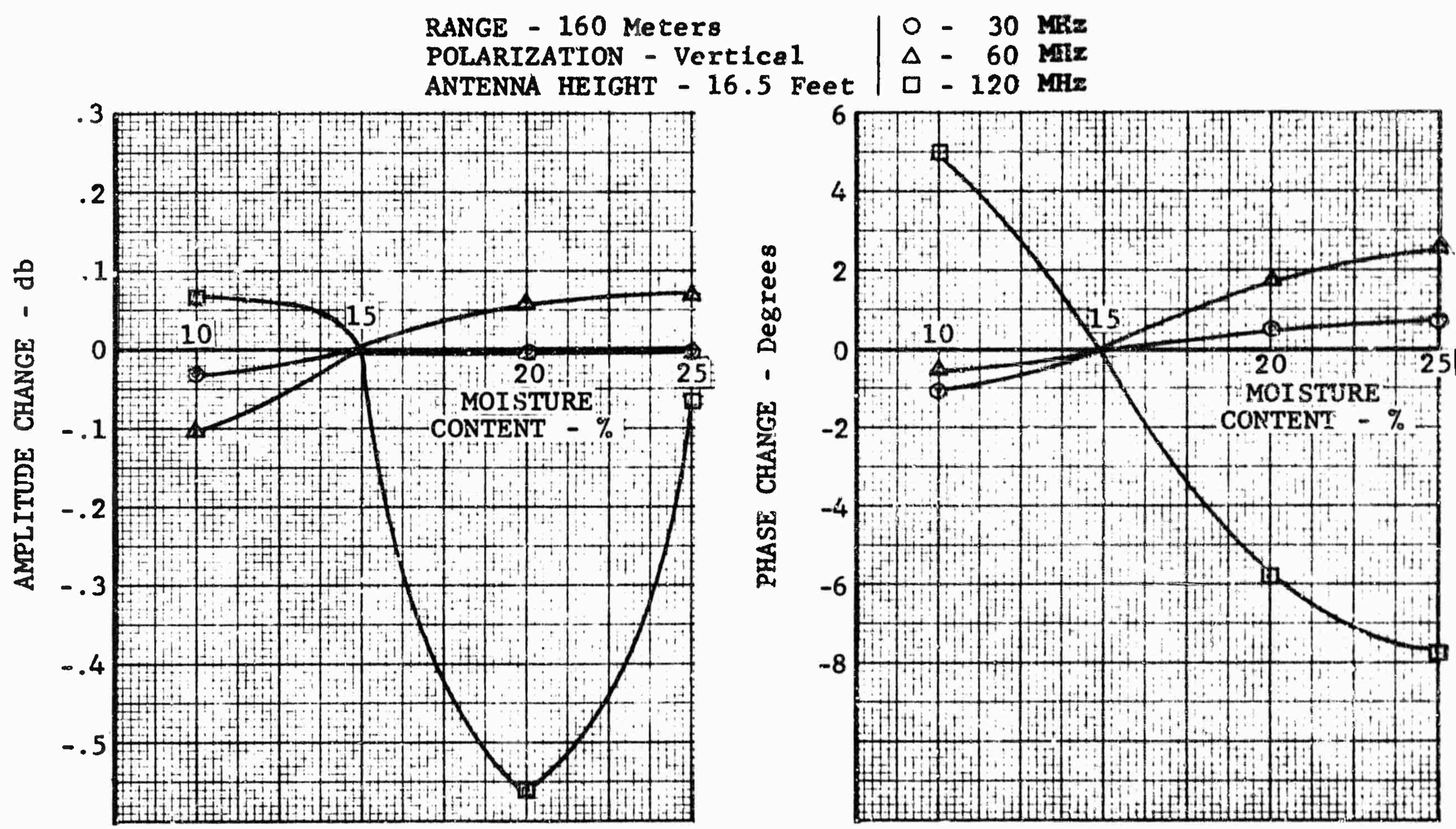

Fig. 33 FIELD GRADIENTS PRODUCED BY SOIL MOISTURE CHANGE
(16.5-FOOT ANTENNA HEIGHT, VERTICAL, 160-METER RANGE)

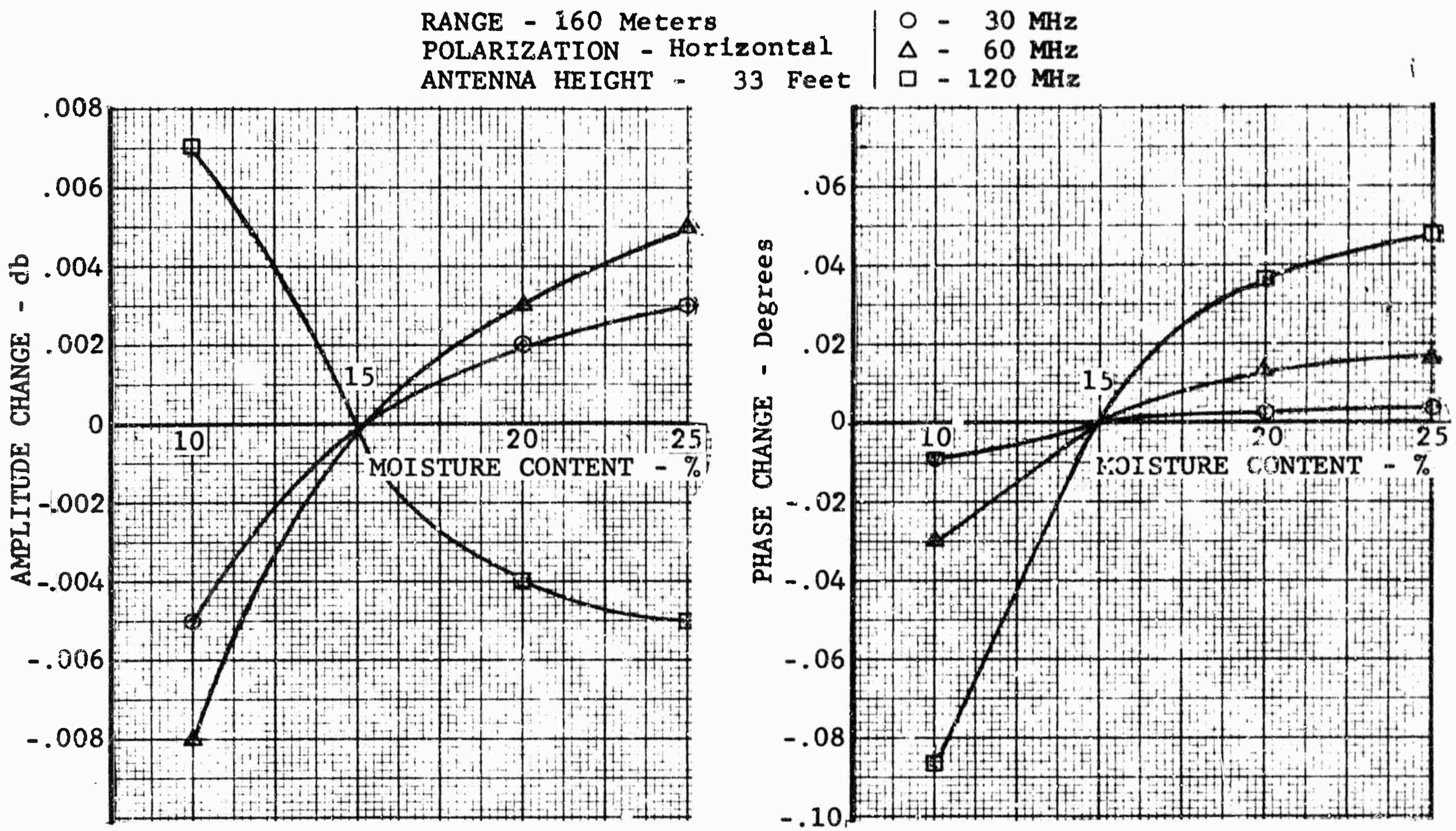

Fig. 34 FIELD GRADIENTS PRODUCED BY SOIL MOISTURE CHANGE (33-FOOT ANTENNA HEIGHT, HORIZONTAL, 160-METER RANGE)

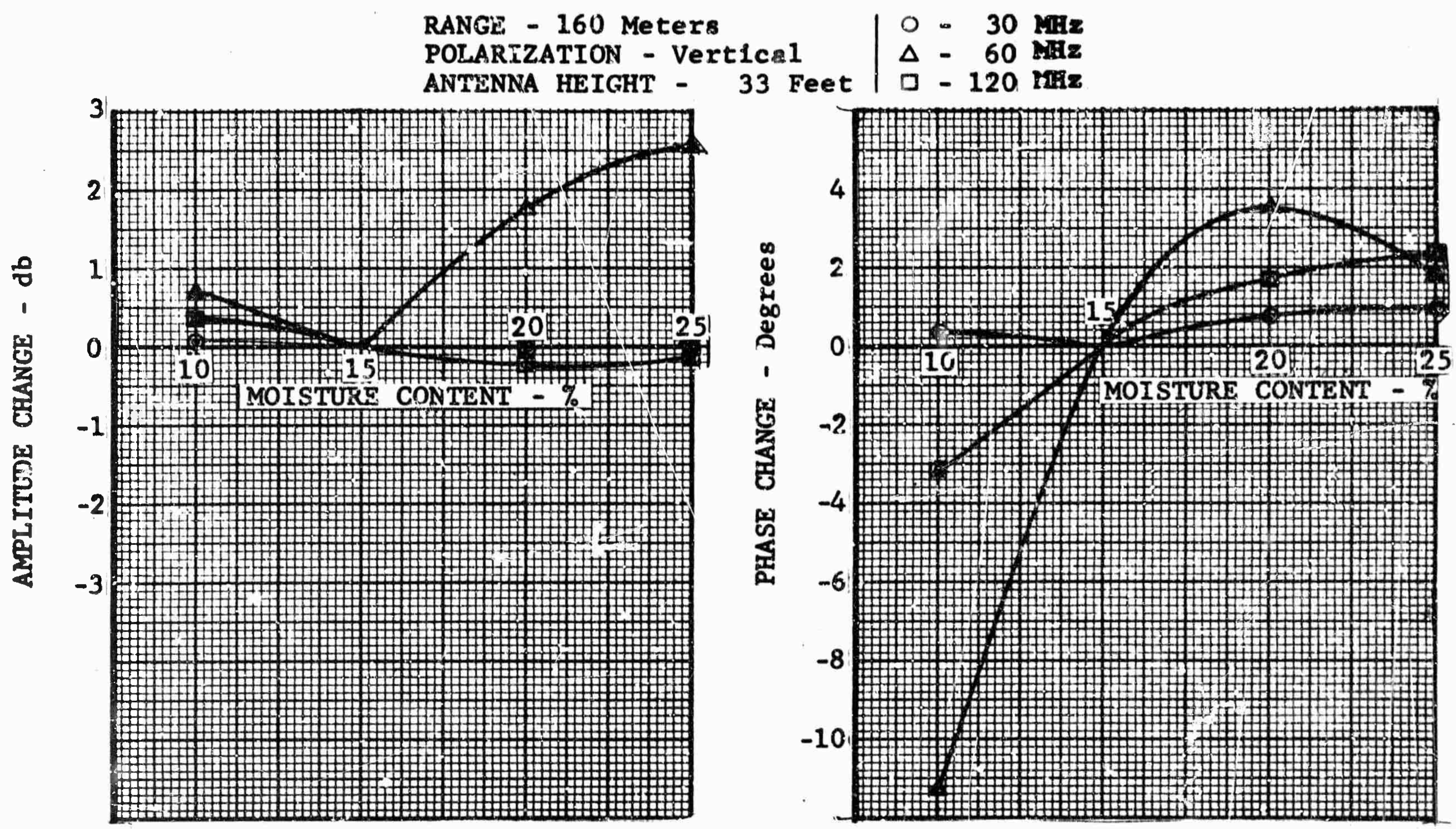

Fig. 35 FIELD GRADIENTS PRODUCED BY SOIL MOISTURE CHANGE (33-FOOT ANTENNA HEIGHT, VERTICAL, 160-METER RANGE)

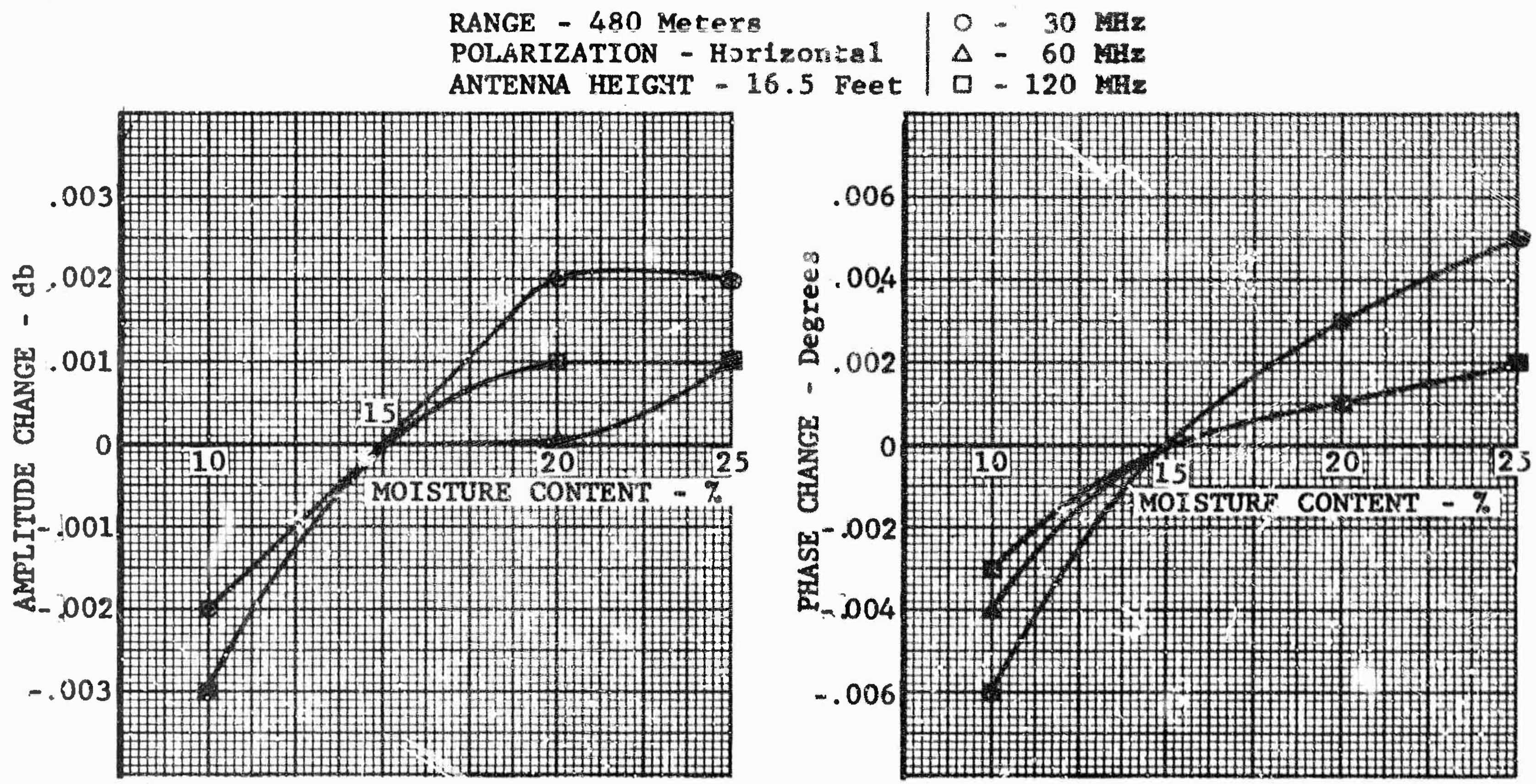

Fig. 36 FIELD GRADIENTS PRODUCED BY SOIL MOISTURE CHANGE (16.5-FOOT ANTENNA HEIGHT, HORIZONTAL, 480-METER RANGE)

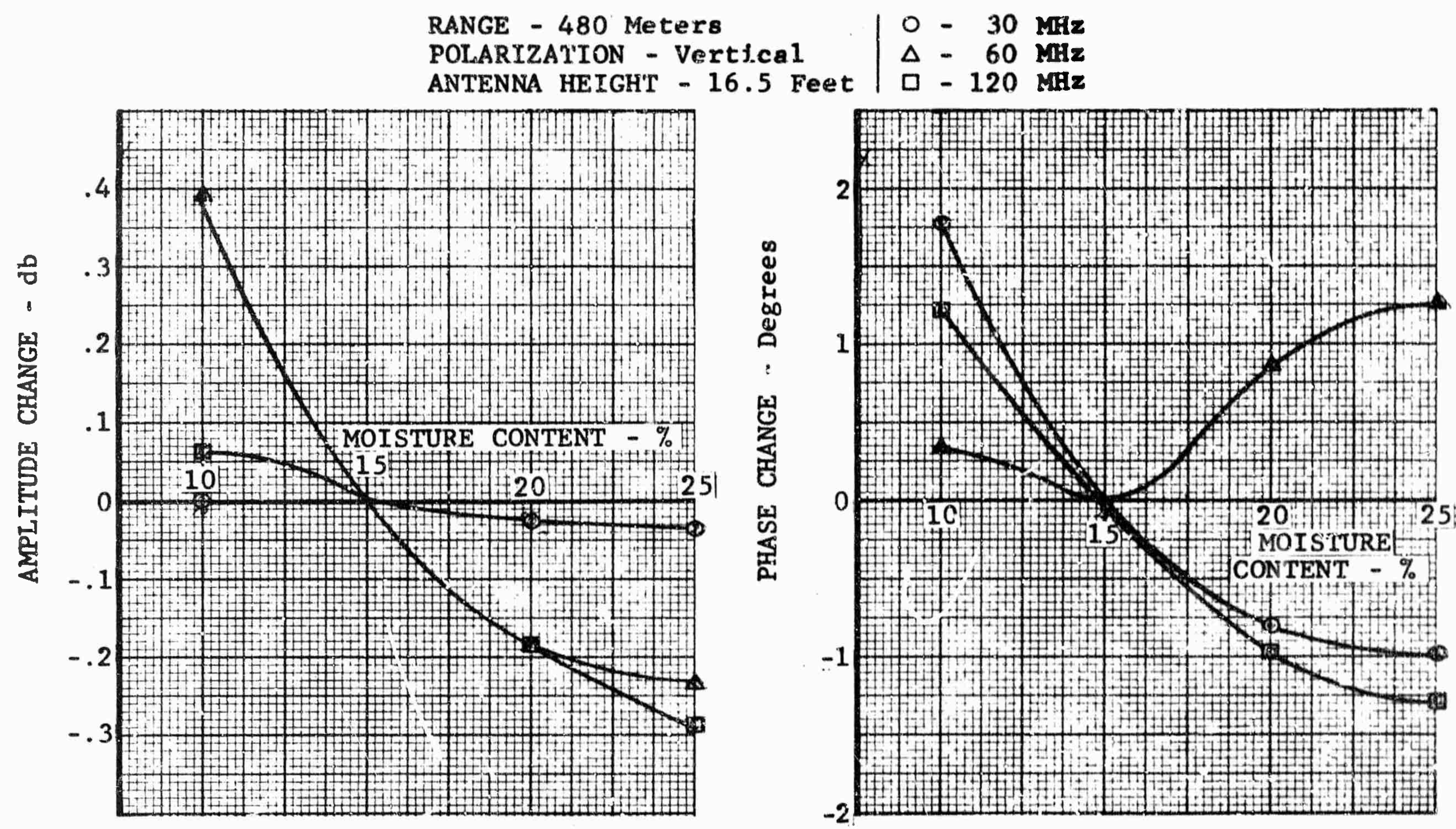

Fig. 37 FIELD GRADIENTS PRODUCED BY SOIL MOISTURE CHANGE (16.5-FOOT ANTENNA HEIGHT, VERTICAL, 480-METER RANGE)

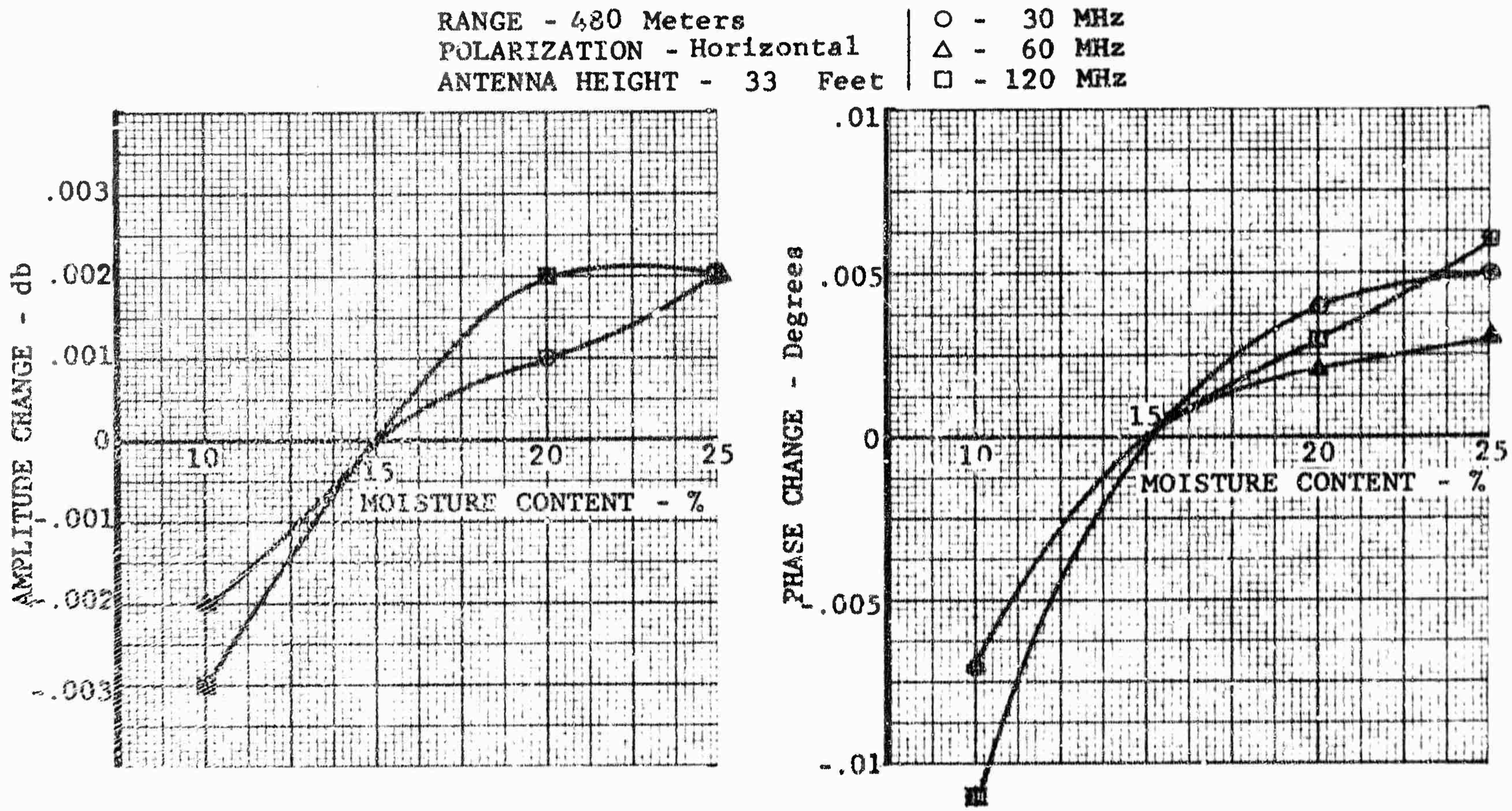

Fig. 38 FIELD GRADIENTS PRODUCED BY SOIL MOISTURE CHANGE
(33-FOOT ANTENNA HEIGHT, HORIZONTAL, 480-METER RANGE)

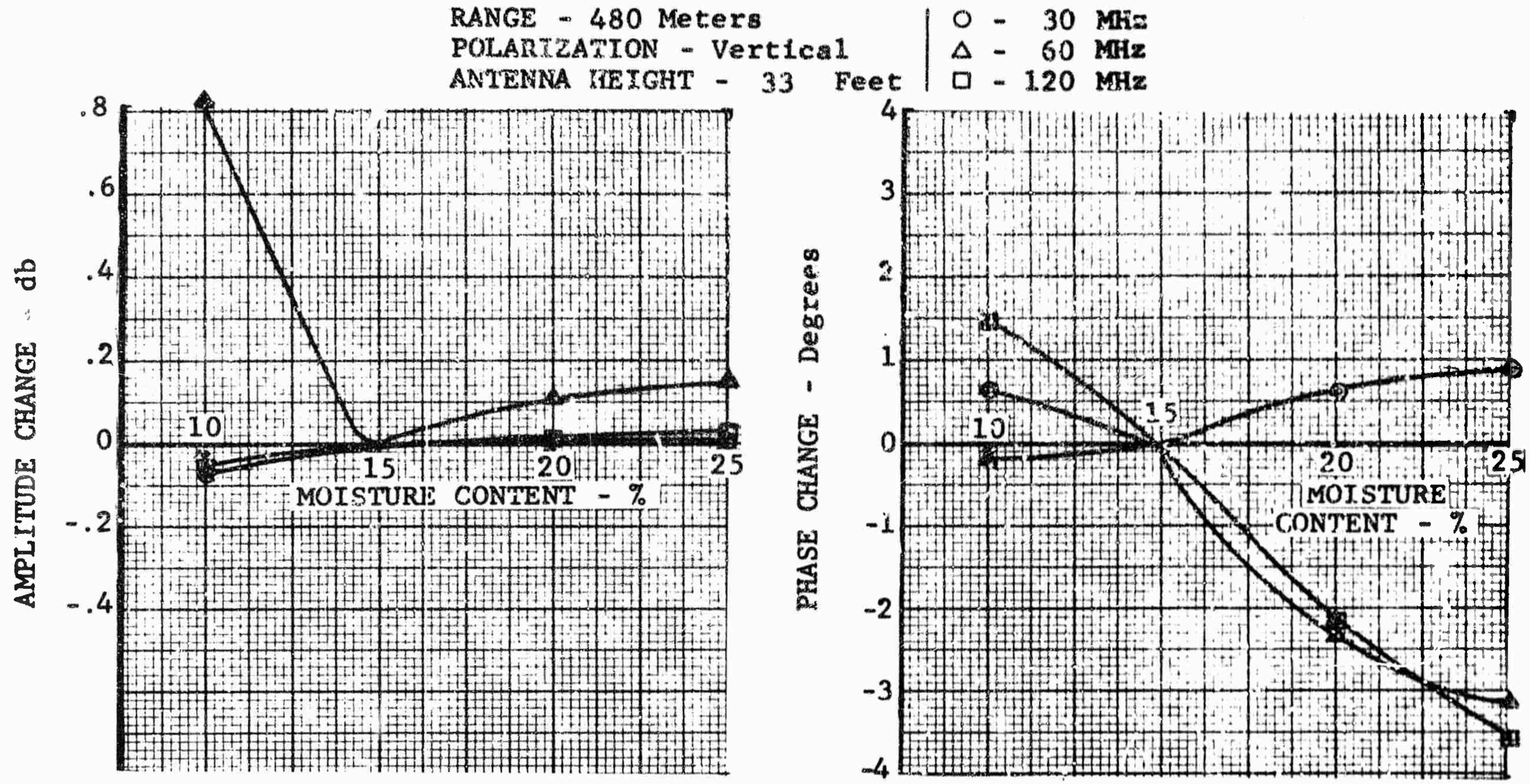

Fig. 39 FIELD GRADIENTS PRODUCED BY SOIL MOISTURE CHANGE (33-FOOT ANTENNA HEIGHT, VERTICAL, 480-METER RANGE)

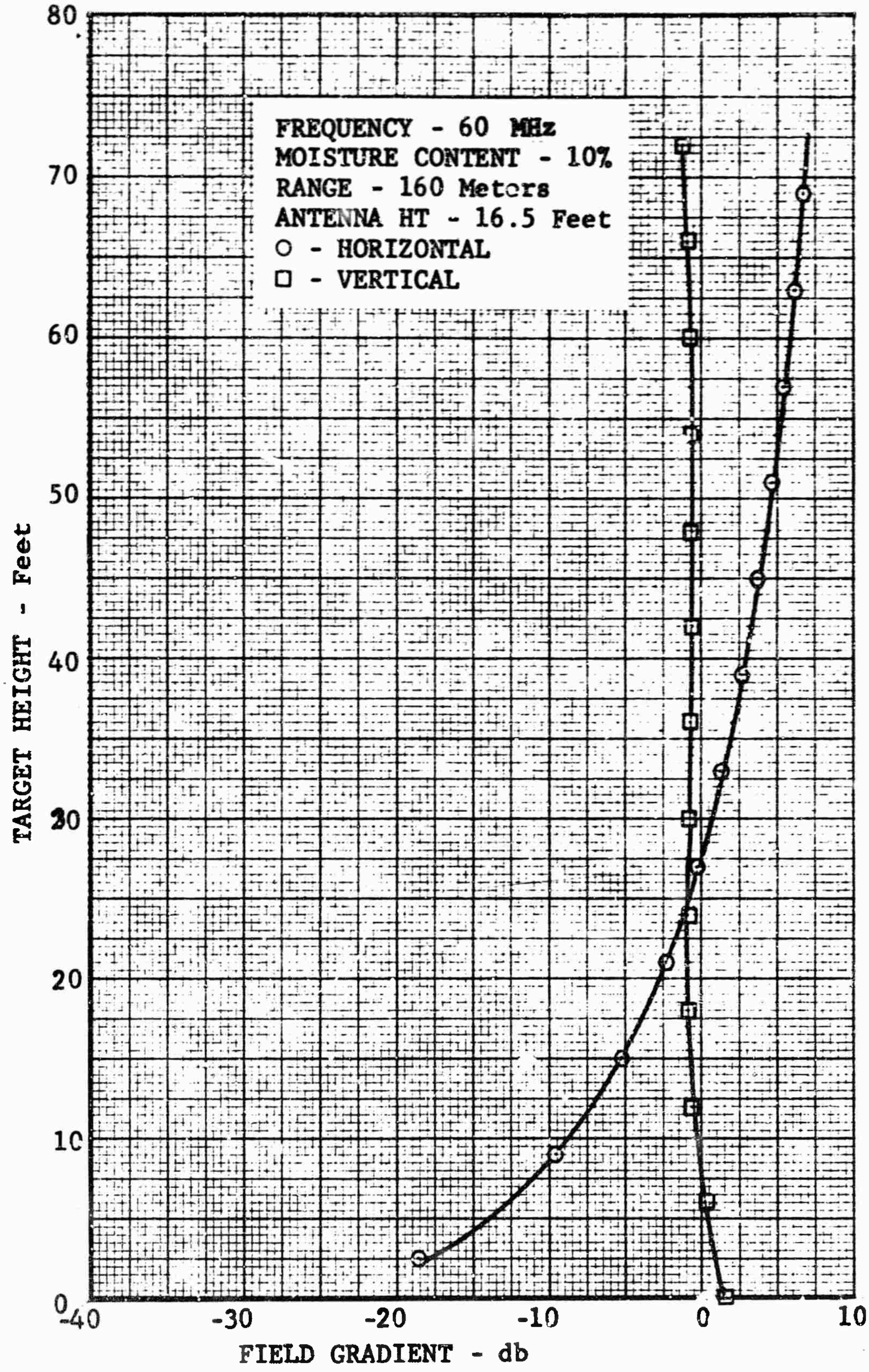

Fig. 40 AMPLITUDE FOR 10 PERCENT MOISTURE

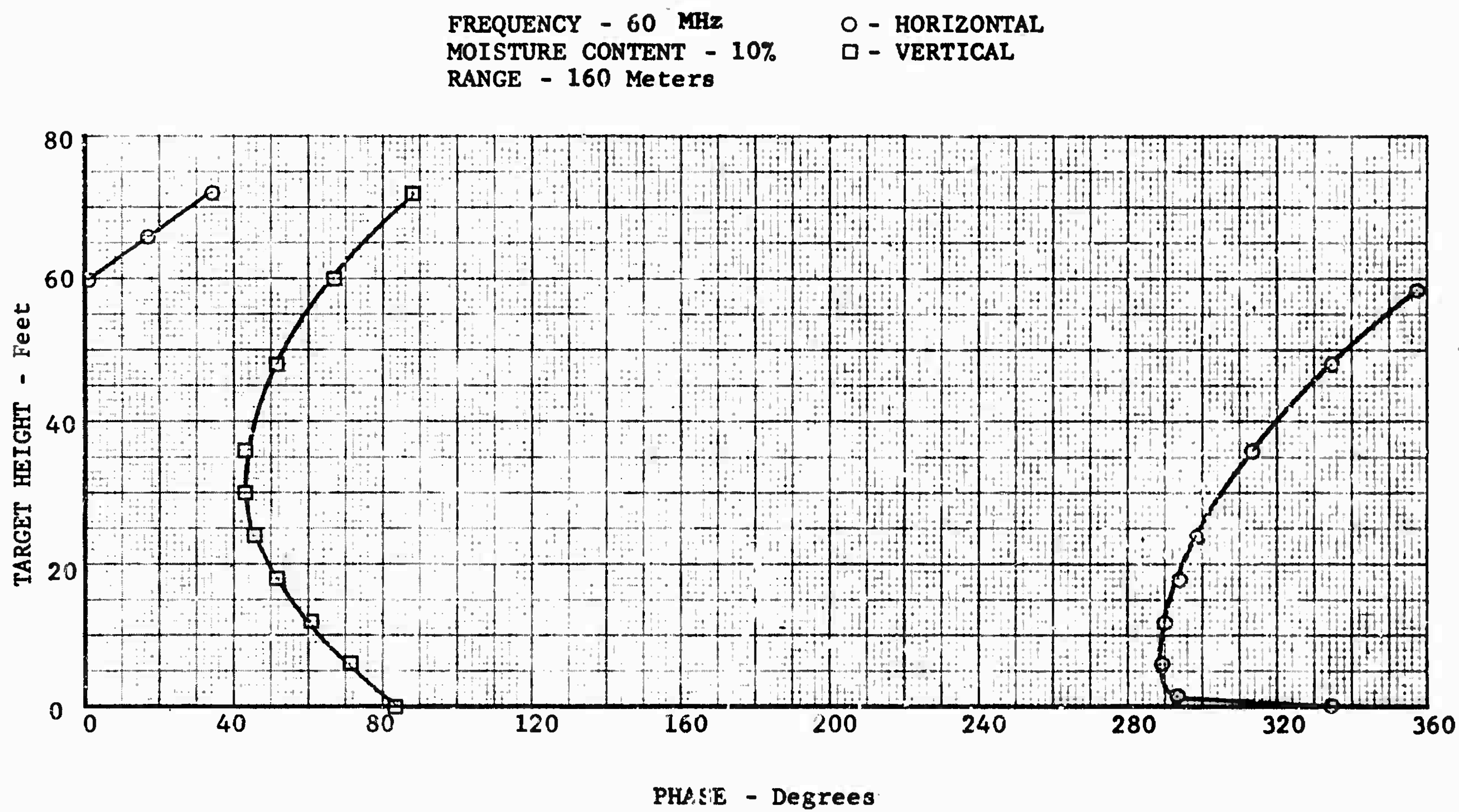

Fig. 41 PHASE FOR 10 PERCENT MOISTURE

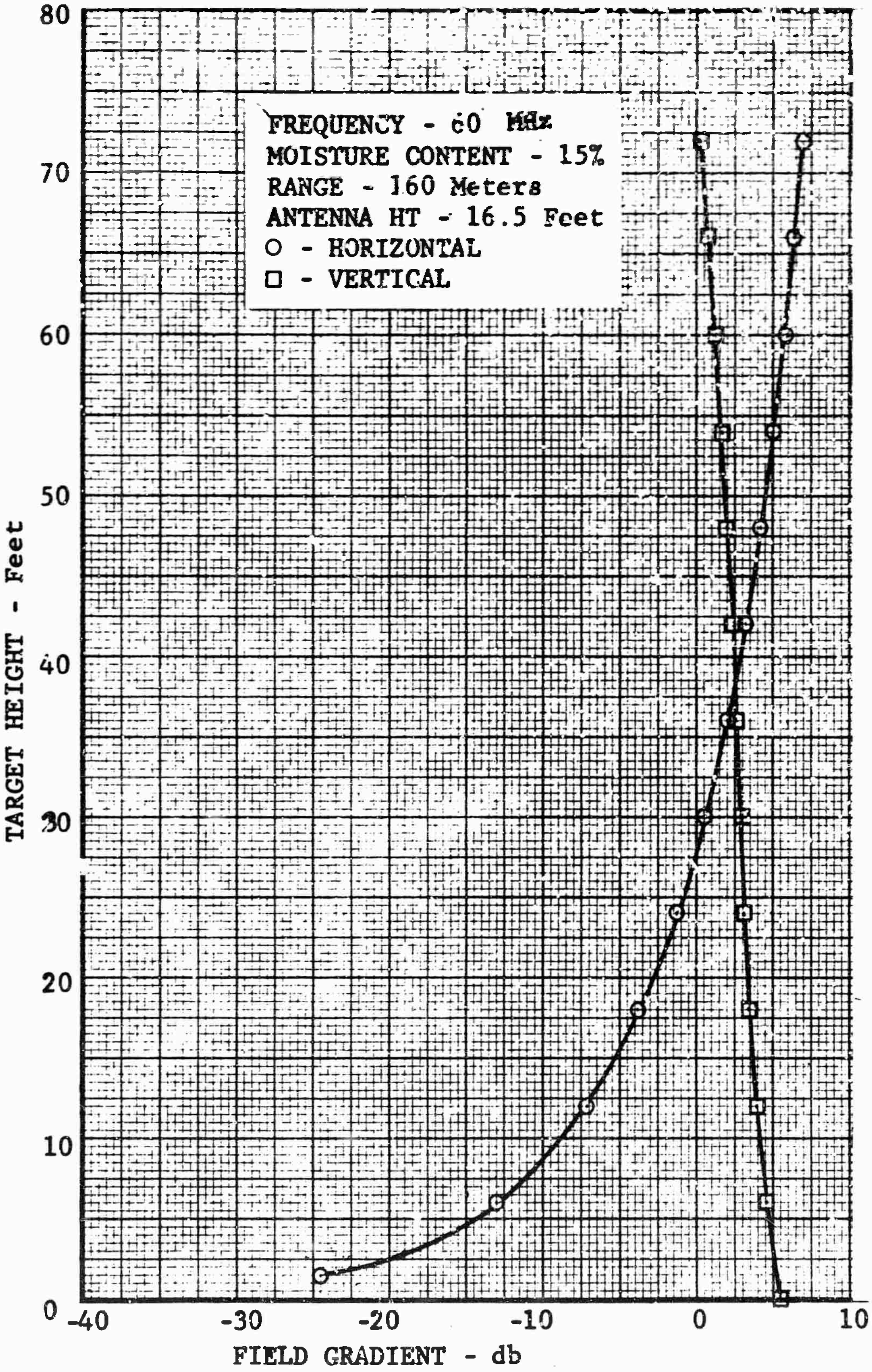

Fig. 42 AMPLITUDE FOR 15 PERCENT MOISTURE

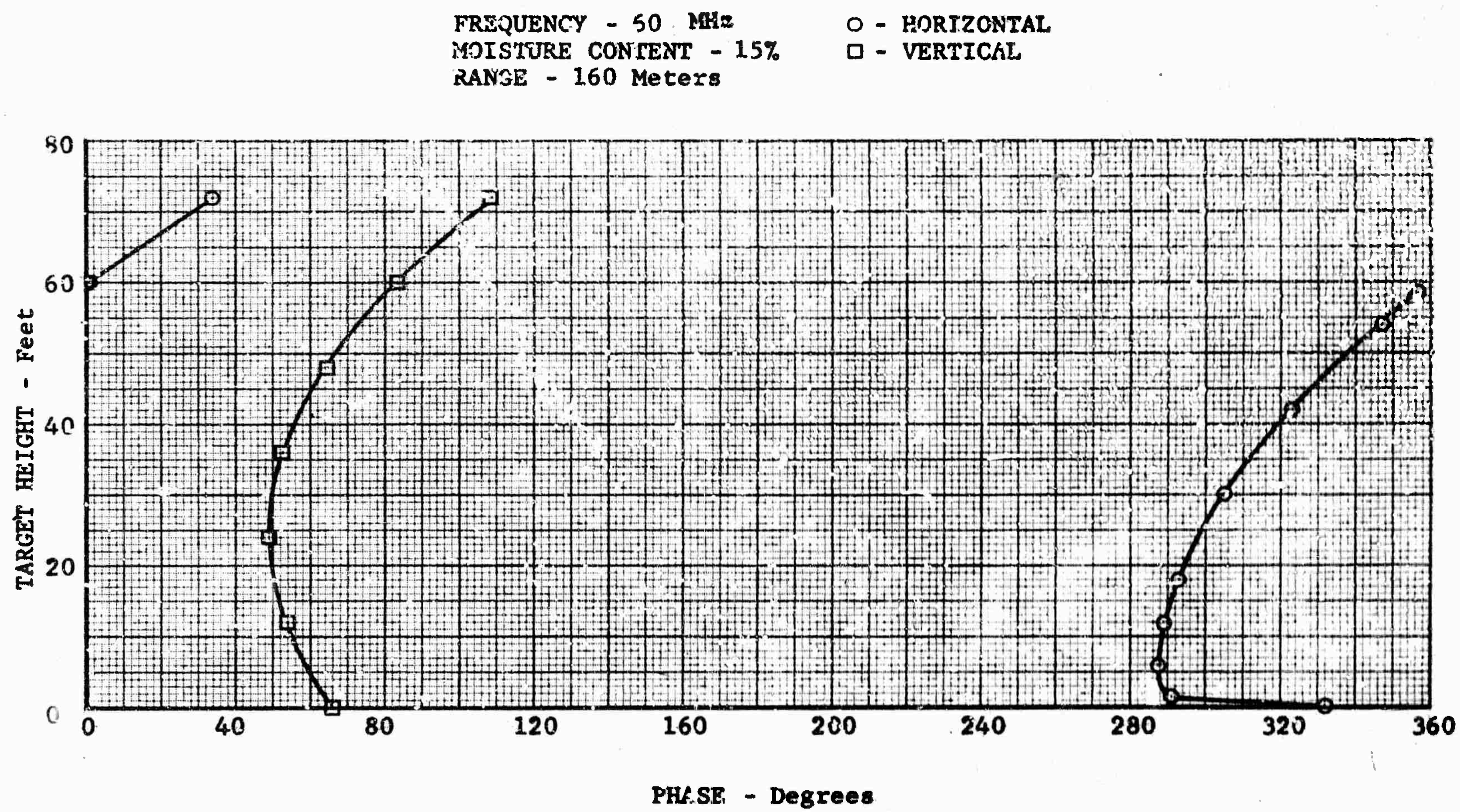

Fig. 43 PHASE FOR 15 PERCENT MOISTURE

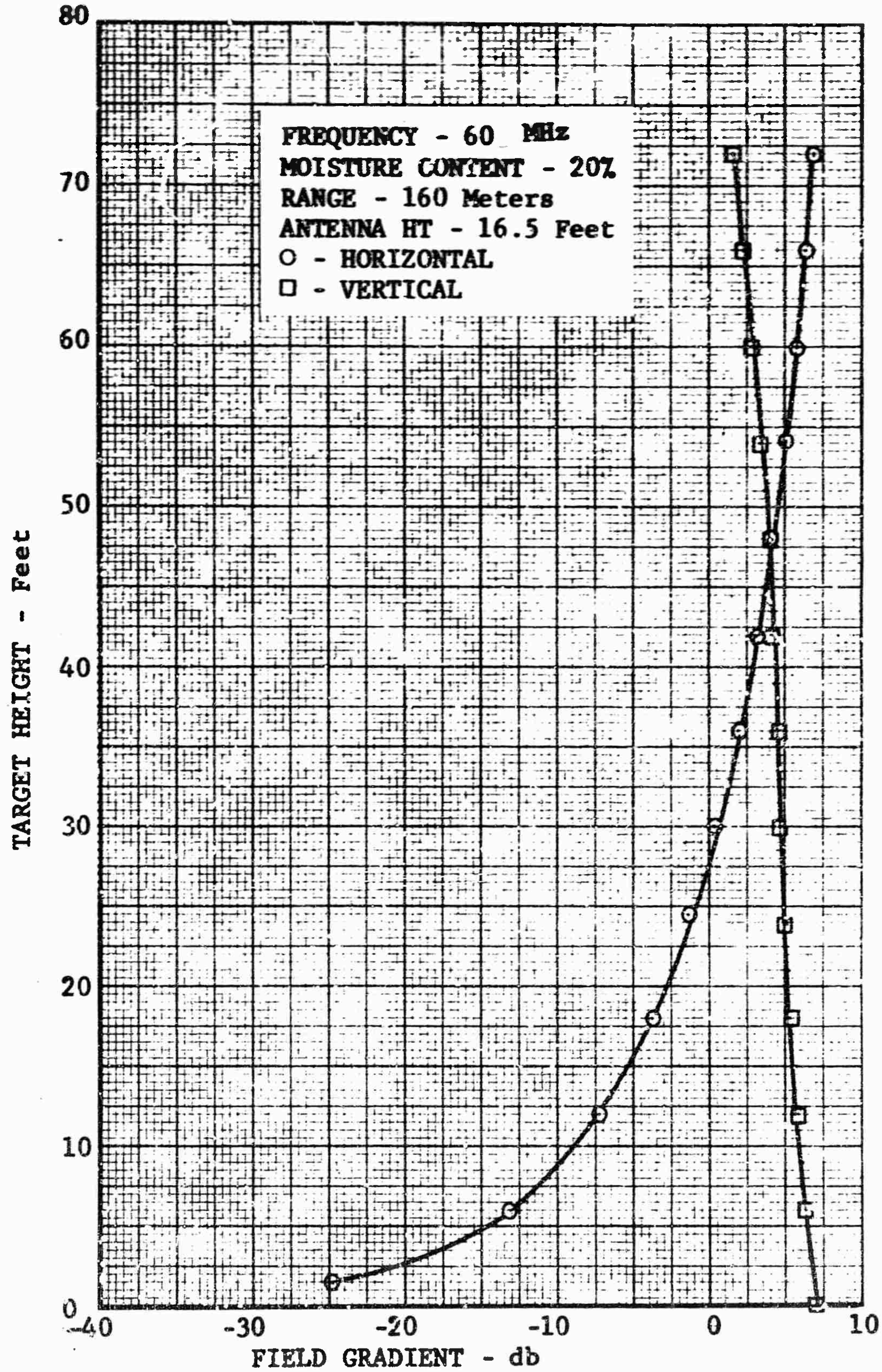

Fig. 44 AMPLITUDE FOR 20 PERCENT MOISTURE

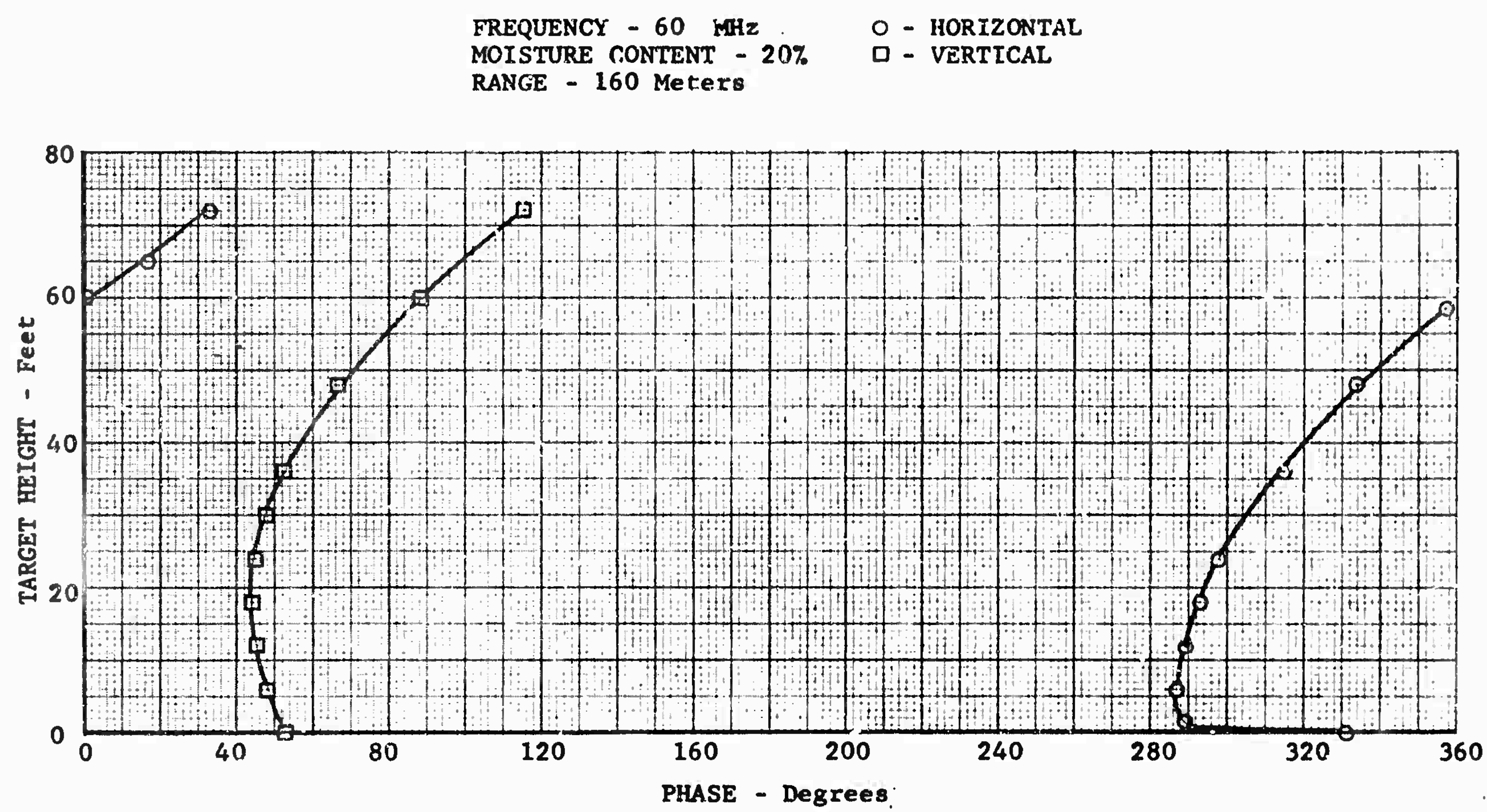

Fig. 45 PHASE FOR 20 PERCENT MOISTURE

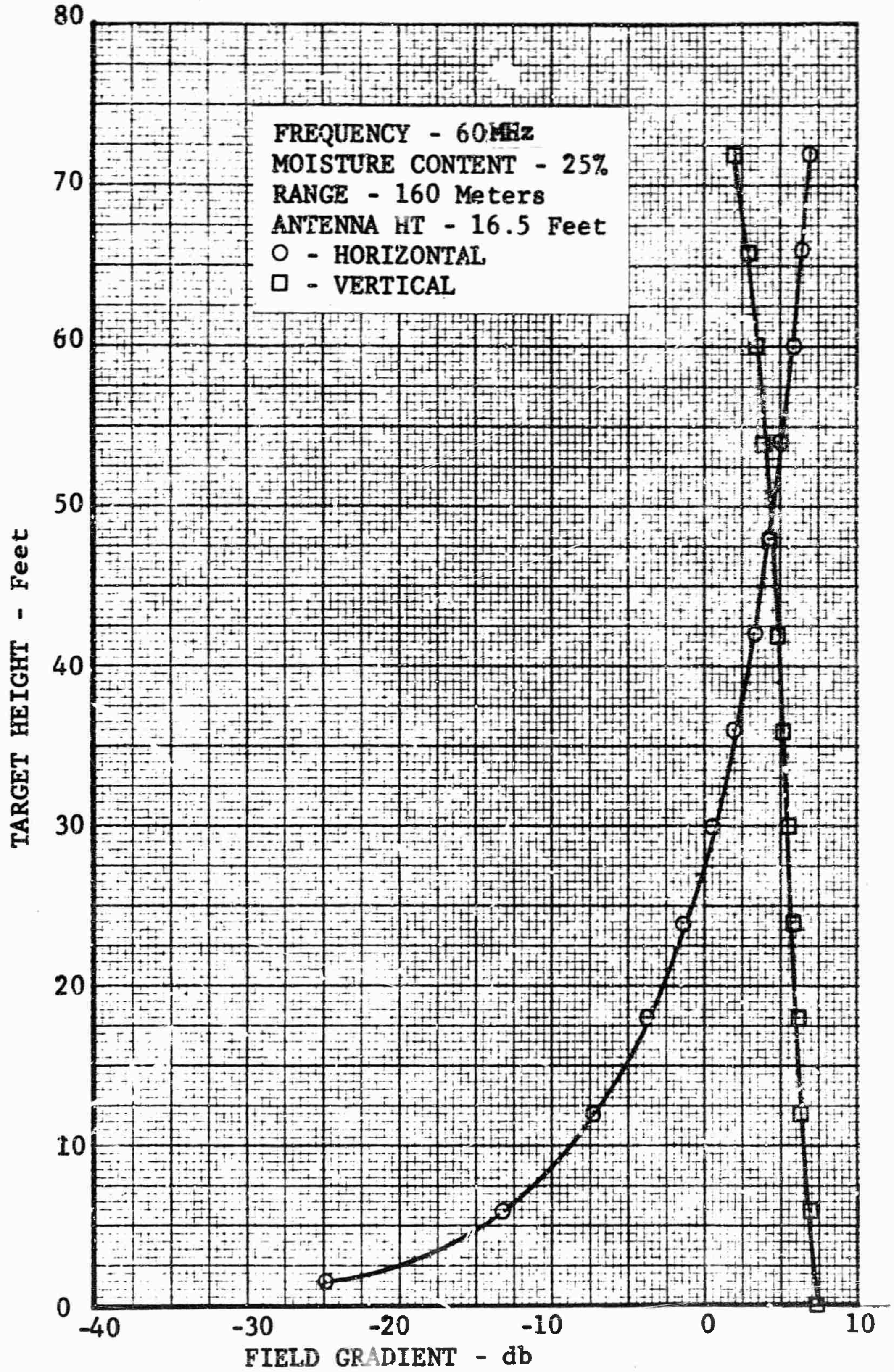

Fig. 46 AMPLITUDE FOR 25 PERCENT MOISTURE

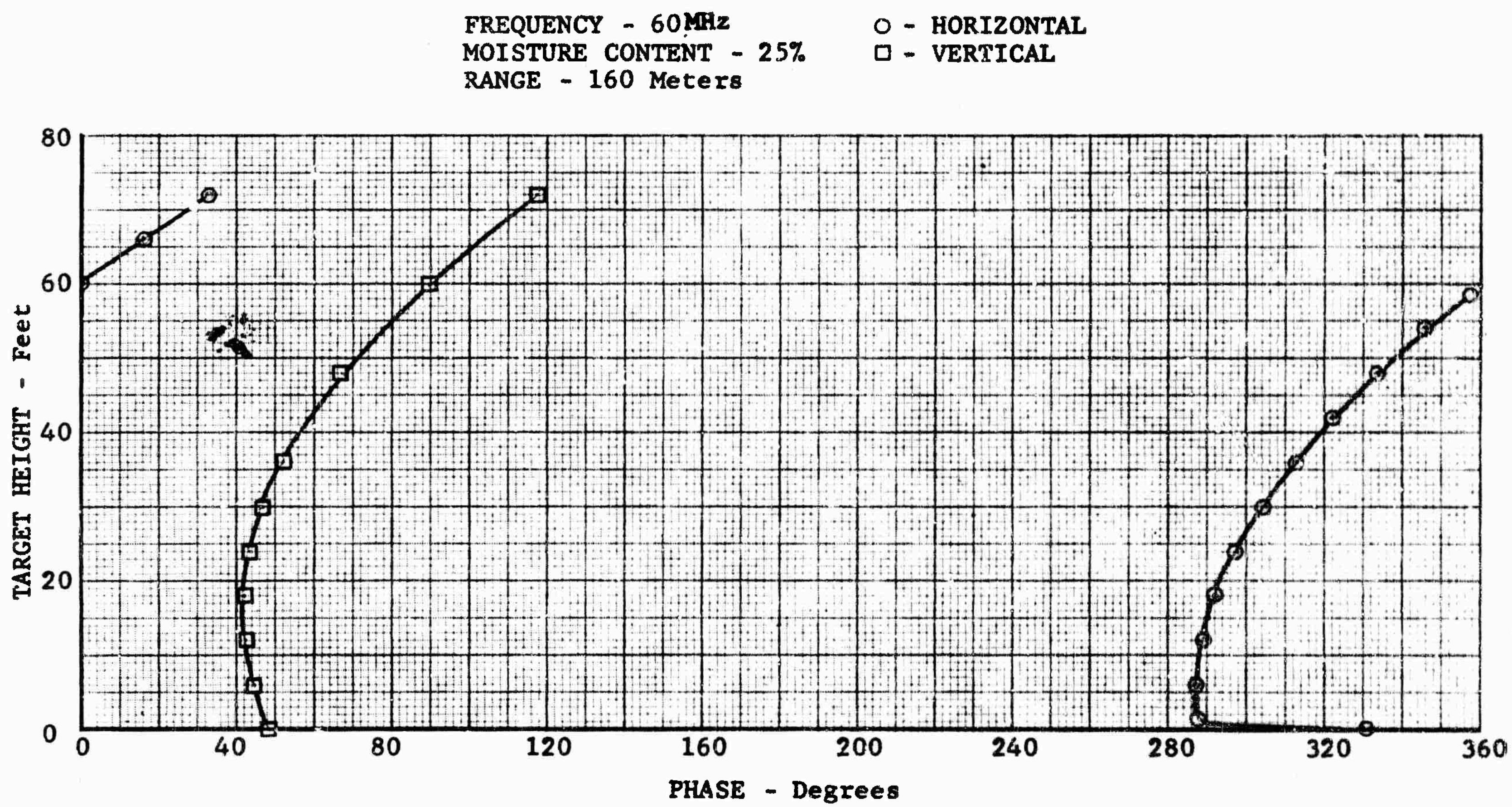

Fig. 47 PHASE FOR 25 PERCENT MOISTURE

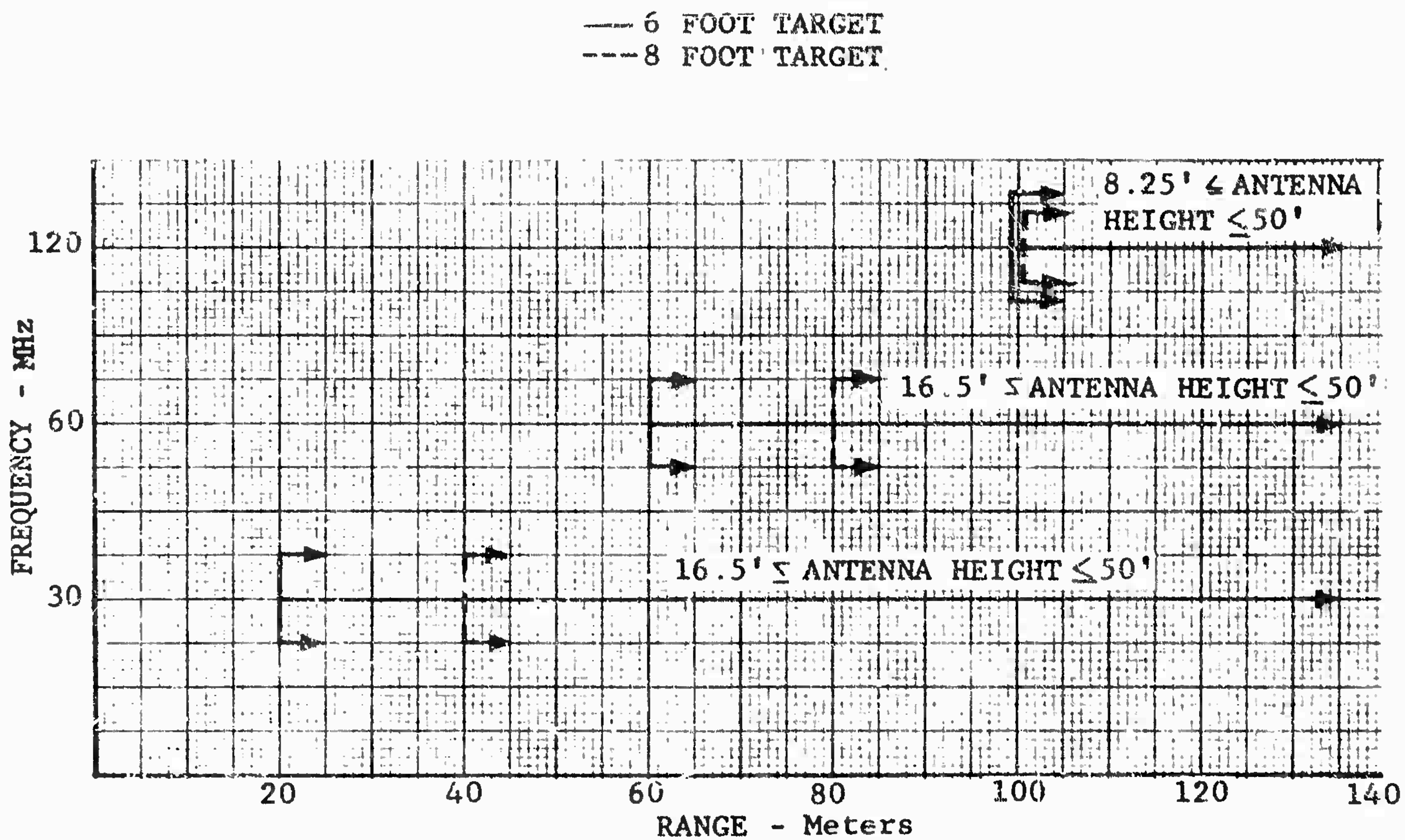

Fig. 48 OPERATING REGIONS FOR HORIZONTAL POLARIZATION

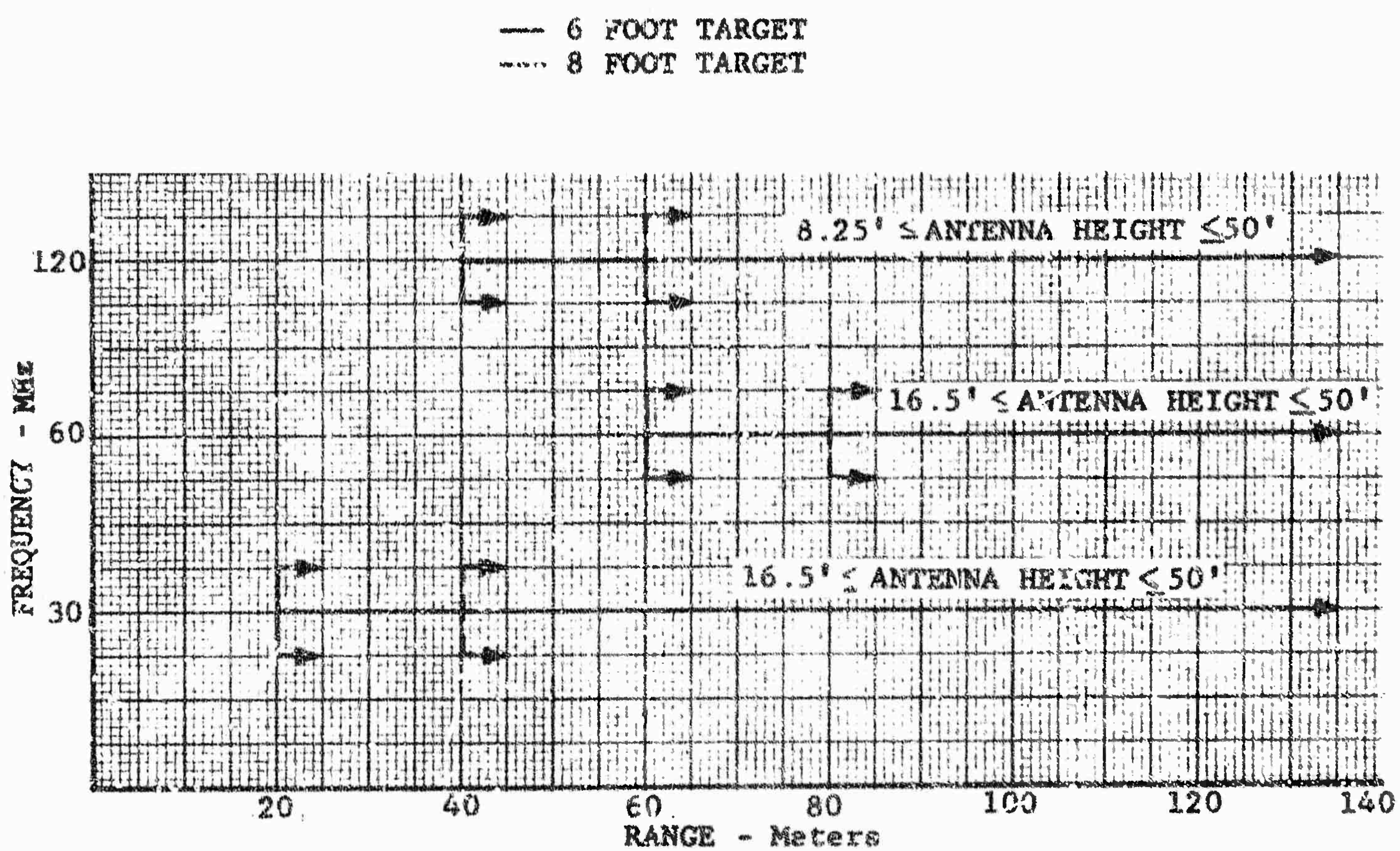

Fig. 49 OPERATING REGIONS FOR VERTICAL POLARIZATION

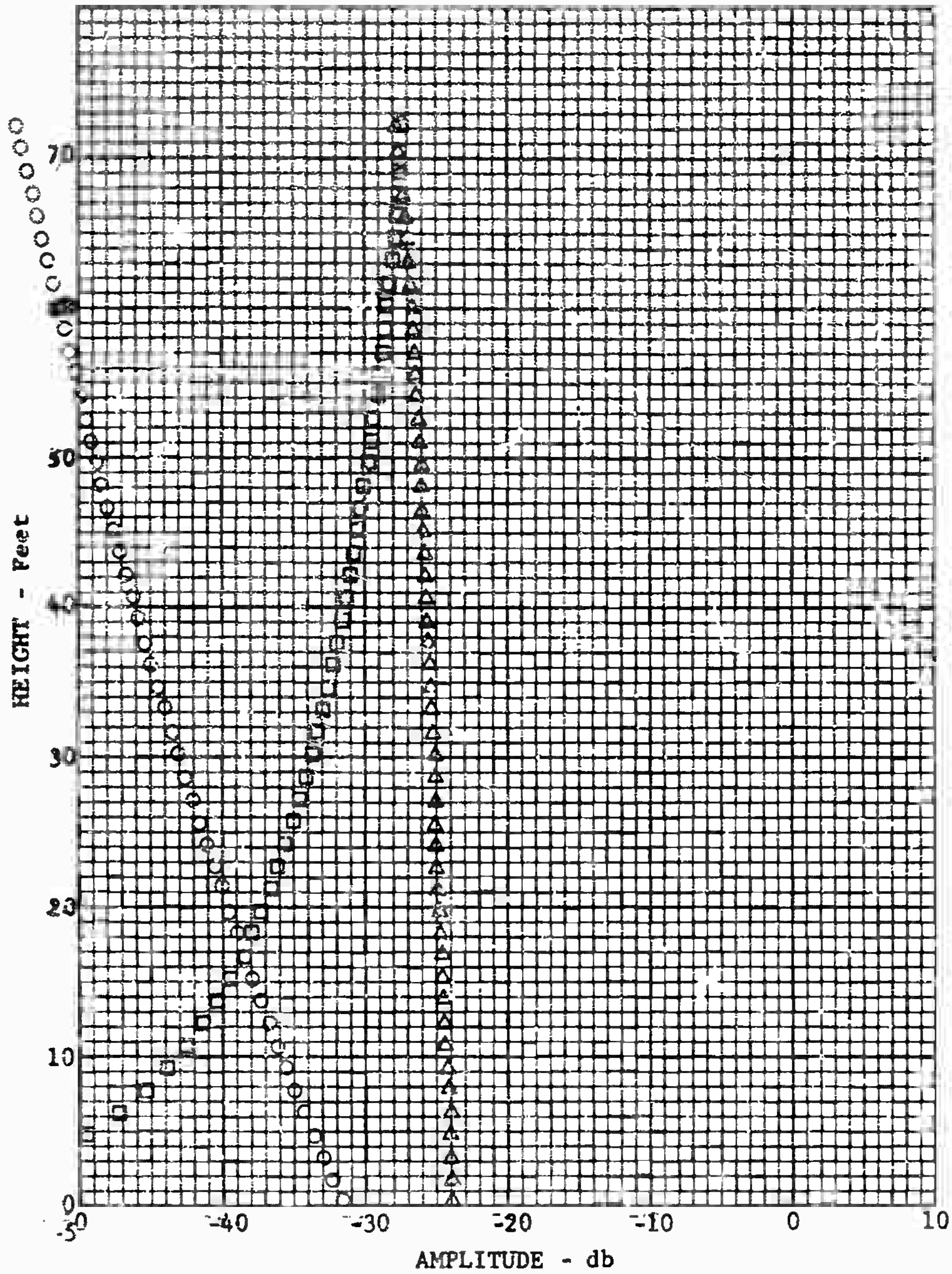

□ HORIZONTAL

△ TOTAL VERTICAL

○ SURFACE

RANGE - Feet	328.10
ANTENNA HEIGHT - Meters	4.998720
FREQUENCY - Megacycles	30.0
SIGMA - mhos/Meter	.610
EPSILON	14.48

Fig. 50 AMPLITUDE FOR 30 MHz FREQUENCY

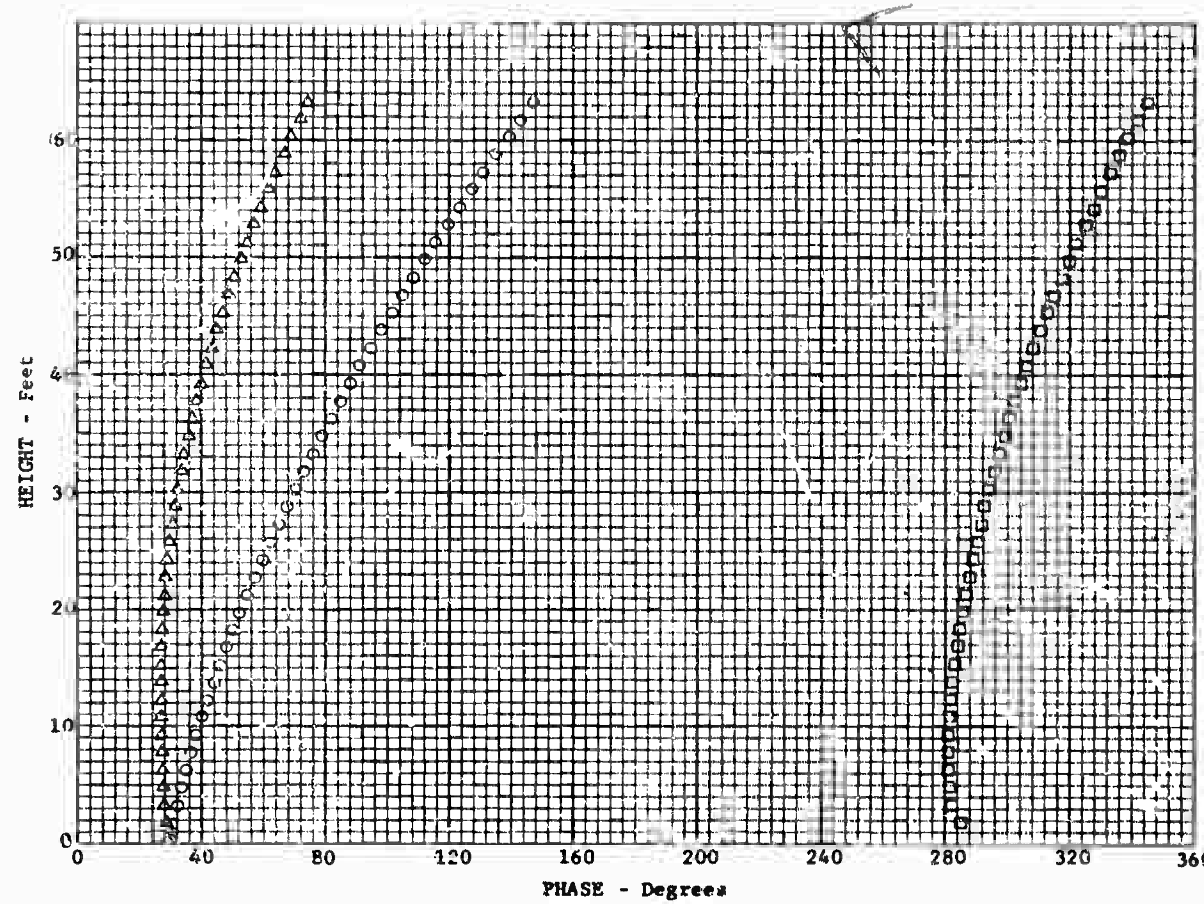

□ HORIZONTAL
△ TOTAL VERTICAL
○ SURFACE

RANGE - Feet	328.10
ANTENNA HEIGHT - Meters	4.998720
FREQUENCY - Megacycles	30.0
SIGMA - mhos/Meter	.610
EPSILON	14.48

Fig. 51 PHASE FOR 30 MHz FREQUENCY

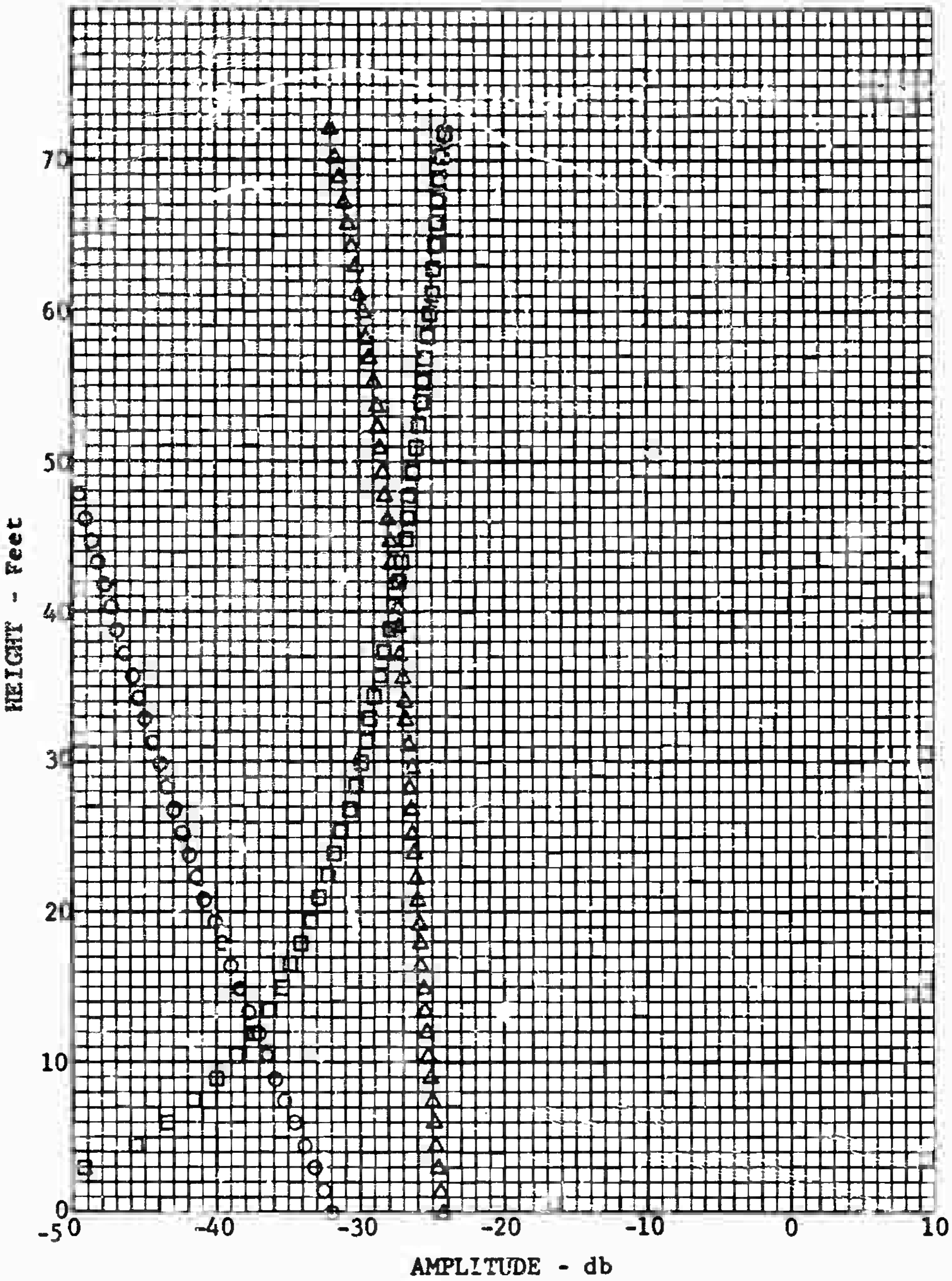

□ HORIZONTAL
△ TOTAL VERTICAL
○ SURFACE

RANGE - Feet	328.10
ANTENNA HEIGHT - Meters	4.998720
FREQUENCY - Megacycles	45.0
SIGMA - mhos/Meter	.610
EPSILON	14.48

Fig. 52 AMPLITUDE FOR 45 MHz FREQUENCY

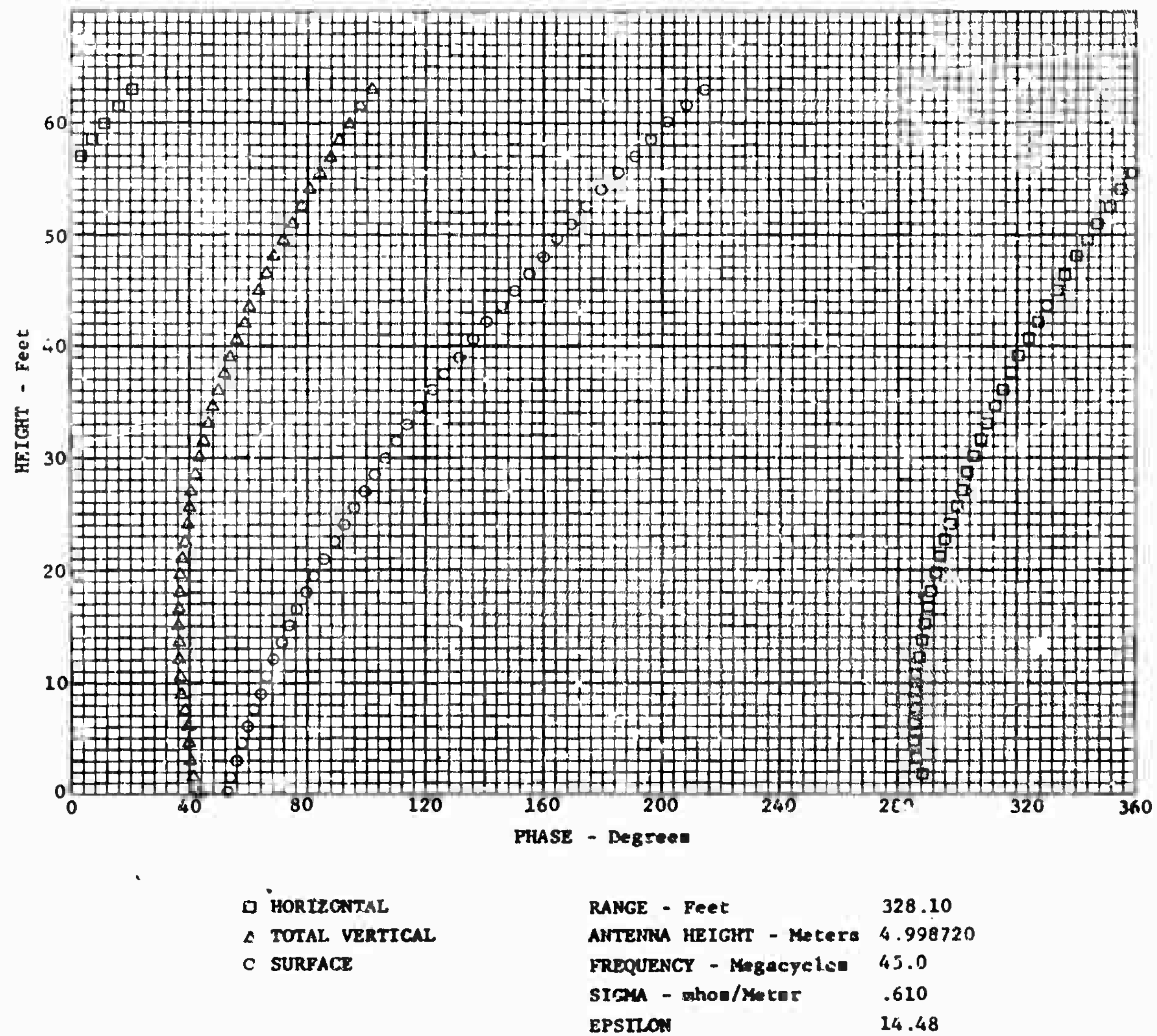

Fig. 53 PHASE FOR 45 MHz FREQUENCY

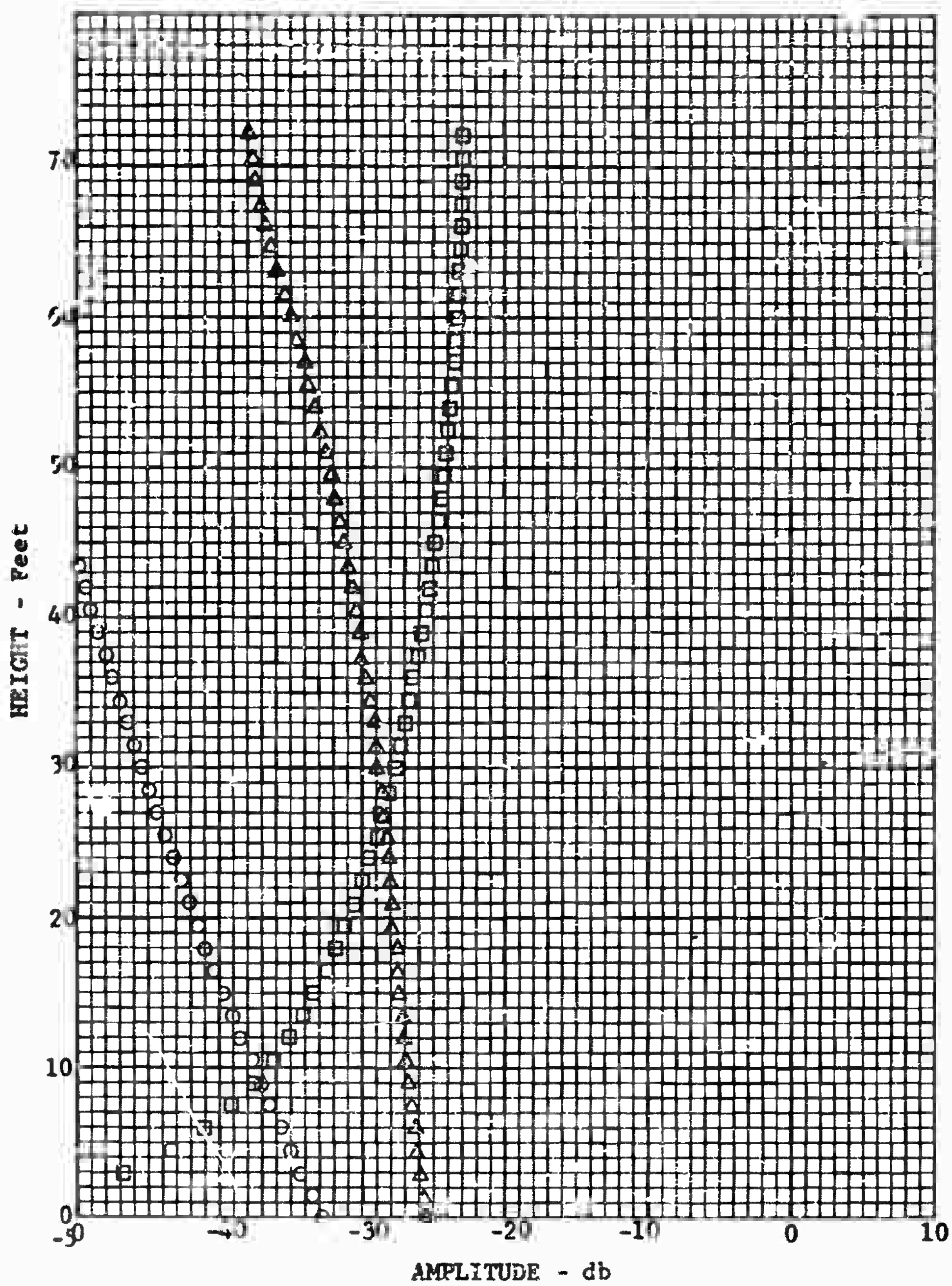

□ HORIZONTAL
△ TOTAL VERTICAL
○ SURFACE

RANGE - Feet	328.10
ANTENNA HEIGHT - Meters	4.998720
FREQUENCY - Megacycles	60.0
SIGMA - mhos/Meter	.610
EPSILON	14.48

Fig. 54 AMPLITUDE FOR 60 MHz FREQUENCY

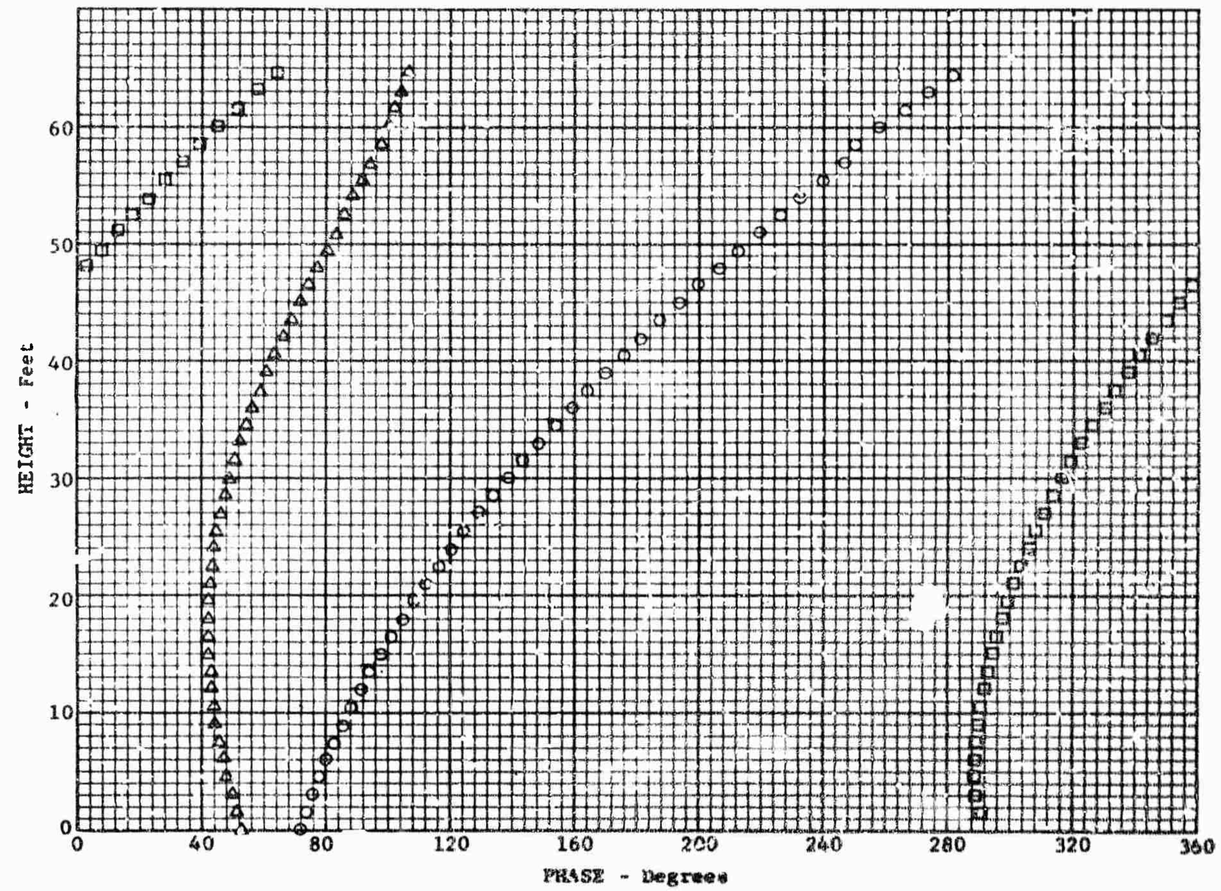

□ HORIZONTAL
△ TOTAL VERTICAL
○ SURFACE

RANGE - Feet	328.10
ANTENNA HEIGHT - Meters	4.998720
FREQUENCY - Megacycles	60.0
SIGMA - mhos/Meter	.610
EPSILON	14.48

Fig. 55 PHASE FOR 60 MHz FREQUENCY

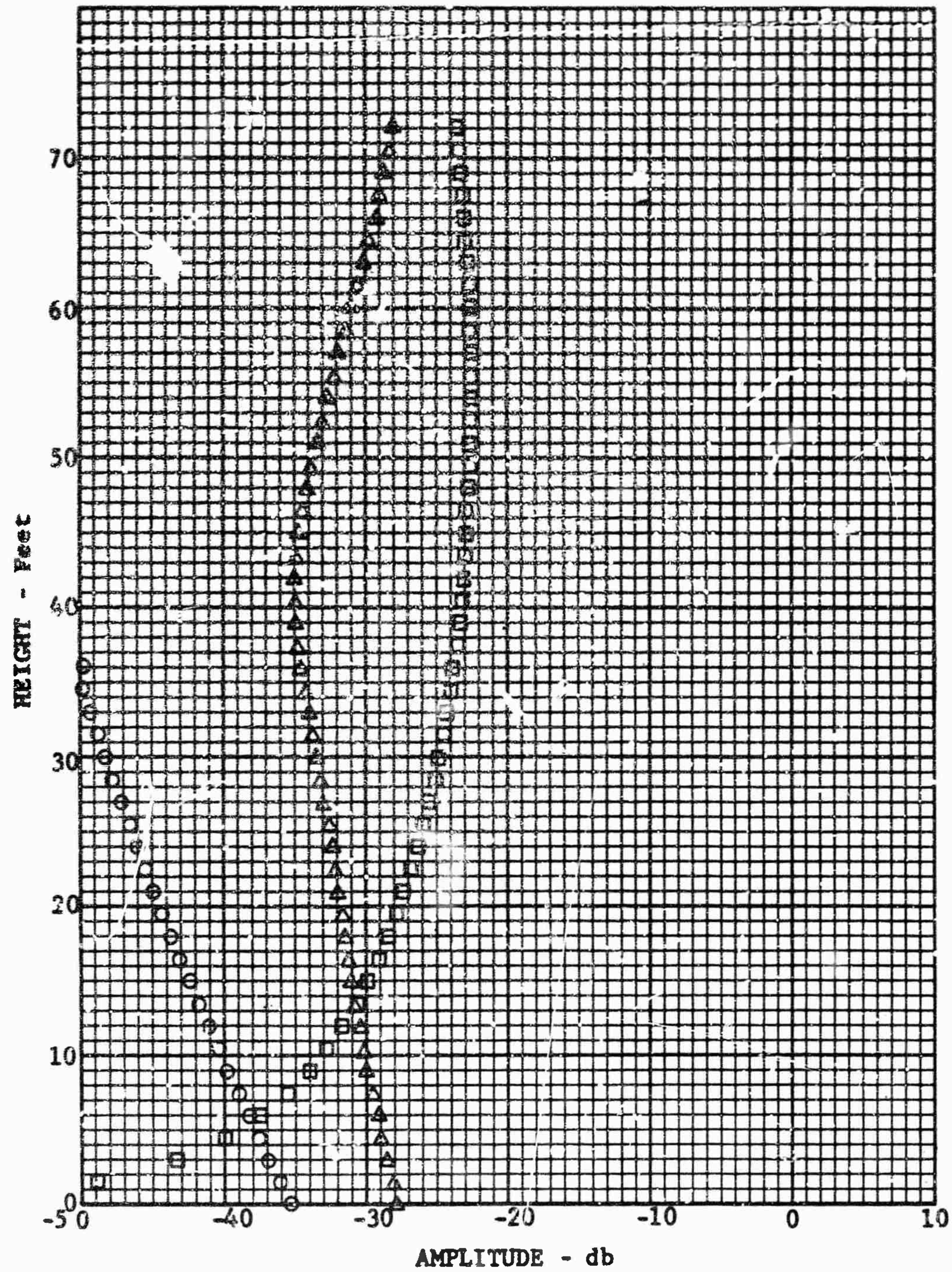

□ HORIZONTAL

△ TOTAL VERTICAL

○ SURFACE

RANGE - Feet	328.10
ANTENNA HEIGHT - Meters	4.998720
FREQUENCY - Megacycles	90.0
SIGMA - mhos/Meter	.610
EPSILON	14.48

Fig. 56 AMPLITUDE FOR 90 MHz FREQUENCY

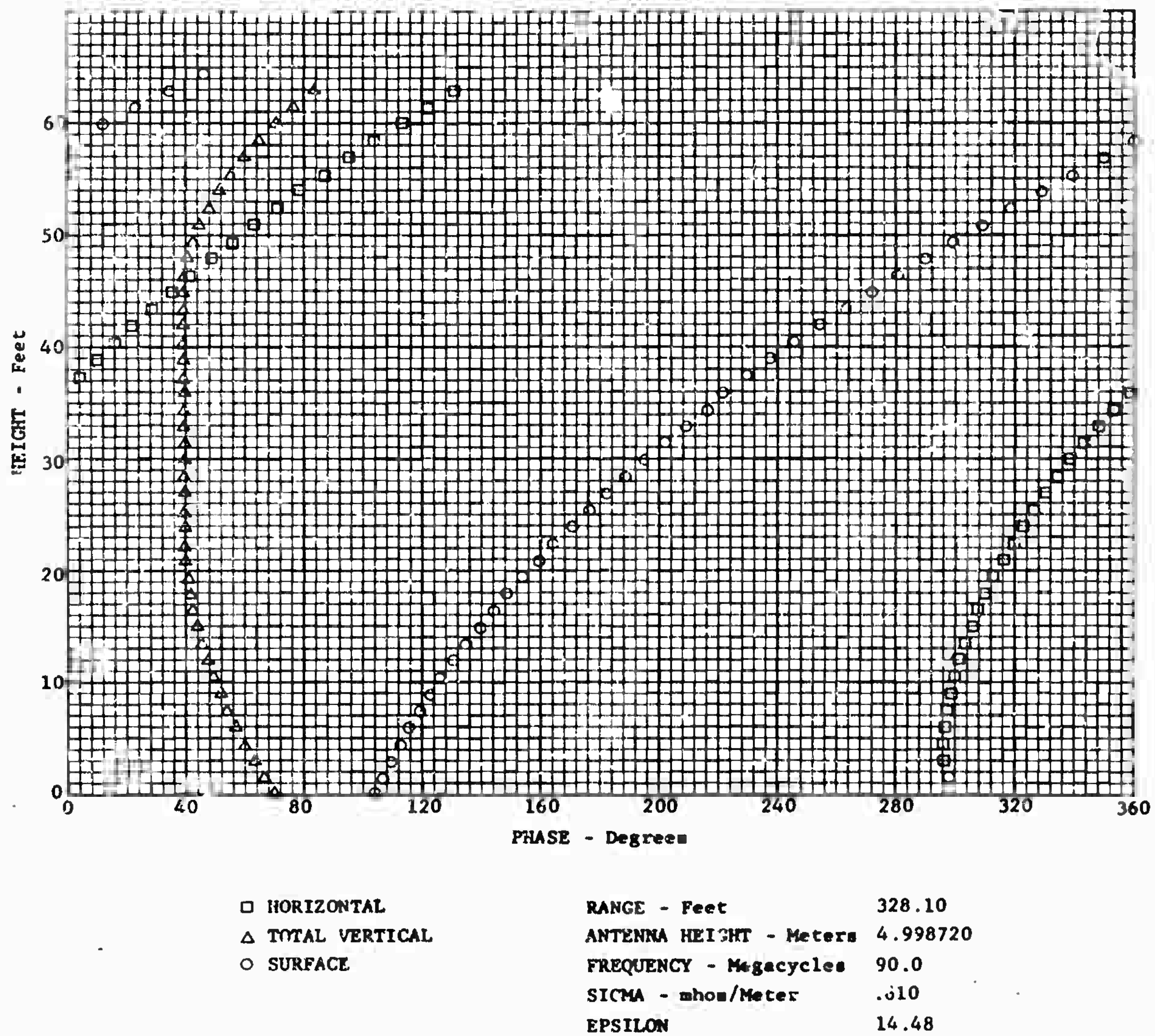

Fig. 57 PHASE FOR 90 MHz FREQUENCY

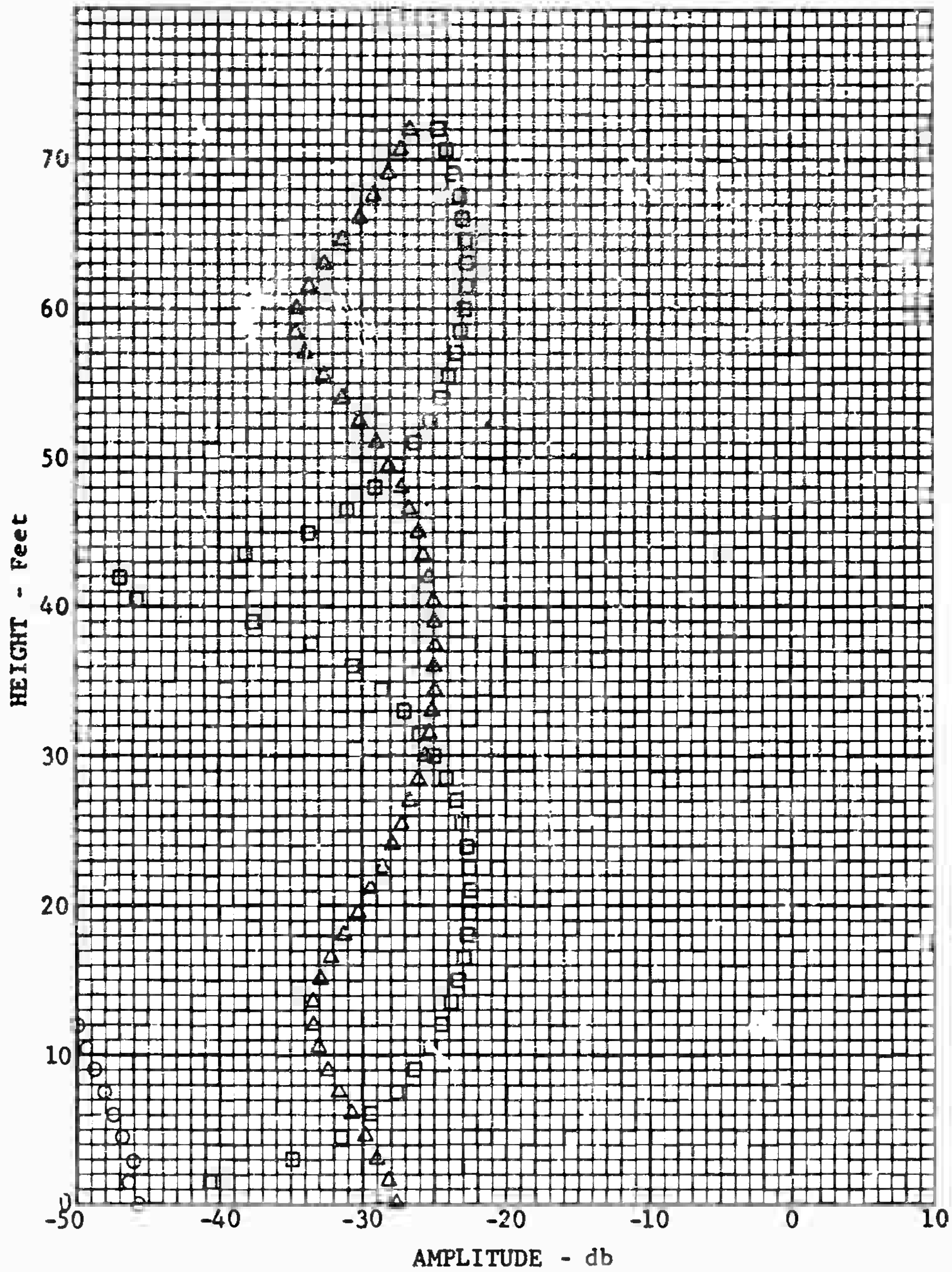

□ HORIZONTAL
△ TOTAL VERTICAL
○ SURFACE

RANGE - Feet	328.10
ANTENNA HEIGHT - Meters	9.997440
FREQUENCY - Megacycles	120.0
SIGMA - mhos/Meter	.610
EPSILON	14.48

Fig. 58 AMPLITUDE FOR 120 MHz FREQUENCY

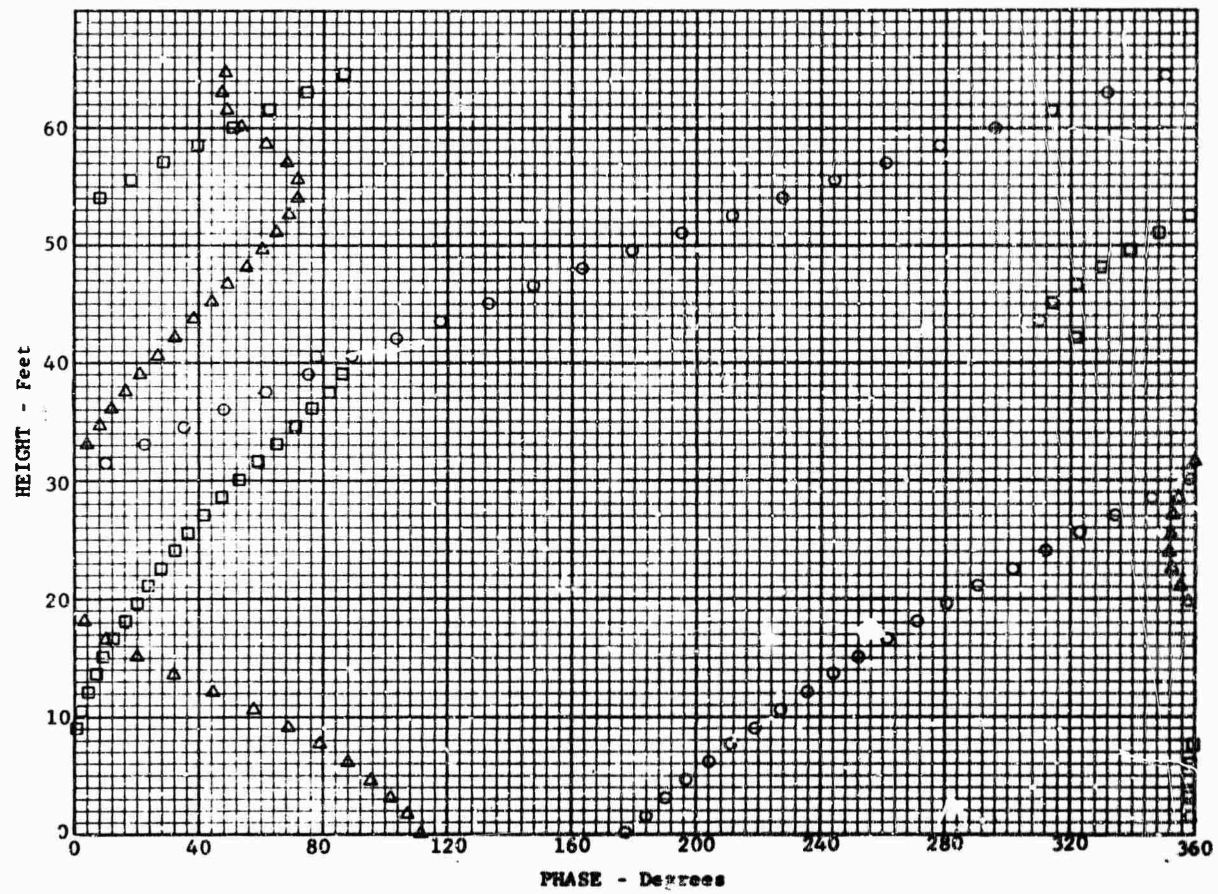

□ HORIZONTAL
△ TOTAL VERTICAL
○ SURFACE

RANGE - Feet	328.10
ANTENNA HEIGHT - Meters	9.997440
FREQUENCY - Megacycles	120.0
SIGMA - mhos/Meter	.610
EPSILON	14.48

Fig. 59 PHASE FOR 120 MHz FREQUENCY

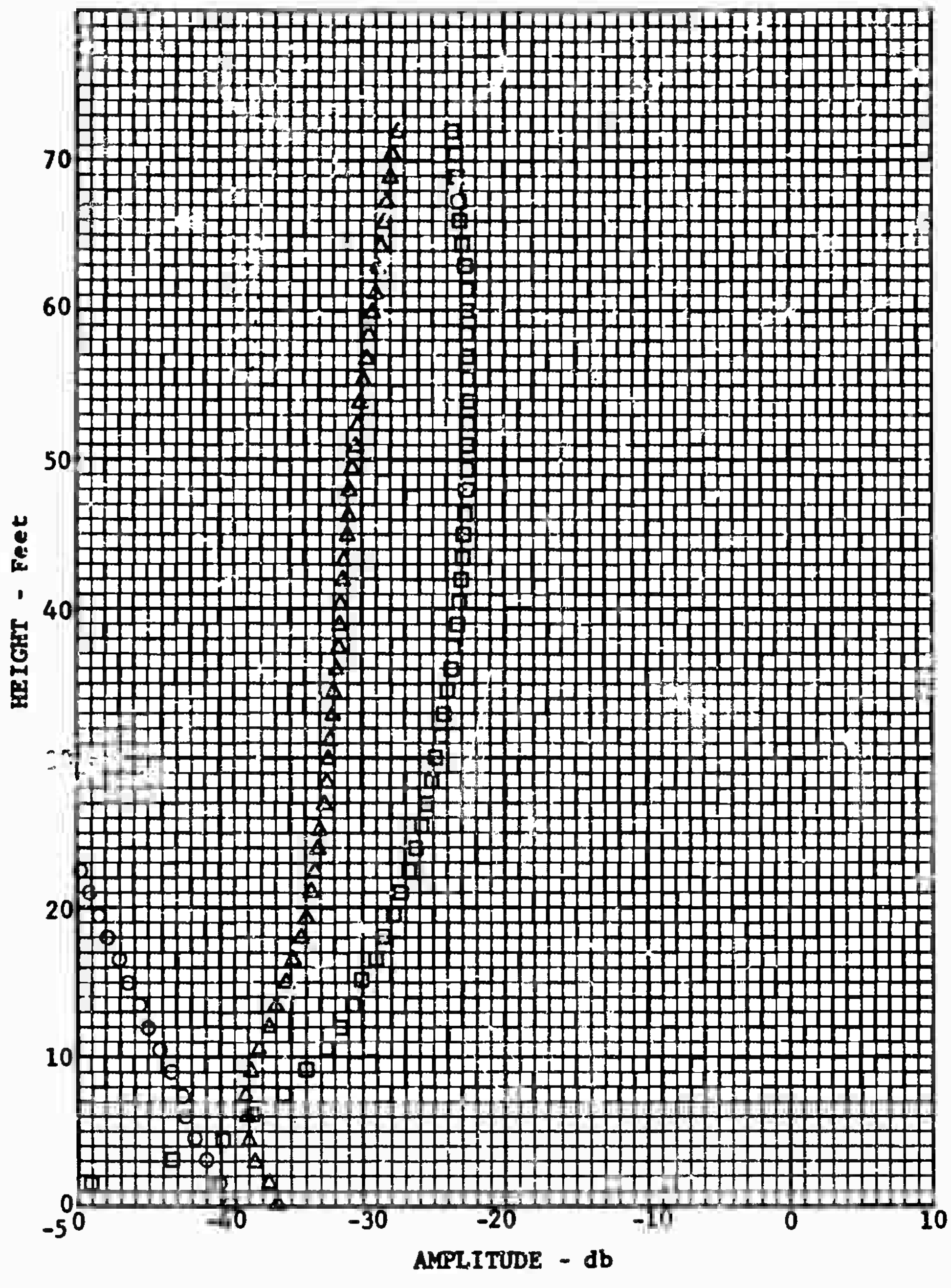

□ HORIZONTAL

△ TOTAL VERTICAL

○ SURFACE

RANGE - Feet	328.10
ANTENNA HEIGHT - Meters	2.499360
FREQUENCY - Megacycles	180.0
SIGMA - mhos/Meter	.010
EPSILON	14.48

Fig. 60 AMPLITUDE FOR 180 MHz FREQUENCY

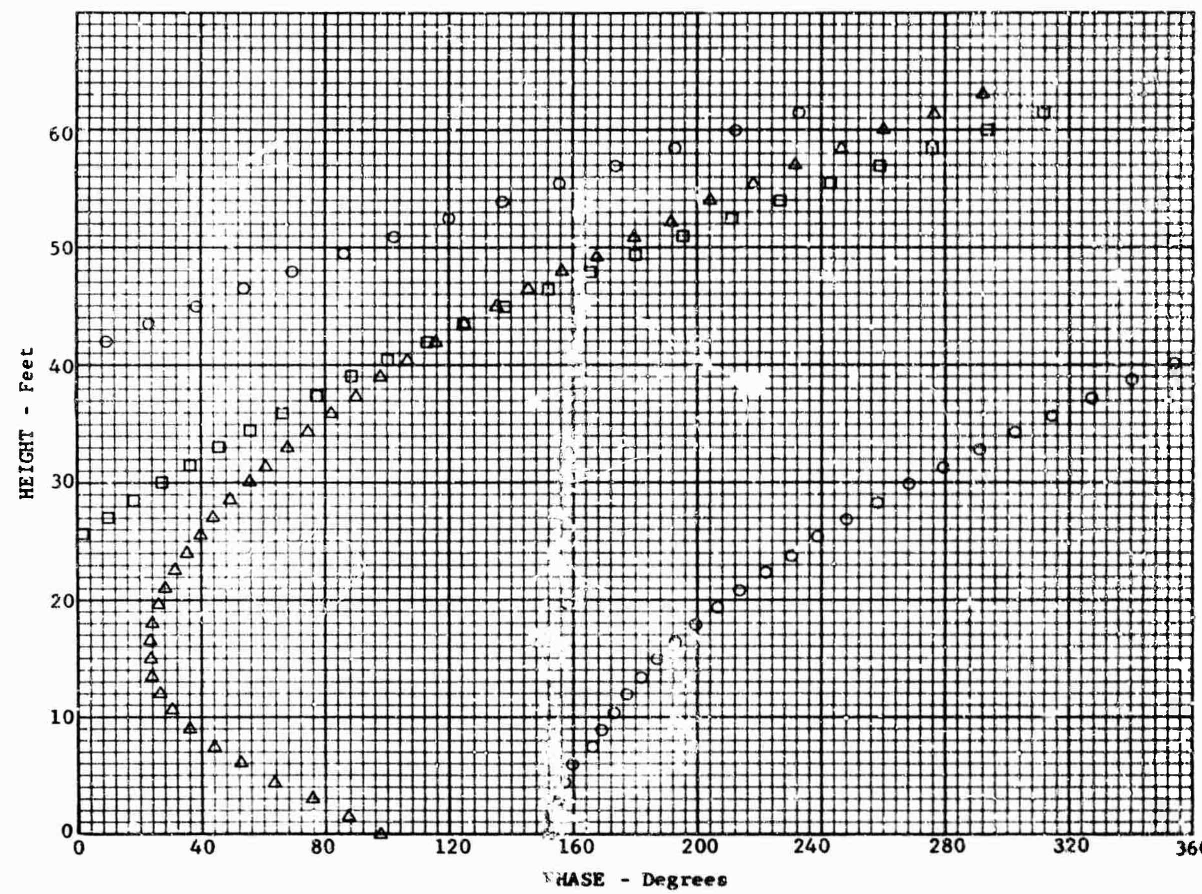

□ HORIZONTAL	
△ TOTAL VERTICAL	
○ SURFACE	

RANGE - Feet	328.10
ANTENNA HEIGHT - Meters	2.499360
FREQUENCY - Megacycles	180.0
SIGMA - mhos/Meter	.610
EPSILON	14.43

Fig. 61 PHASE FOR 180 MHz FREQUENCY

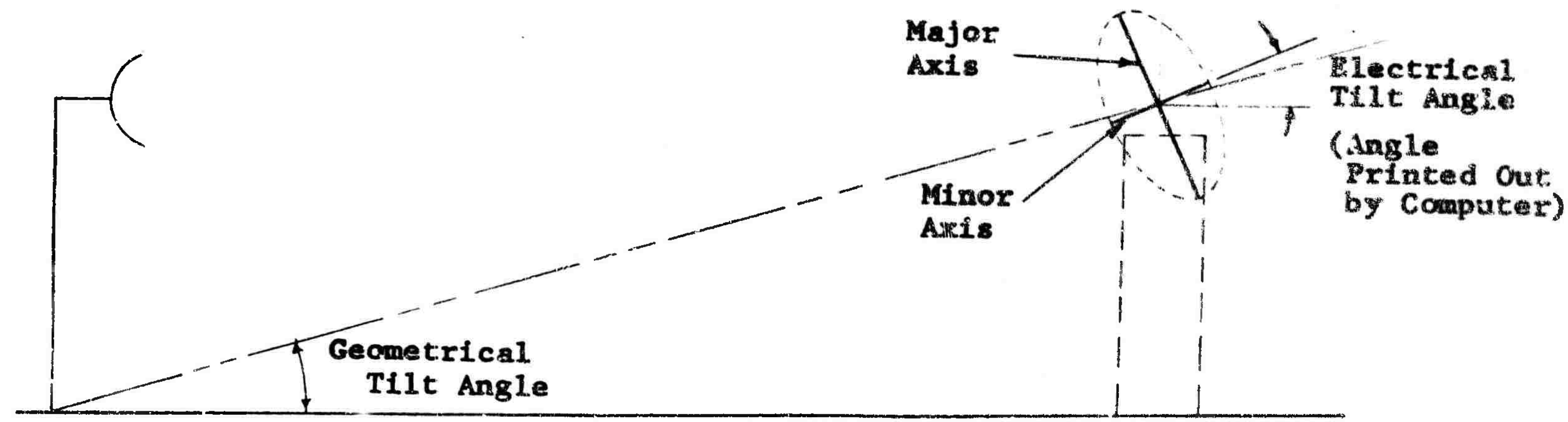

Fig. 62 ILLUSTRATION OF FIELD ELLIPTICITY

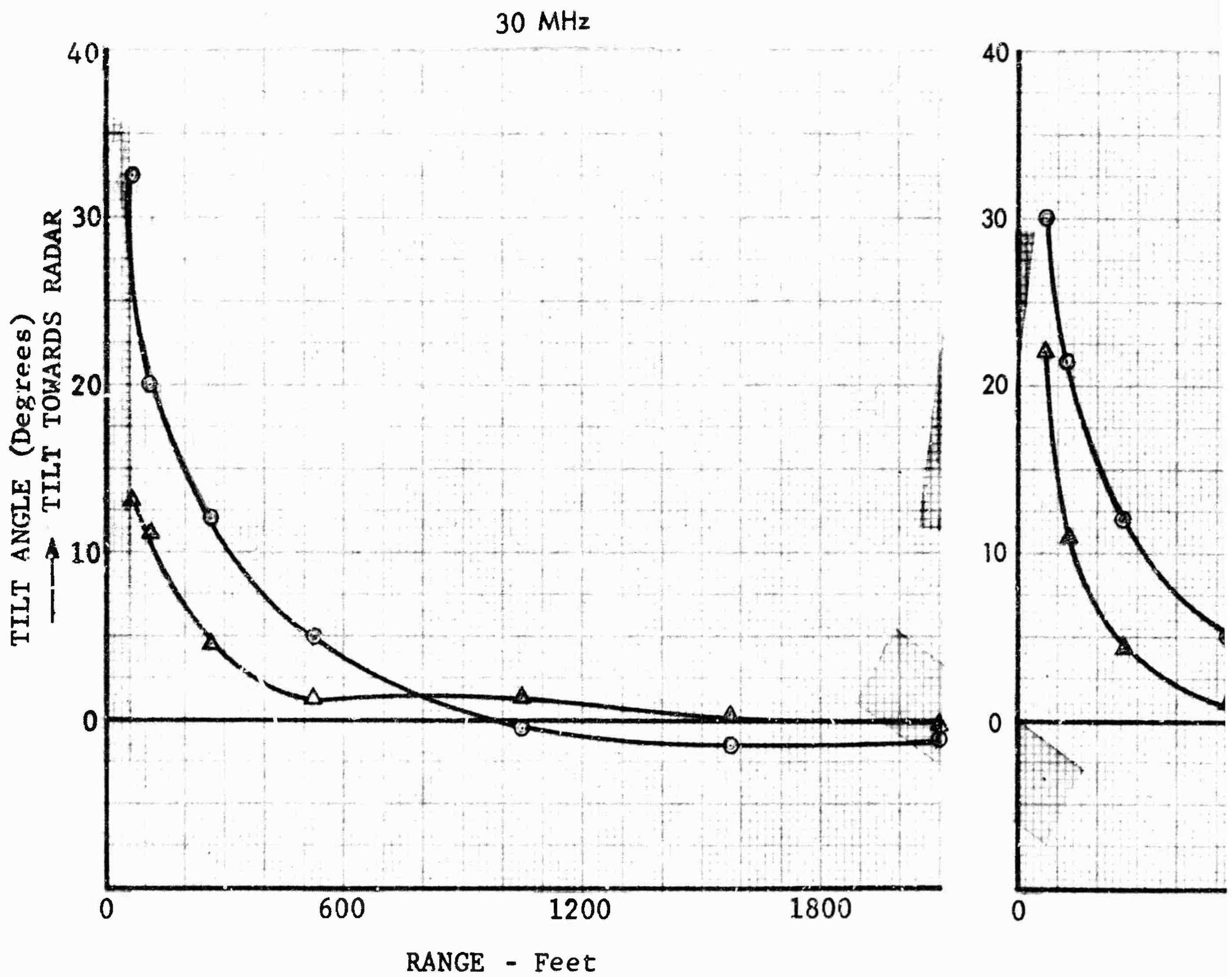
30 MHz
40
30
20
10
0
TILT ANGLE (Degrees)
TILT TOWARDS RADAR
0
600
1200
1800
RANGE - Feet
40
30
20
10
0
0

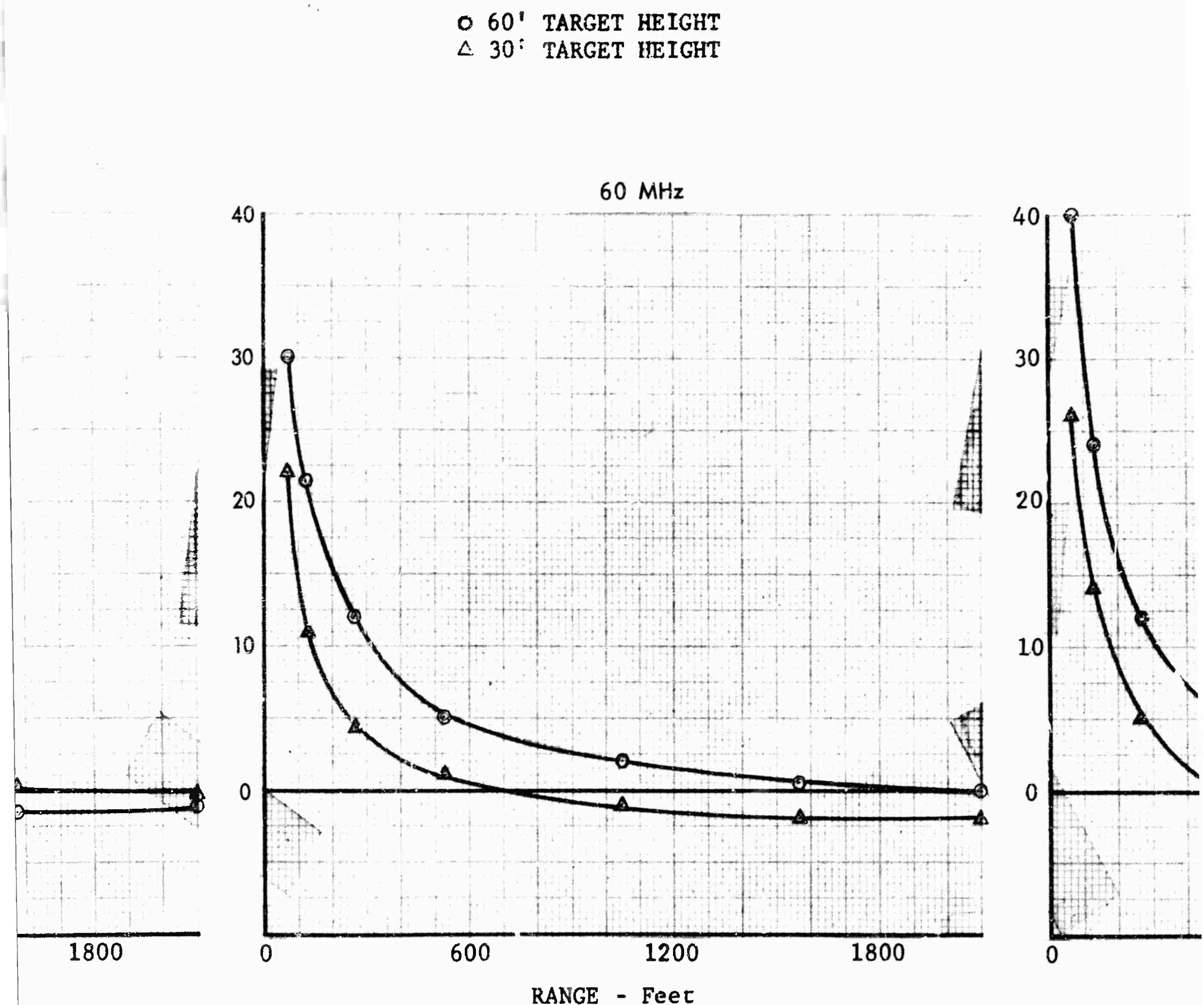

o 60' TARGET HEIGHT
△ 30' TARGET HEIGHT
60 MHz
40
30
20
10
0
1800
0
600
1200
1800
RANGE - Feet

Fig. 63

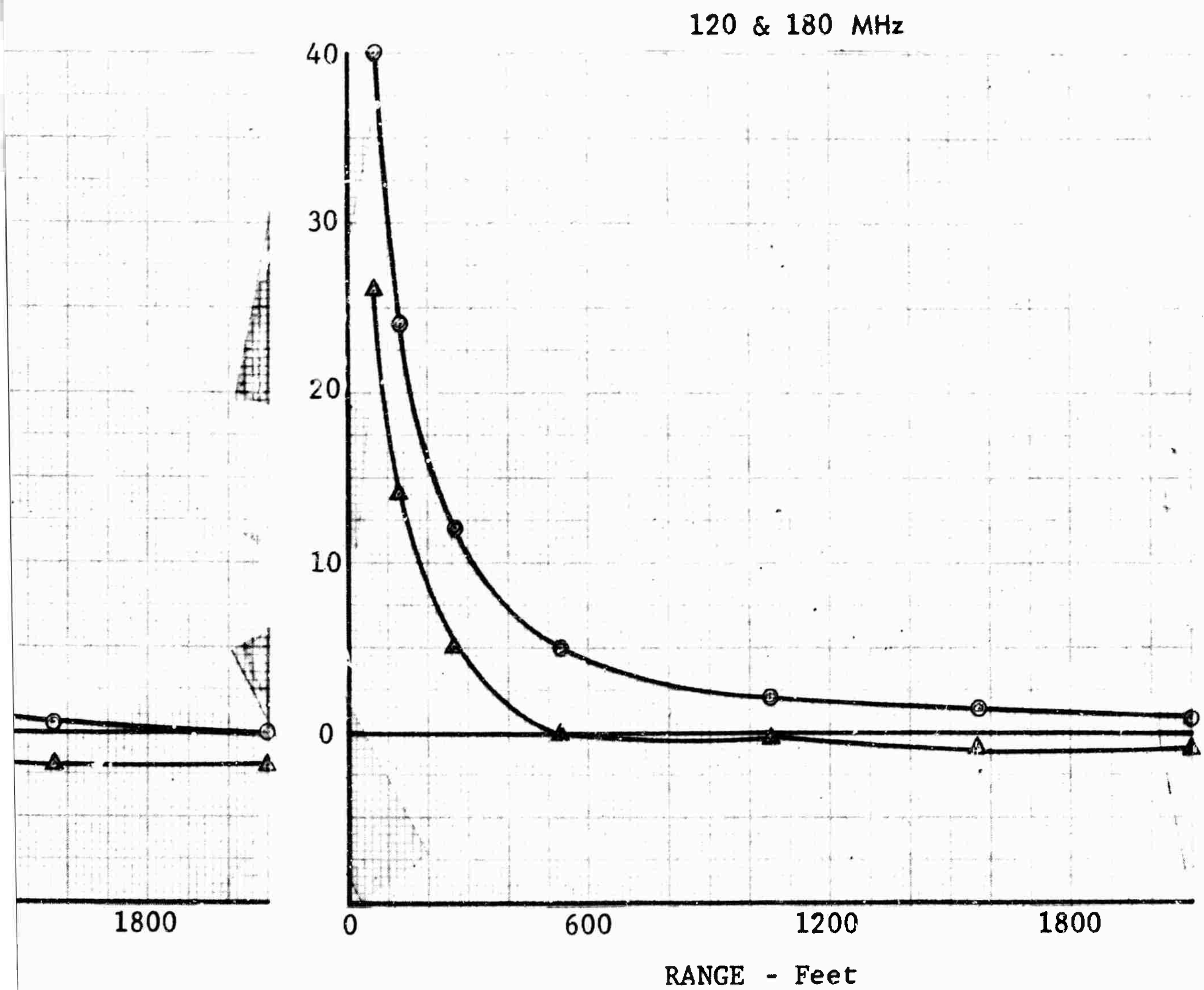

Fig. 63 TILT ANGLE AS A FUNCTION OF RANGE
(VERTICAL POLARIZATION)

3

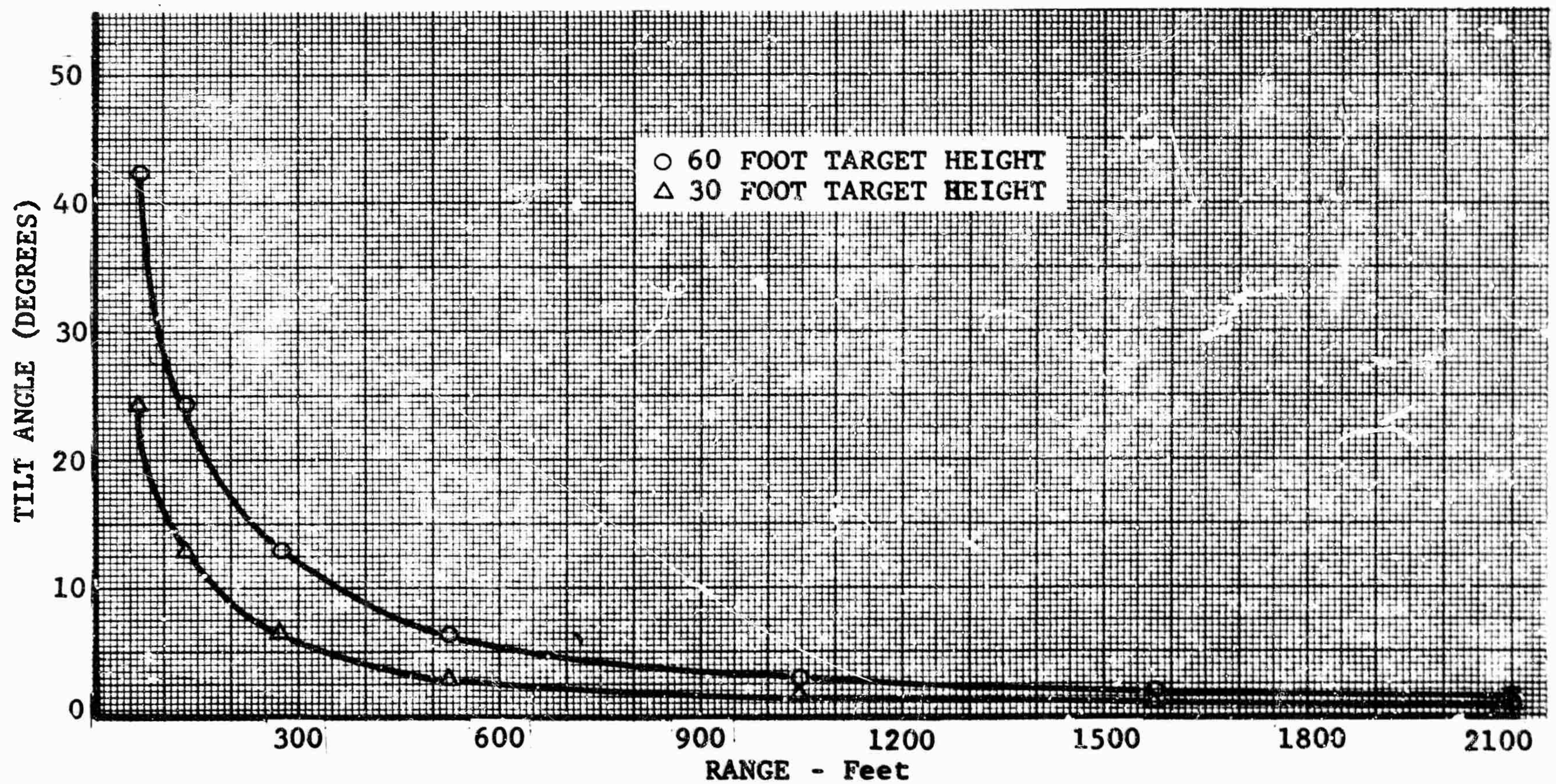

Fig. 64 TILT ANGLE VERSUS RANGE (HORIZONTAL POLARIZATION)

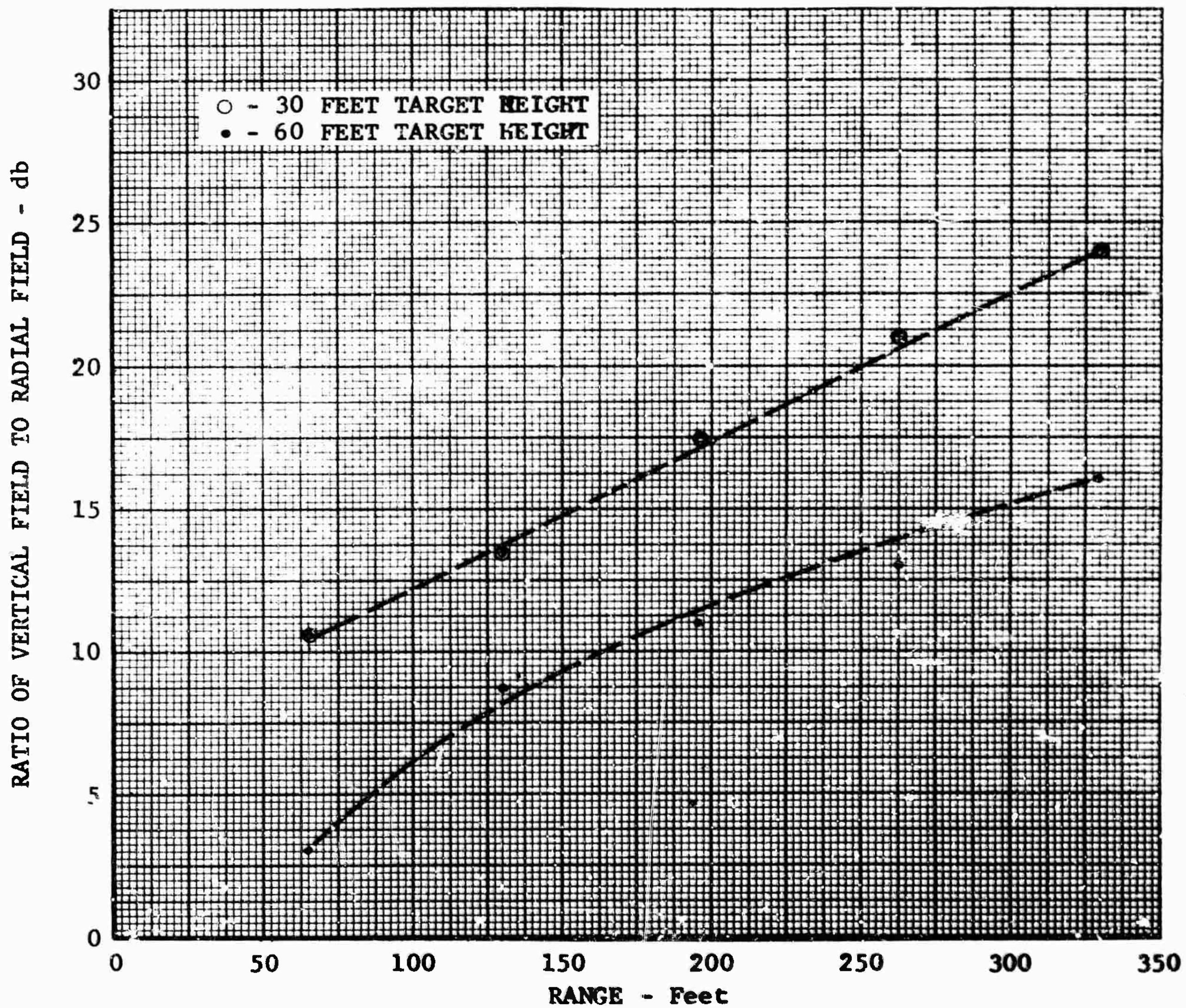

Fig. 65 AXIAL RATIO VERSUS RANGE (30 MHz)

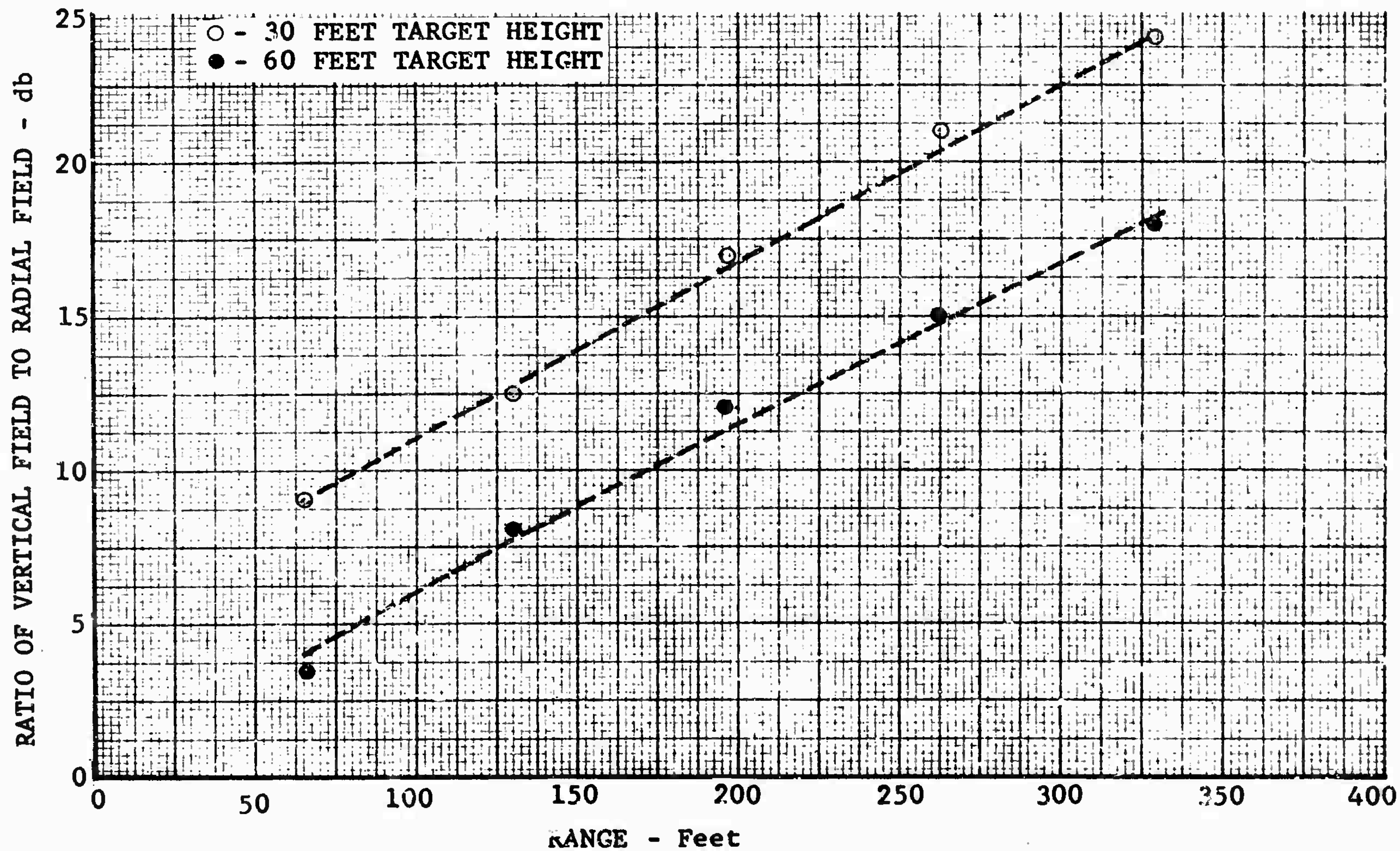

Fig. 66 AXIAL RATIO VERSUS RANGE (60 MHz)

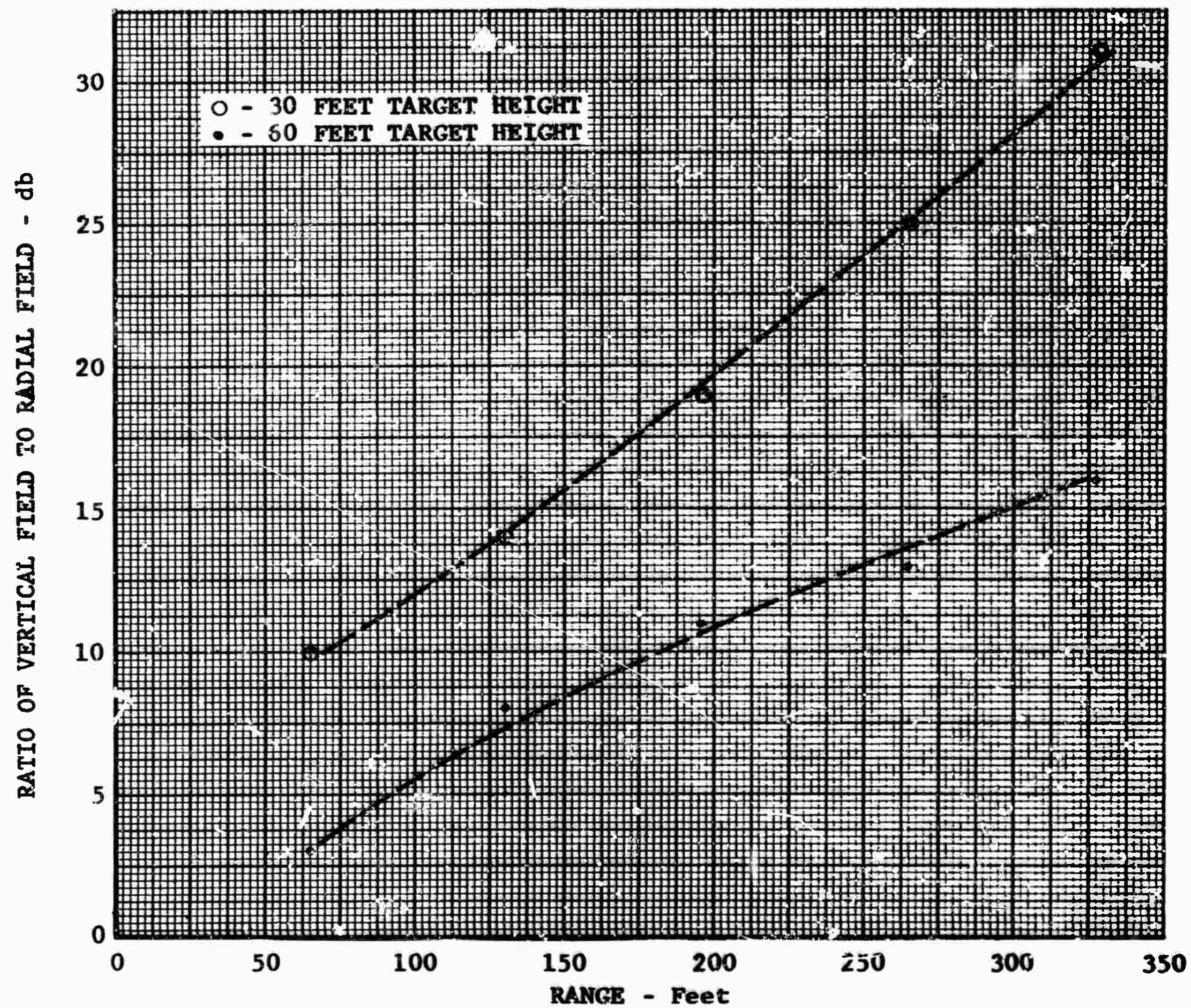

Fig. 67 AXIAL RATIO VERSUS RANGE (120 MHz)

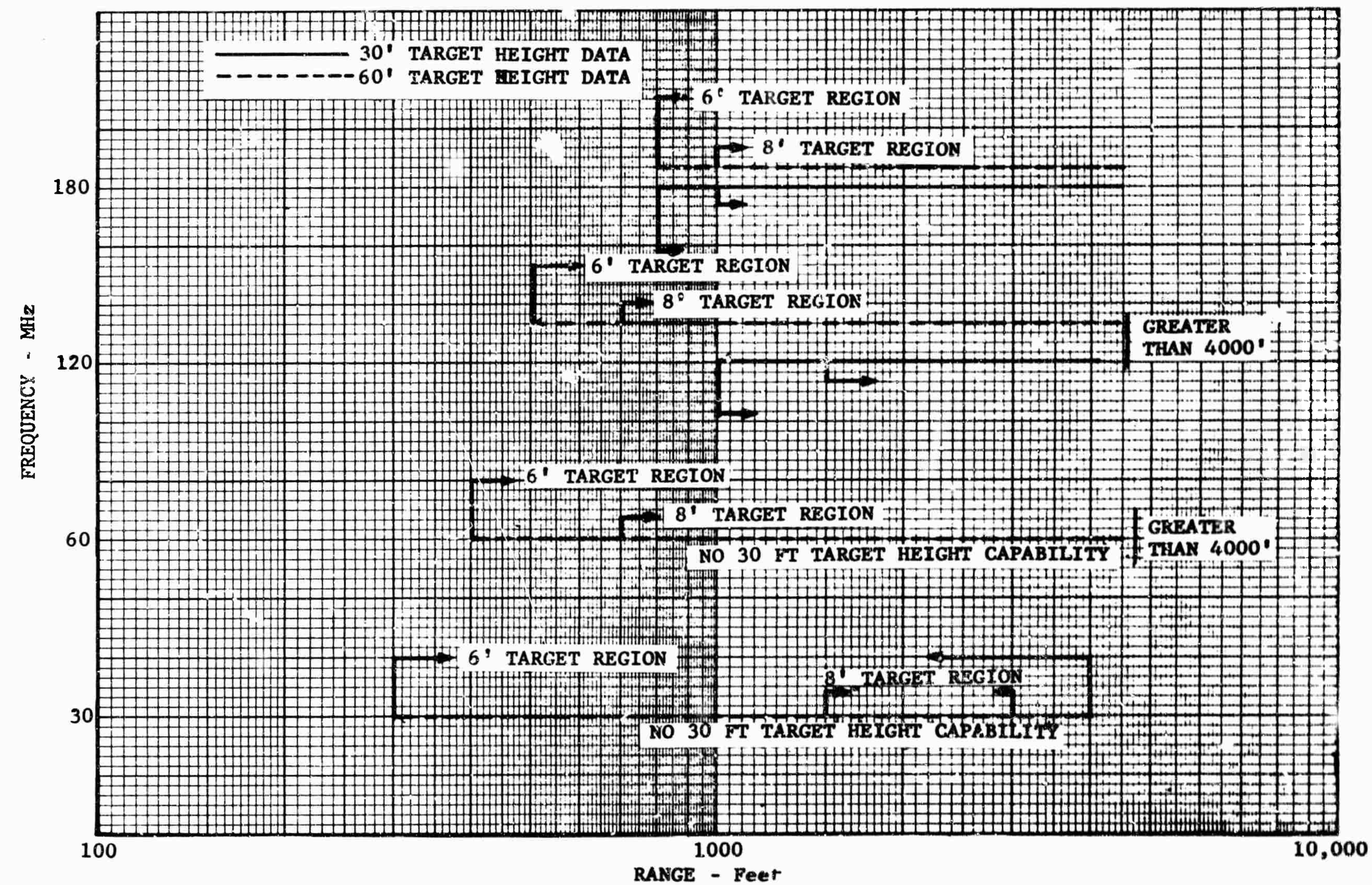

Fig. 38 OPERATING CONDITIONS FOR POLARIZATION VERSATILITY

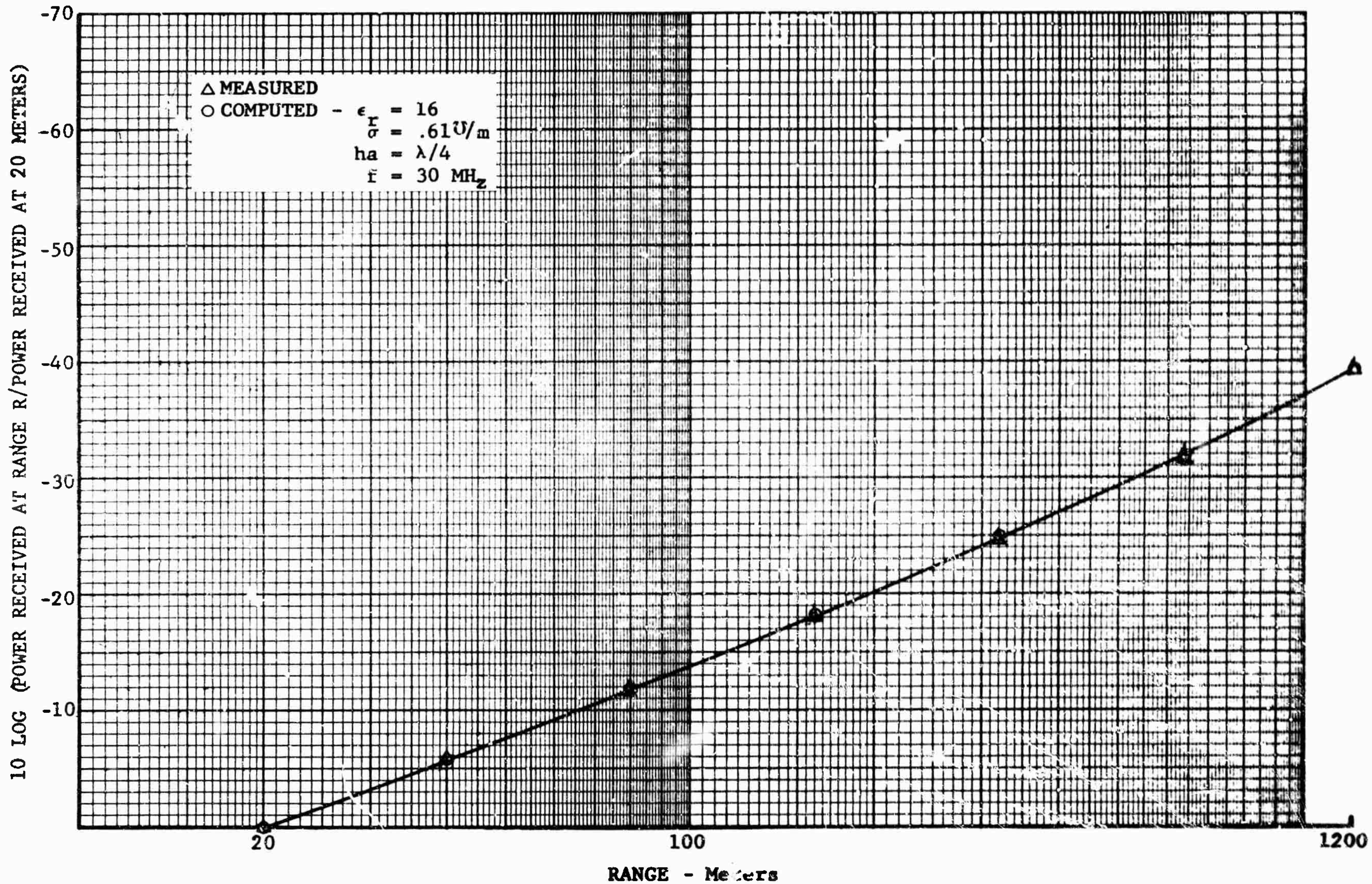

Fig. 69 MEASURED VERSUS COMPUTED SURFACE FIELD AMPLITUDE (30 MHz)

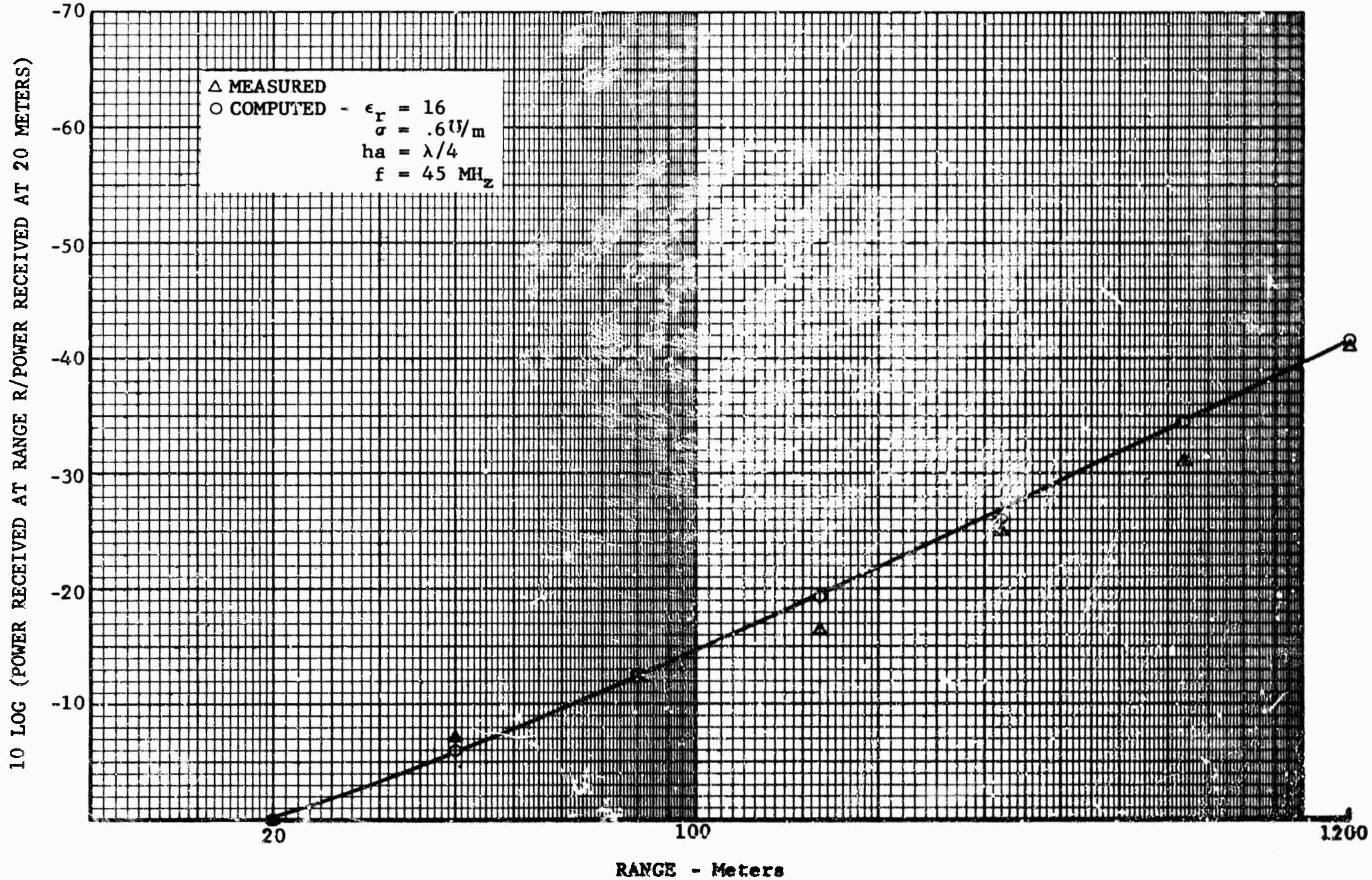

Fig. 70 MEASURED VERSUS COMPUTED SURFACE FIELD AMPLITUDE (45 MHz)

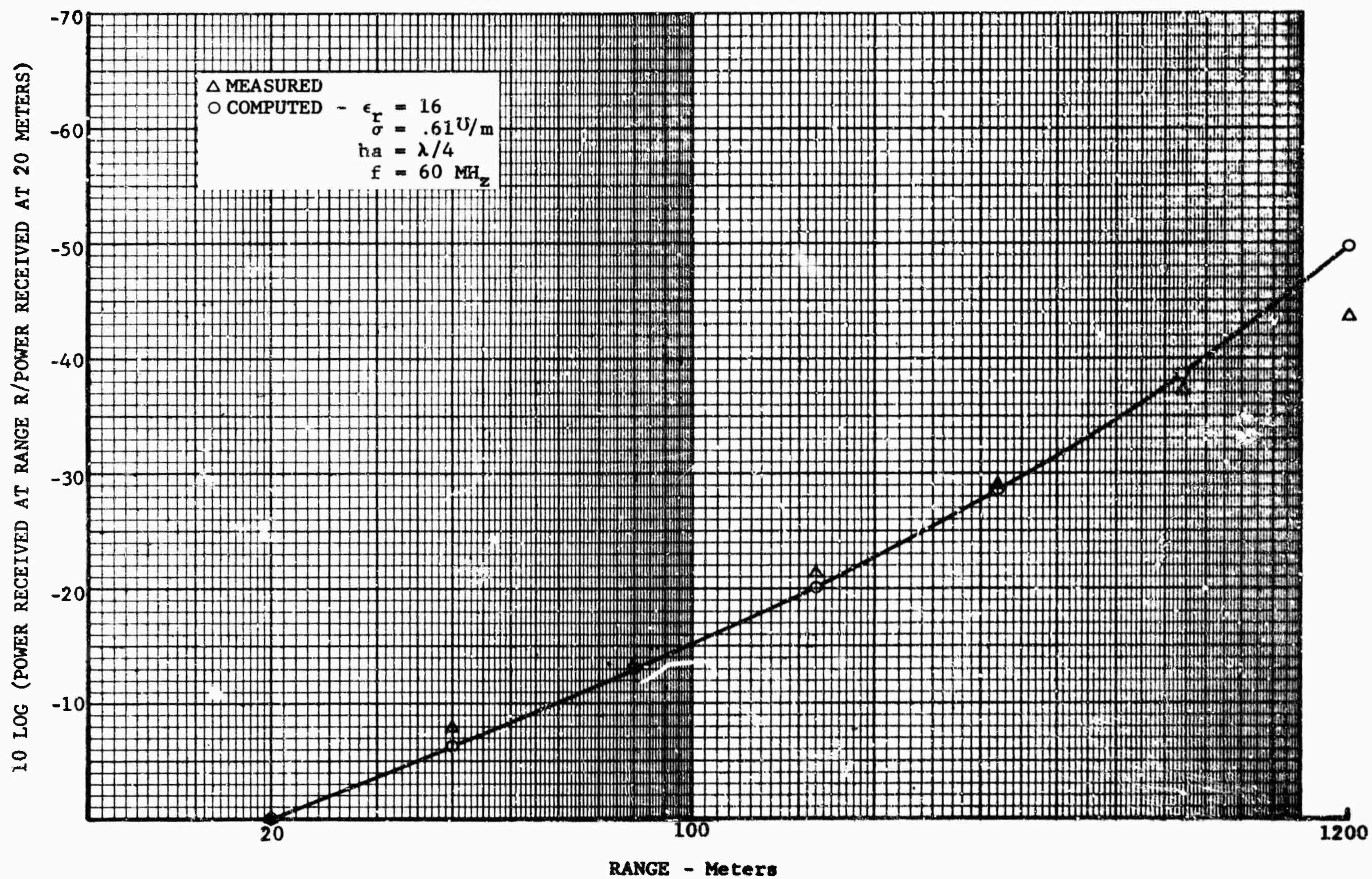

Fig. 71 MEASURED VERSUS COMPUTED SURFACE FIELD AMPLITUDE (60 MHz)

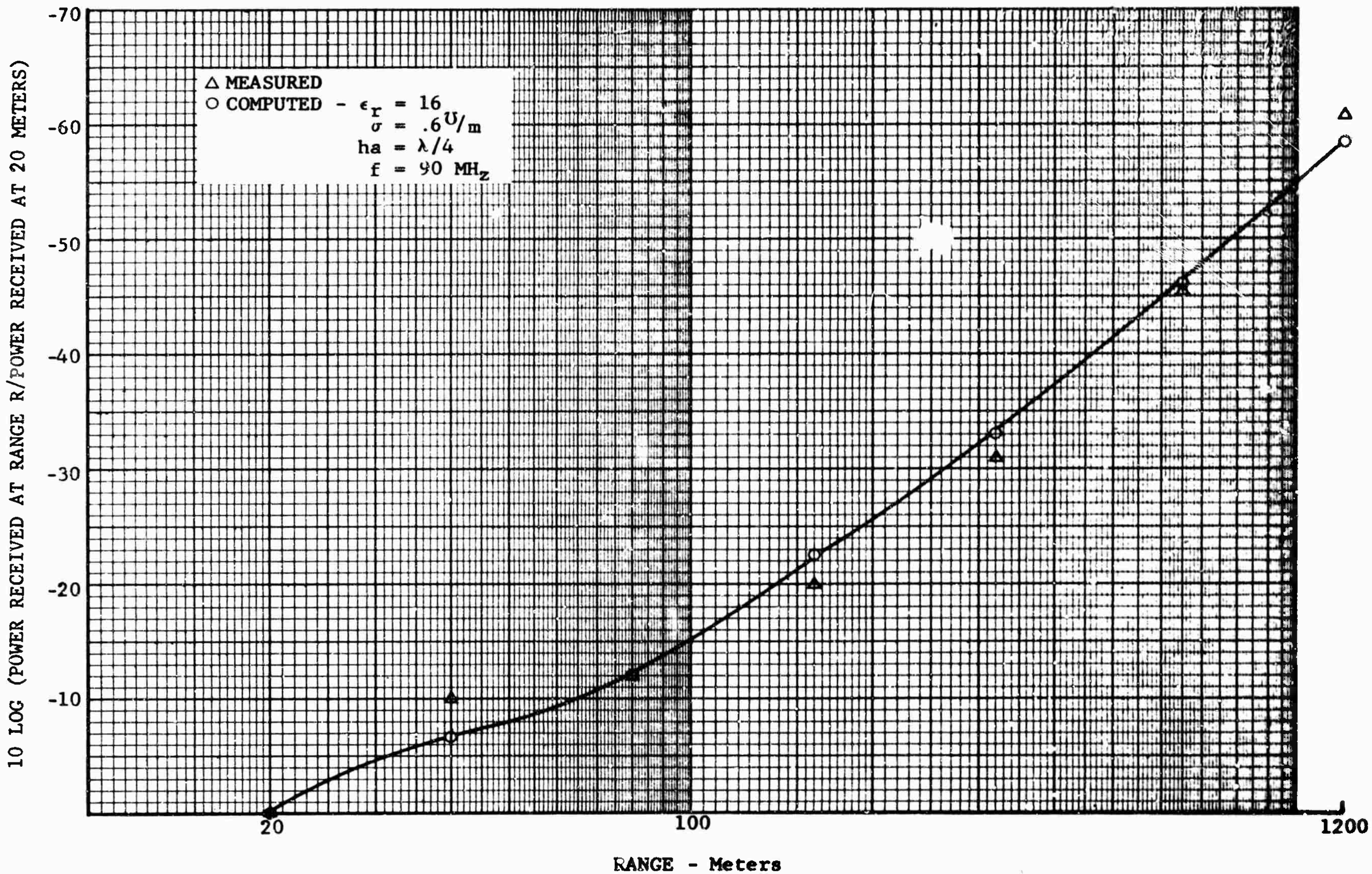

Fig. 72 MEASURED VERSUS COMPUTED SURFACE FIELD AMPLITUDE (90 MHz)

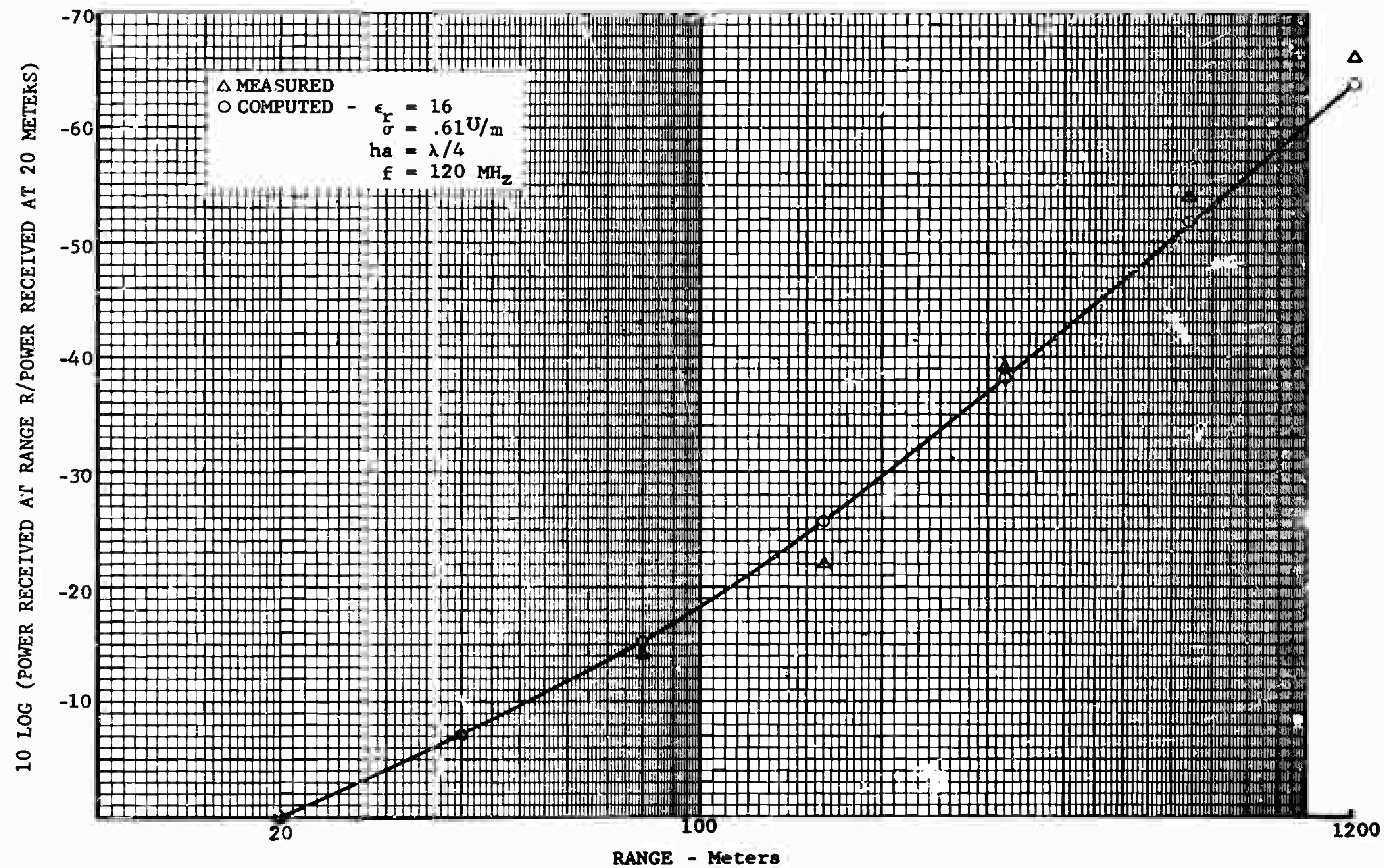

Fig. 73 MEASURED VERSUS COMPUTED SURFACE FIELD AMPLITUDE (120 MHz)

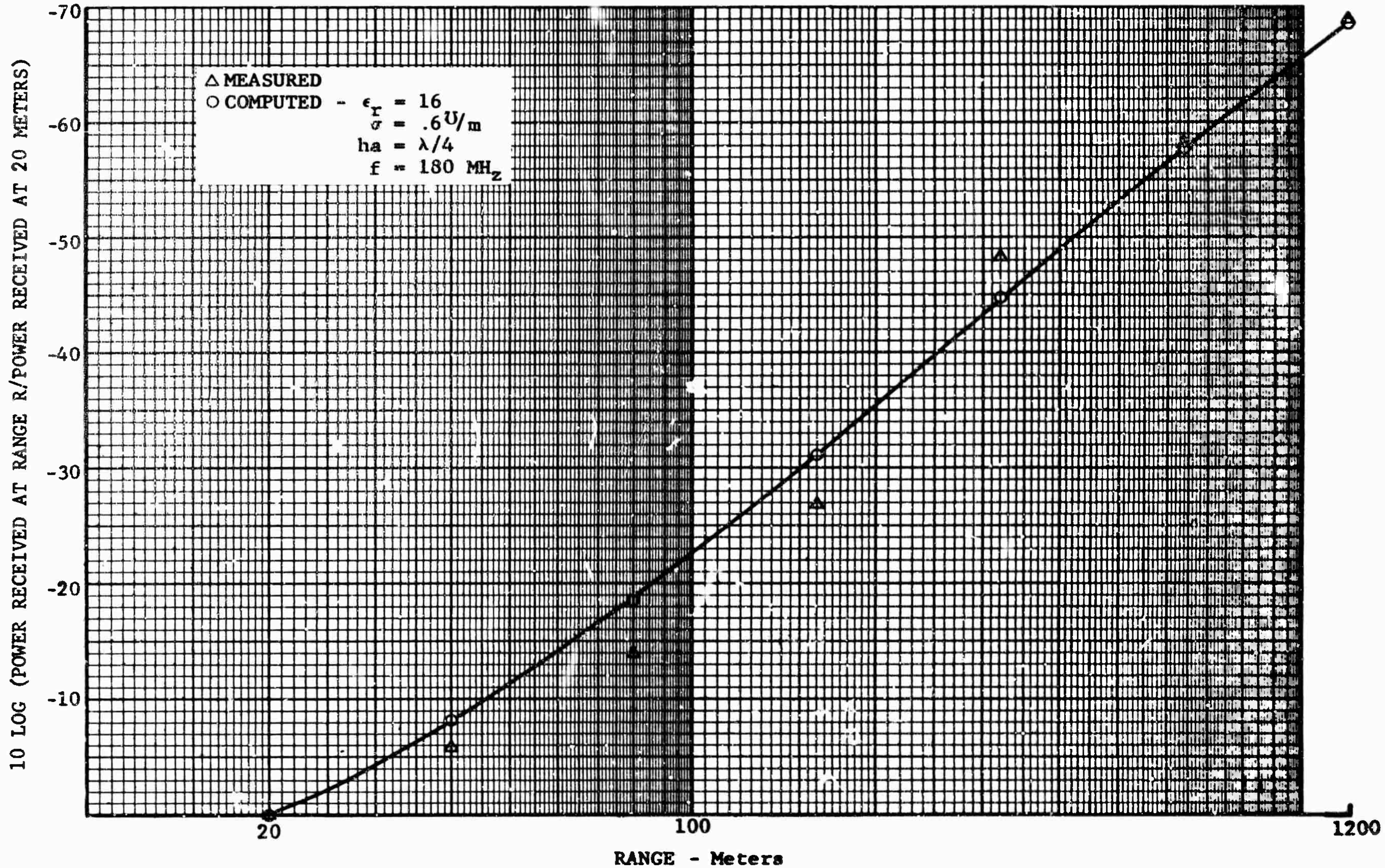

Fig. 74 MEASURED VERSUS COMPUTED SURFACE FIELD AMPLITUDE (180 MHz)

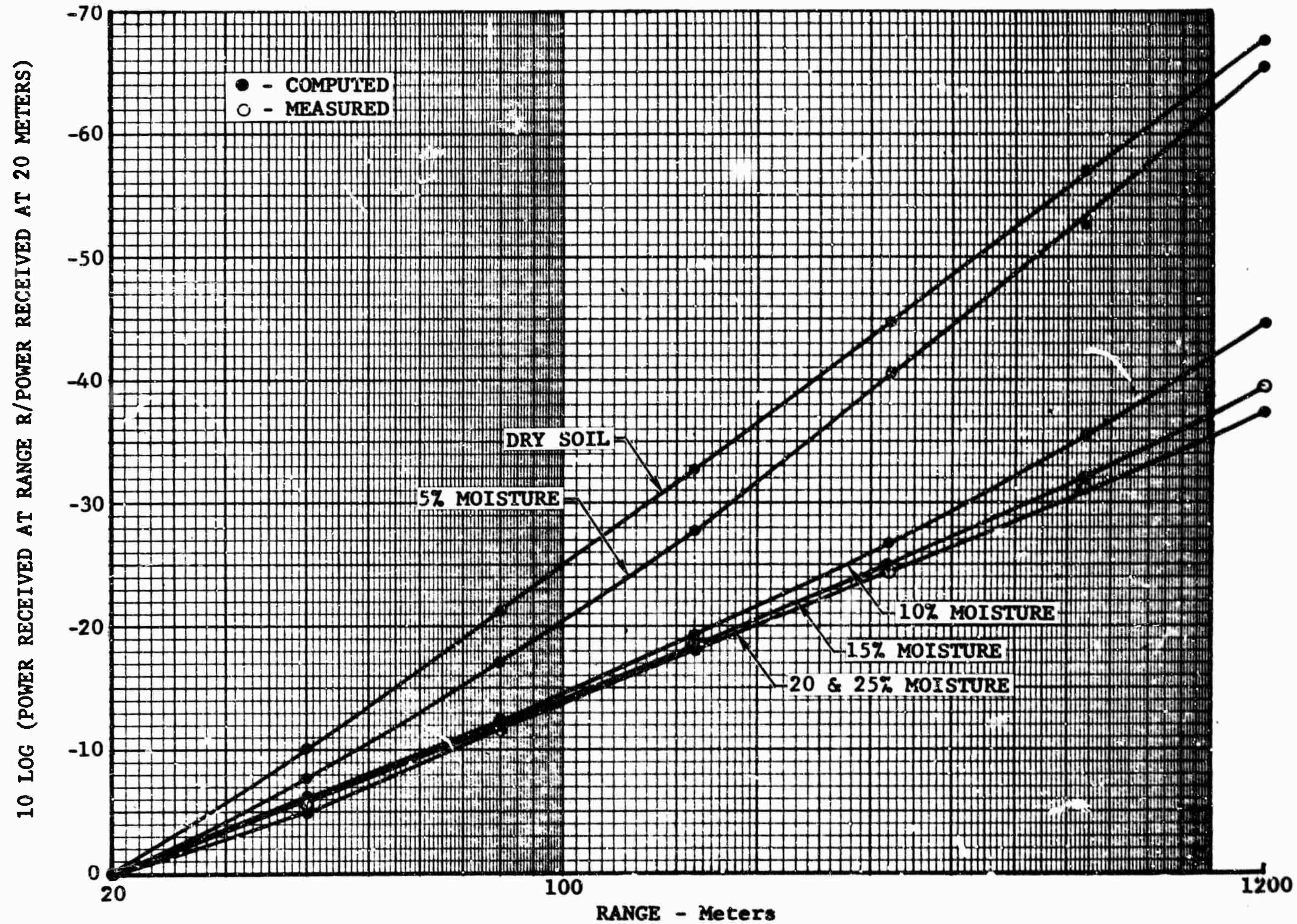

Fig. 75 SURFACE FIELD AMPLITUDE RANGE VARIATION WITH SOIL MOISTURE (30 MHz)

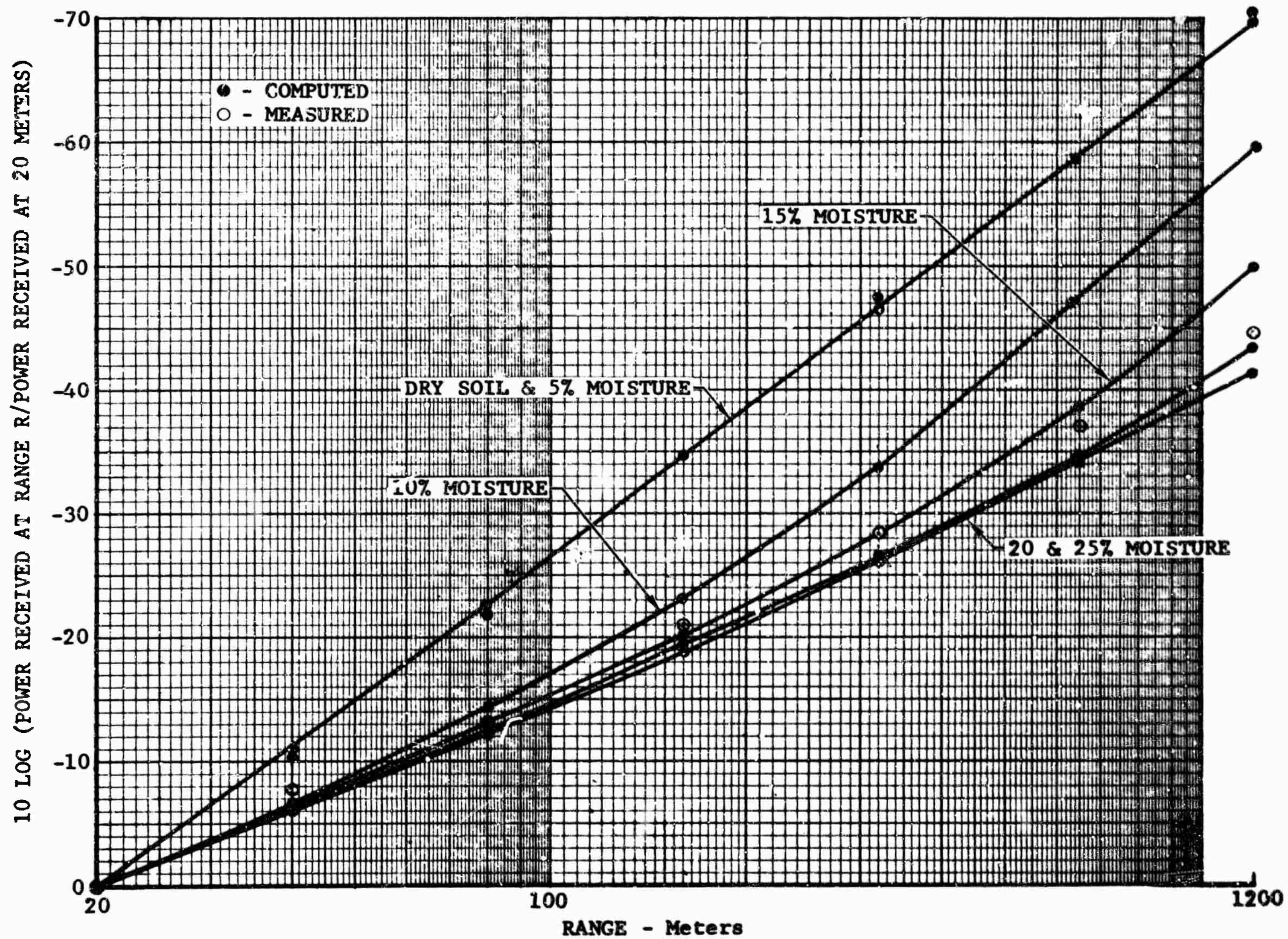

Fig. 76 SURFACE FIELD AMPLITUDE RANGE VARIATION WITH SOIL MOISTURE (60 MHz)

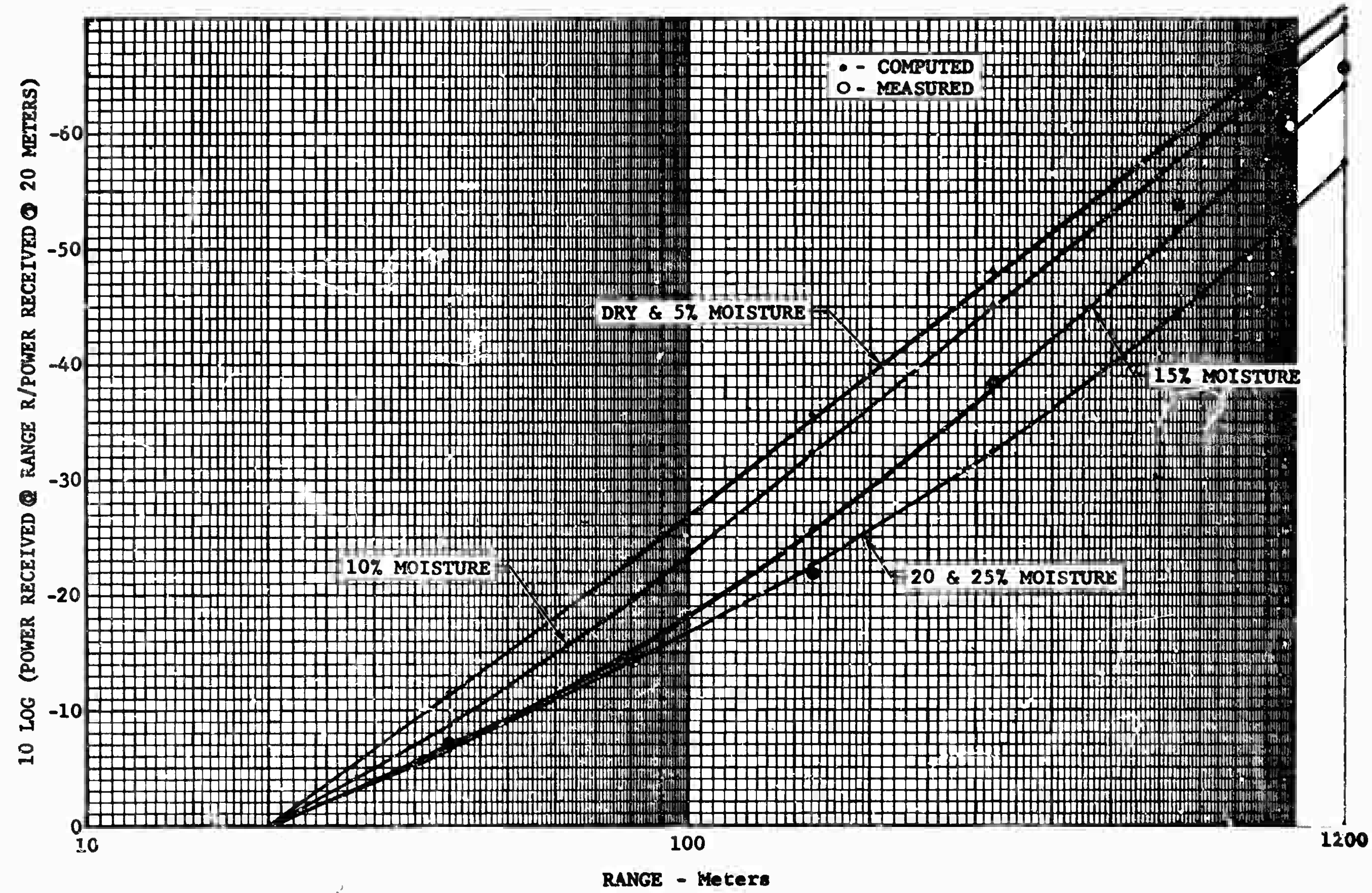

Fig. 77 SURFACE FIELD AMPLITUDE RANGE VARIATION WITH SOIL MOISTURE (120 MHz)

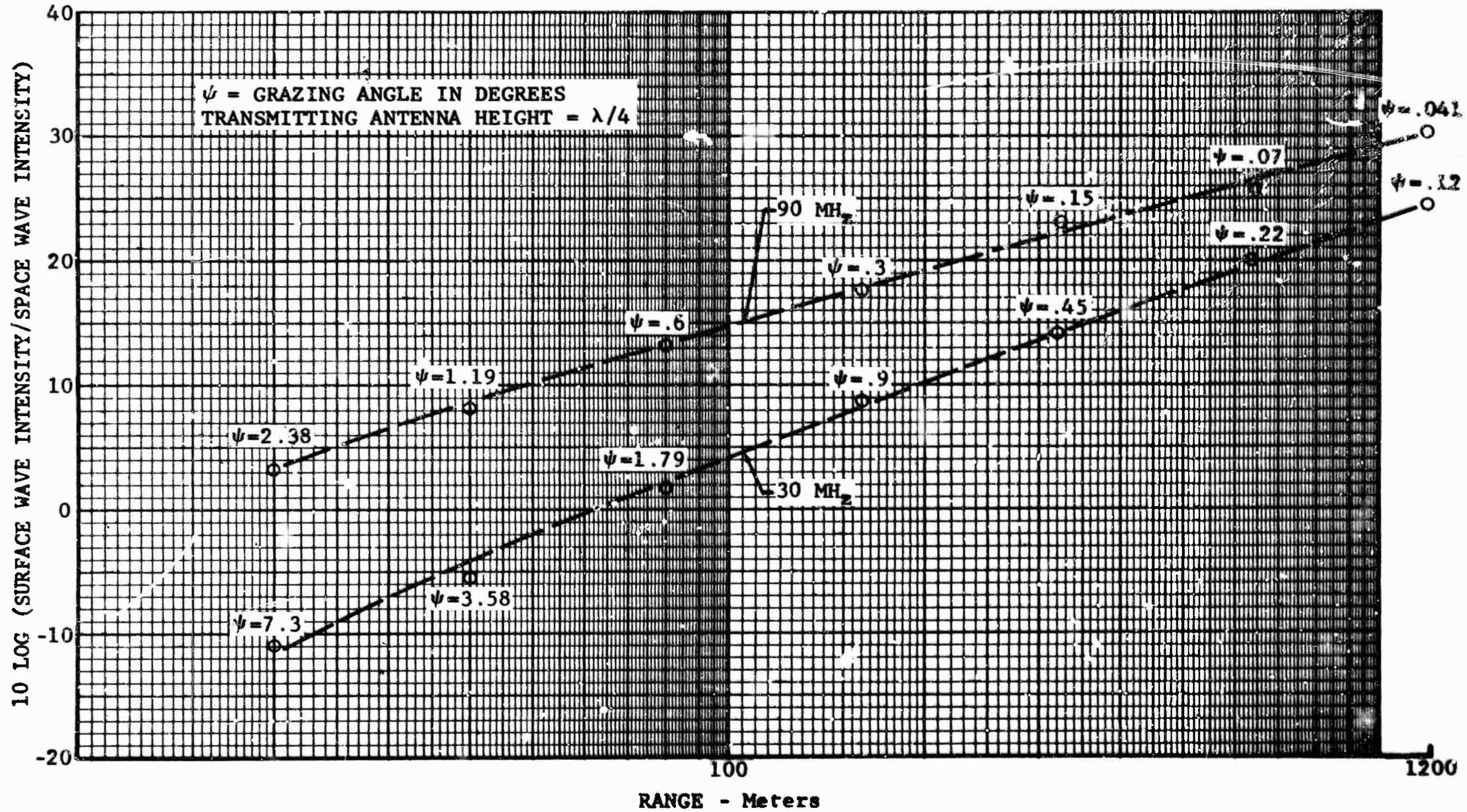

Fig. 78 SURFACE WAVE VERSUS SPACE WAVE

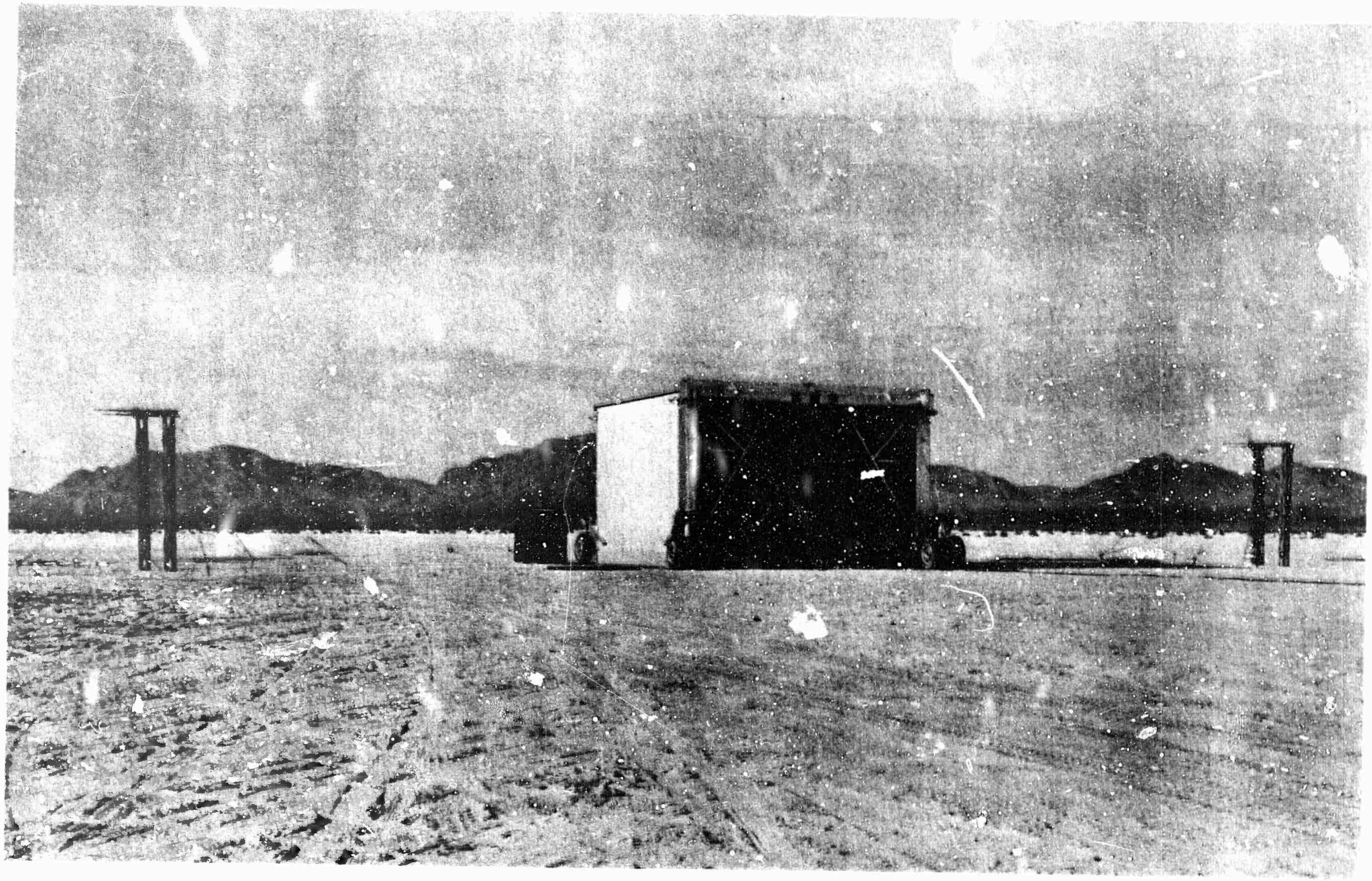

Fig. 79 VHF ANTENNA SYSTEM

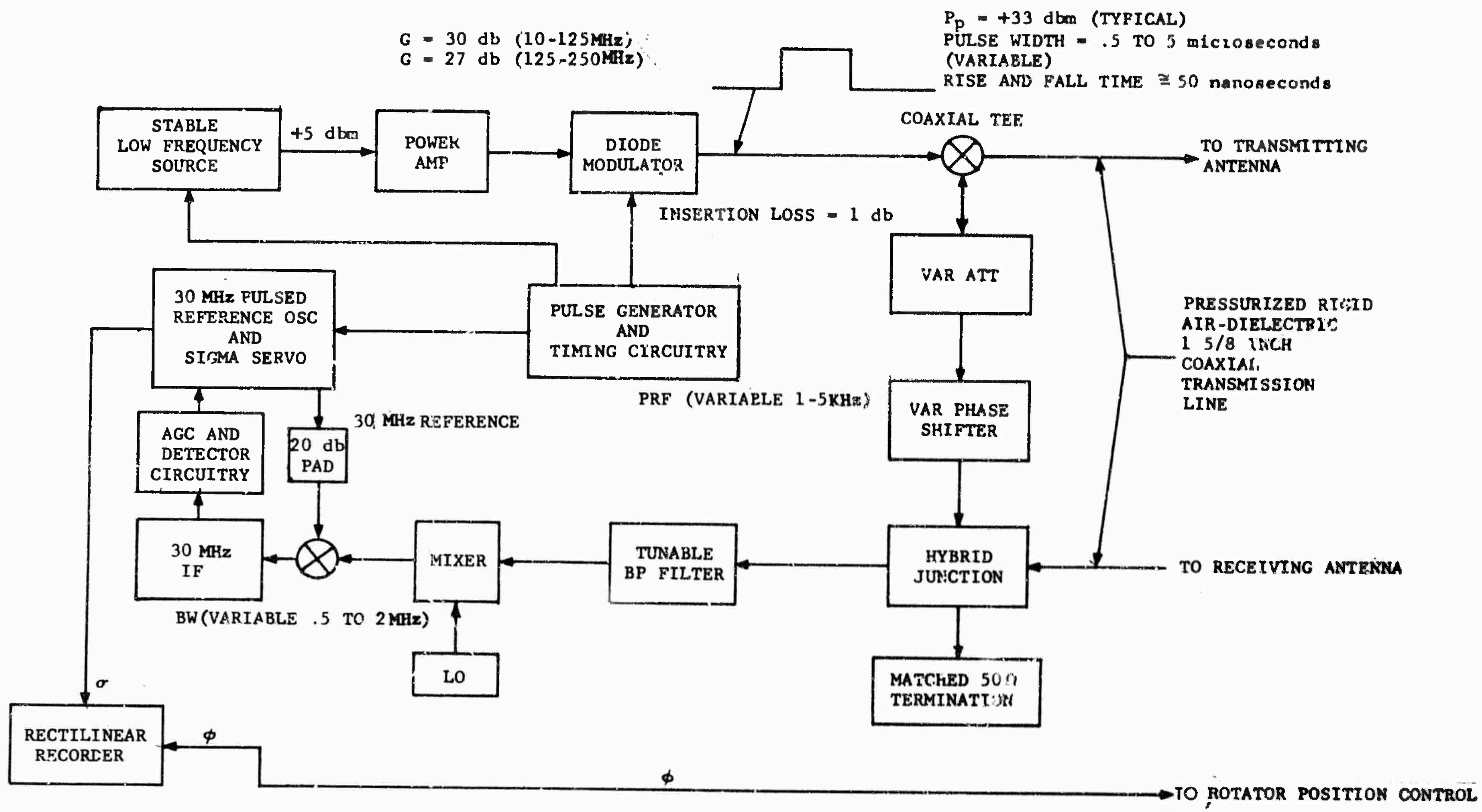

Fig. 80 ELECTRONIC SYSTEM BLOCK DIAGRAM

Fig. 81 FIBER GLASS TARGET SUPPORT AND PULLEY SYSTEM

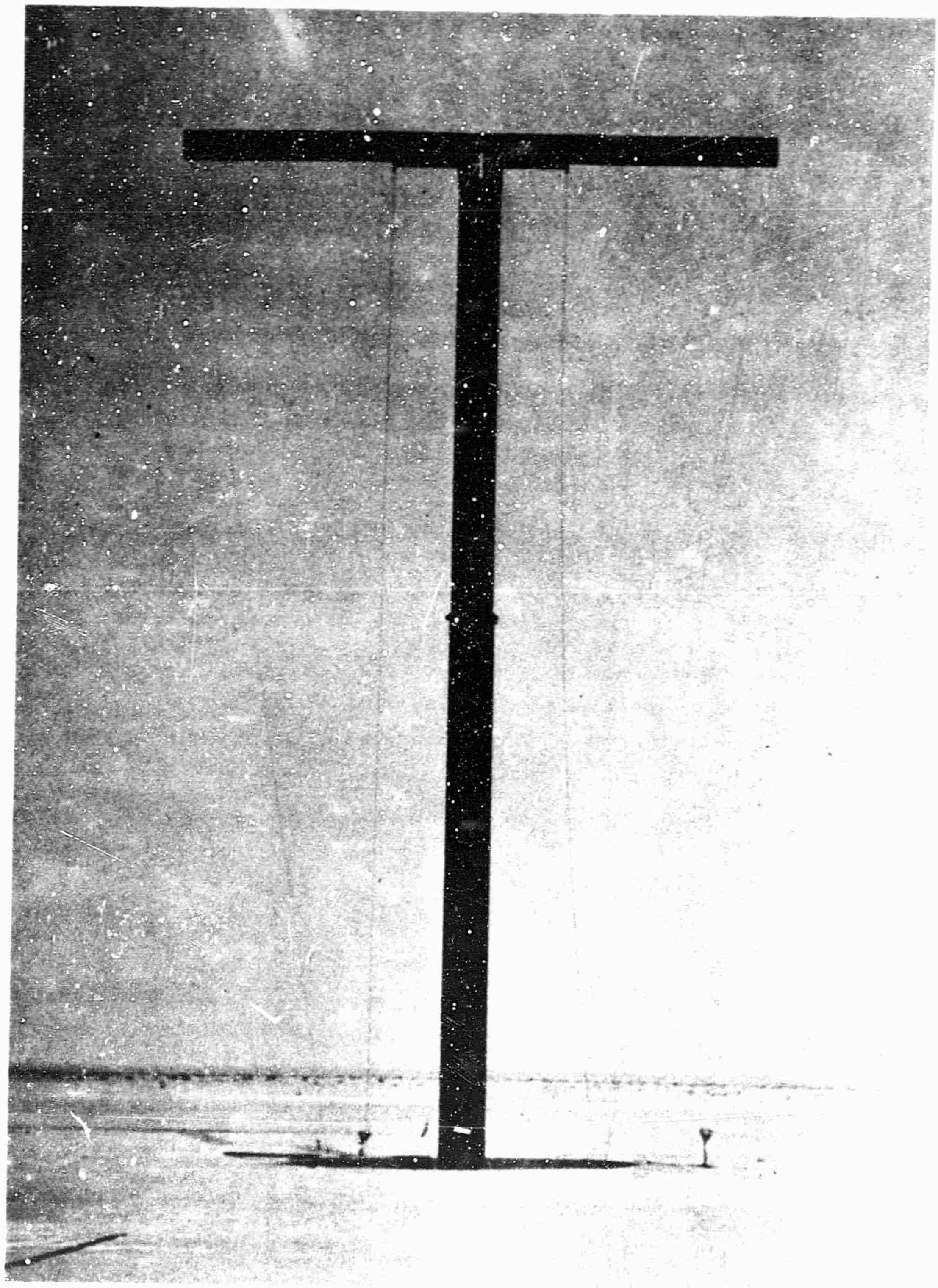

Fig. 82 42 FOOT CYLINDER USED IN COUPLING INVESTIGATION

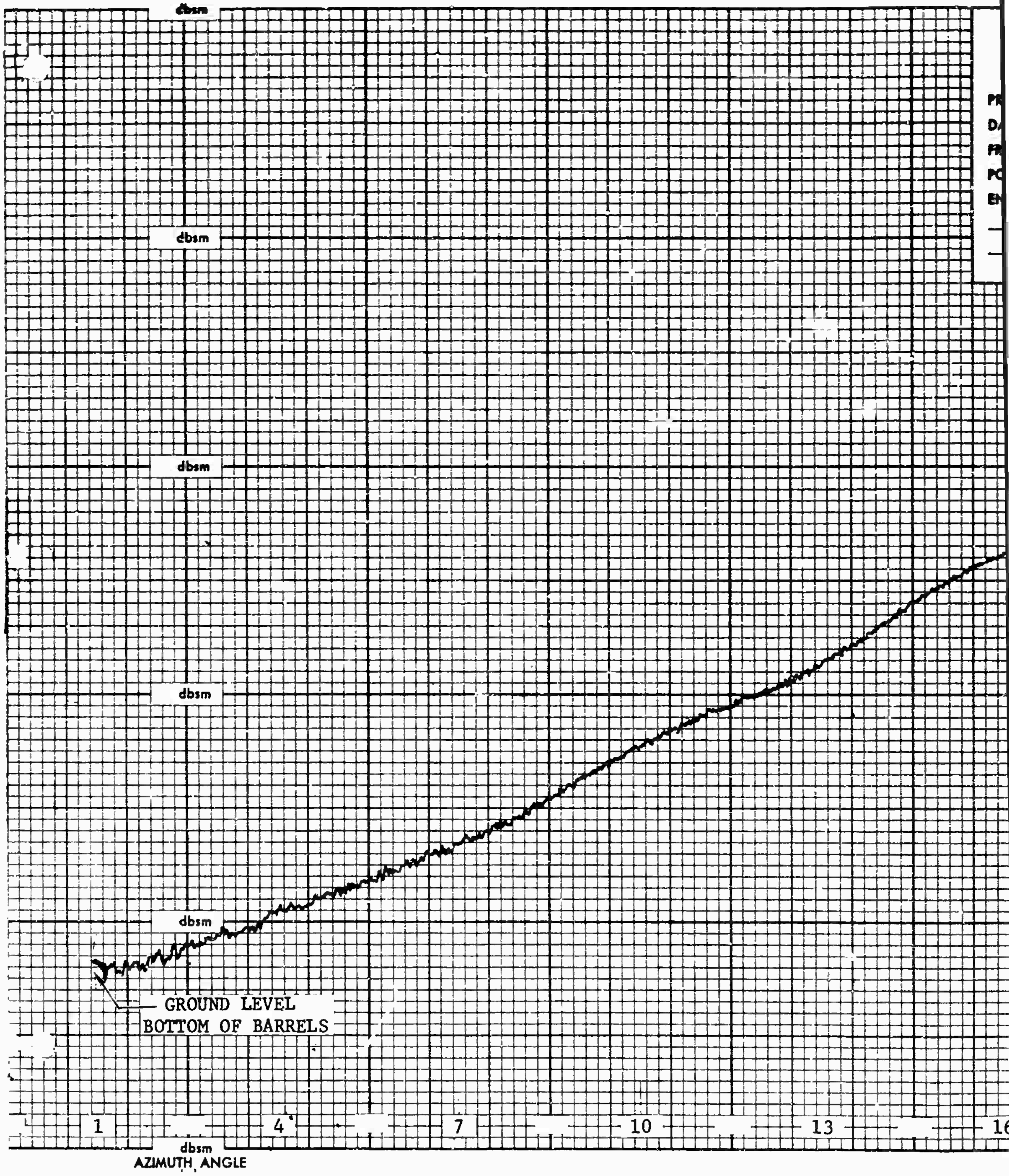

dbsm
dbsm
dbsm
dbsm
dbsm
GROUND LEVEL
BOTTOM OF BARRELS
1
4
7
10
13
dbsm
AZIMUTH ANGLE

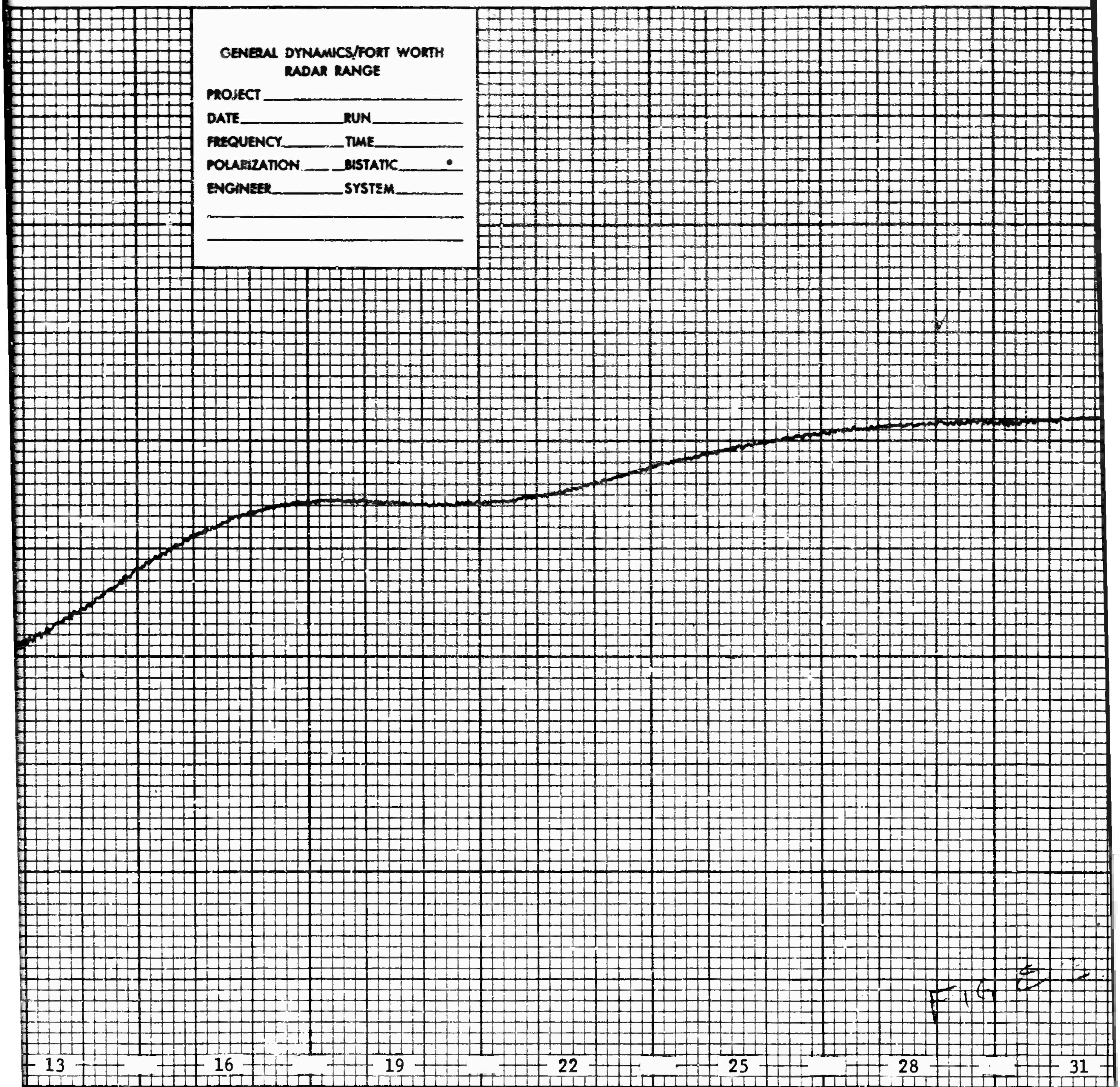
GENERAL DYNAMICS/FORT WORTH
RADAR RANGE
PROJECT
DATE
RUN
FREQUENCY
TIME
POLARIZATION
BISTATIC
ENGINEER
SYSTEM
13
16
19
22
25
28
31

2

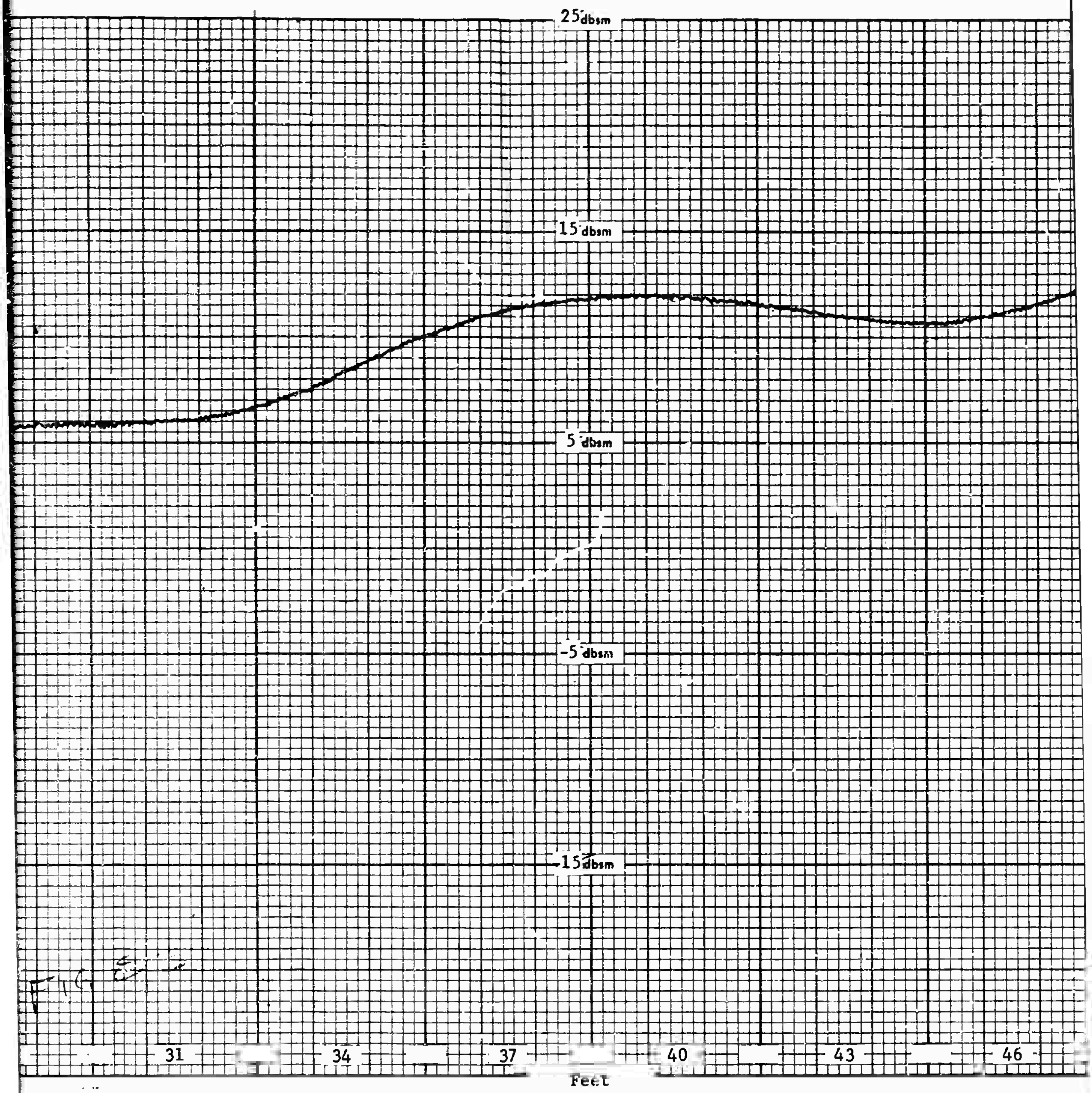

Fig. 83

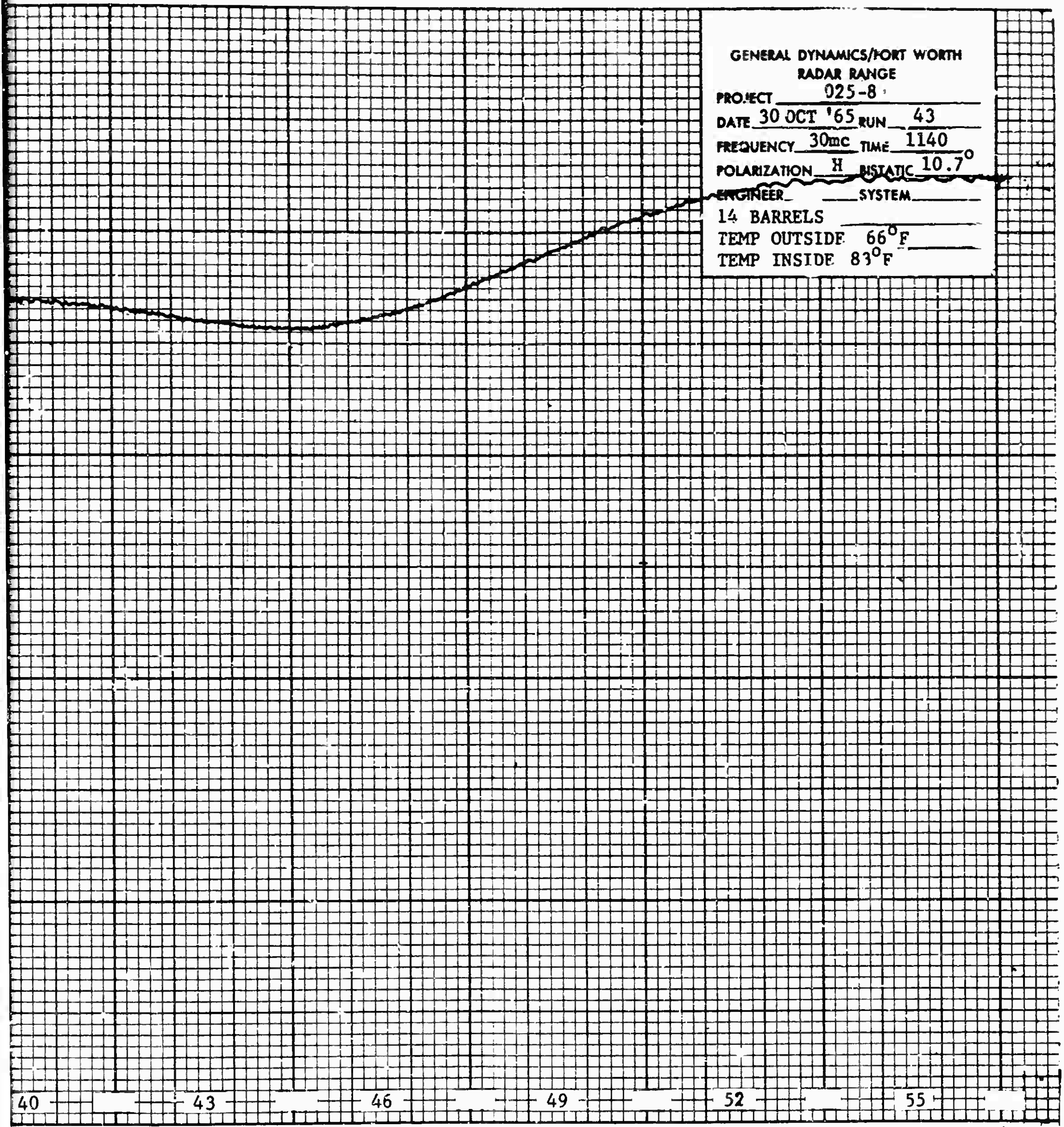

Fig. 83 CYLINDER CROSS SECTION VERSUS HEIGHT
(30 MHz, HORIZONTAL POLARIZATION)

4

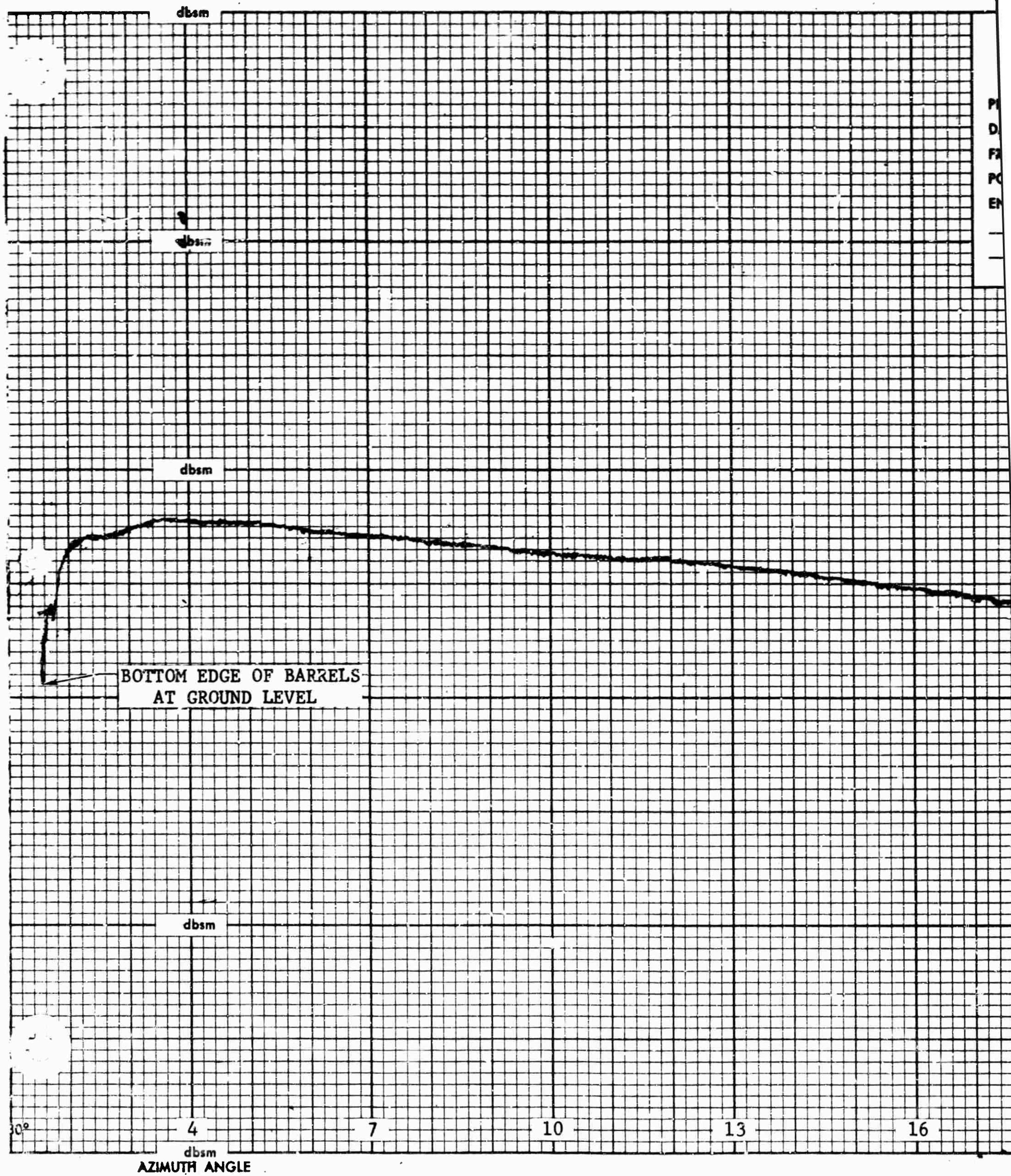

dbsm
dbsm
dbsm
BOTTOM EDGE OF BARRELS AT GROUND LEVEL
dbsm
30°
4
7
10
13
16
dbsm
AZIMUTH ANGLE

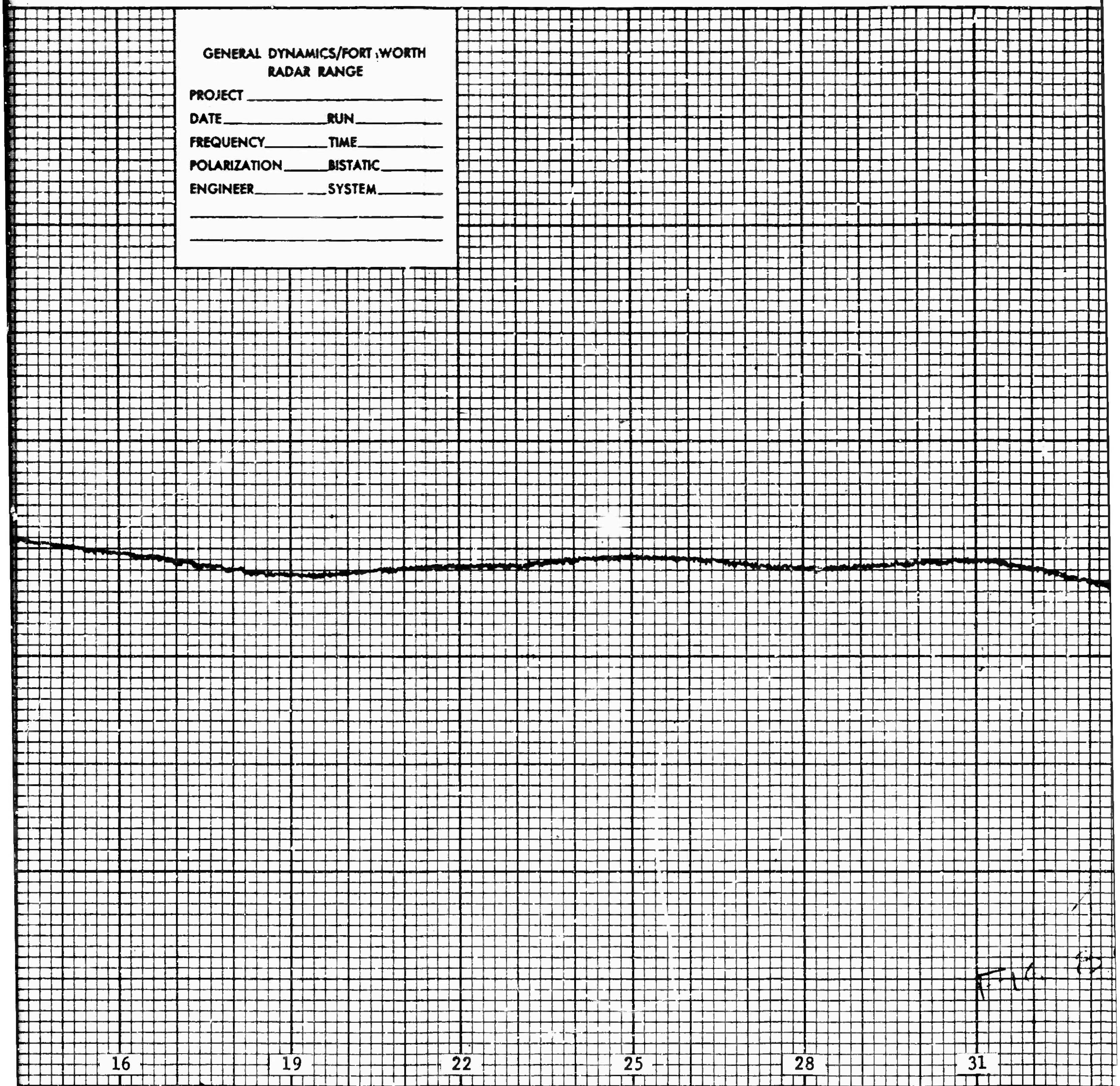
GENERAL DYNAMICS/FORT WORTH
RADAR RANGE
PROJECT
DATE
RUN
FREQUENCY
TIME
POLARIZATION
BISTATIC
ENGINEER
SYSTEM
16
19
22
25
28
31

2

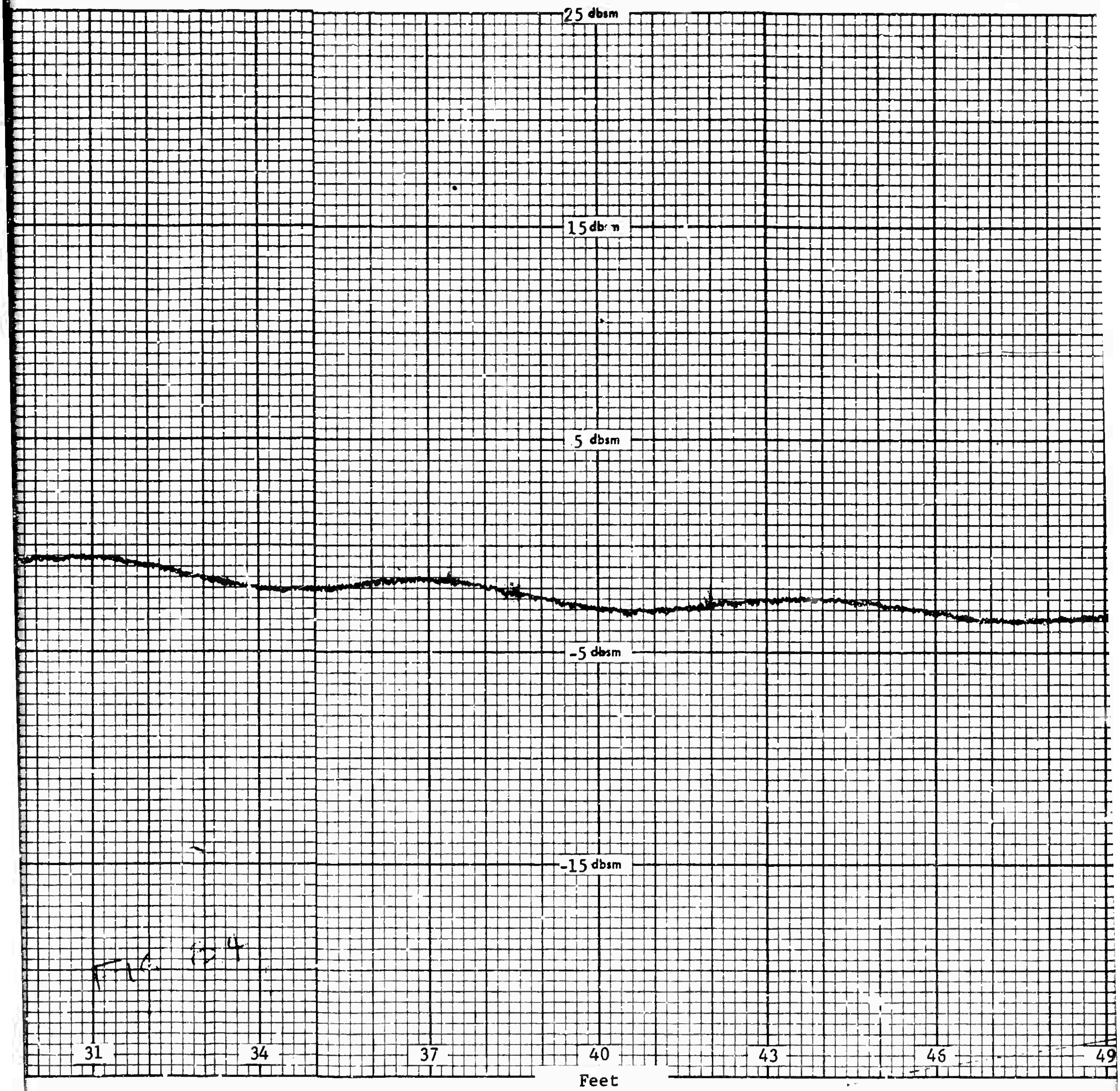

Fig. 8

3

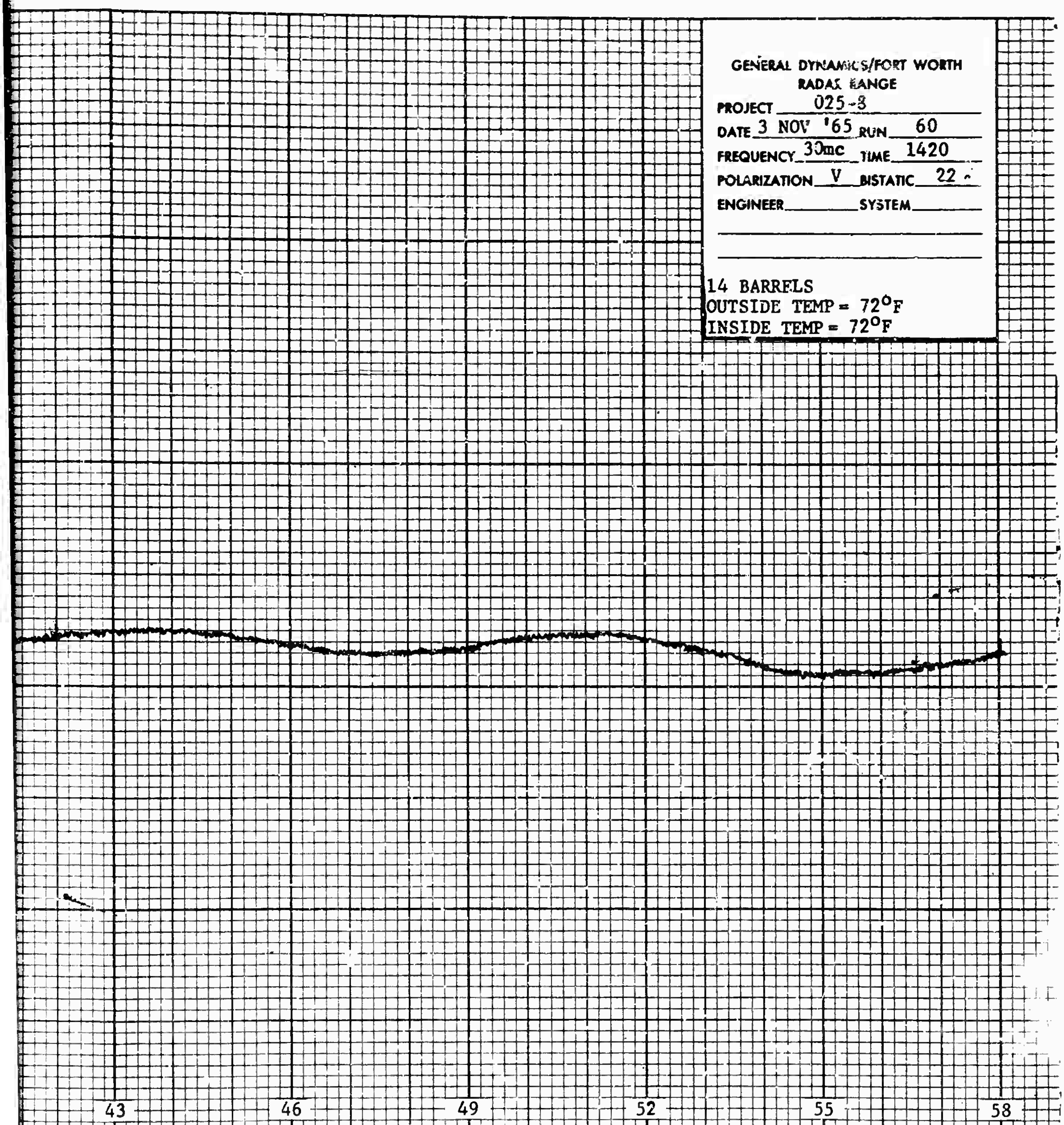

Fig. 84 CYLINDER CROSS SECTION VERSUS HEIGHT
(30 MHz, VERTICAL POLARIZATION)

4

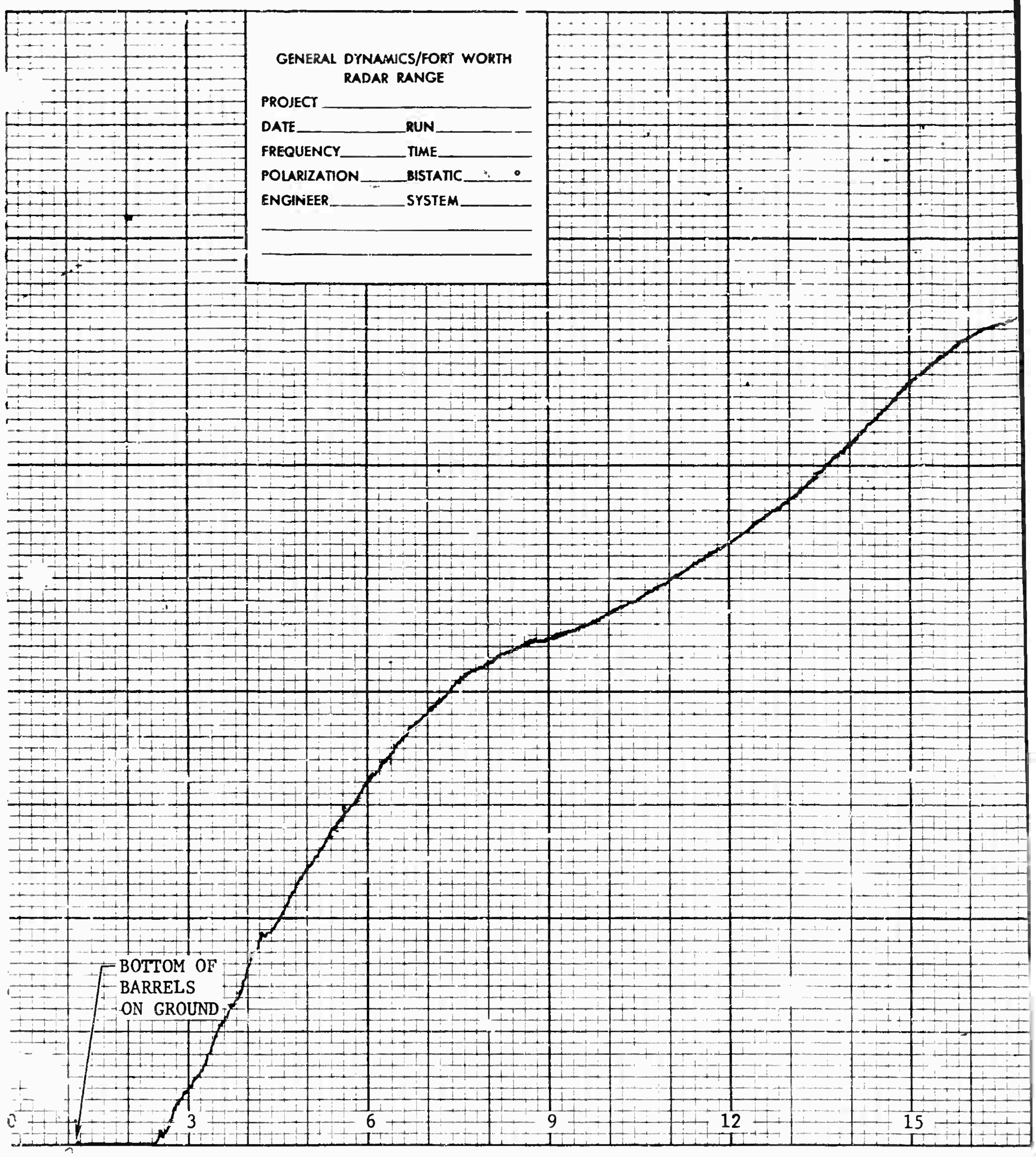
GENERAL DYNAMICS/FORT WORTH
RADAR RANGE
PROJECT
DATE
RUN
FREQUENCY
TIME
POLARIZATION
BISTATIC
ENGINEER
SYSTEM
BOTTOM OF
BARRELS
ON GROUND
0
3
6
9
12
15

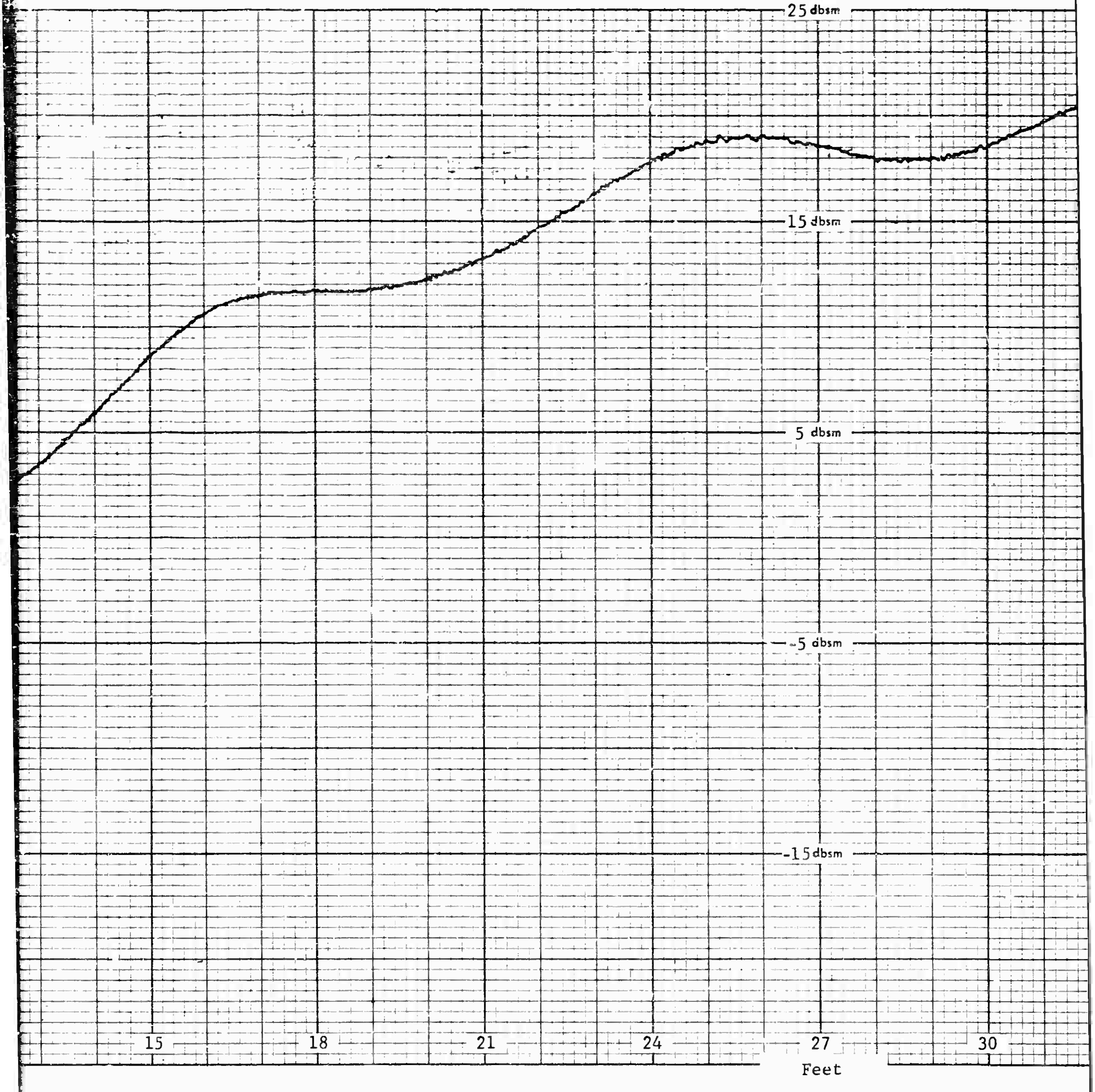

2

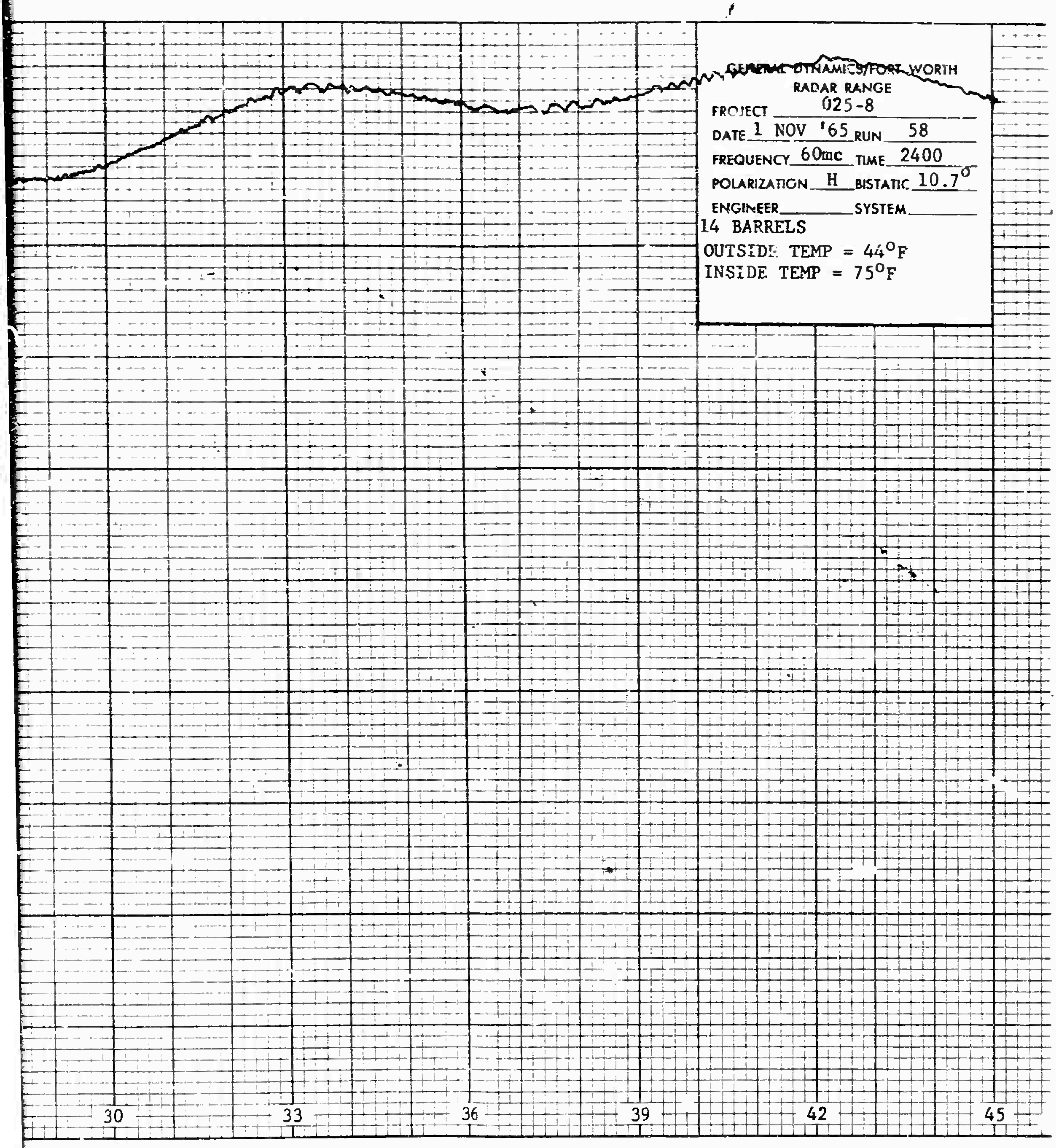

Fig. 85 CYLINDER, CROSS SECTION VERSUS HEIGHT
(60 MHz, HORIZONTAL POLARIZATION)

3

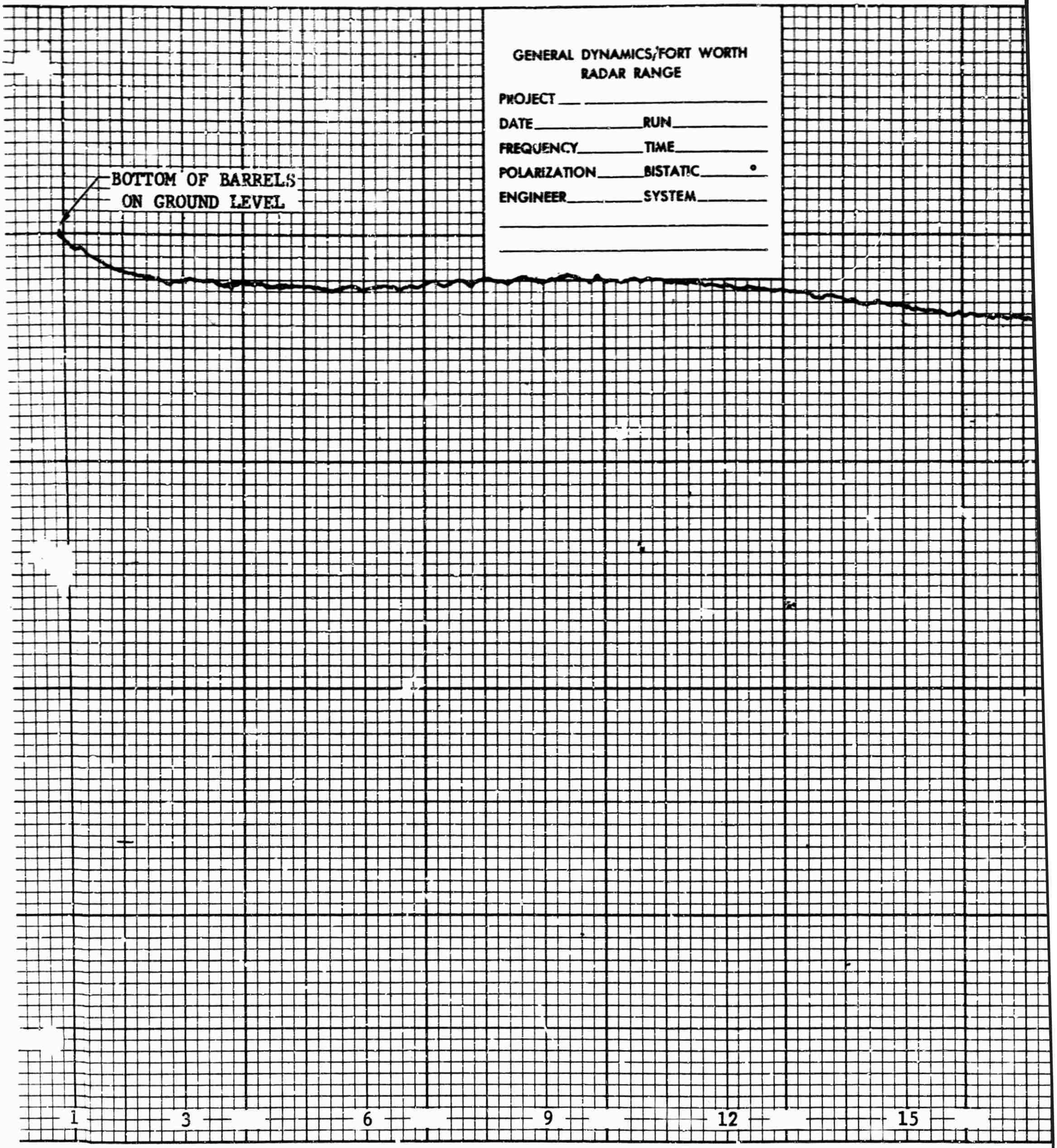

GENERAL DYNAMICS/FORT WORTH
RADAR RANGE
PROJECT
DATE
RUN
FREQUENCY
TIME
POLARIZATION
BISTATIC
ENGINEER
SYSTEM
BOTTOM OF BARRELS ON GROUND LEVEL
1
3
6
9
12
15

1

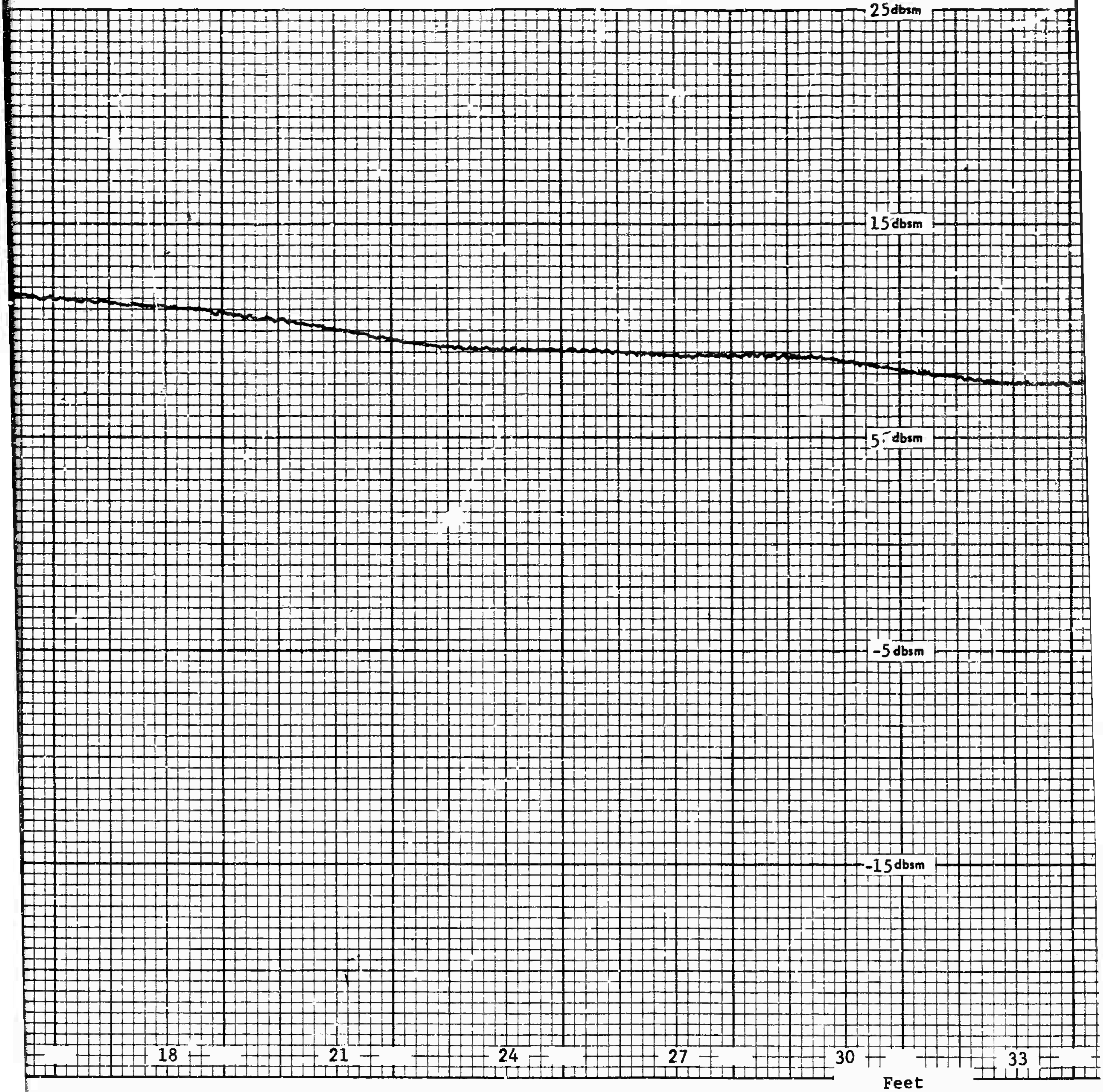

2

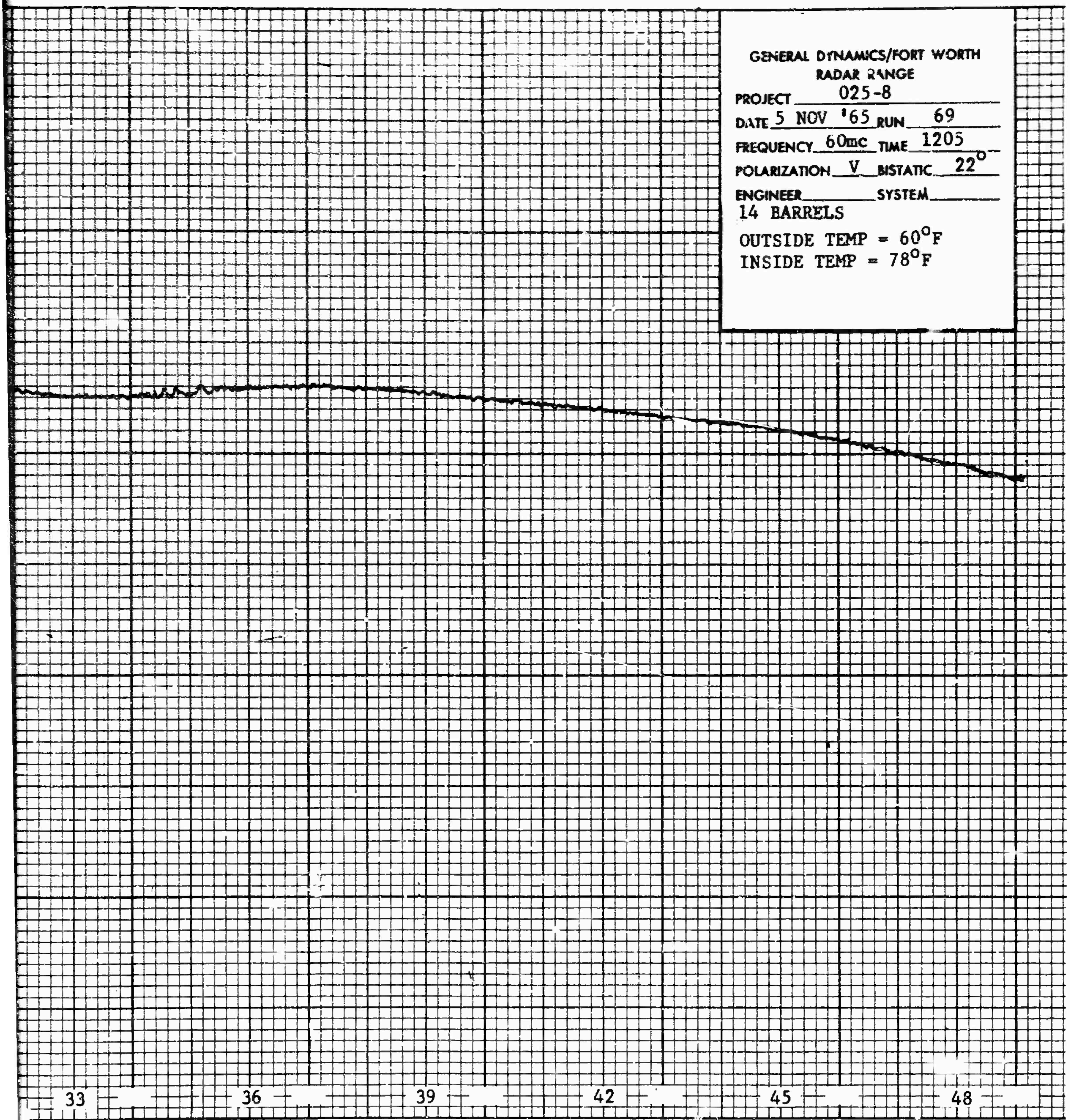

Fig. 86 CYLINDER CROSS SECTION VERSUS HEIGHT
(60 MHz, VERTICAL POLARIZATION)

3

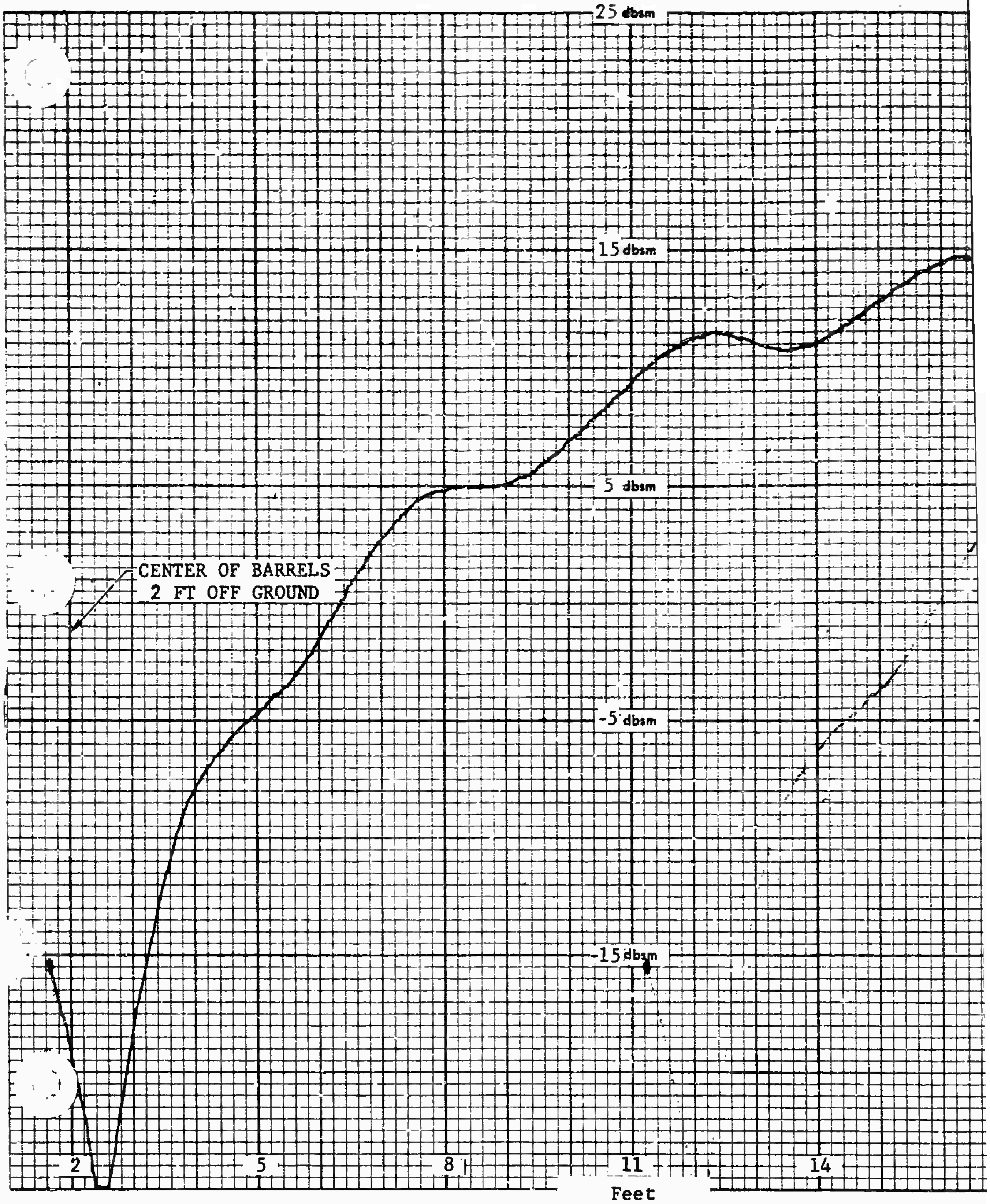
25 dbsm
15 dbsm
5 dbsm
-5 dbsm
-15 dbsm
CENTER OF BARRELS
2 FT OFF GROUND
2
5
8
11
14
Feet

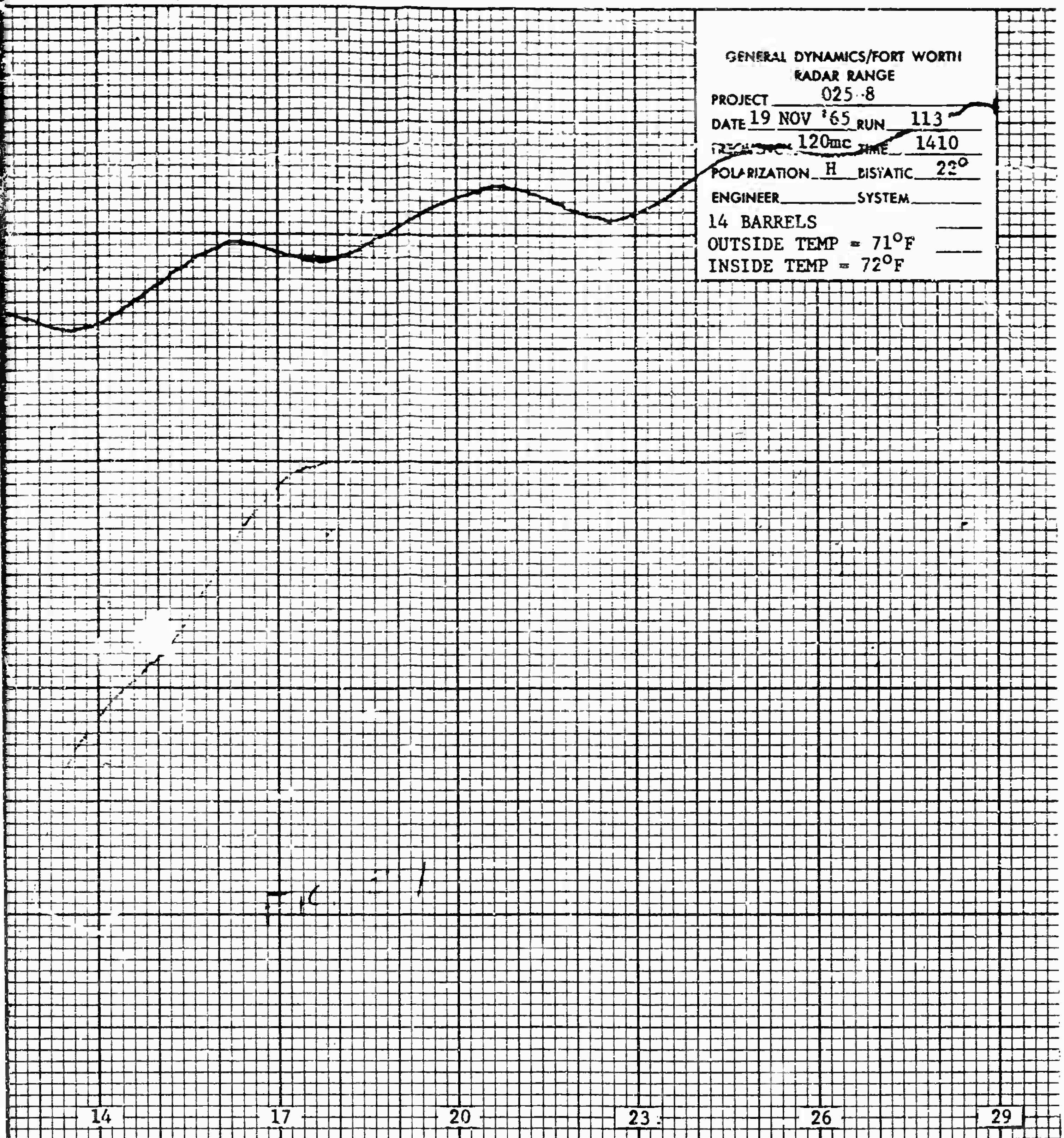

Fig. 87 CYLINDER CROSS SECTION VERSUS HEIGHT
(120 MHz, HORIZONTAL POLARIZATION)

25 dbsm
15 dbsm
5 dbsm
-5 dbsm
-15 dbsm
CENTER OF BARRELS
2 FT OFF GROUND
2
5
8
11
14
17
Feet

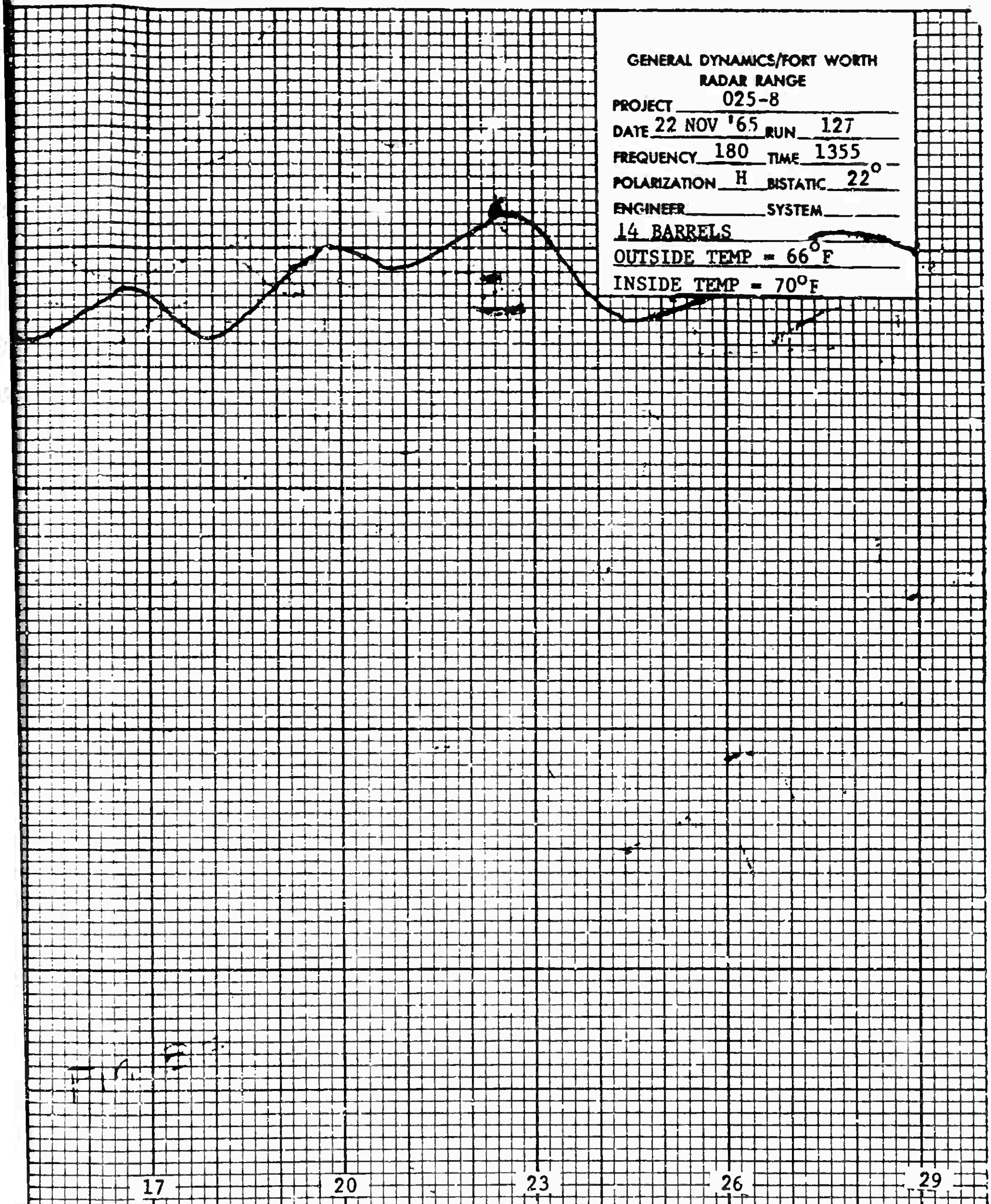

Fig. 38 CYLINDER CROSS SECTION VERSUS HEIGHT (180 MHz, HORIZONTAL POLARIZATION)

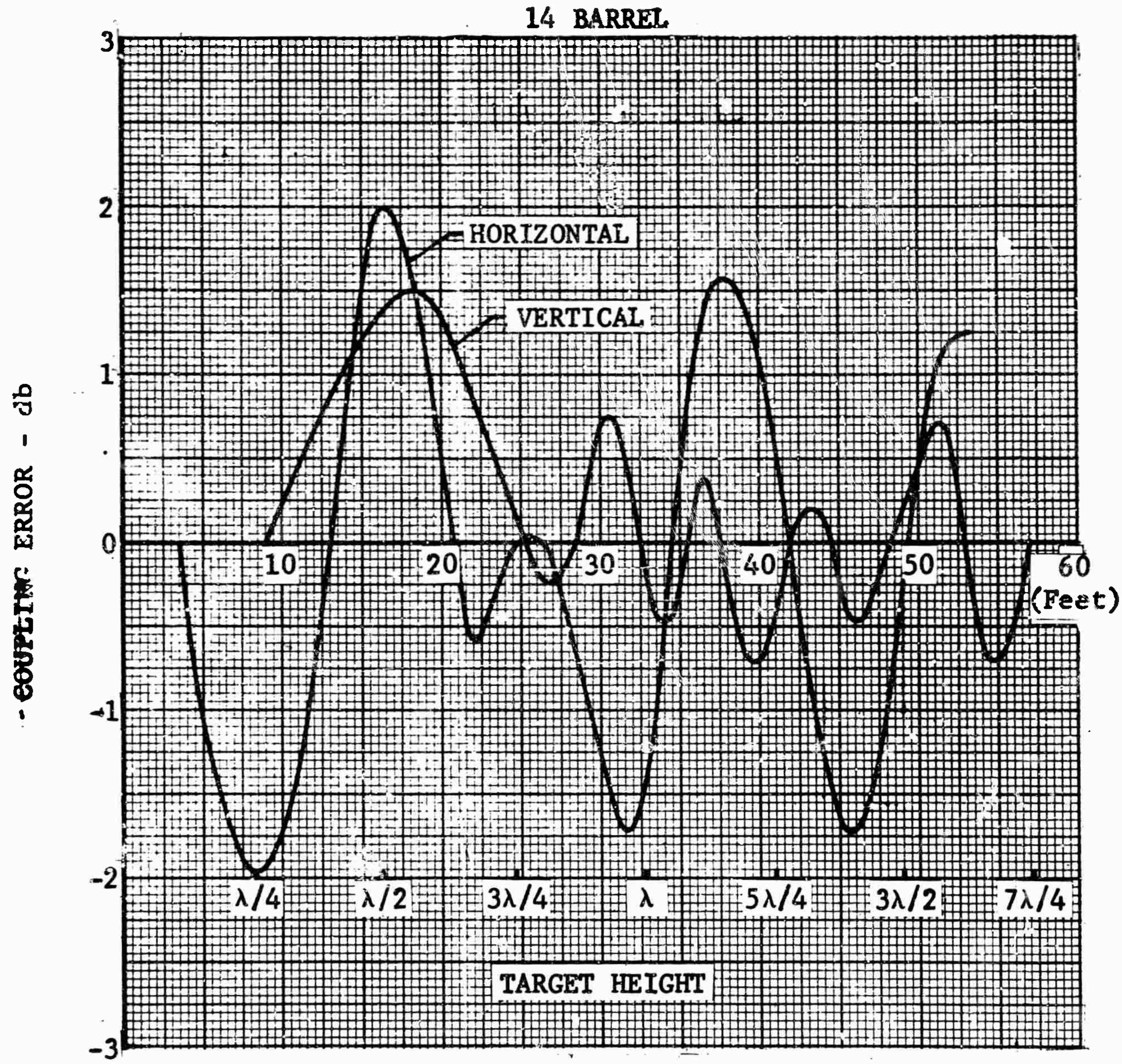

14 BARREL
HORIZONTAL
VERTICAL
COUPLING ERROR - db
3
2
1
0
-1
-2
-3
10
20
30
40
50
60
(Feet)
λ/4
λ/2
3λ/4
λ
5λ/4
3λ/2
7λ/4
TARGET HEIGHT

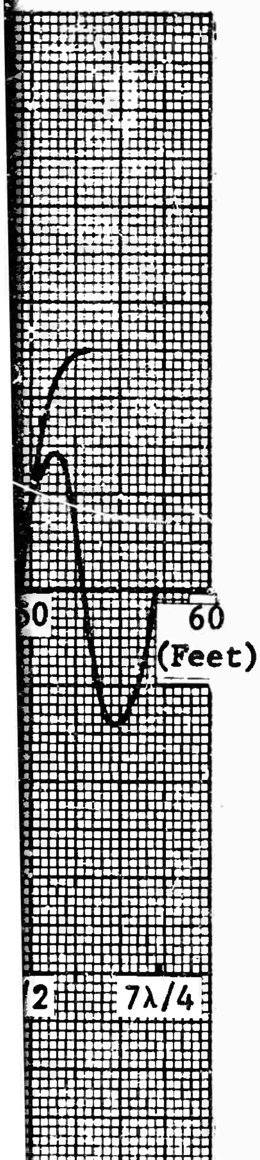
60
(Feet)
7λ/4

7 BARREL

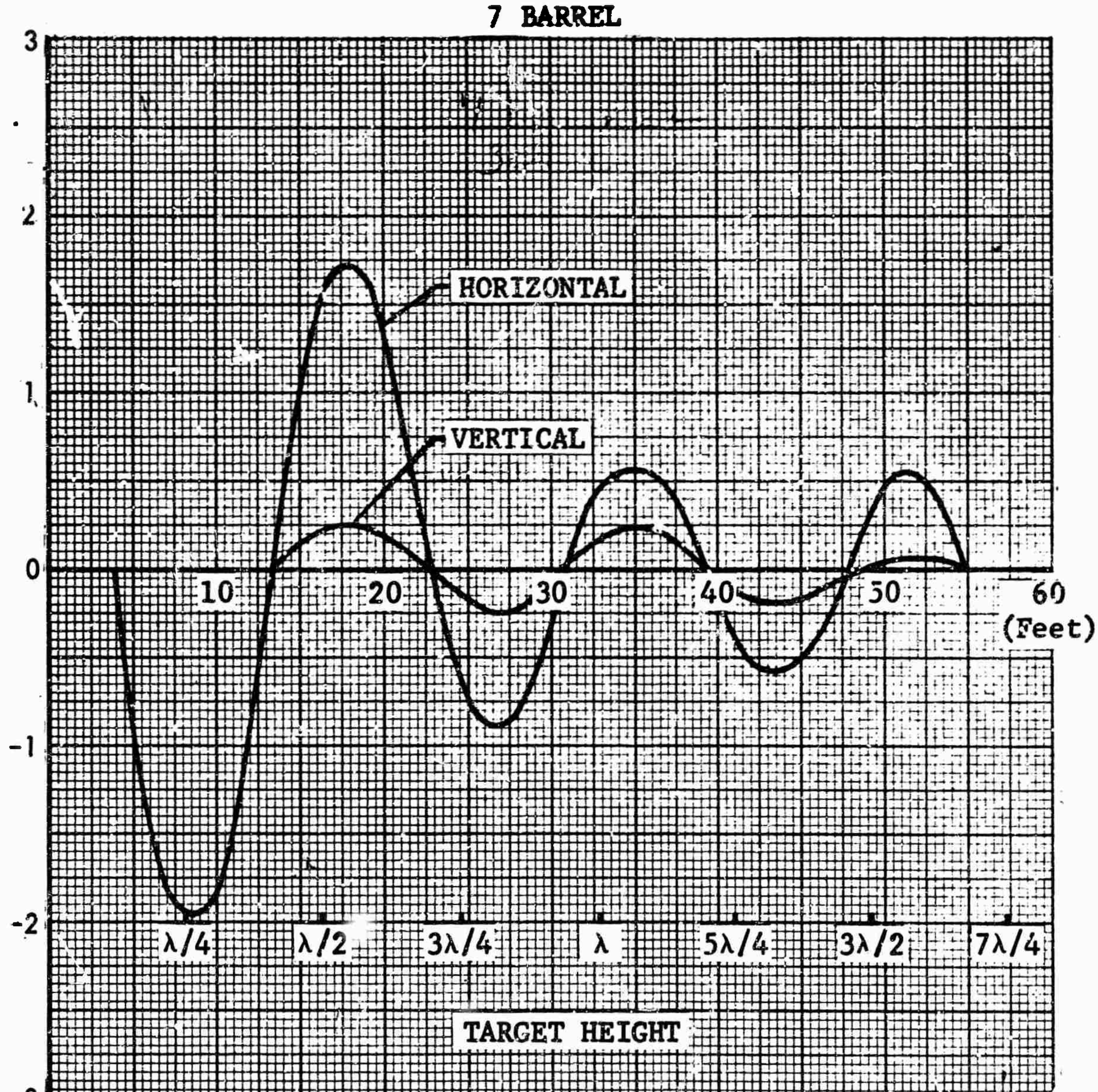
3
2
1
0
-1
-2
-3
HORIZONTAL
VERTICAL
10
20
30
40
50
60
(Feet)
λ/4
λ/2
3λ/4
λ
5λ/4
3λ/2
7λ/4
TARGET HEIGHT

2

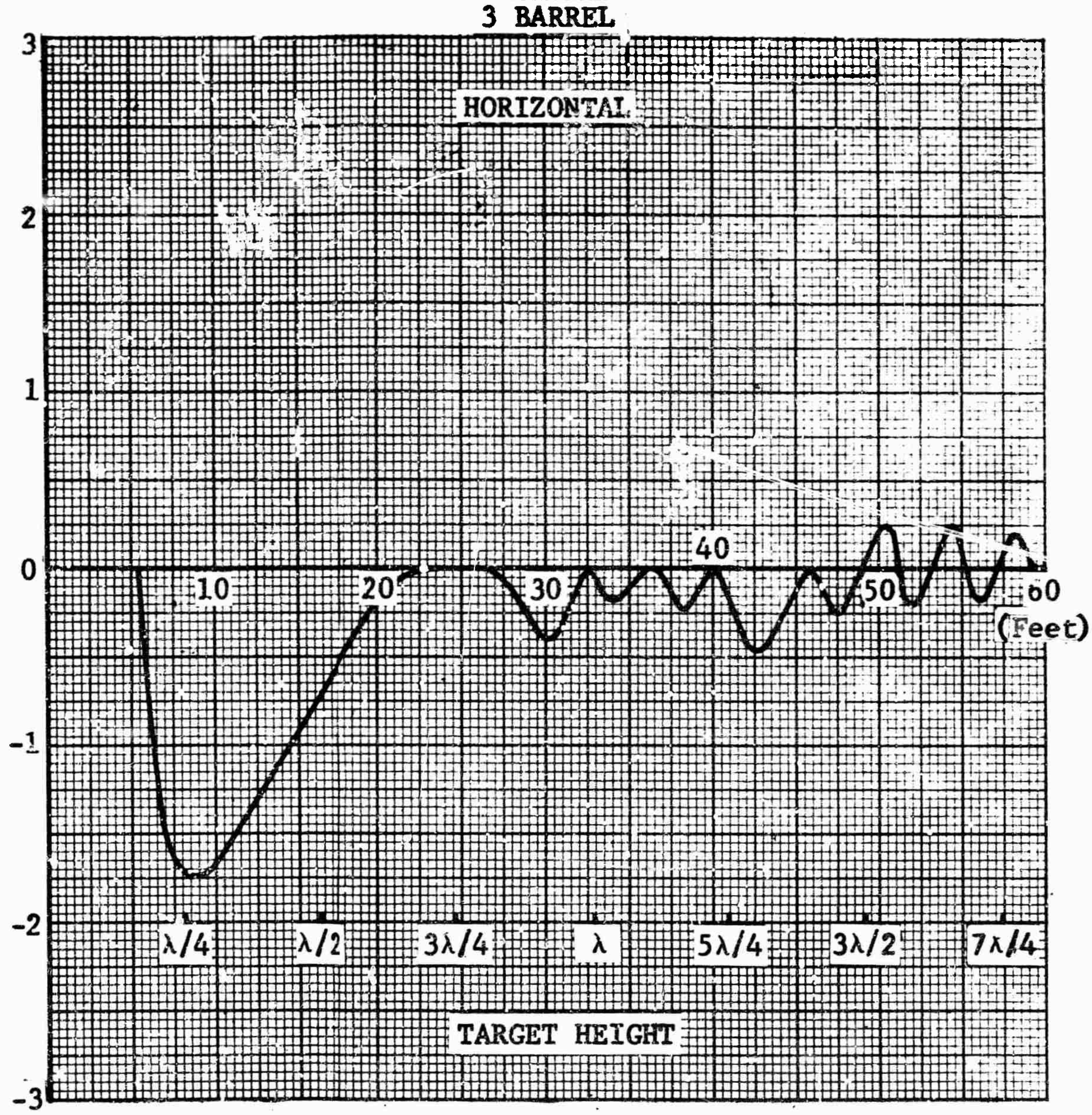

Fig. 89 COUPLING ERROR VERSUS HEIGHT AT 30 MHz

3

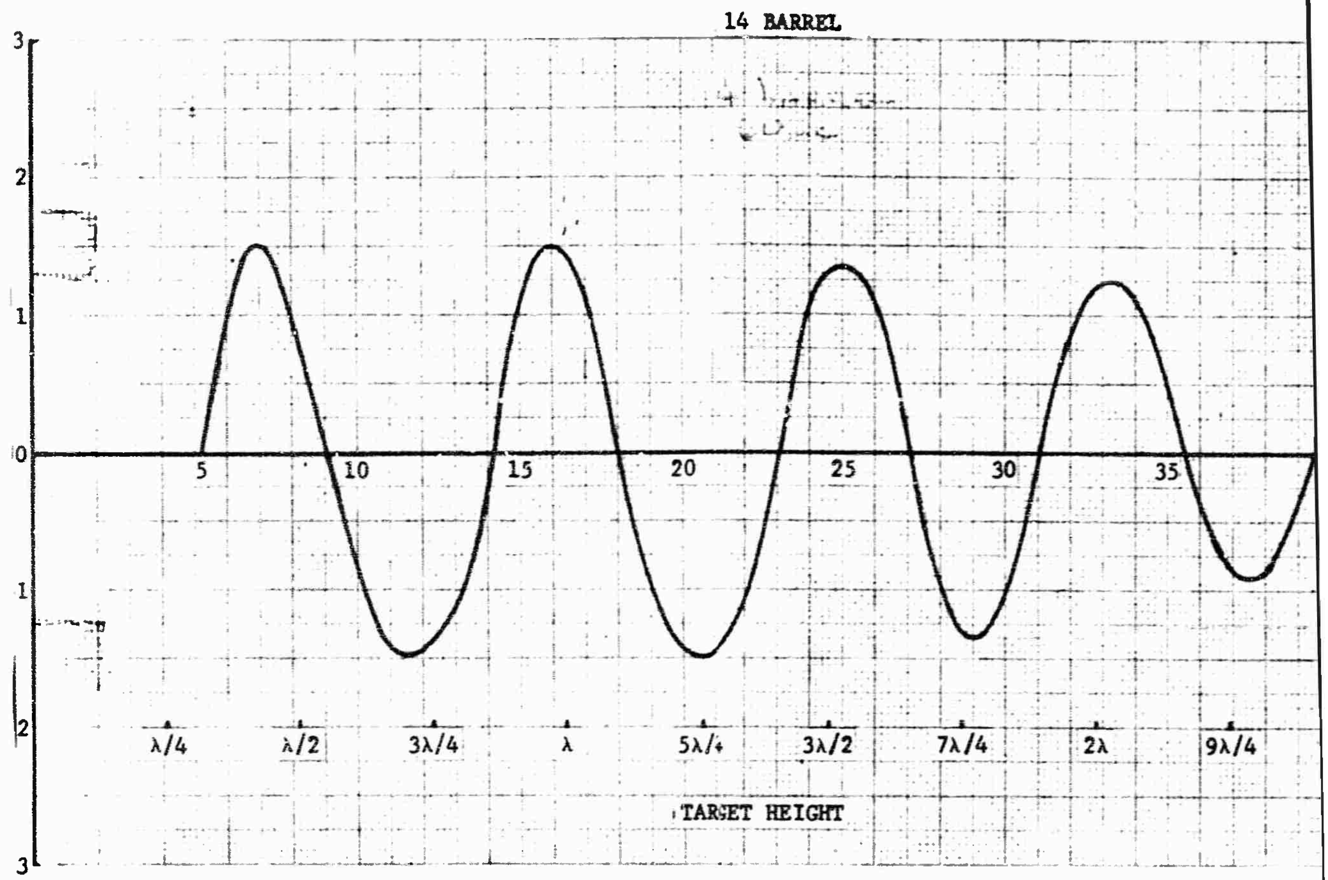
14 BARREL
3
2
1
0
1
2
3
5
10
15
20
25
30
35
λ/4
λ/2
3λ/4
λ
5λ/4
3λ/2
7λ/4
2λ
9λ/4
TARGET HEIGHT

HORIZONTAL POLARITY

7 BARREL

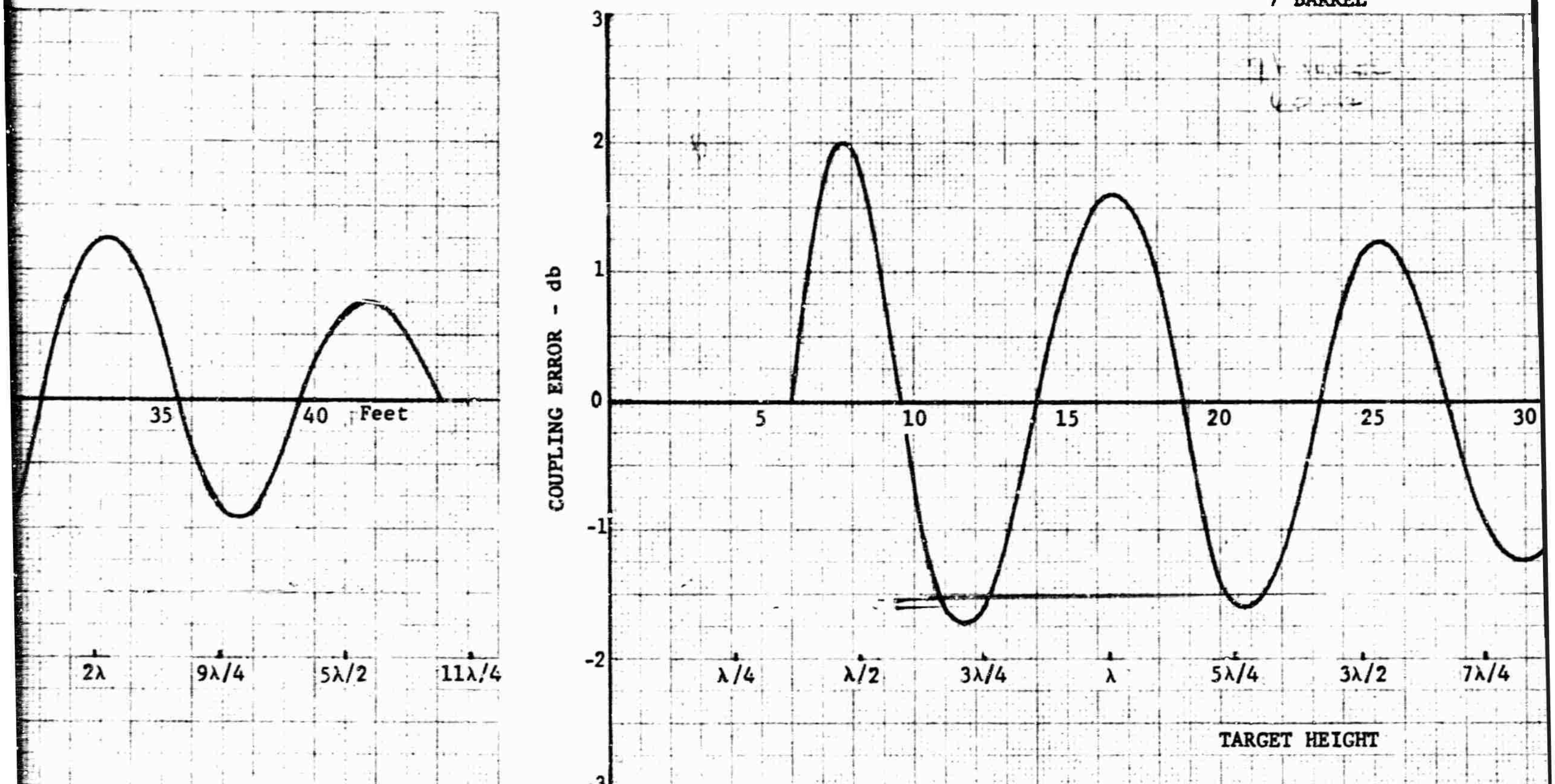

2

AL POLARITY

BARREL

3 BA

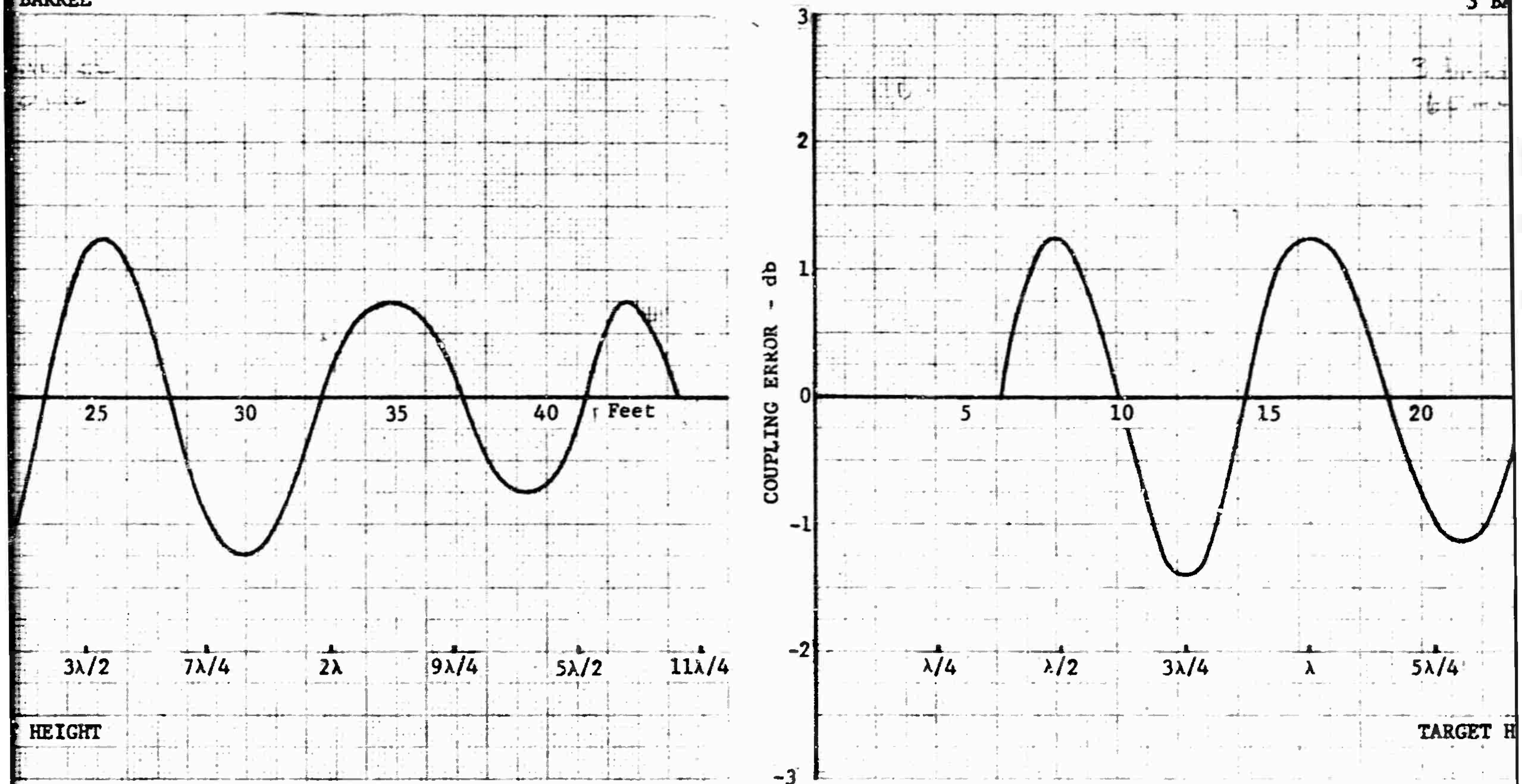

Fig. 90 COUPLING

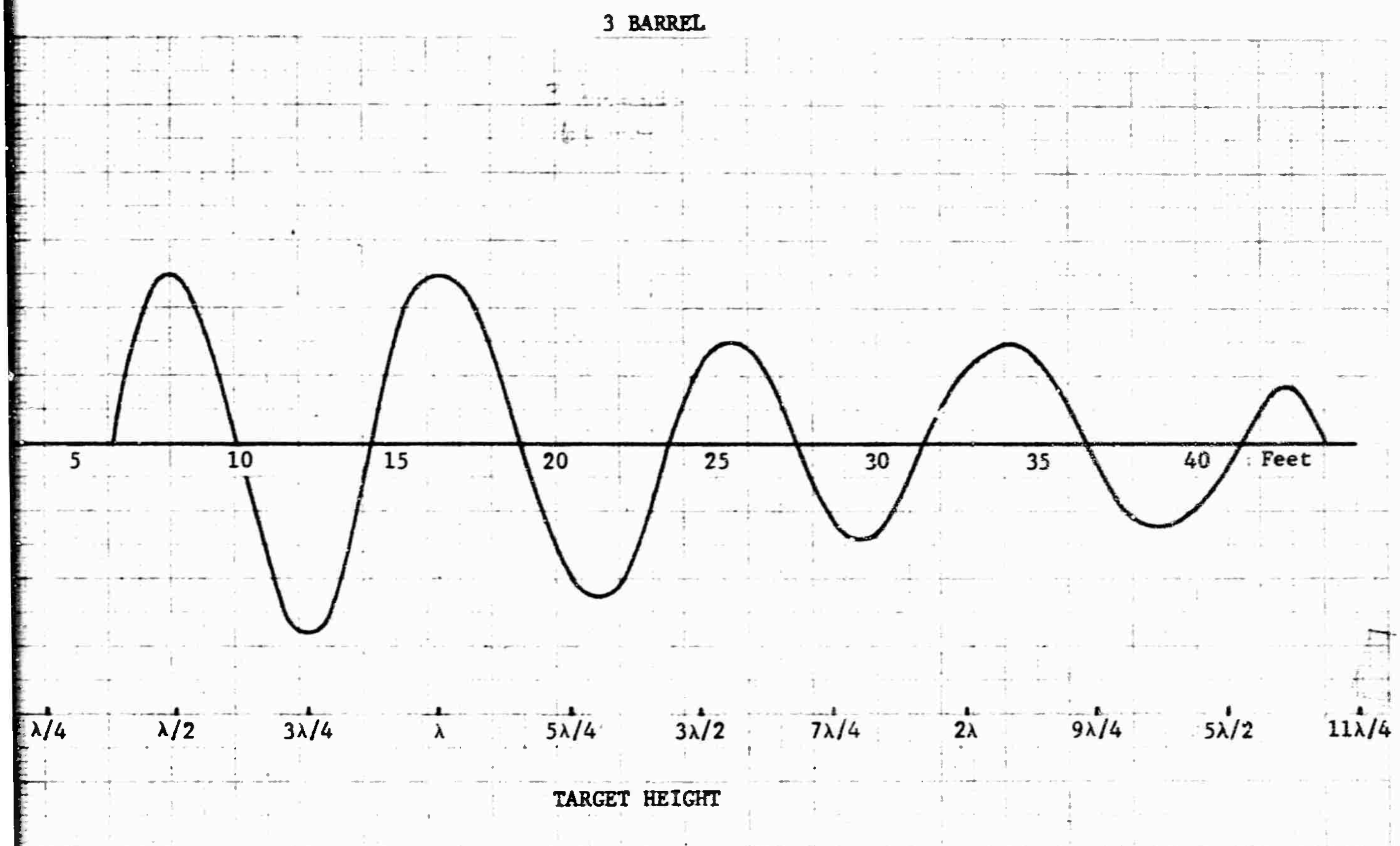

Fig. 90 COUPLING ERROR VERSUS HEIGHT AT 60 MHz

4

14 BARREL

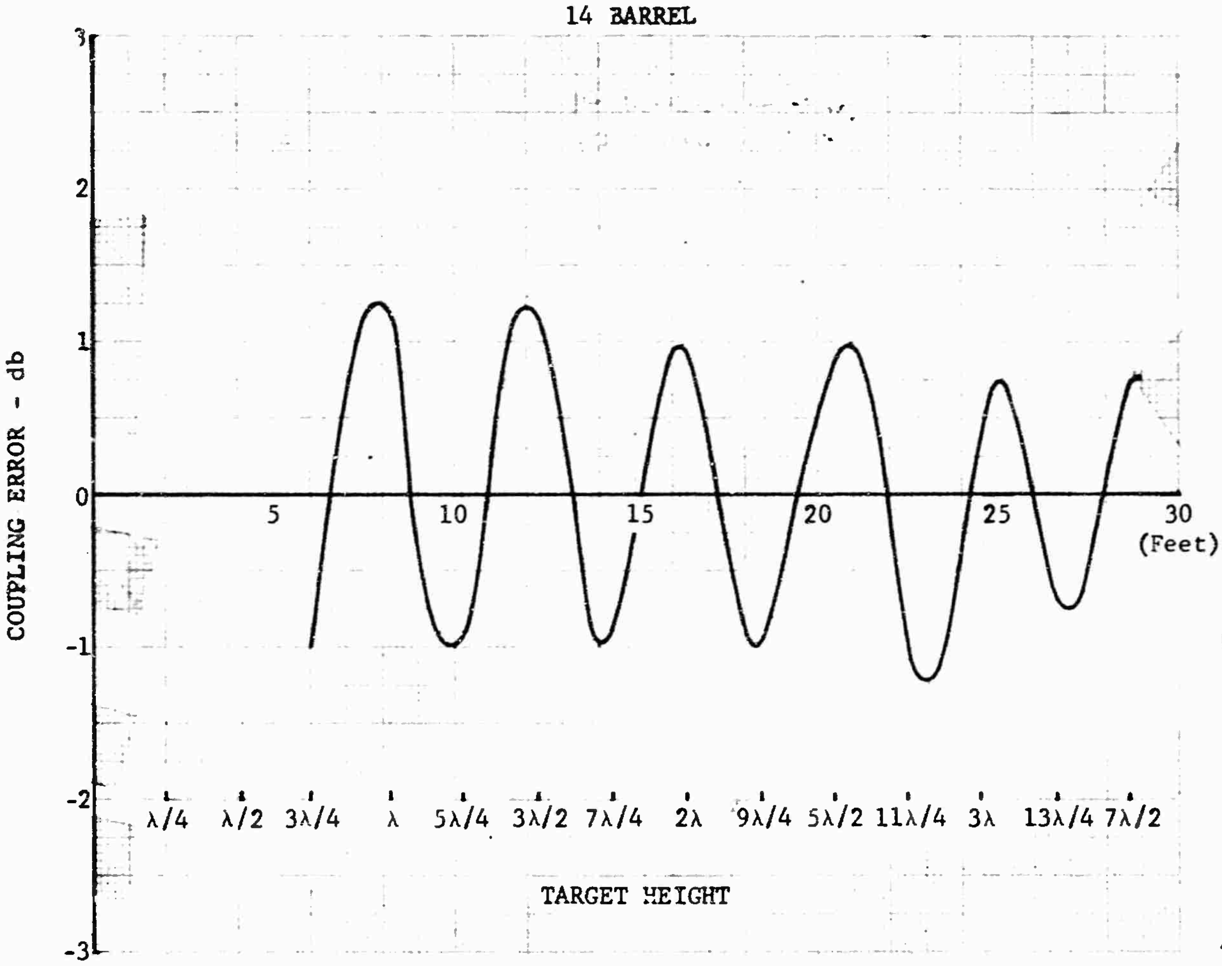
COUPLING ERROR - db
3
2
1
0
-1
-2
-3
5
10
15
20
25
30
(Feet)
λ/4 λ/2 3λ/4 λ 5λ/4 3λ/2 7λ/4 2λ 9λ/4 5λ/2 11λ/4 3λ 13λ/4 7λ/2
TARGET HEIGHT

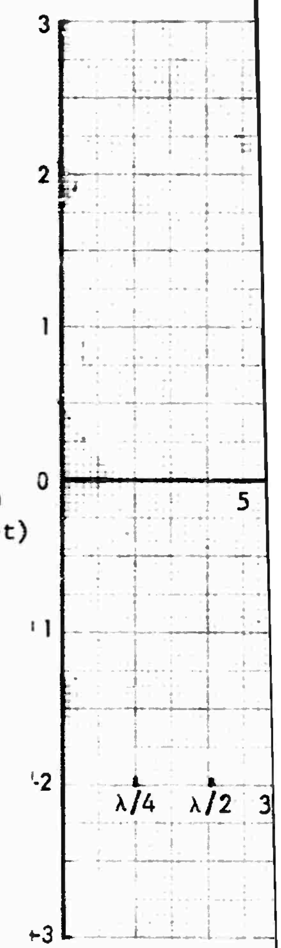
3
2
1
0
5
λ/4 λ/2

HORIZONTAL POLARITY

7 BARREL

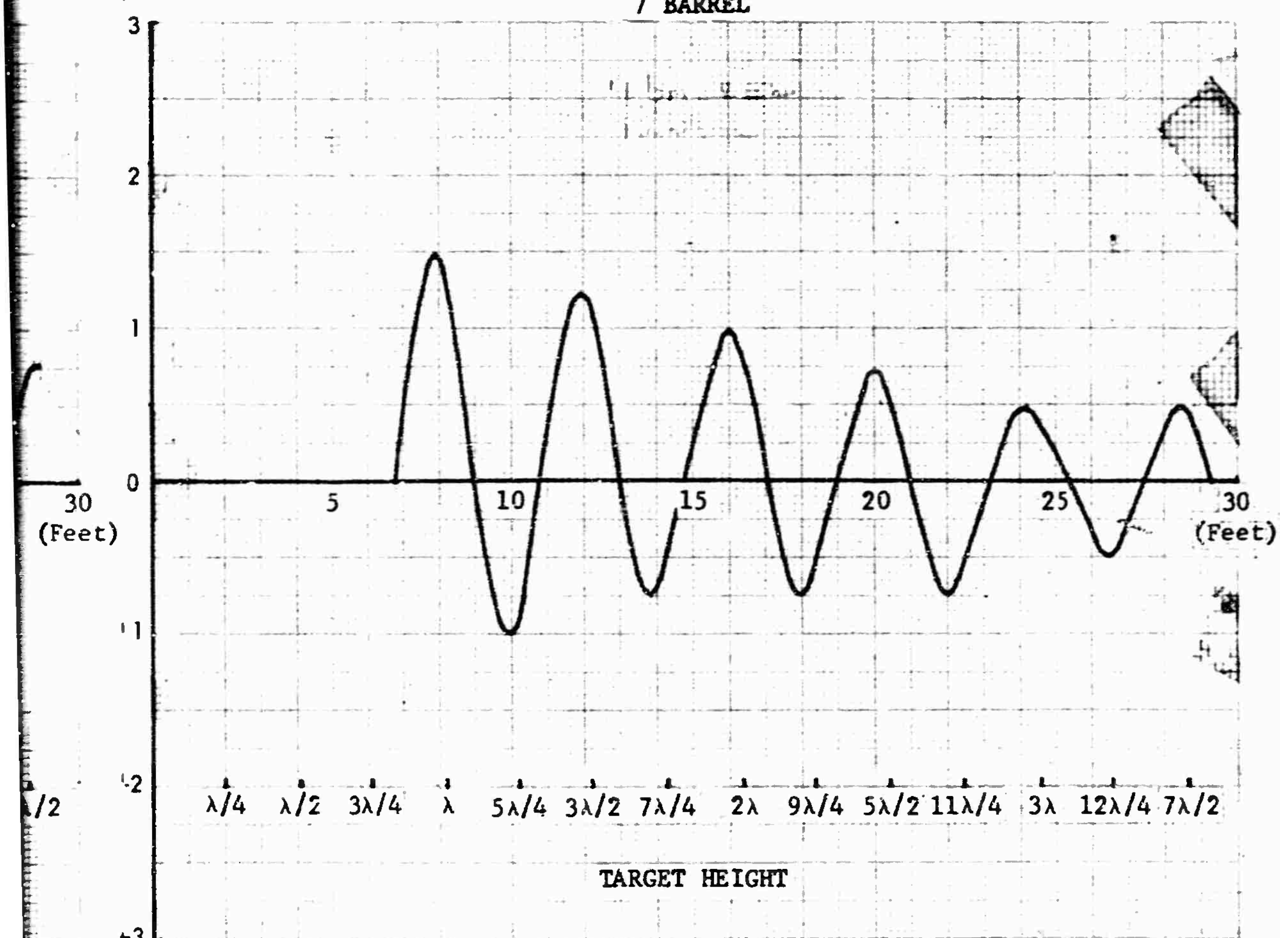

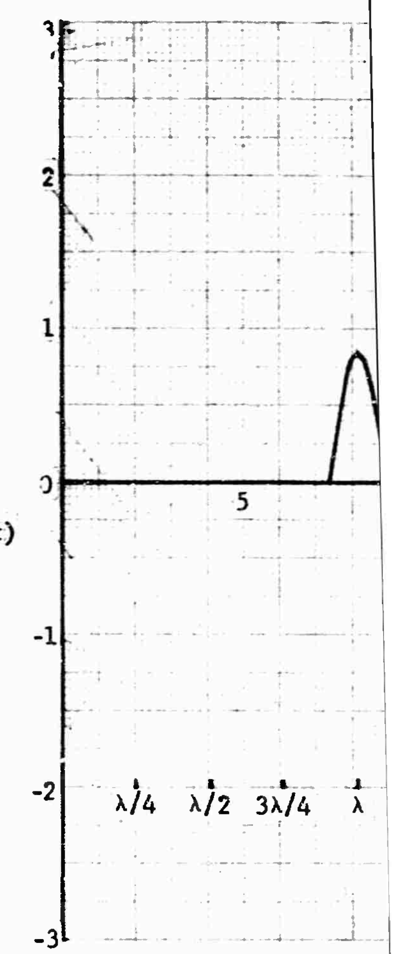

Fig. 91 C

2

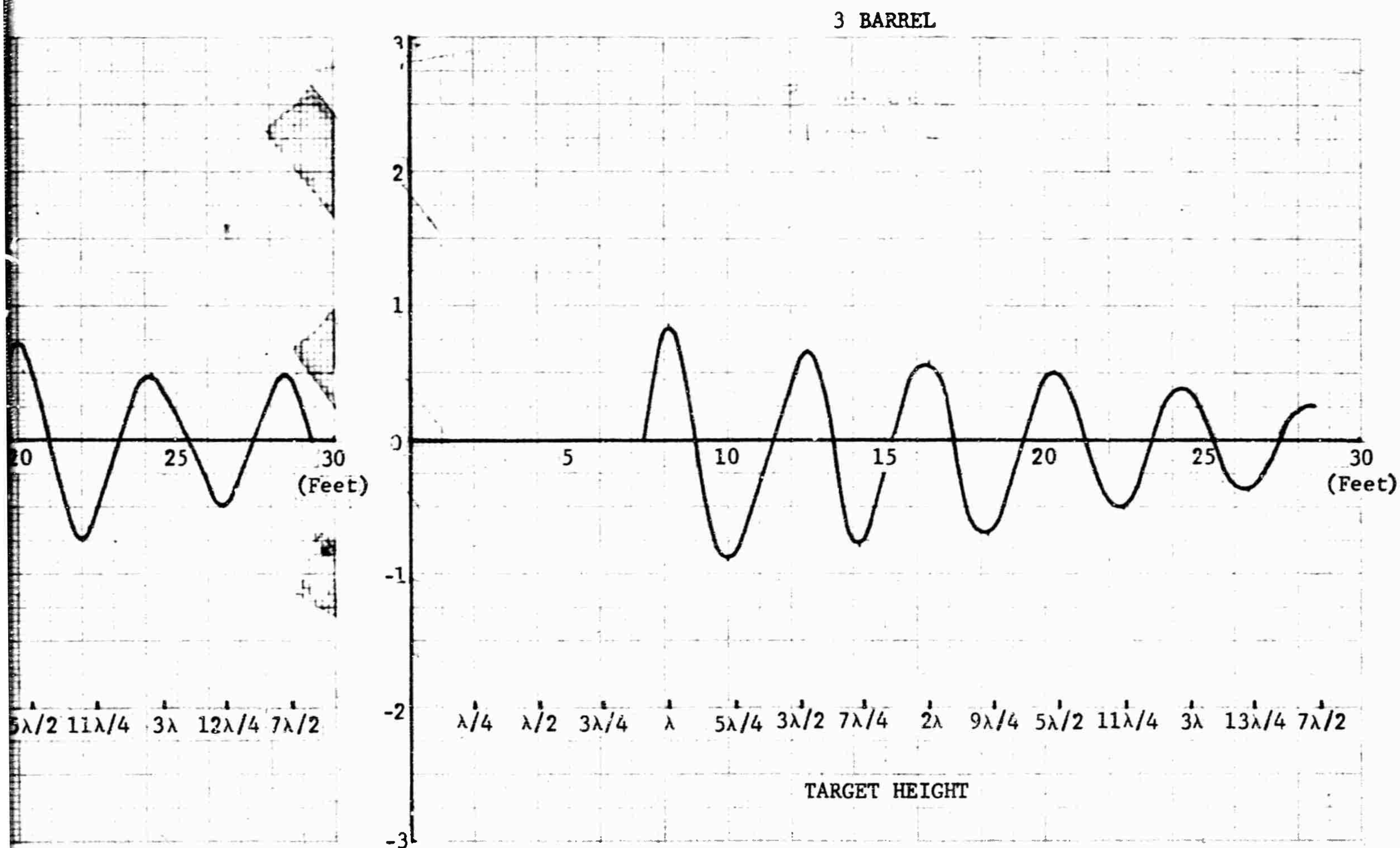

Fig. 91 COUPLING ERROR VERSUS HEIGHT AT 120 MHz

3

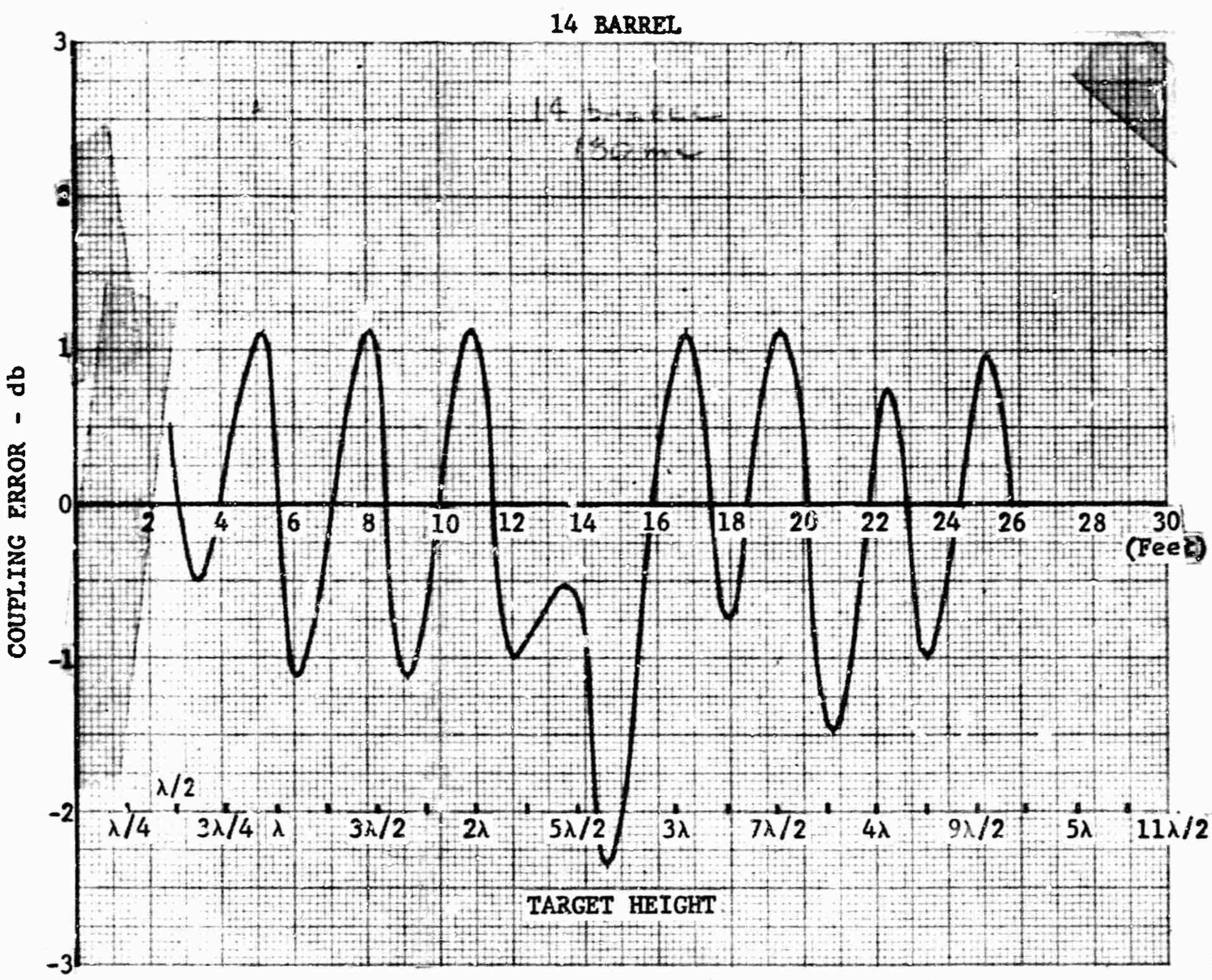
14 BARREL
COUPLING ERROR - db
3
1
0
-1
-2
-3
2
4
6
8
10
12
14
16
18
20
22
24
26
28
30
(Feet)
λ/2
λ/4
3λ/4
λ
3λ/2
2λ
5λ/2
3λ
7λ/2
4λ
9λ/2
5λ
11λ/2
TARGET HEIGHT

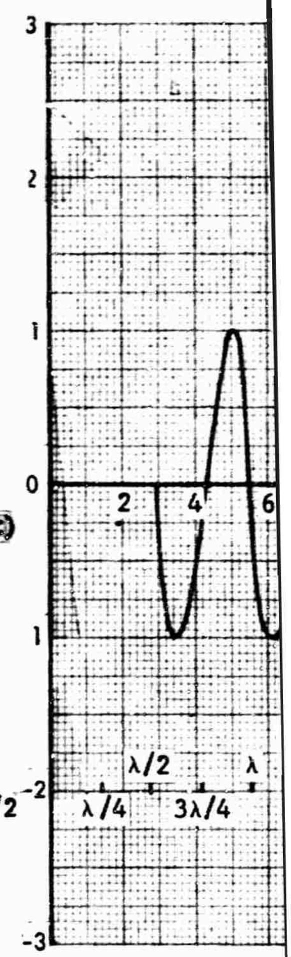
3
2
1
0
1
-2
-3
2
4
6
λ/2
λ
λ/4
3λ/4

HORIZONTAL POLARITY

7 BARREL

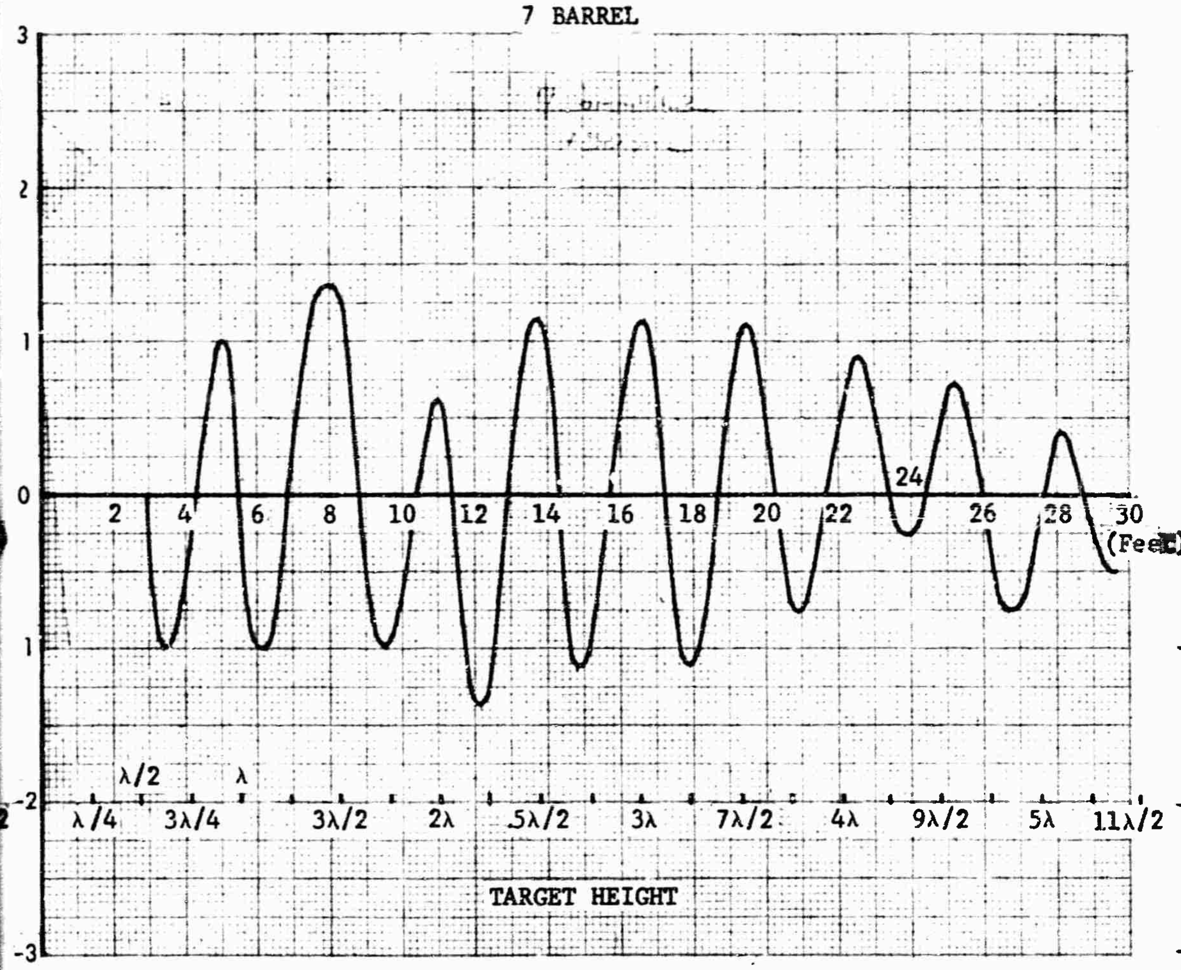

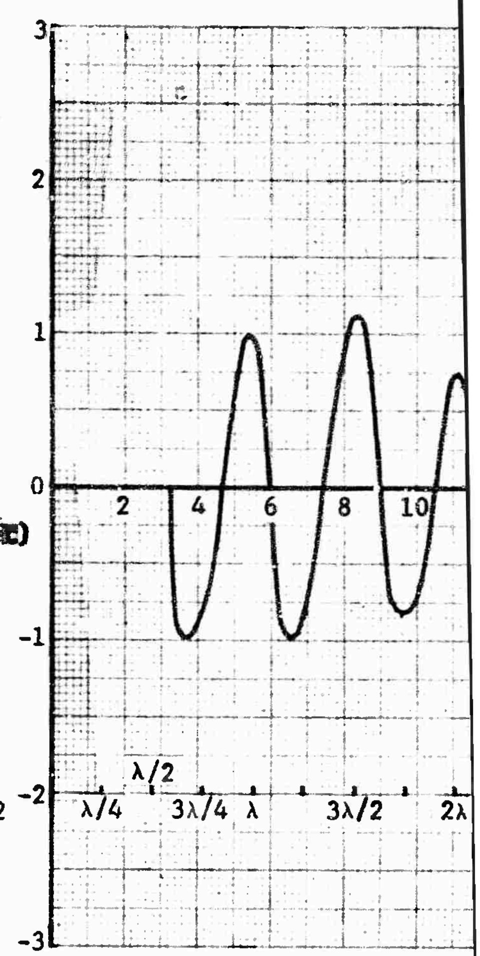

Fig. 92

2

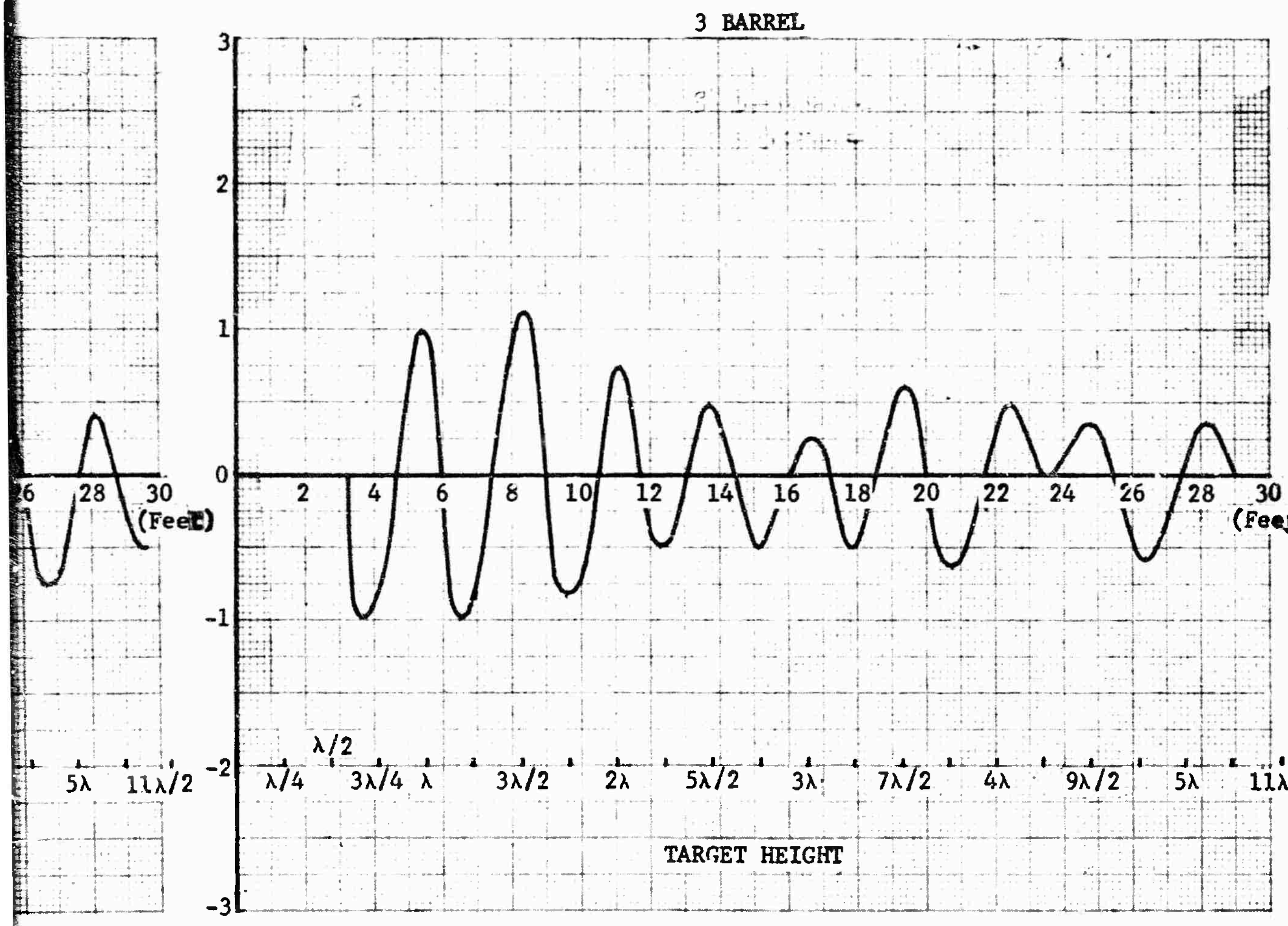

Fig. 92 COUPLING ERROR VERSUS HEIGHT AT 180 MHz

3

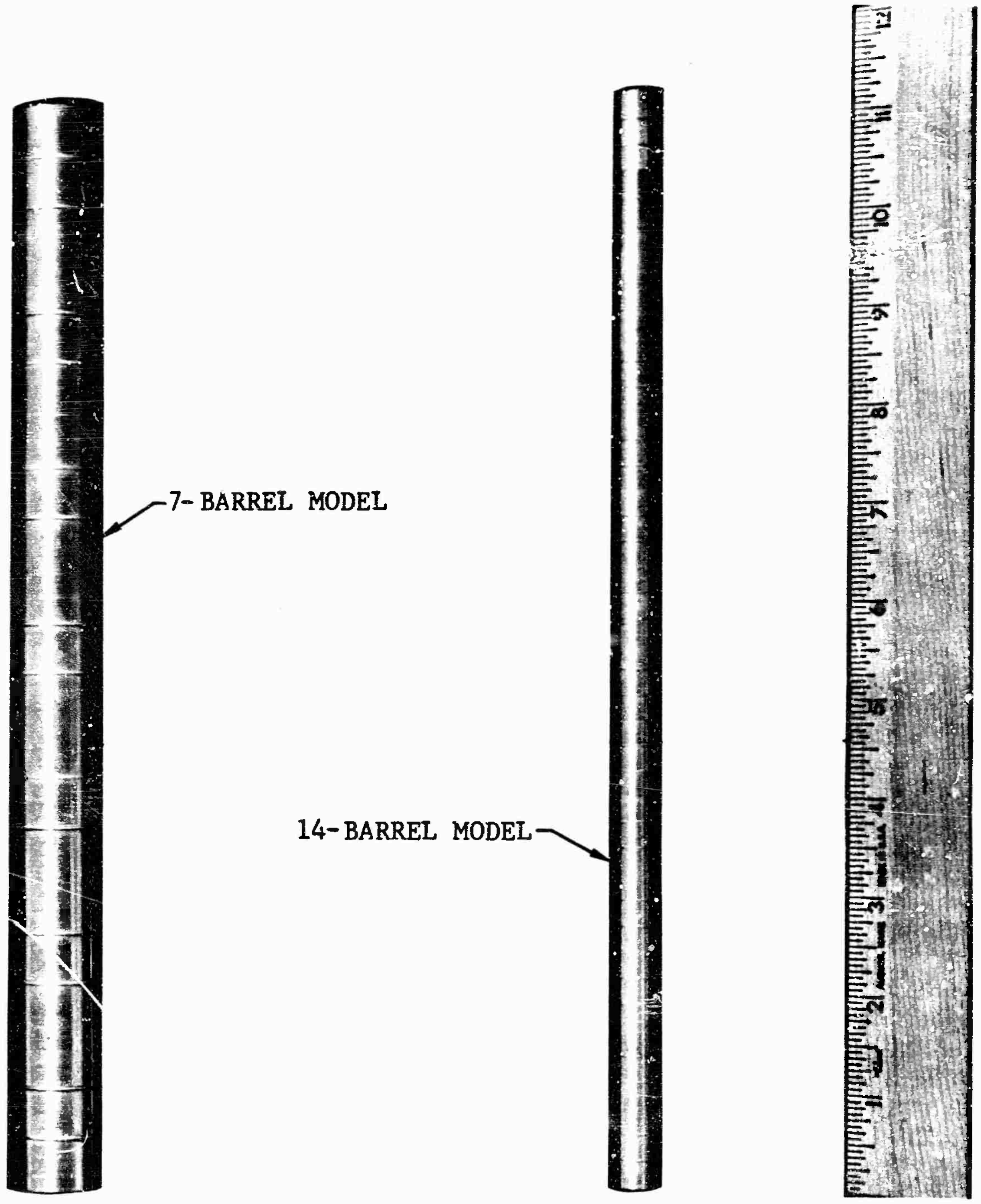

Fig. 93 SCALED MODELS USED TO OBTAIN VALIDATION DATA

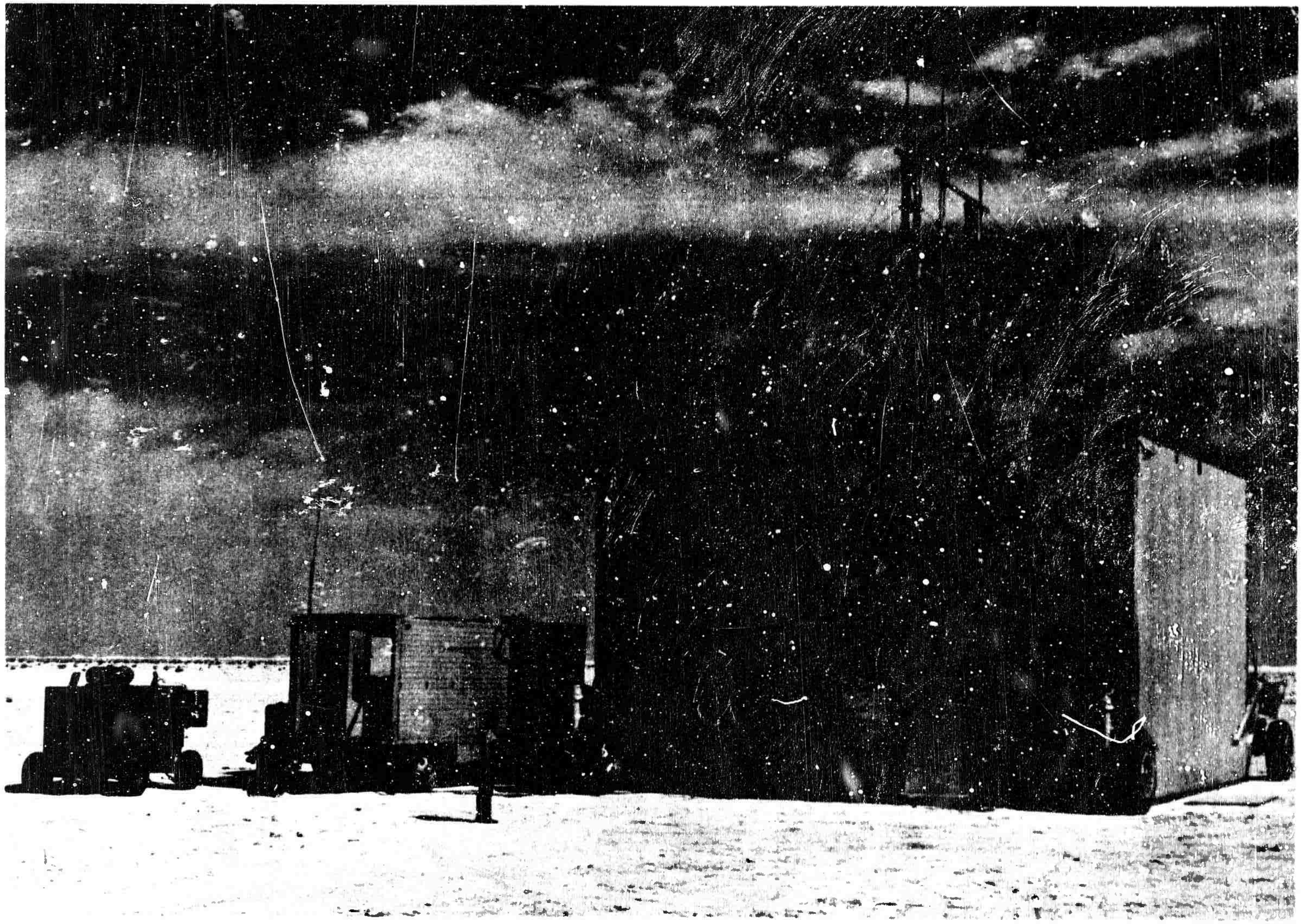

Fig. 94 MOBILE SHELTER USED FOR ANTENNA ISOLATION

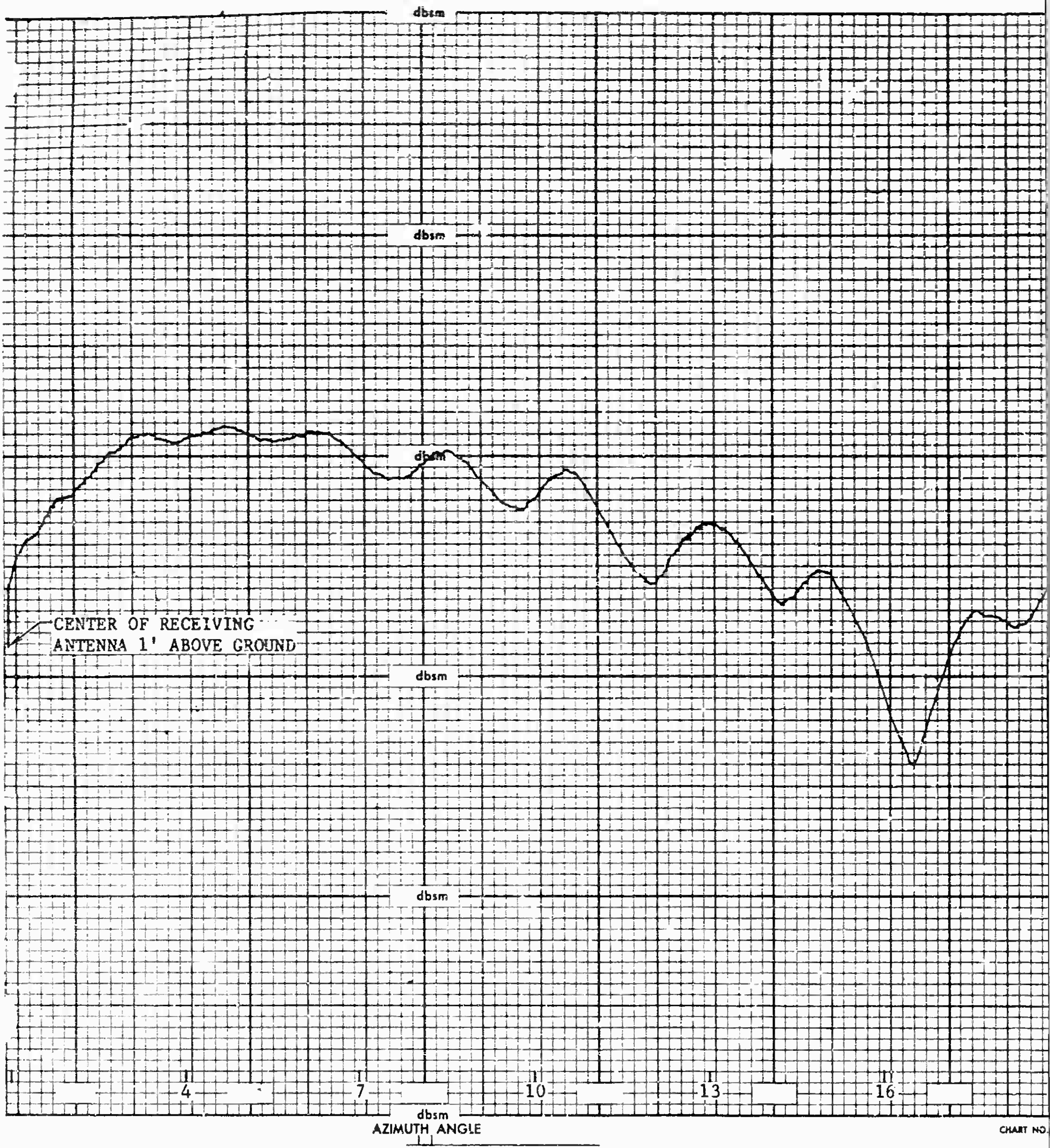
dbsm
dbsm
dbsm
CENTER OF RECEIVING
ANTENNA 1' ABOVE GROUND
dbsm
dbsm
4
7
10
13
16
dbsm
AZIMUTH ANGLE
CHART NO.

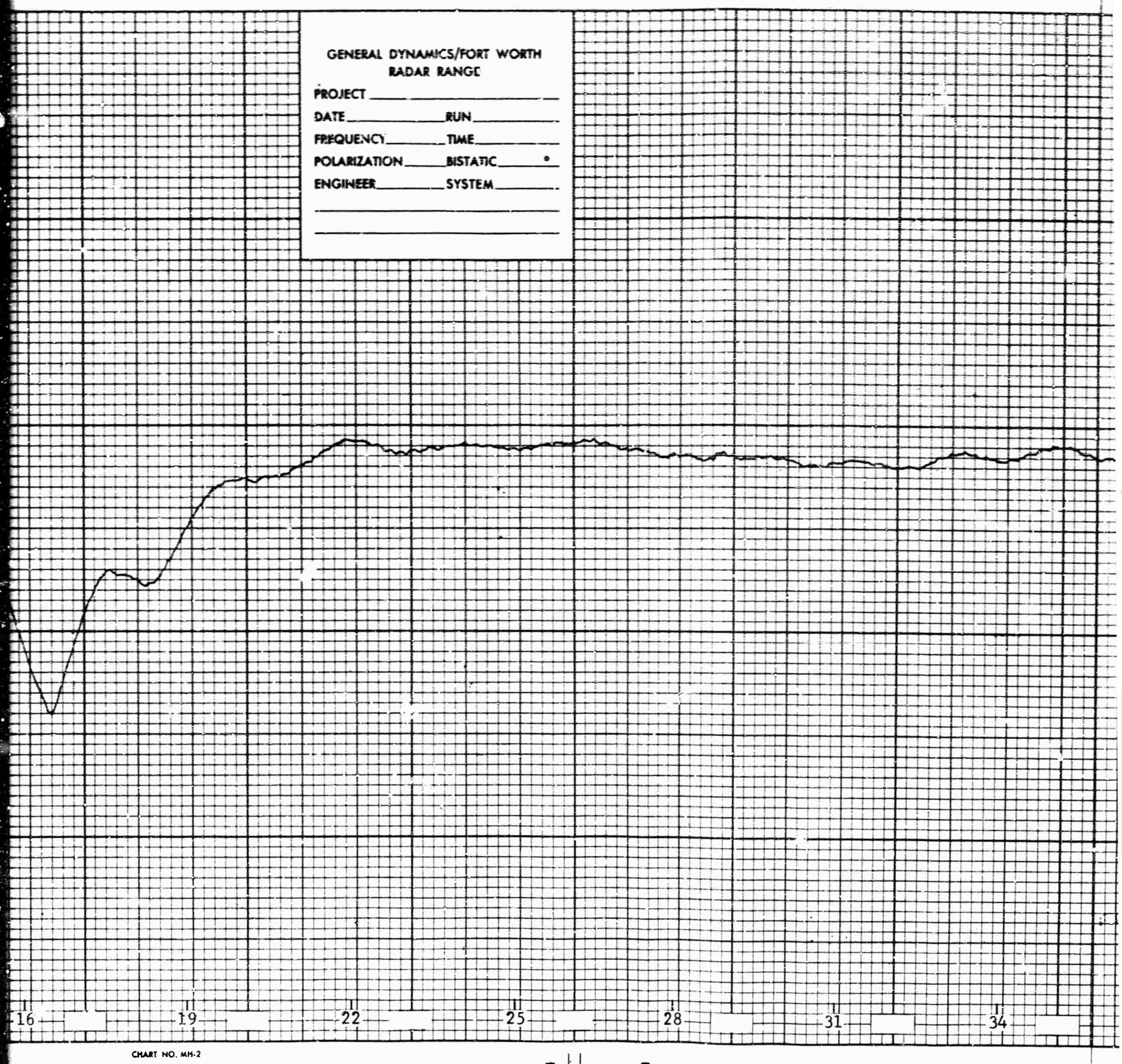
GENERAL DYNAMICS/FORT WORTH
RADAR RANGE
PROJECT
DATE
RUN
FREQUENCY
TIME
POLARIZATION
BISTATIC
ENGINEER
SYSTEM
16
19
22
25
28
31
34
CHART NO. MH-2

2

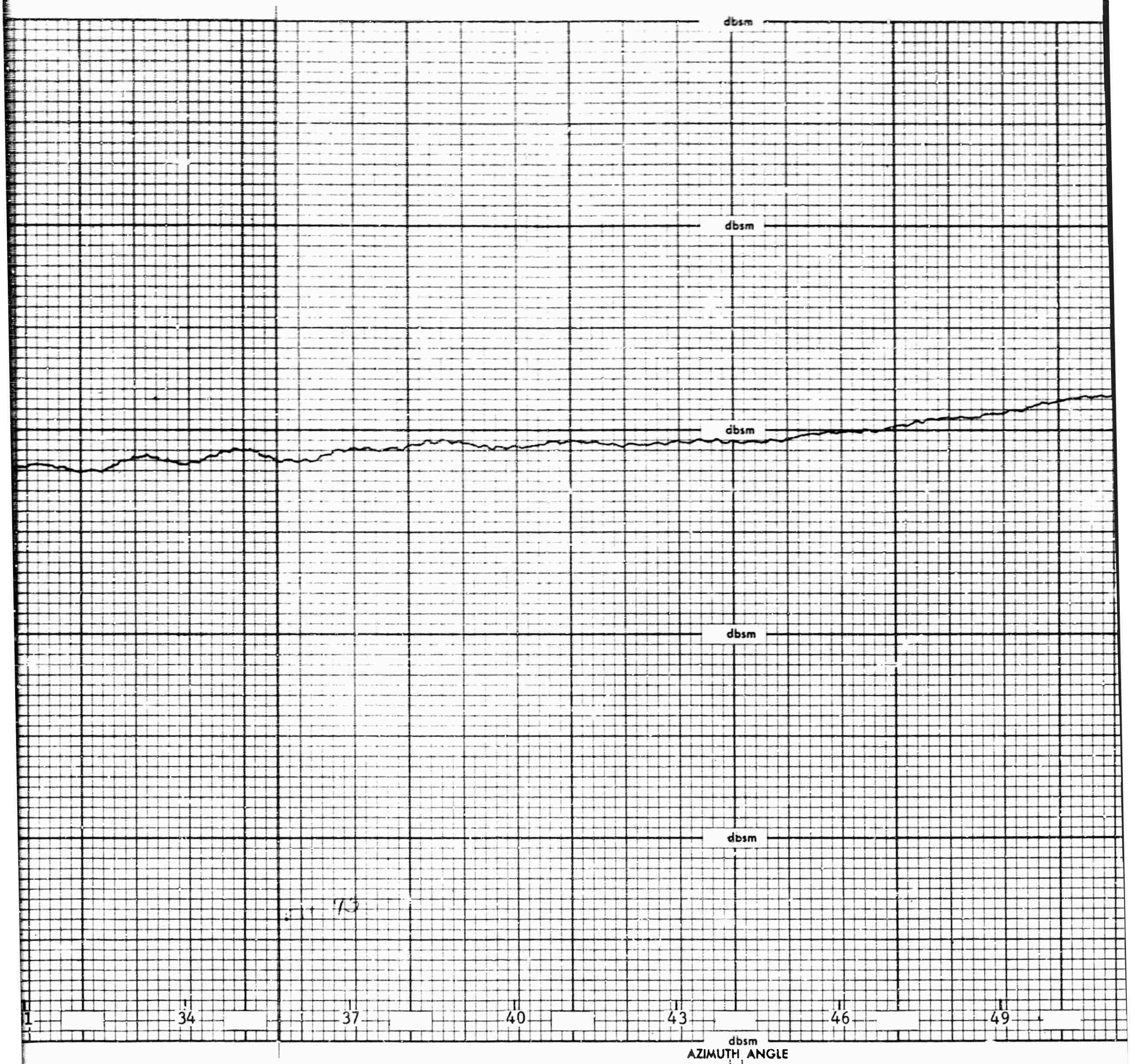

FIG. 9

3

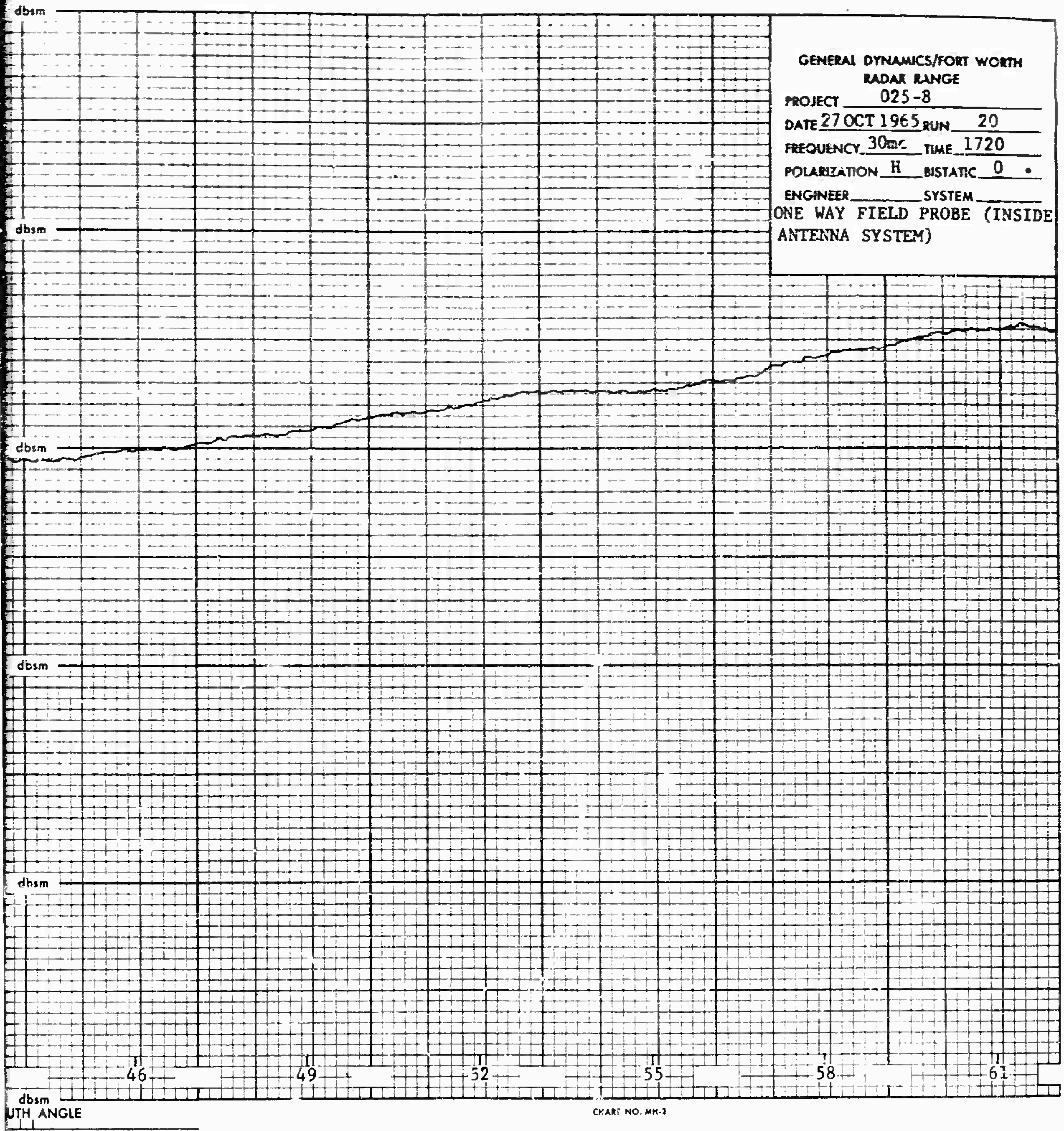

FIG. 35a VERTICAL FIELD PROBE FOR ANTENNA INSIDE MOBILE SHELTER

4

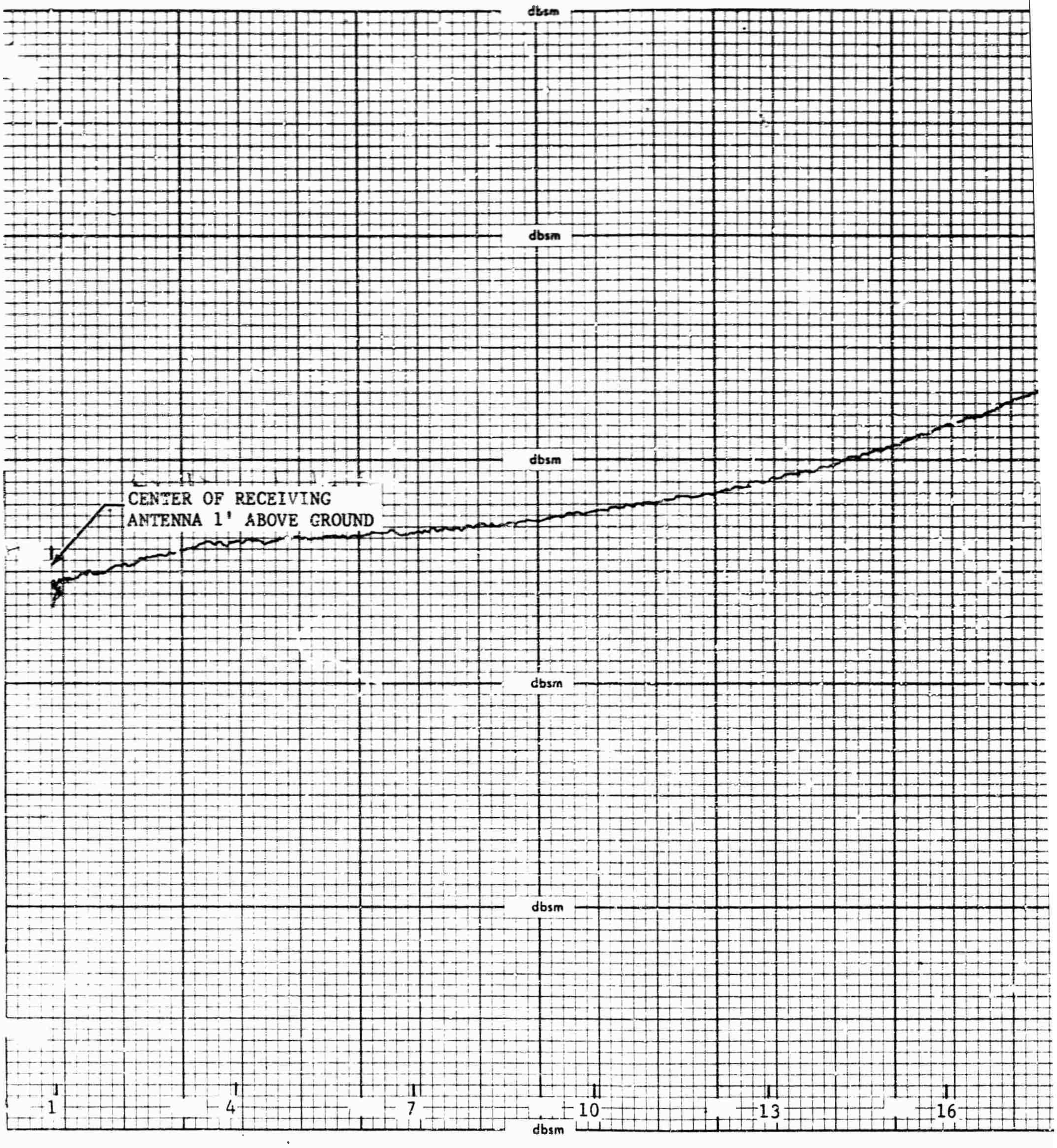

dbsm
dbsm
dbsm
CENTER OF RECEIVING
ANTENNA 1' ABOVE GROUND
dbsm
dbsm
1
4
7
10
13
16
dbsm

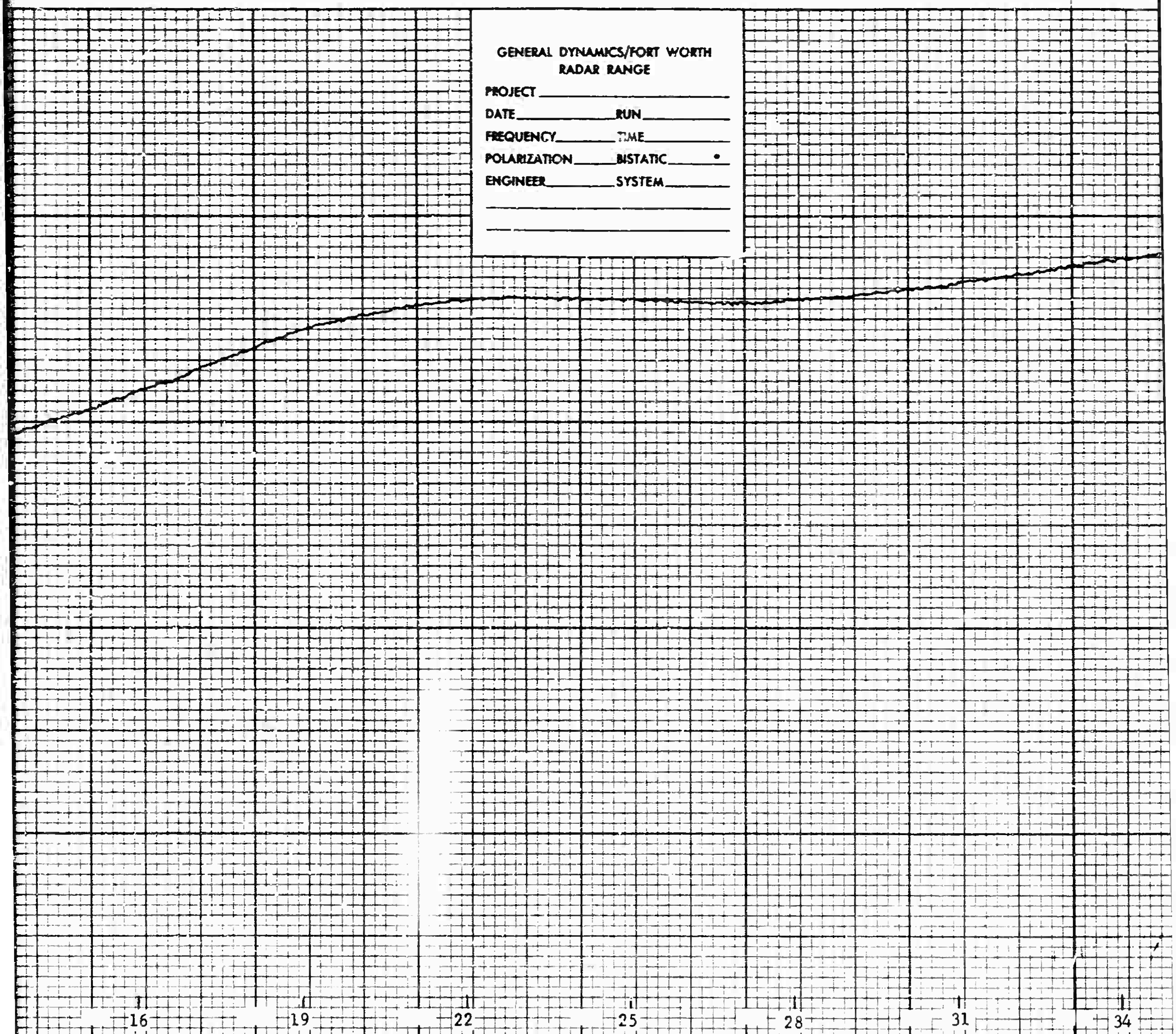
GENERAL DYNAMICS/FORT WORTH
RADAR RANGE
PROJECT
DATE
RUN
FREQUENCY
TIME
POLARIZATION
BISTATIC
ENGINEER
SYSTEM
16
19
22
25
28
31
34

2

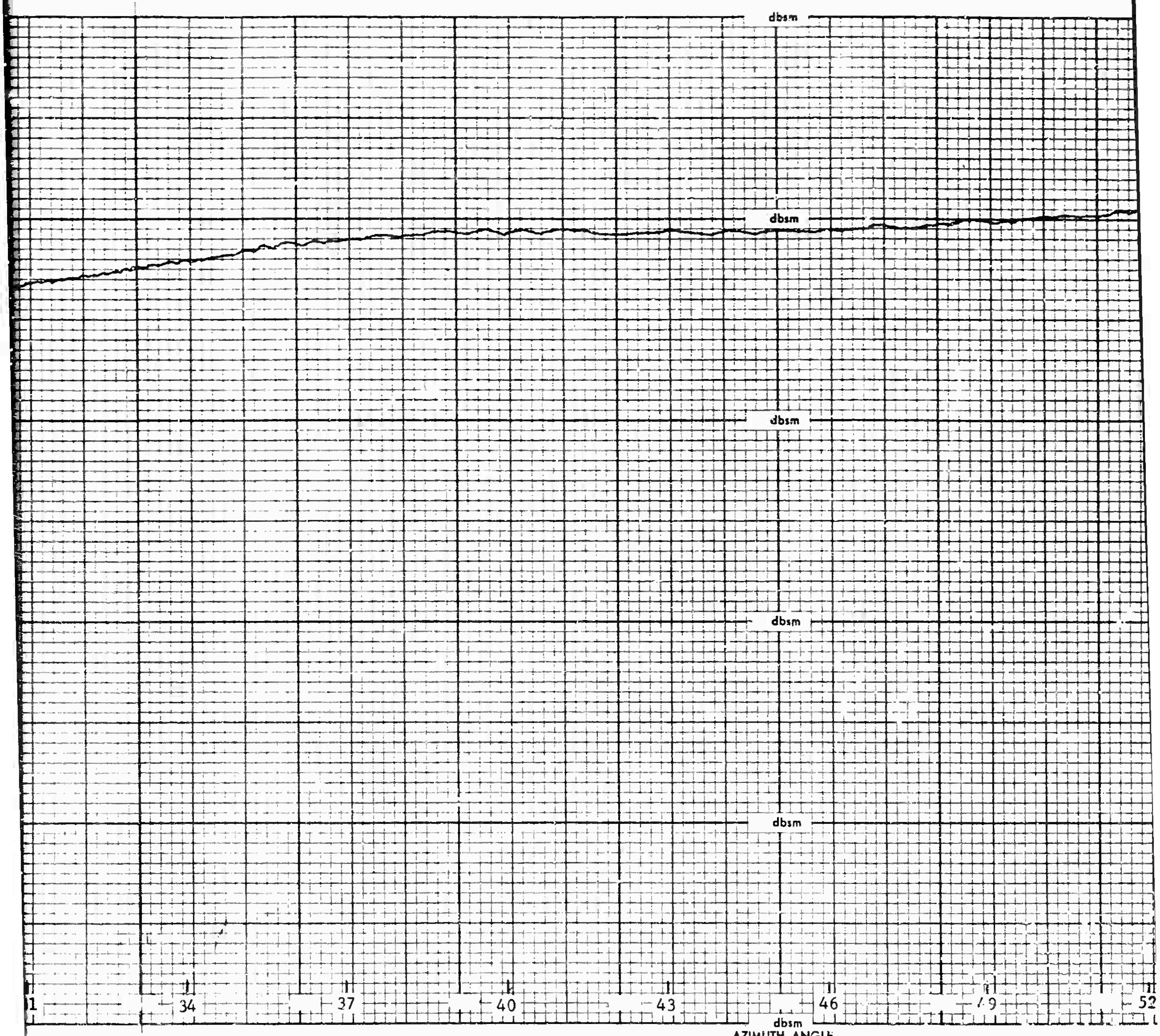

Fig

3

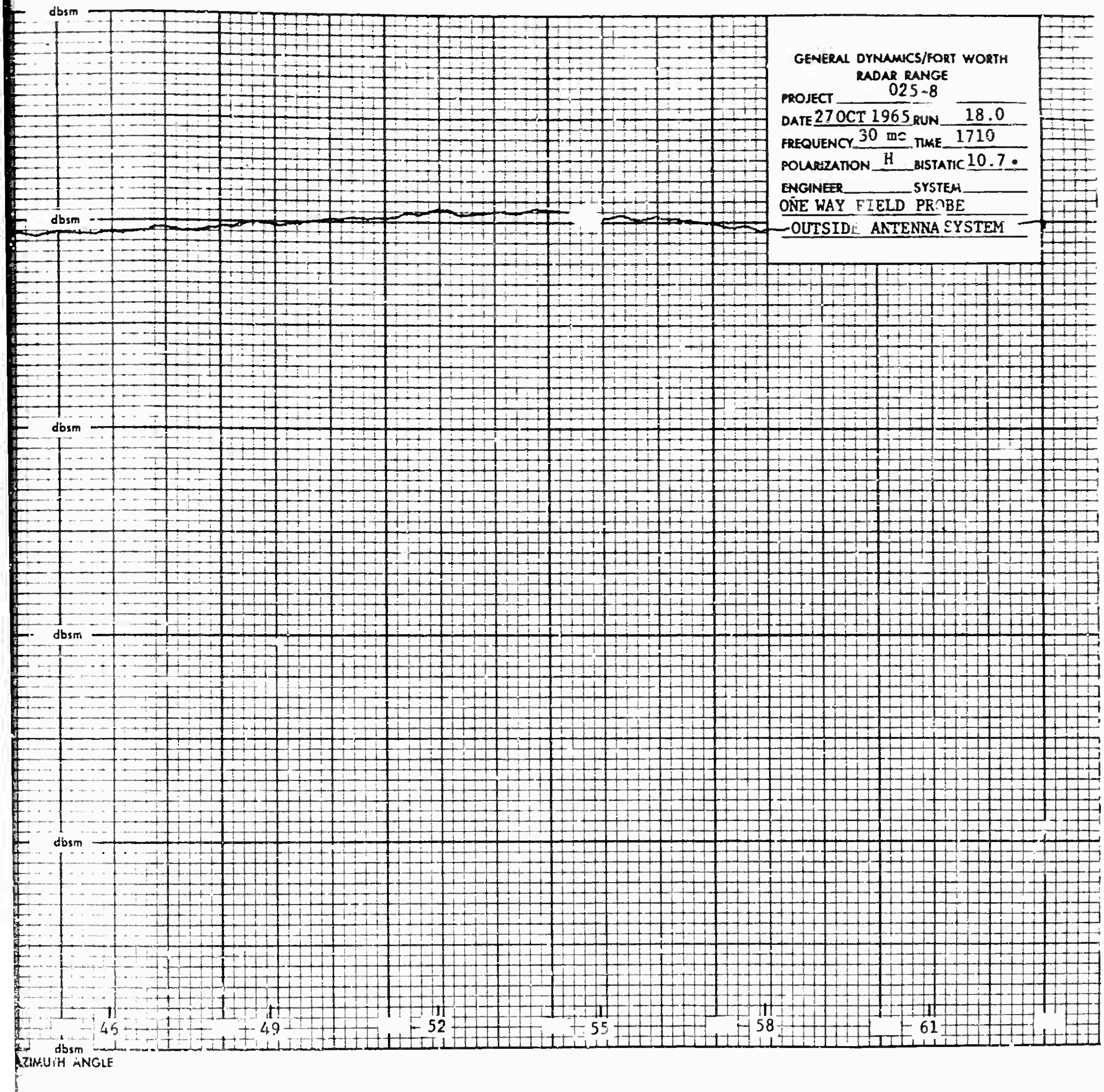

Fig. 95b VERTICAL FIELD PROBE FOR ANTENNA OUTSIDE MOBILE SHELTER

4

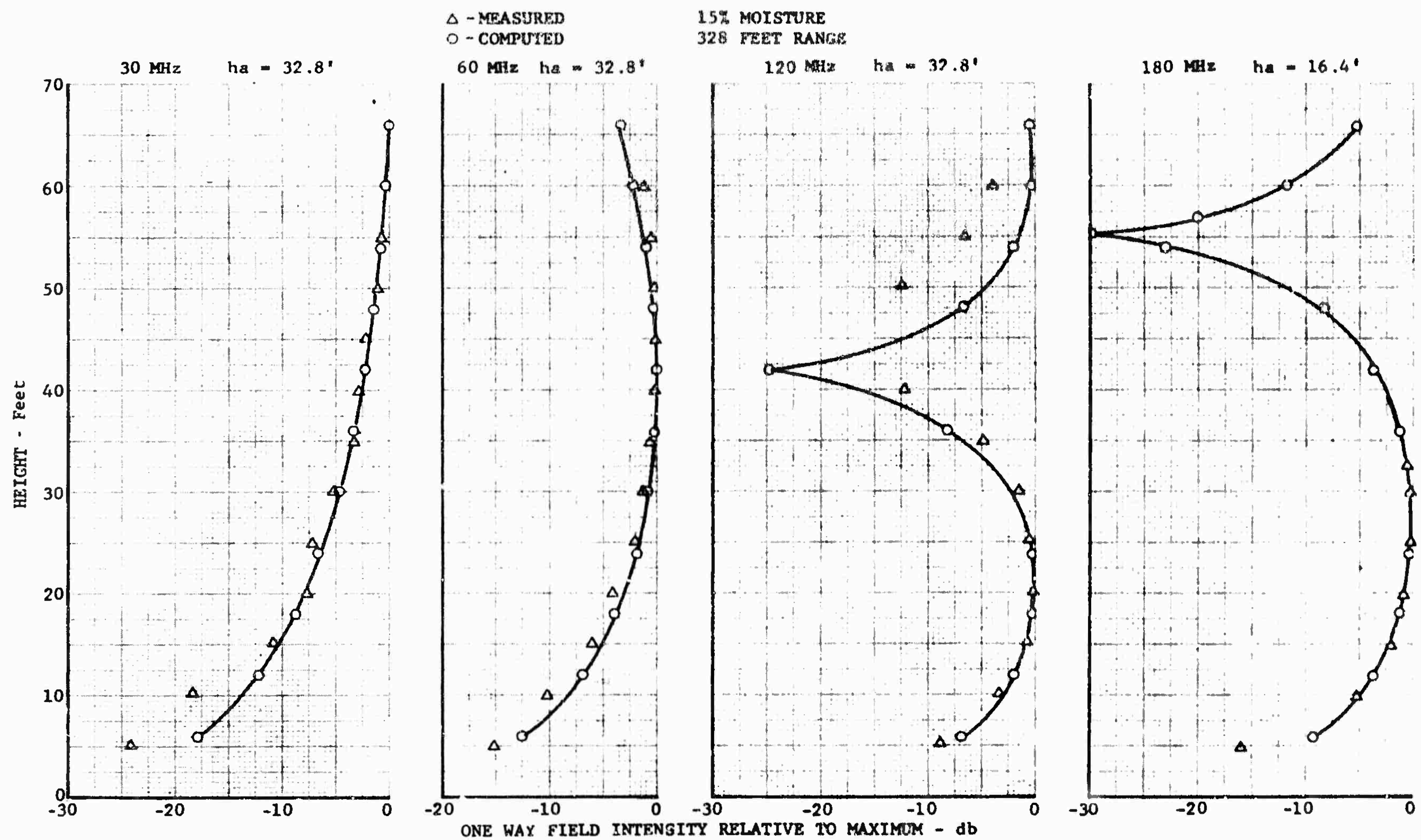

Fig. 96 MEASURED VERSUS COMPUTED VERTICAL FIELD (328 FOOT RANGE, HORIZONTAL POLARIZATION)

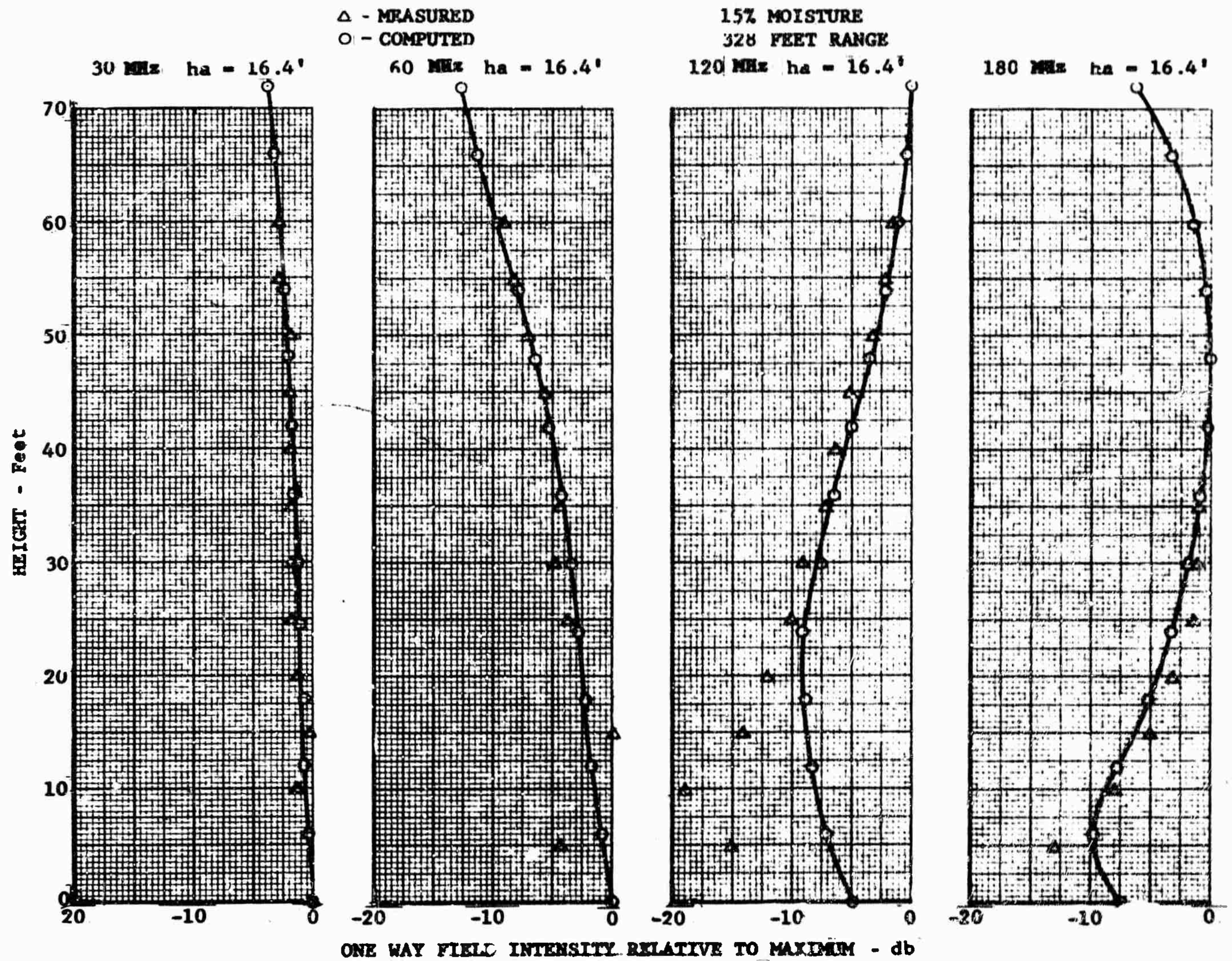

Fig. 97 MEASURED VERSUS COMPUTED VERTICAL FIELD
(328 FOOT RANGE, VERTICAL POLARIZATION)

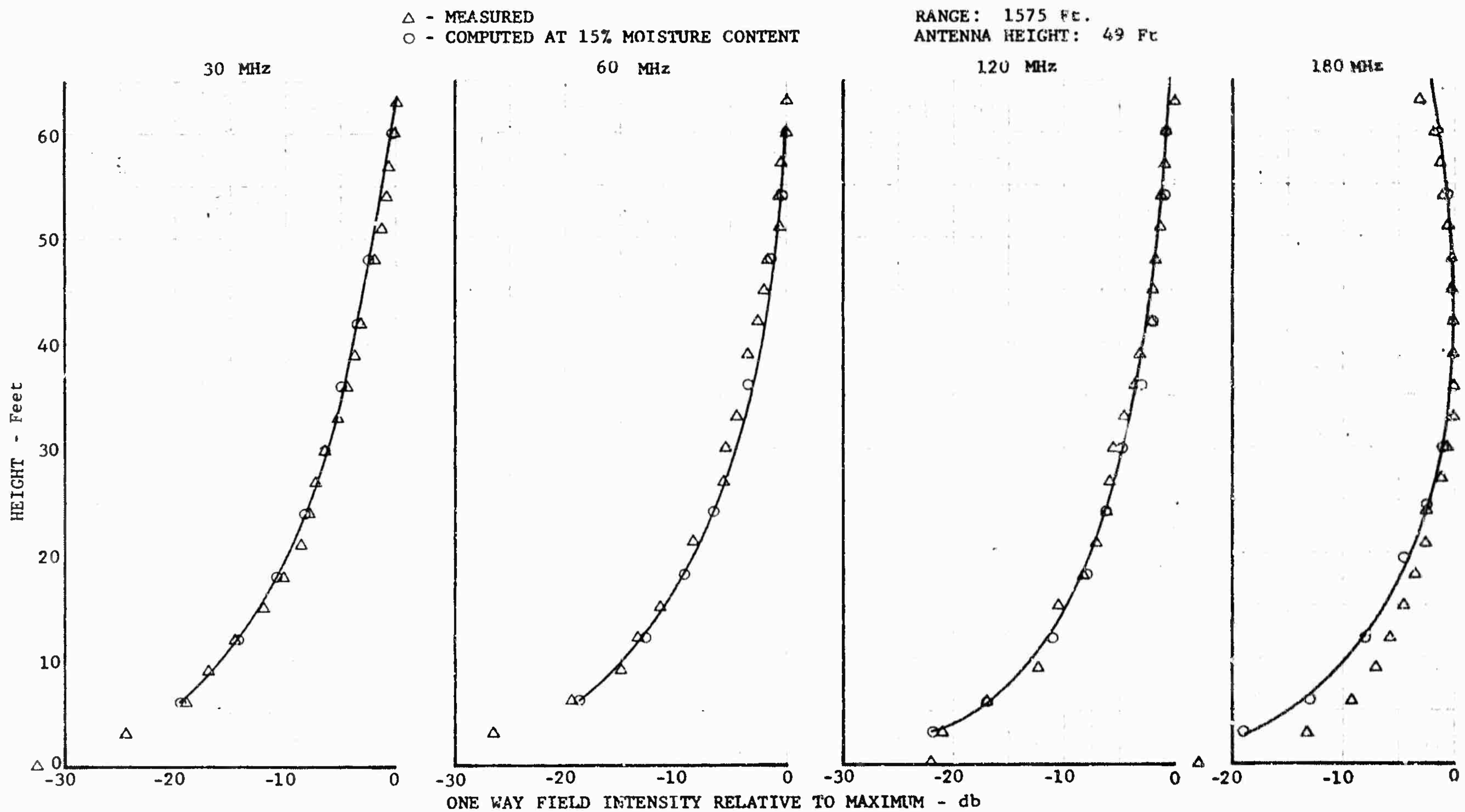

Fig. 98 MEASURED VERSUS COMPUTED VERTICAL FIELD
(1575 FOOT RANGE, HORIZONTAL POLARIZATION)

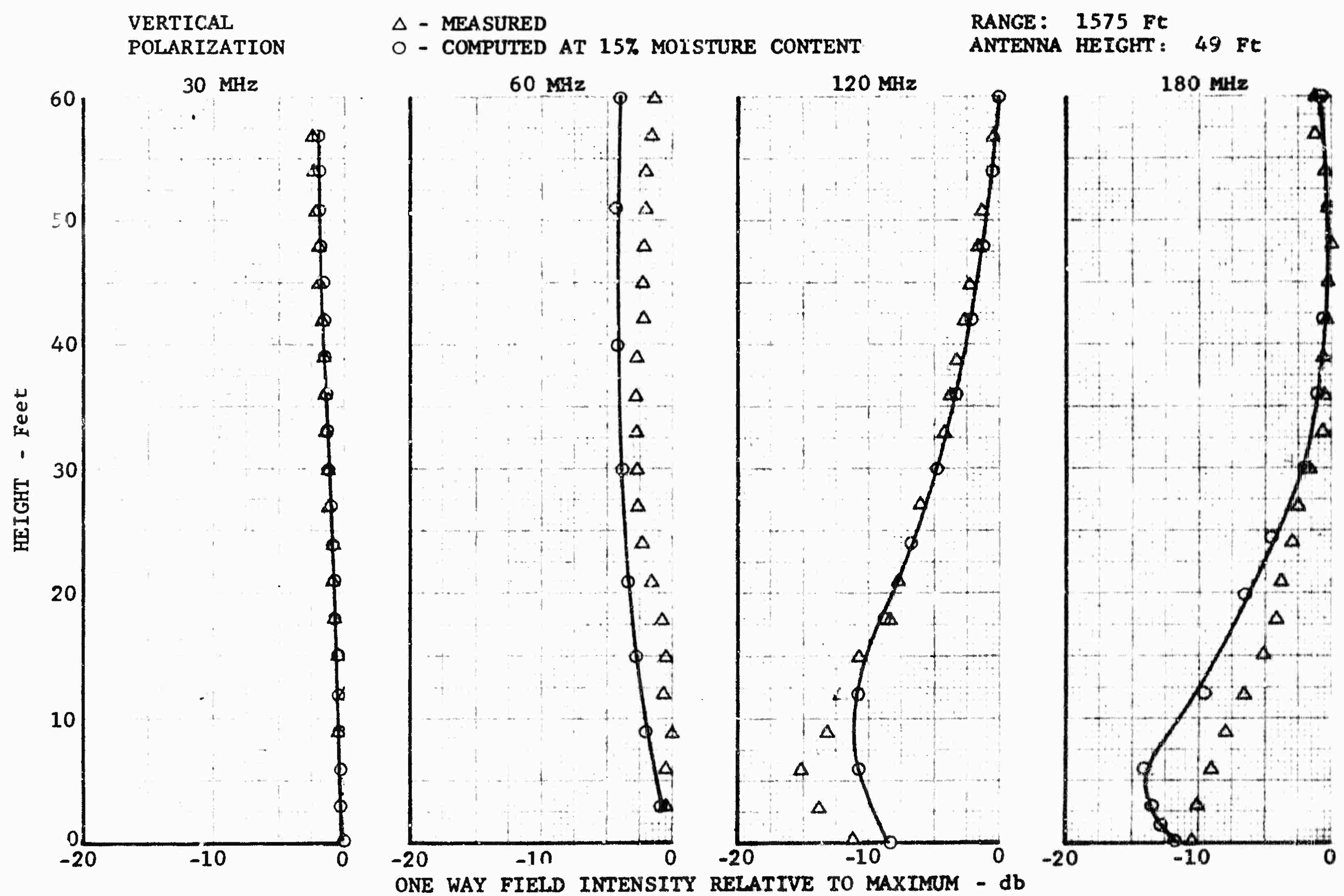

Fig. 99 MEASURED VERSUS COMPUTED VERTICAL FIELD
(1575 FOOT RANGE, VERTICAL POLARIZATION)

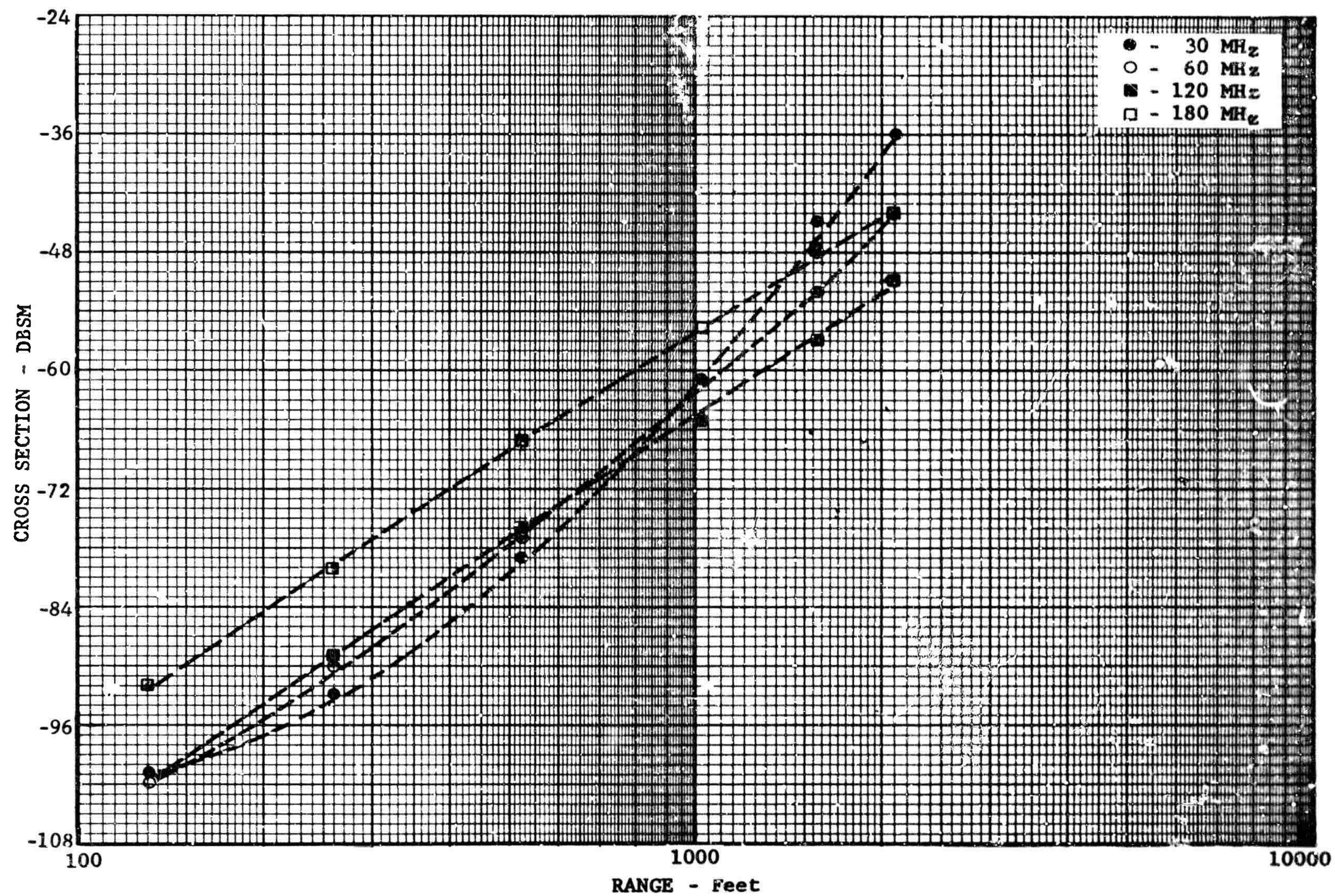

Fig. 100 MEASUREMENT SENSITIVITY VERSUS RANGE (HORIZONTAL POLARIZATION)

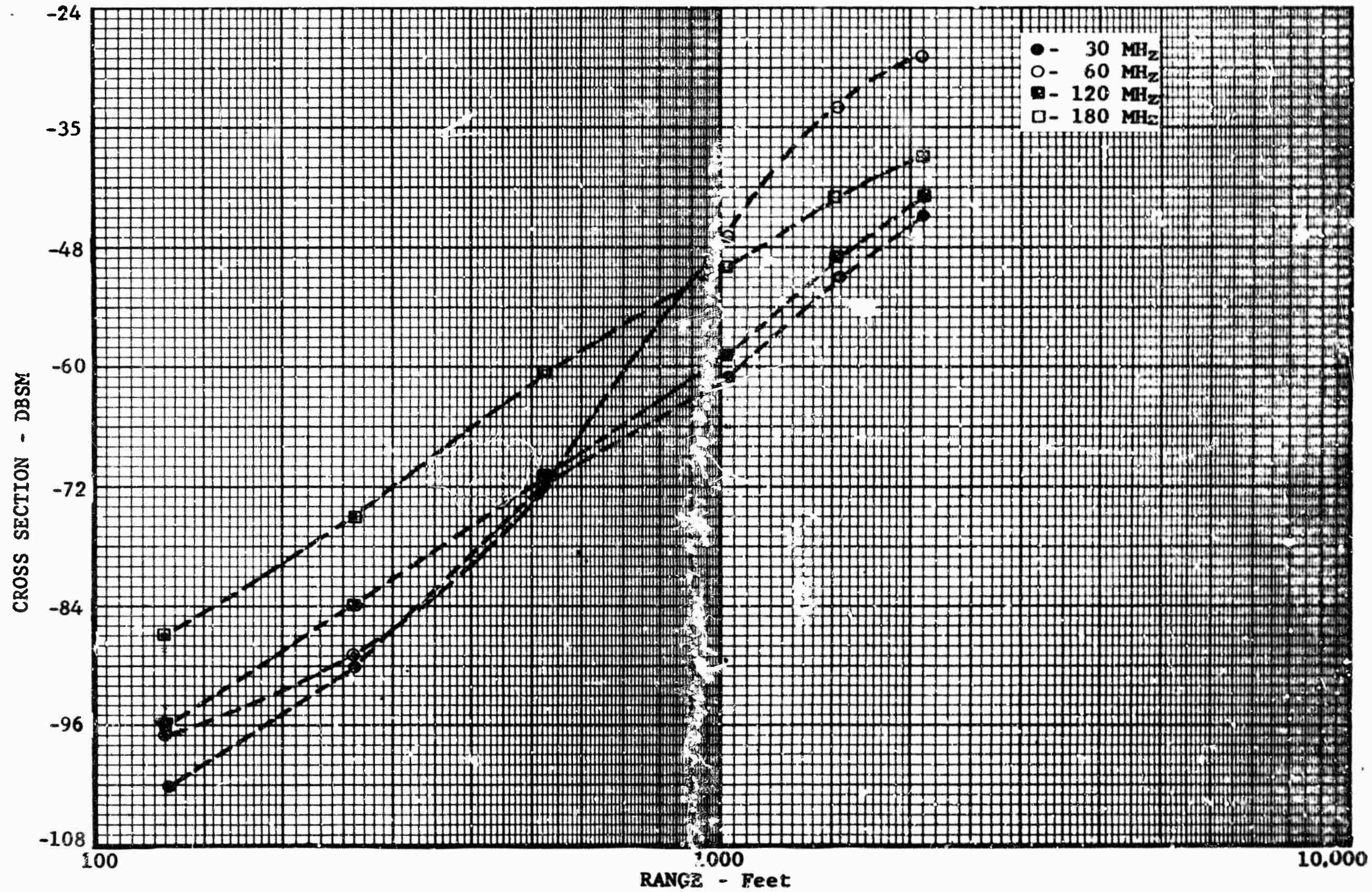

Fig. 101 MEASUREMENT SENSITIVITY VERSUS RANGE (VERTICAL POLARIZATION)

210°
240°
270°
300°

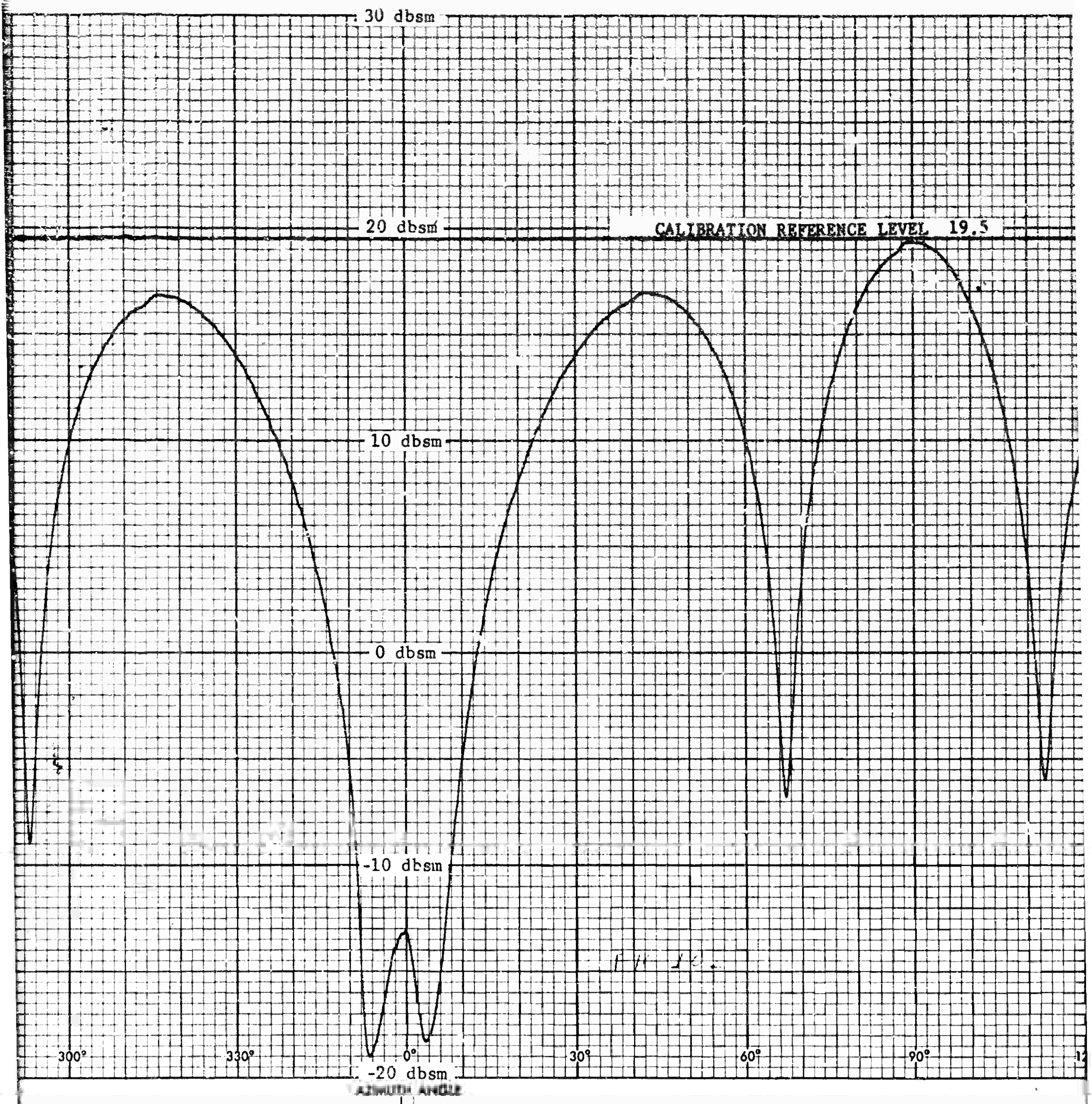

Fig. 102 FULL SCALE C
(HORIZONTAL

2

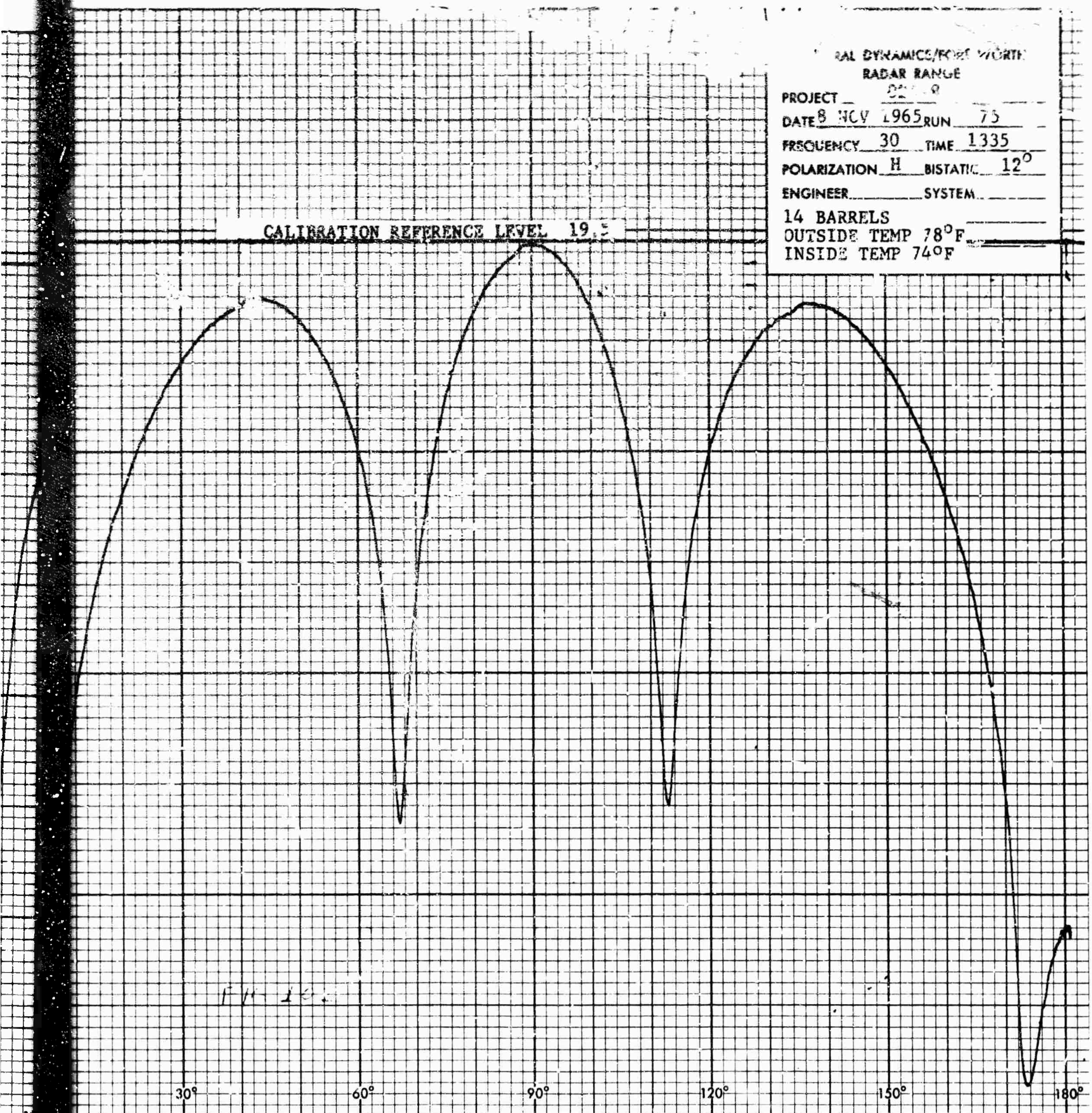

Fig. 102 FULL SCALE CROSS SECTION OF CYLINDER
(HORIZONTAL POLARIZATION, 30 MHz)

3

210°
240°
270°
300°
330°

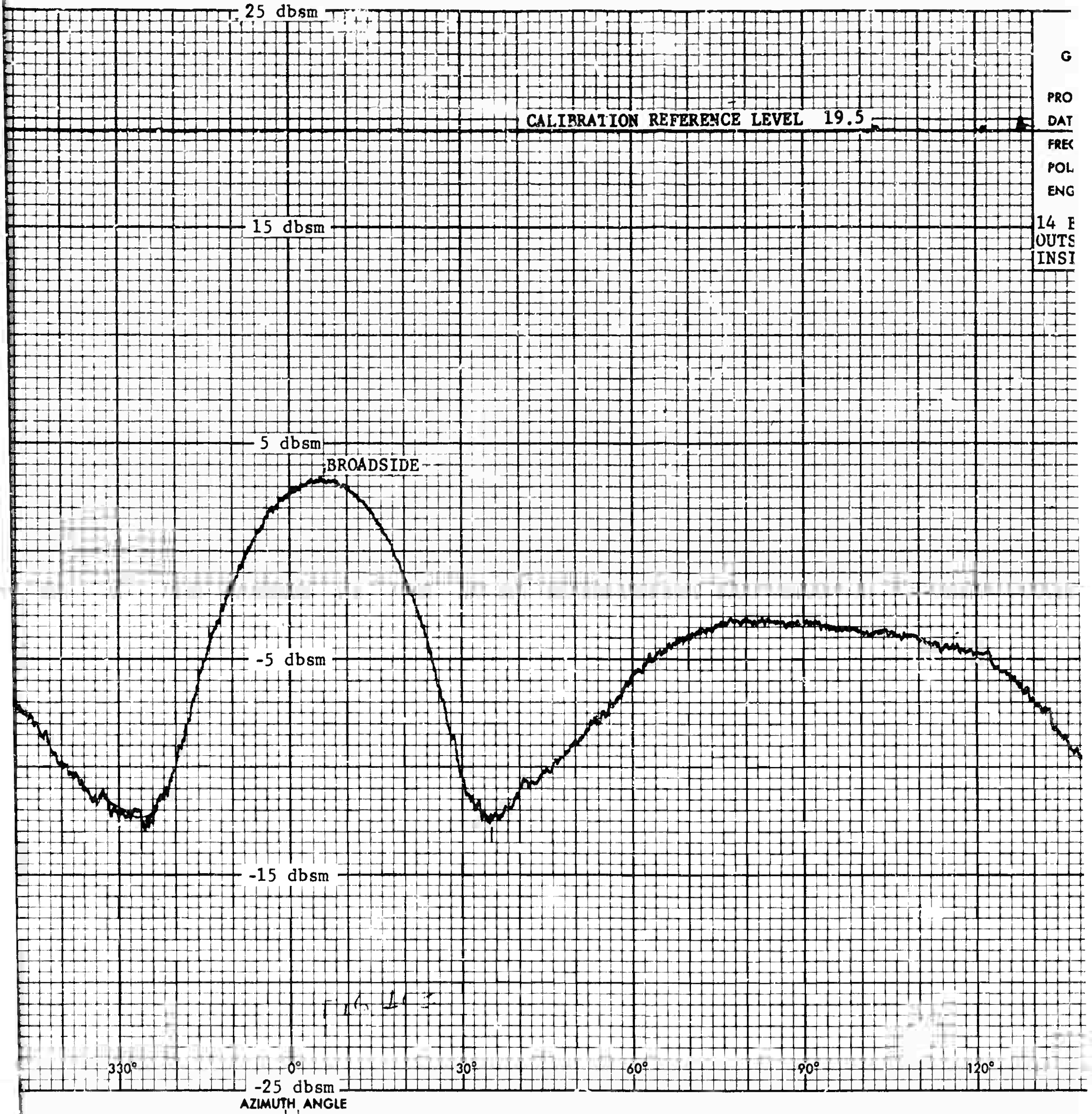

Fig. 103 FULL SCALE CROSS S
(VERTICAL POLARIZA

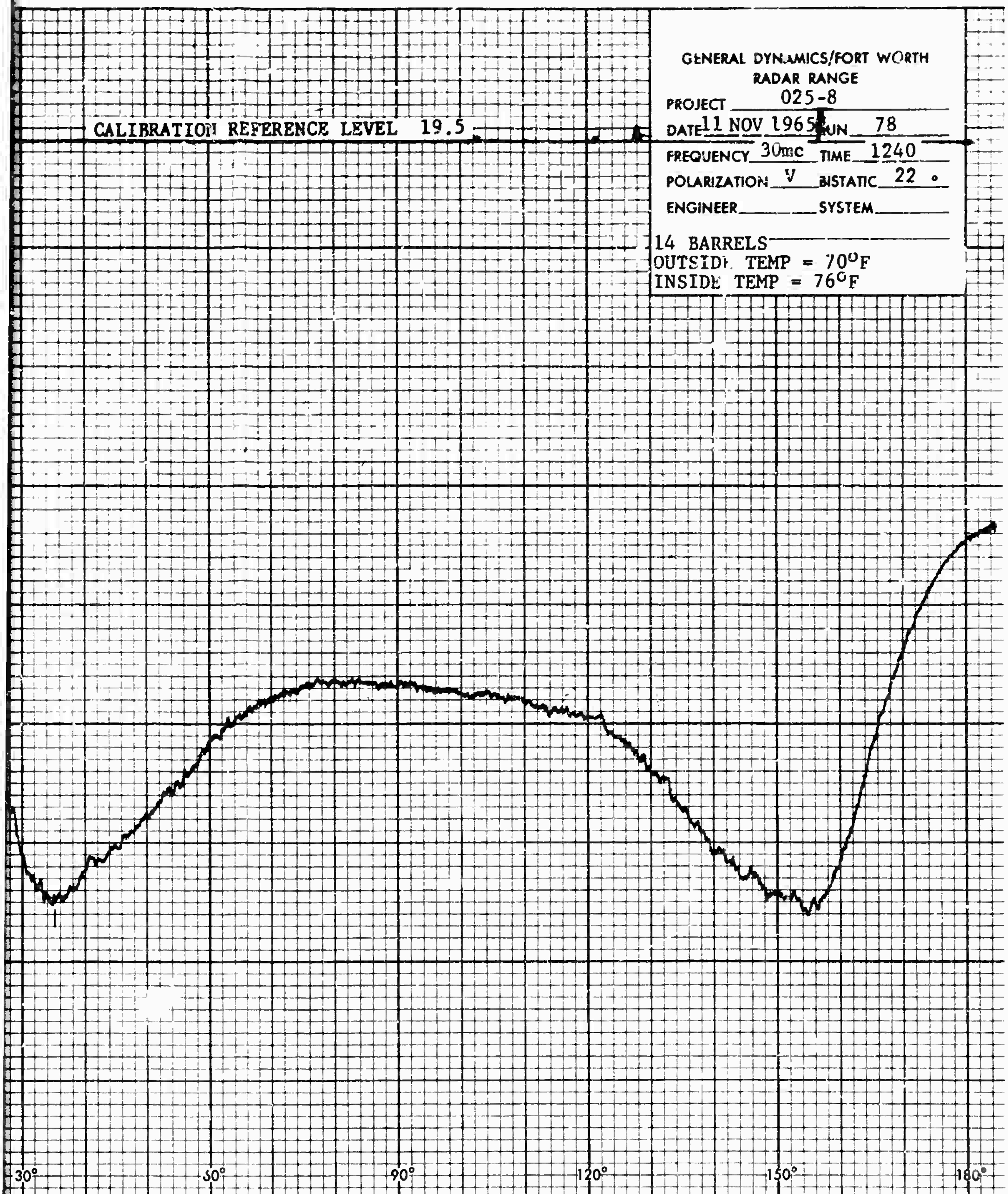

Fig. 103 FULL SCALE CROSS SECTION OF CYLINDER
(VERTICAL POLARIZATION, 30 MHz)

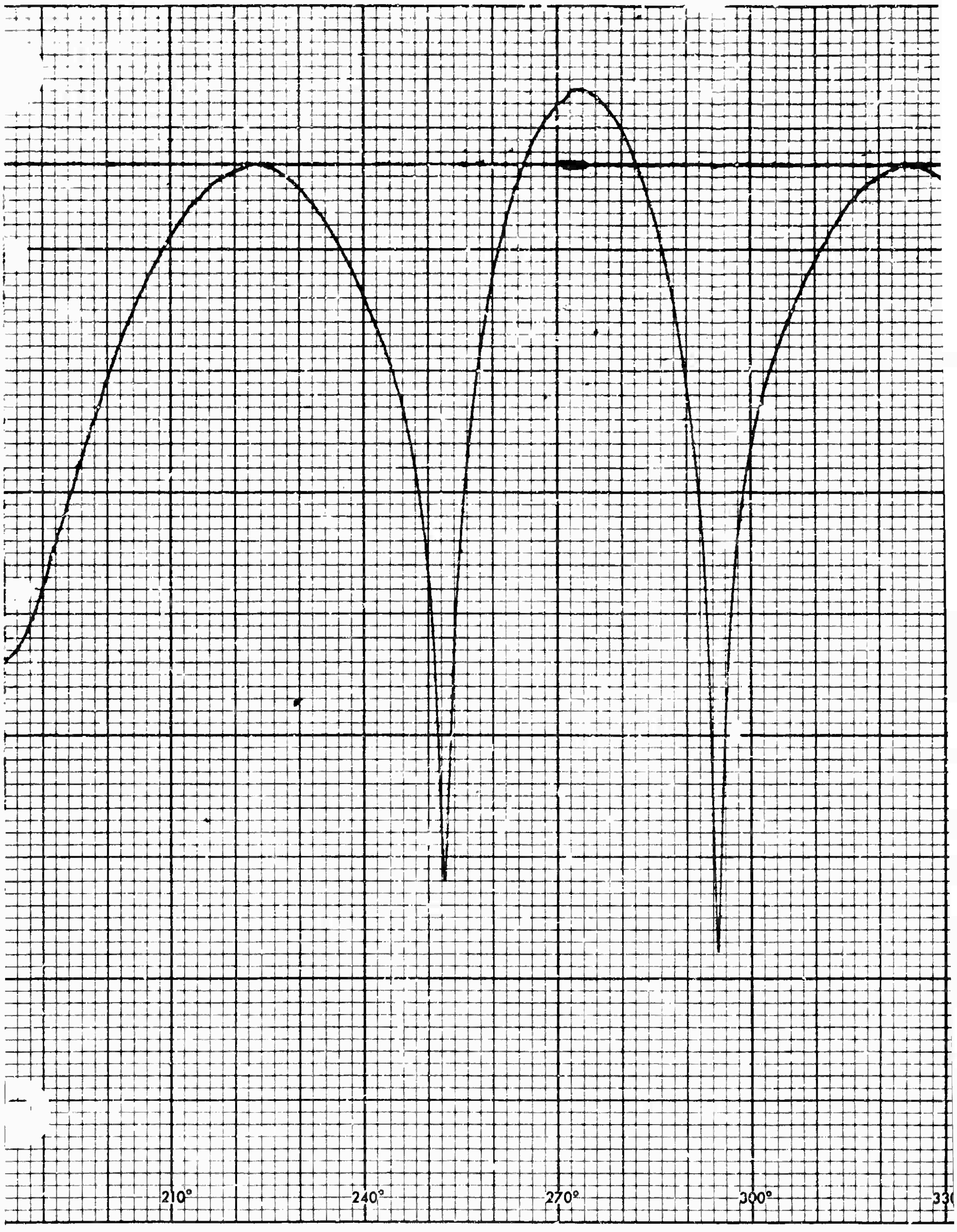

210°
240°
270°
300°

/

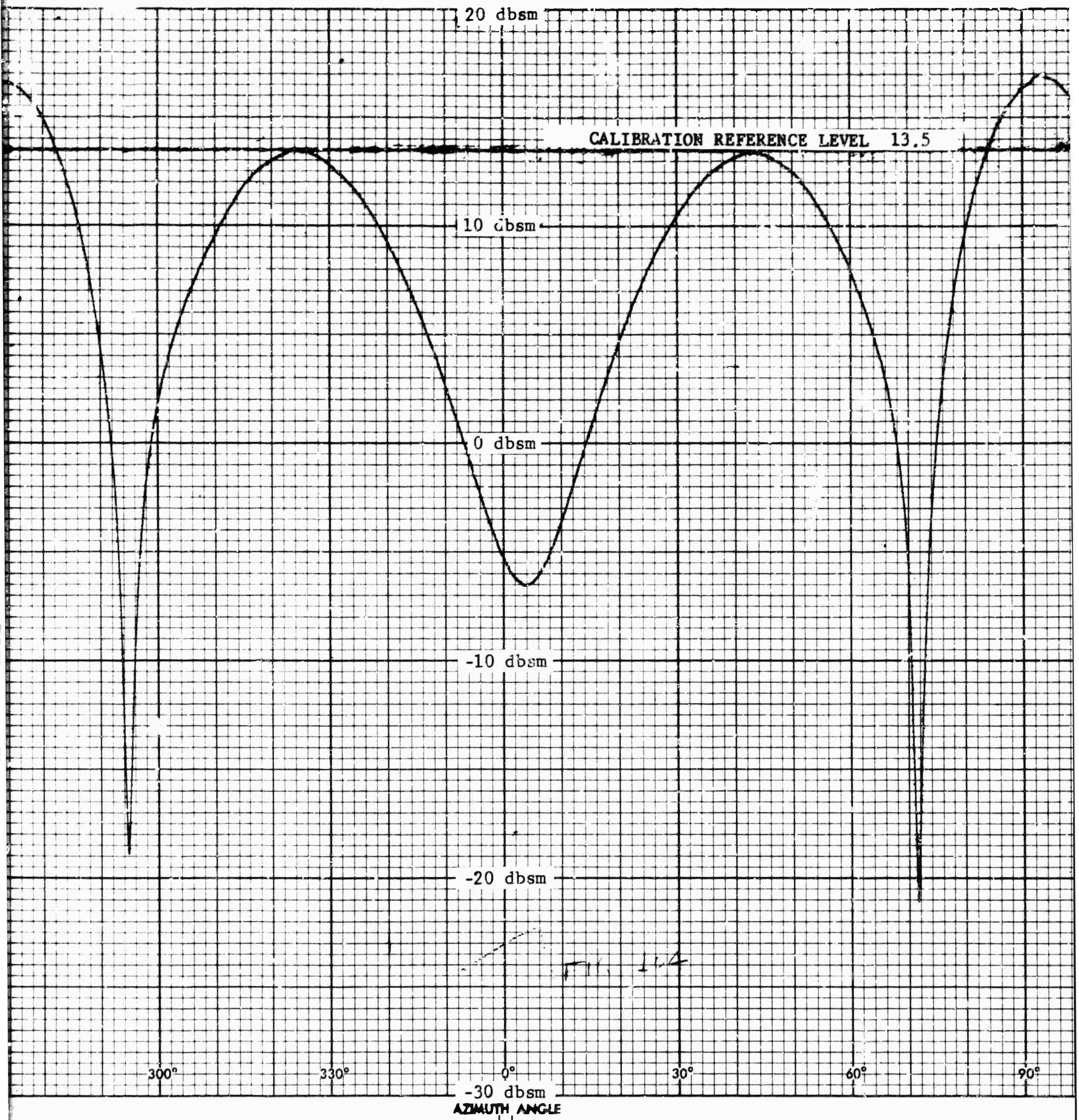
20 dbsm
CALIBRATION REFERENCE LEVEL 13.5
10 dbsm
0 dbsm
-10 dbsm
-20 dbsm
300°
330°
0°
30°
60°
90°
-30 dbsm
AZIMUTH ANGLE

Fig. 104

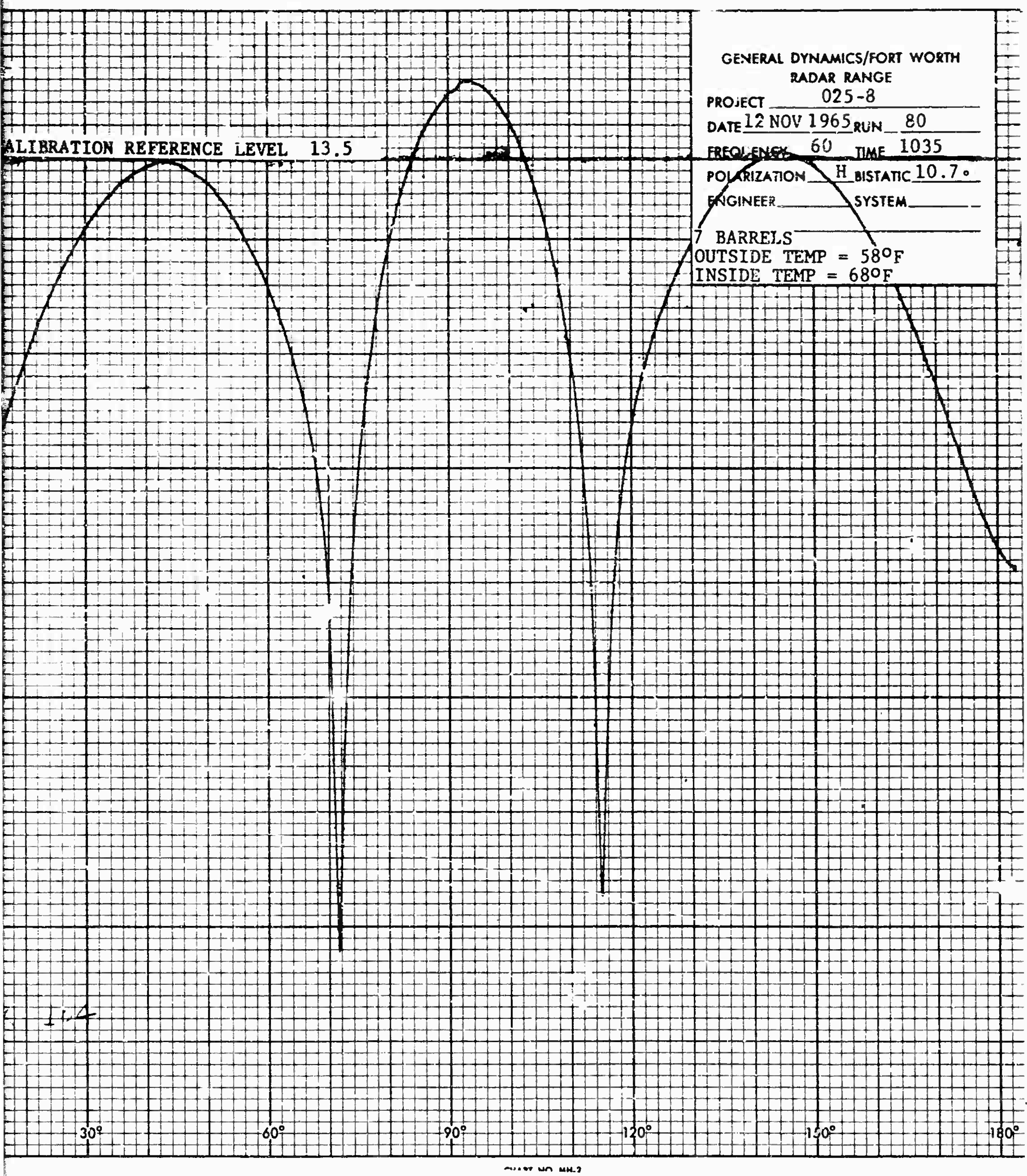

Fig. 104 FULL SCALE CROSS SECTION OF CYLINDER
(HORIZONTAL POLARIZATION, 60 MHz)

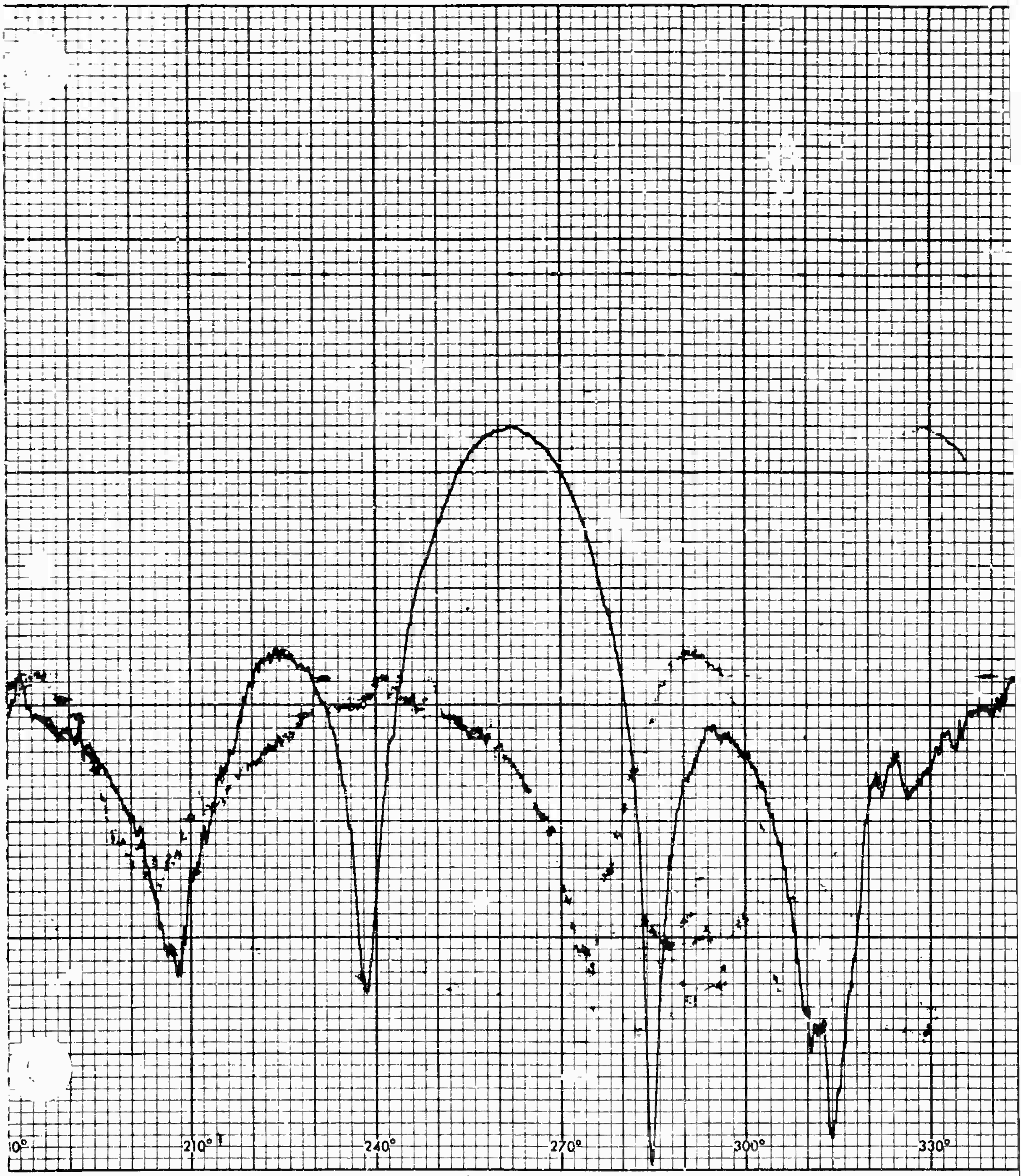
210°
240°
270°
300°
330°

Fig. 105 FULL SCALE CRO
(VERTICAL POLA

2

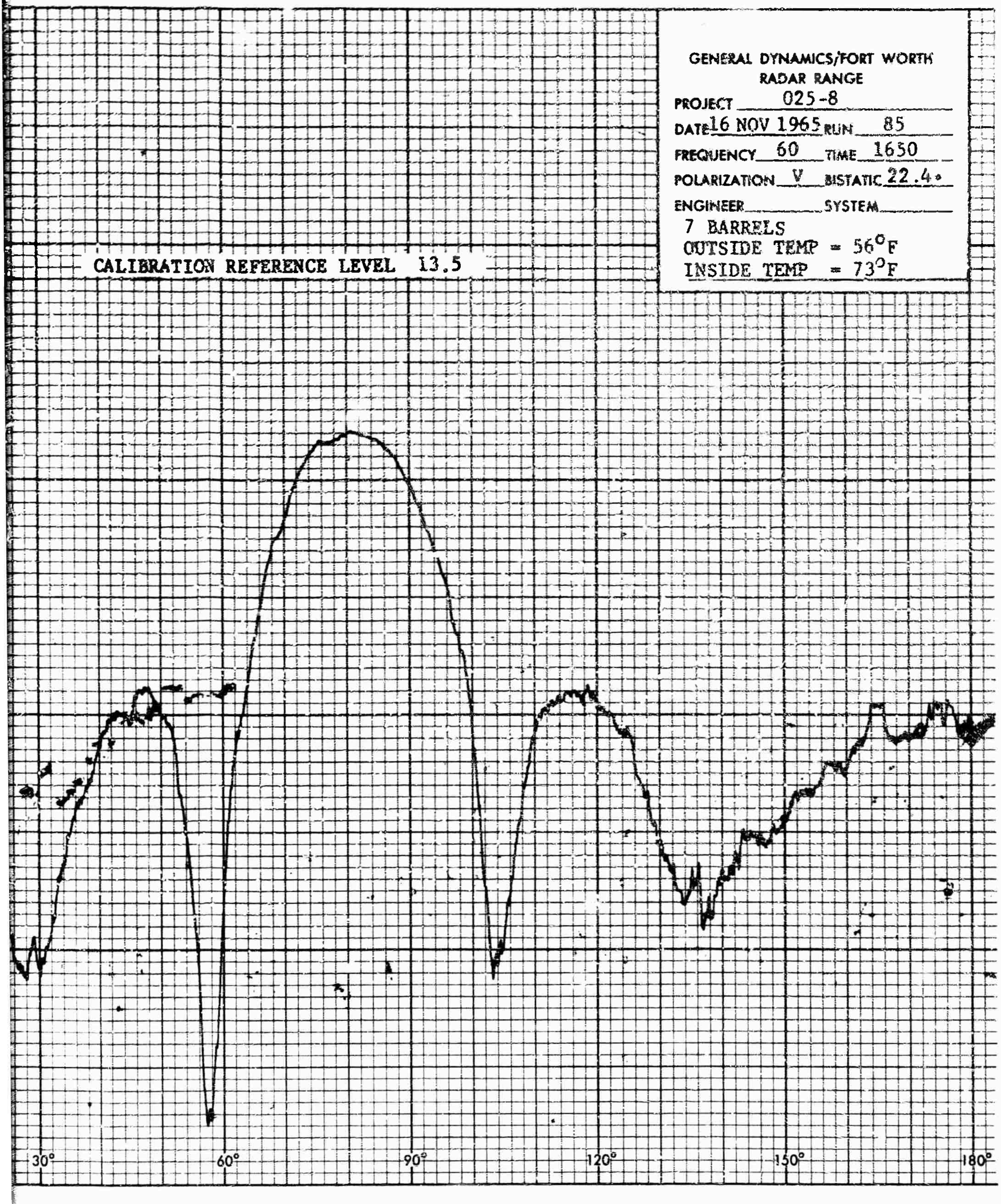

Fig. 105 FULL SCALE CROSS SECTION OF CYLINDER
(VERTICAL POLARIZATION, 60 MHz)

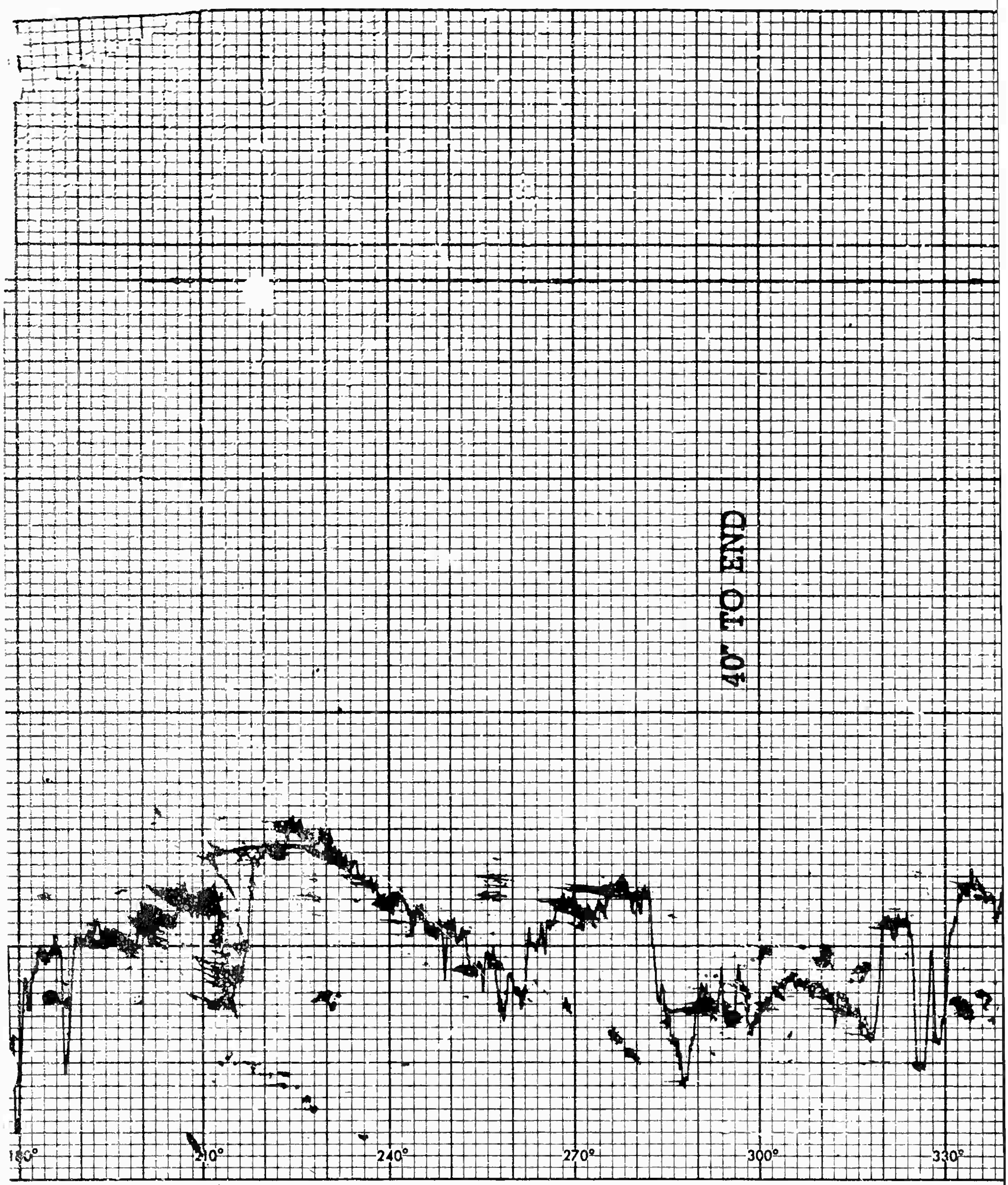
40' TO END
180°
210°
240°
270°
300°
330°

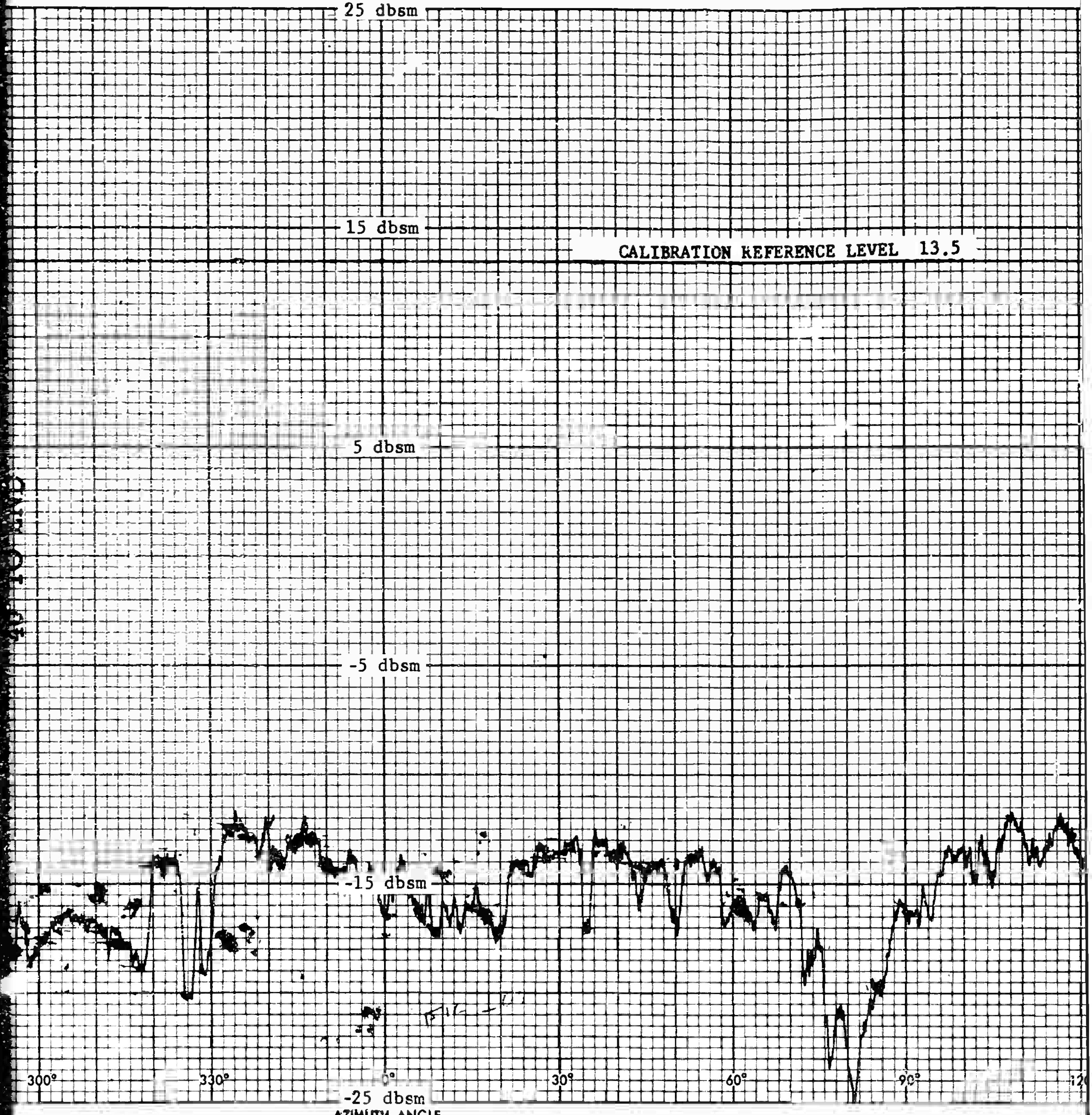

Fig. 106 MEASURED
(VERTICA

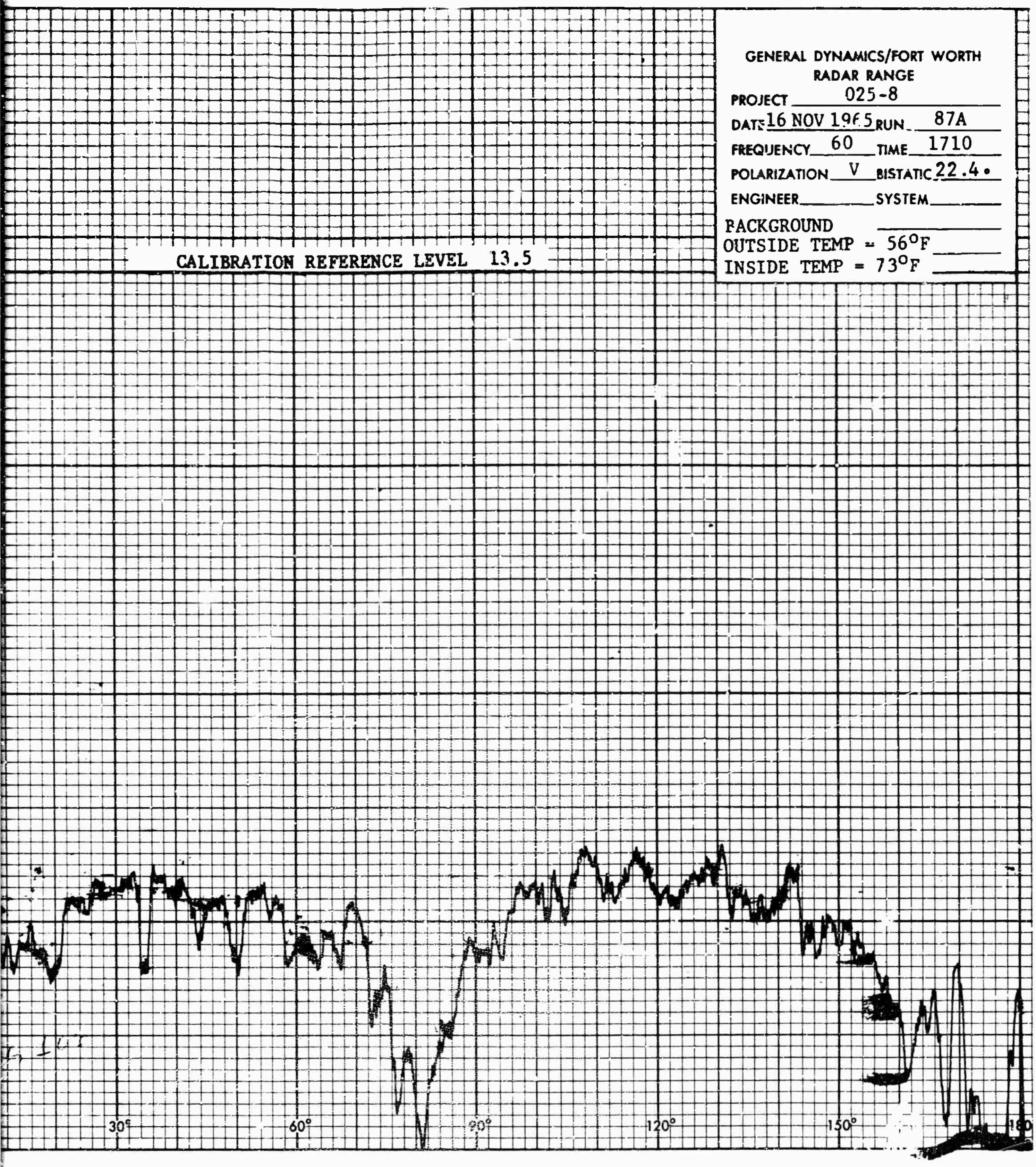

Fig. 106 MEASURED BACKGROUND LEVEL AT 60 MHz (VERTICAL POLARIZATION)

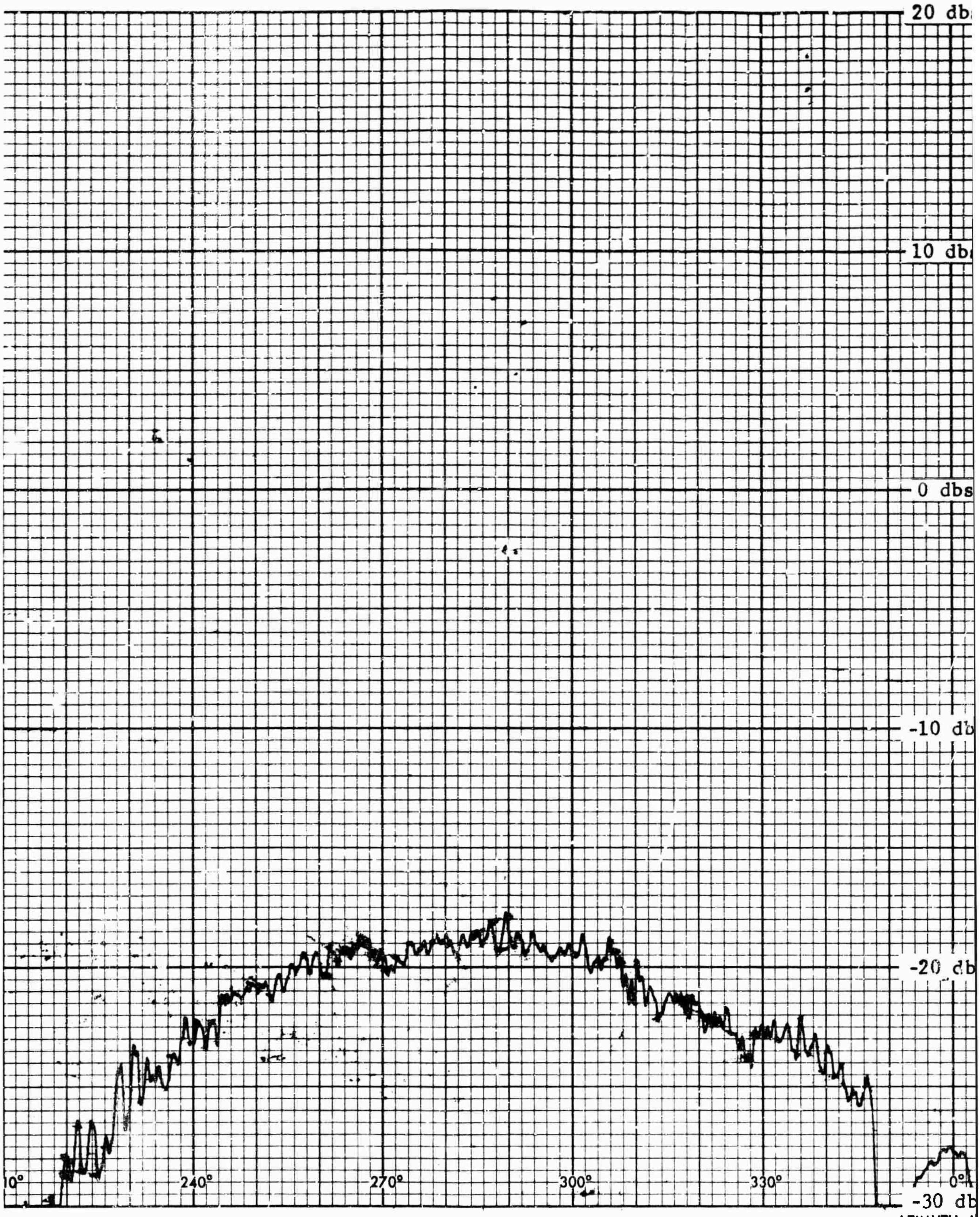
20 db
10 db
0 dbs
-10 db
-20 db
-30 db
10°
240°
270°
300°
330°
0°
AZIMUTH

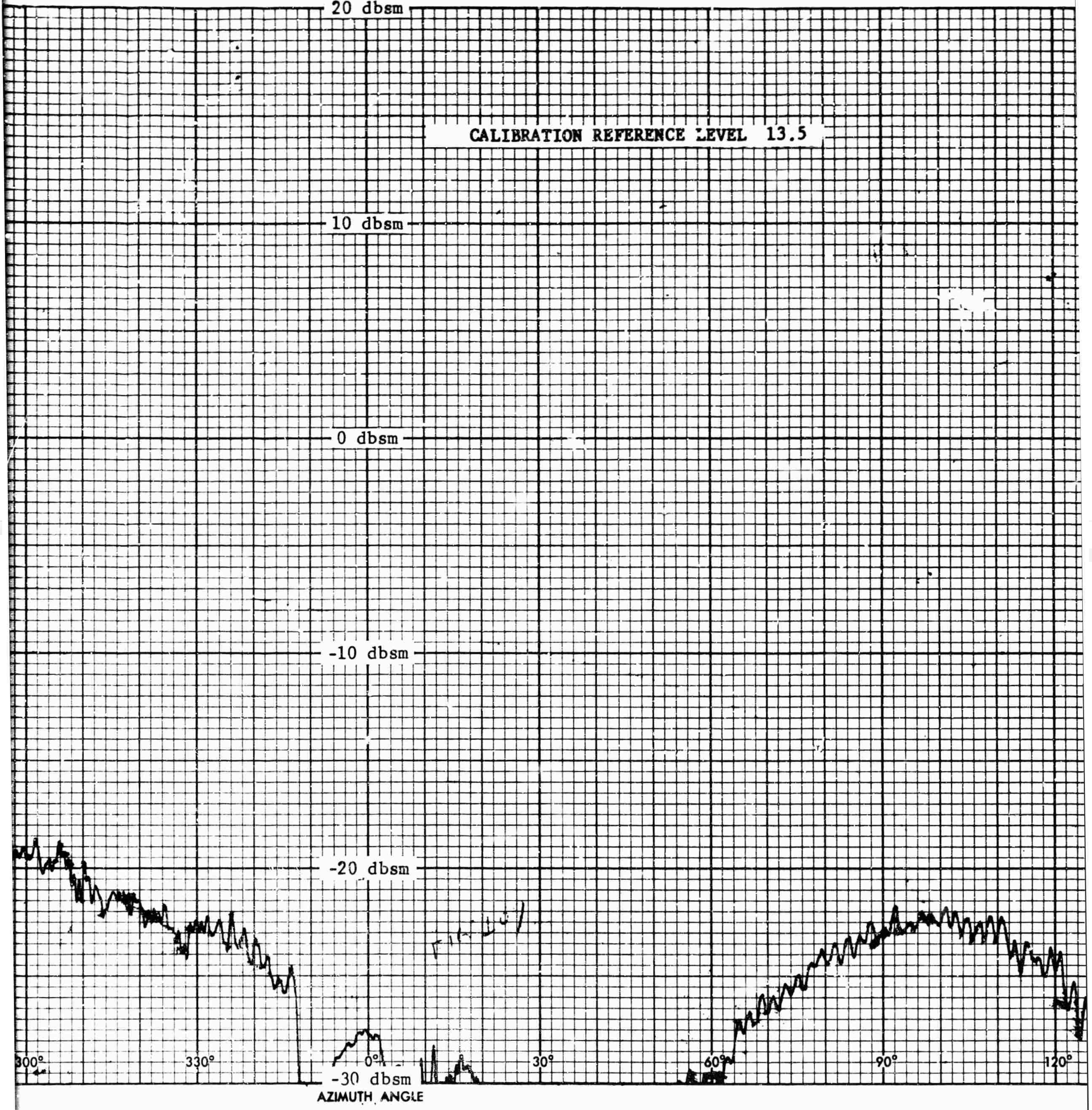

Fig. 107 MEASURED BACKGROU
(HORIZONTAL POLAR

2

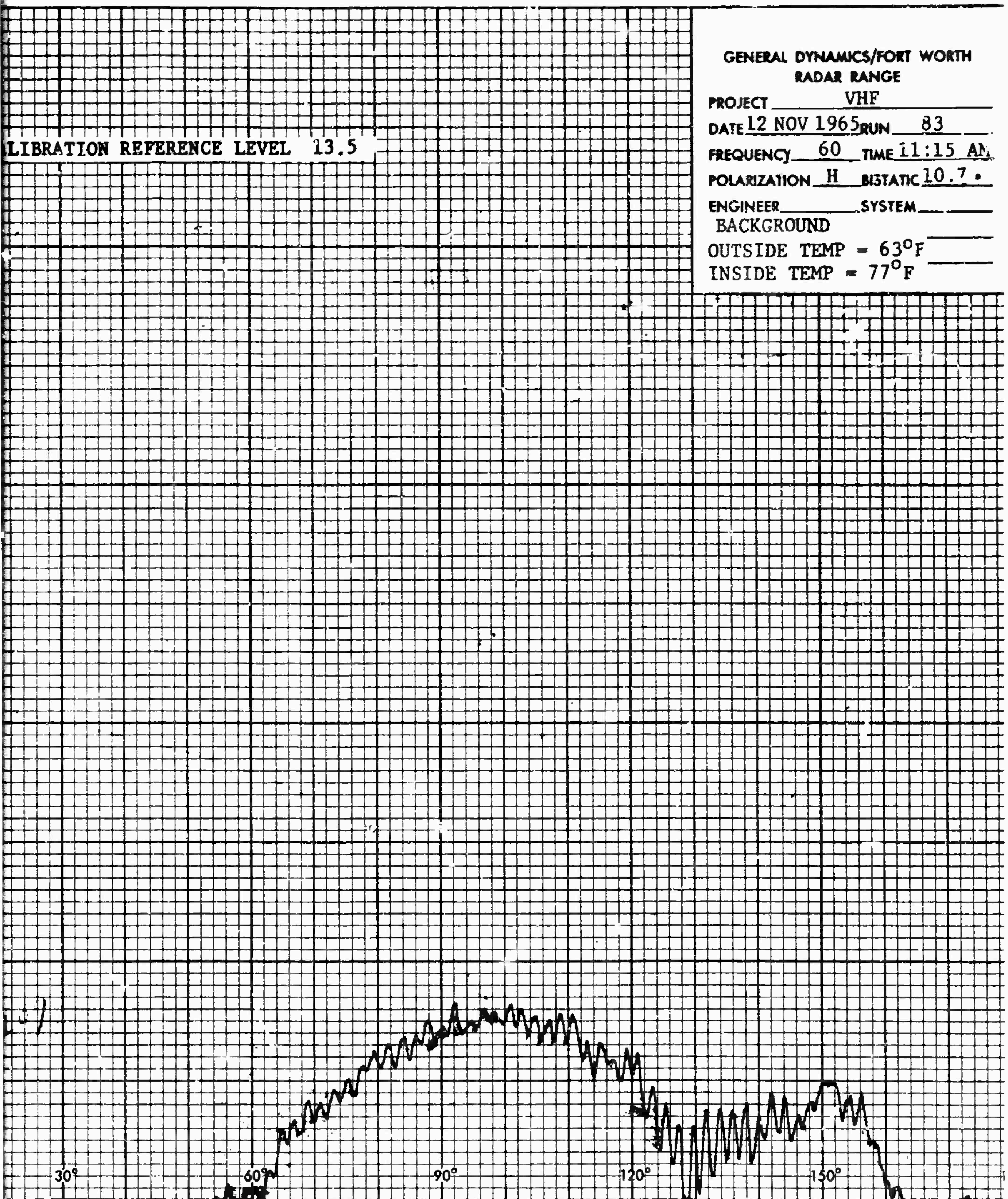

Fig. 107 MEASURED BACKGROUND LEVEL AT 60 MHz
(HORIZONTAL POLARIZATION)

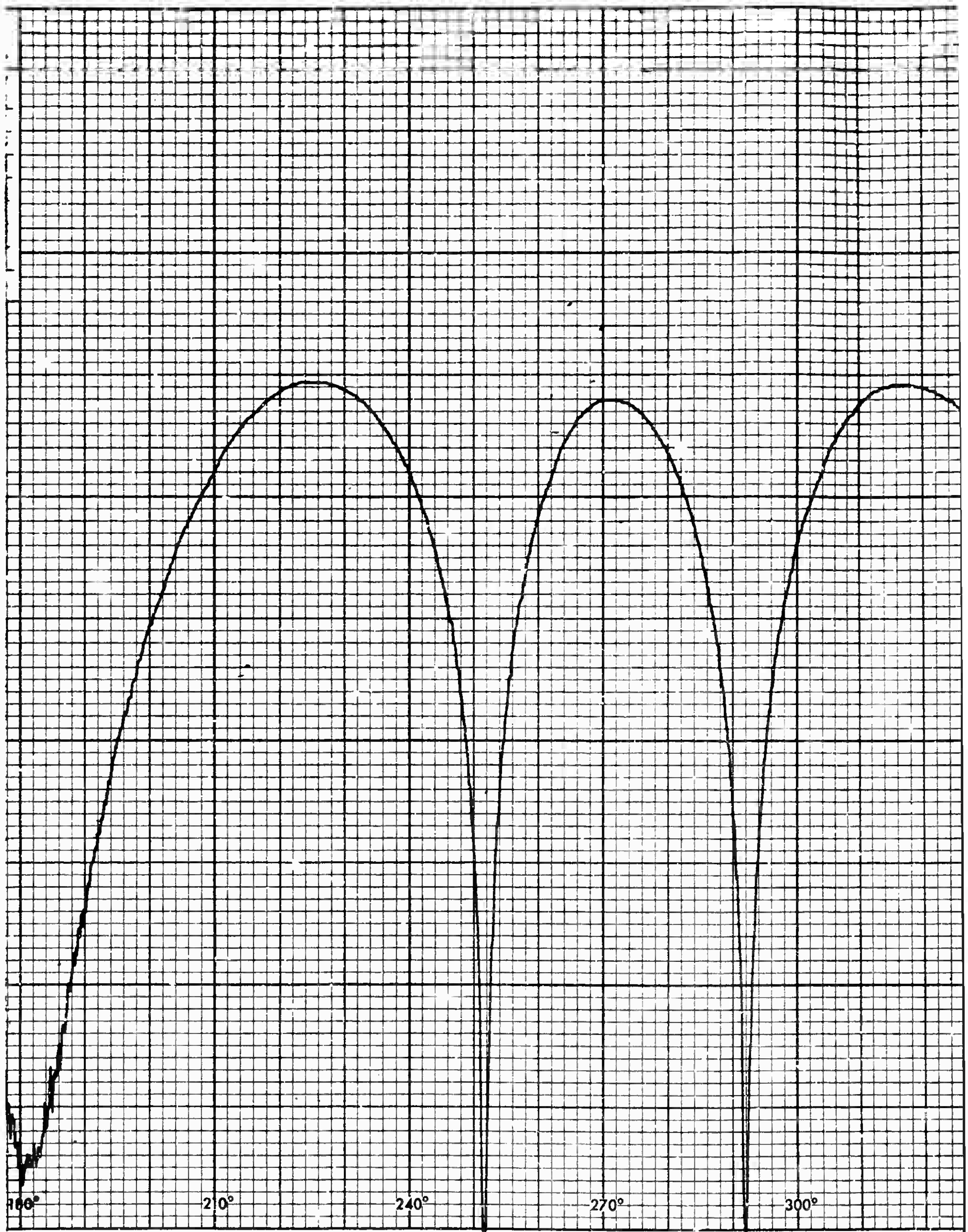

180°
210°
240°
270°
300°

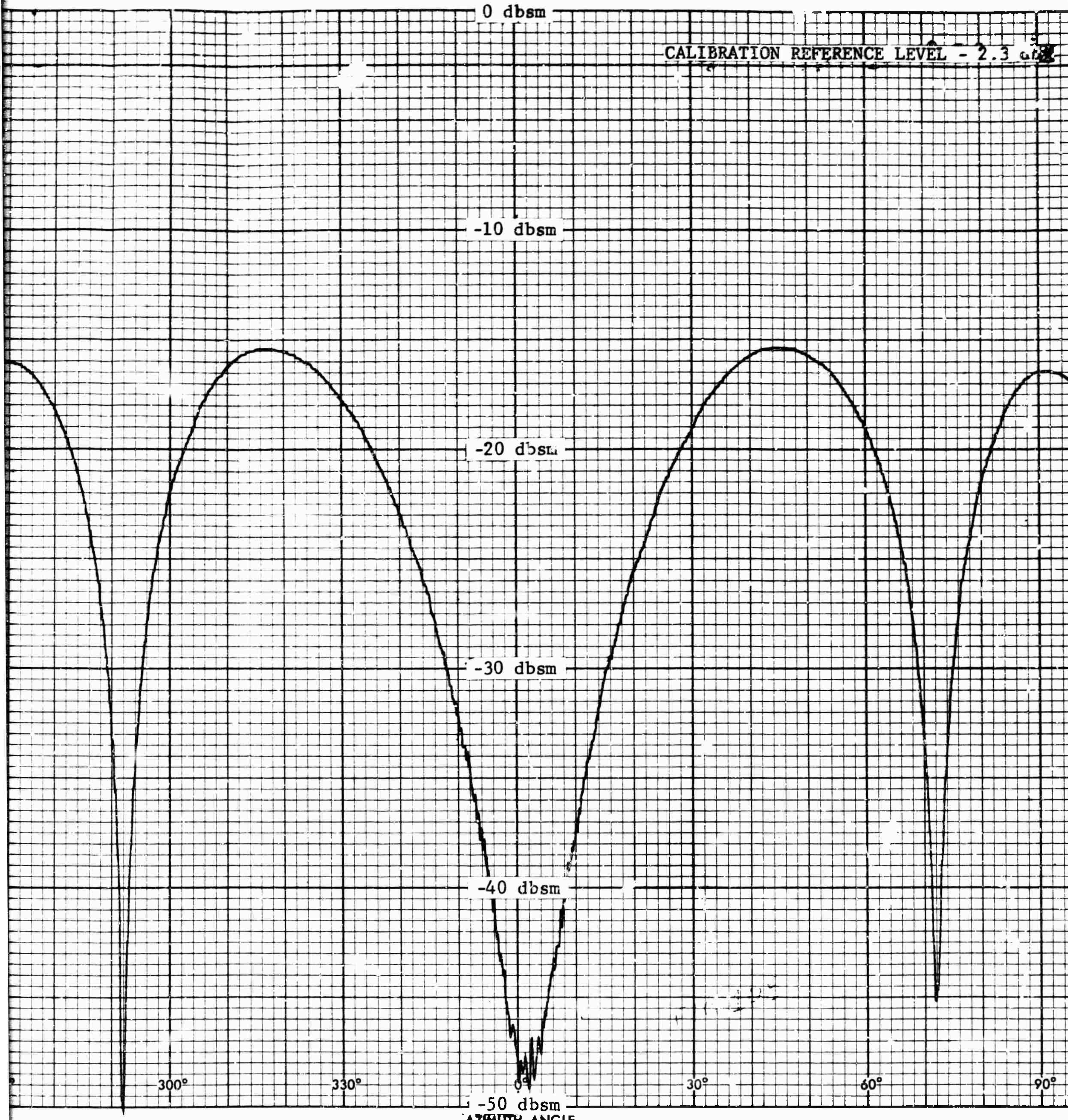

Fig. 108 SC
30

2

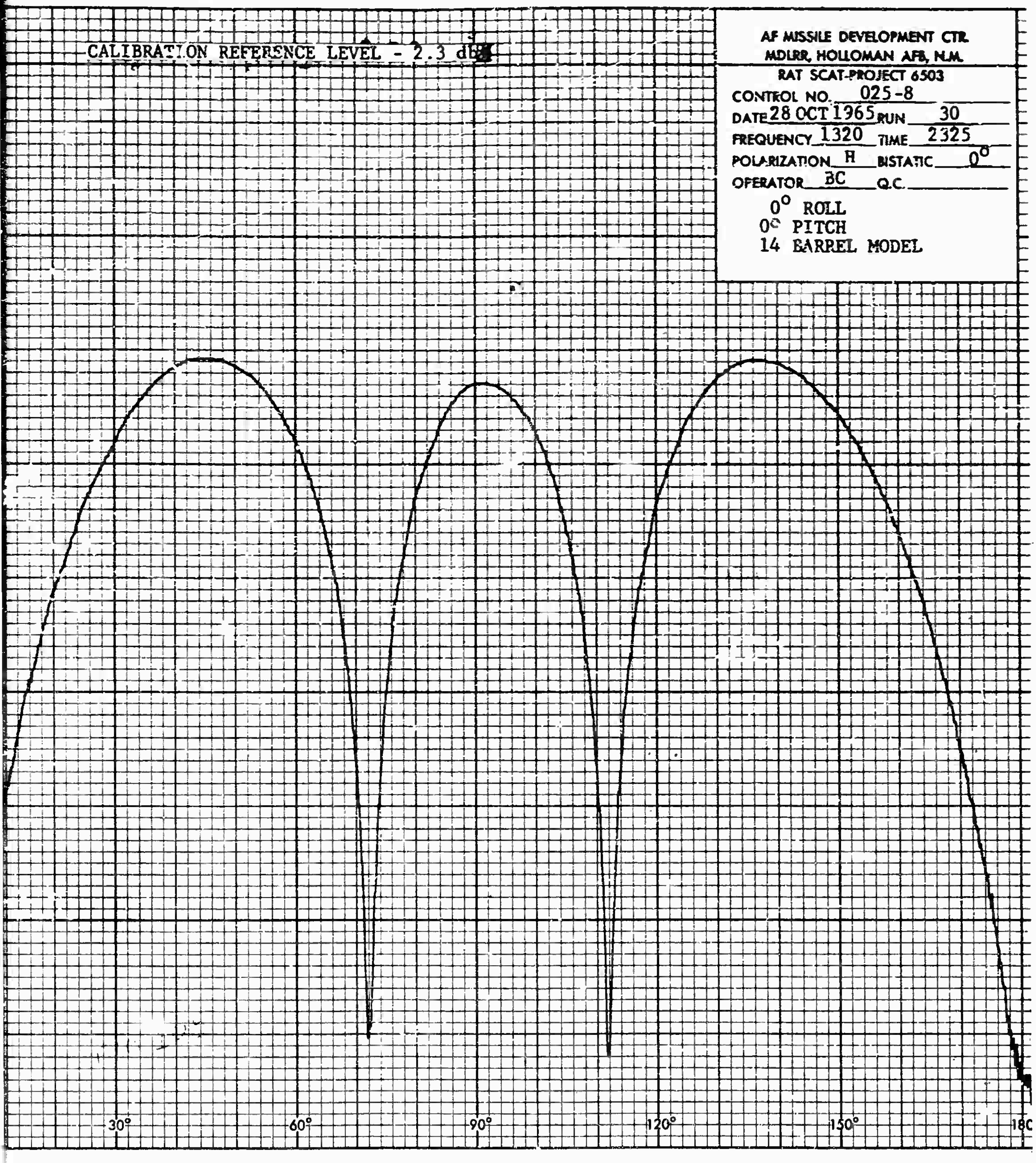

Fig. 108 SCALED MODEL CROSS SECTION CORRESPONDING TO 30 MHz FULL SCALE (HORIZONTAL POLARIZATION)

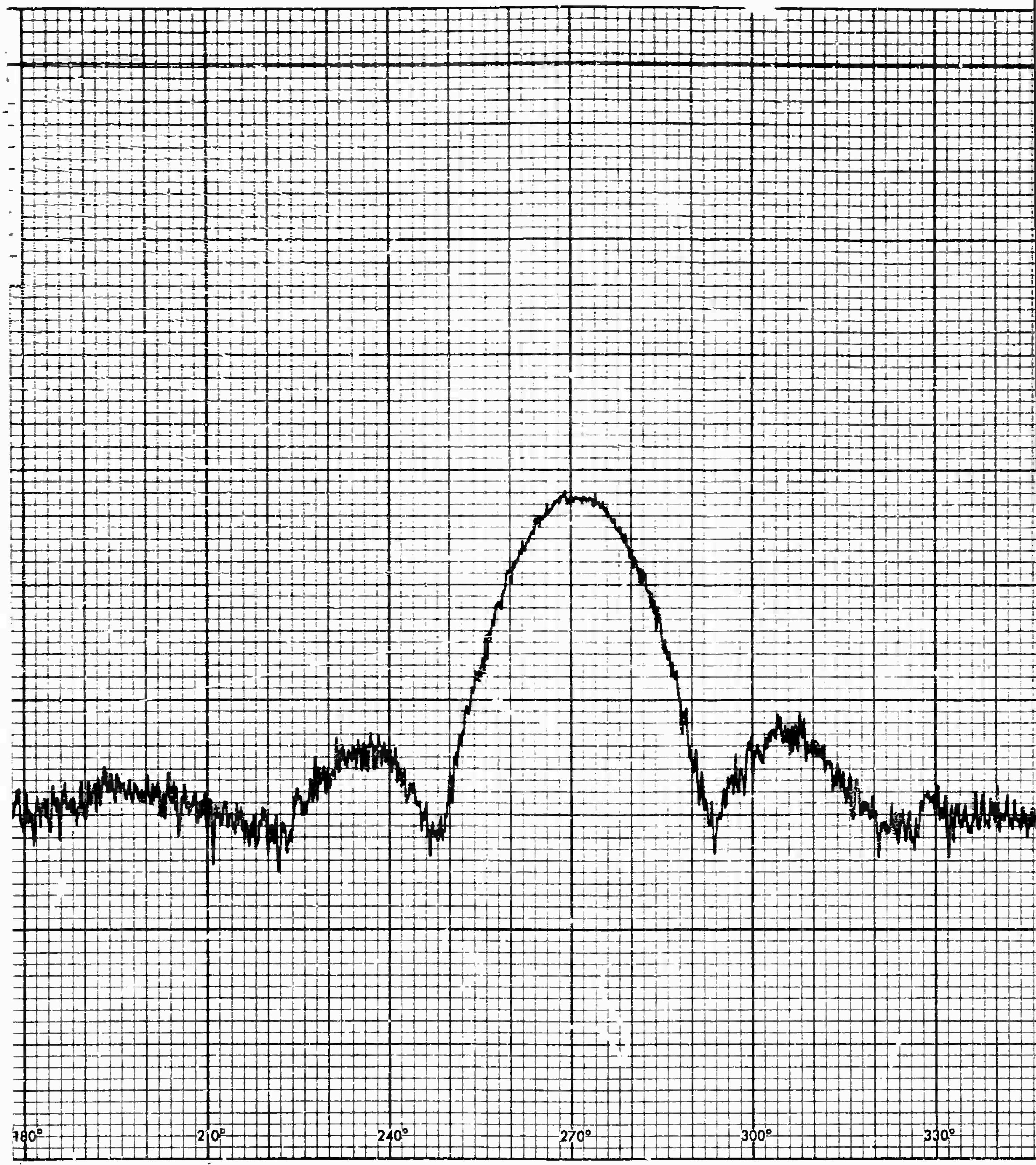

1

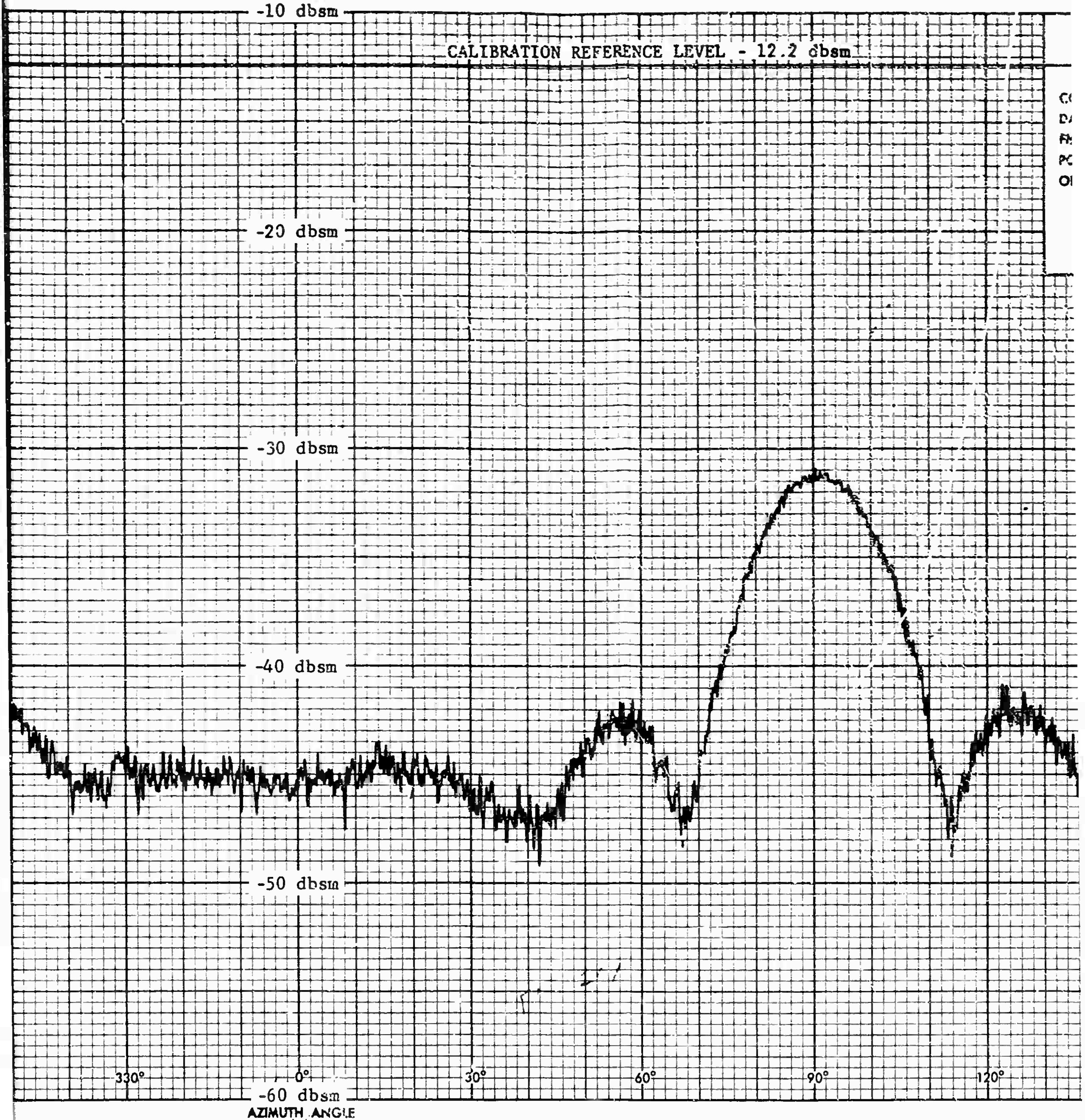

2

Fig. 109 SCALED MODEL CROSS SEC
30 MHz FULL SCALE (VER

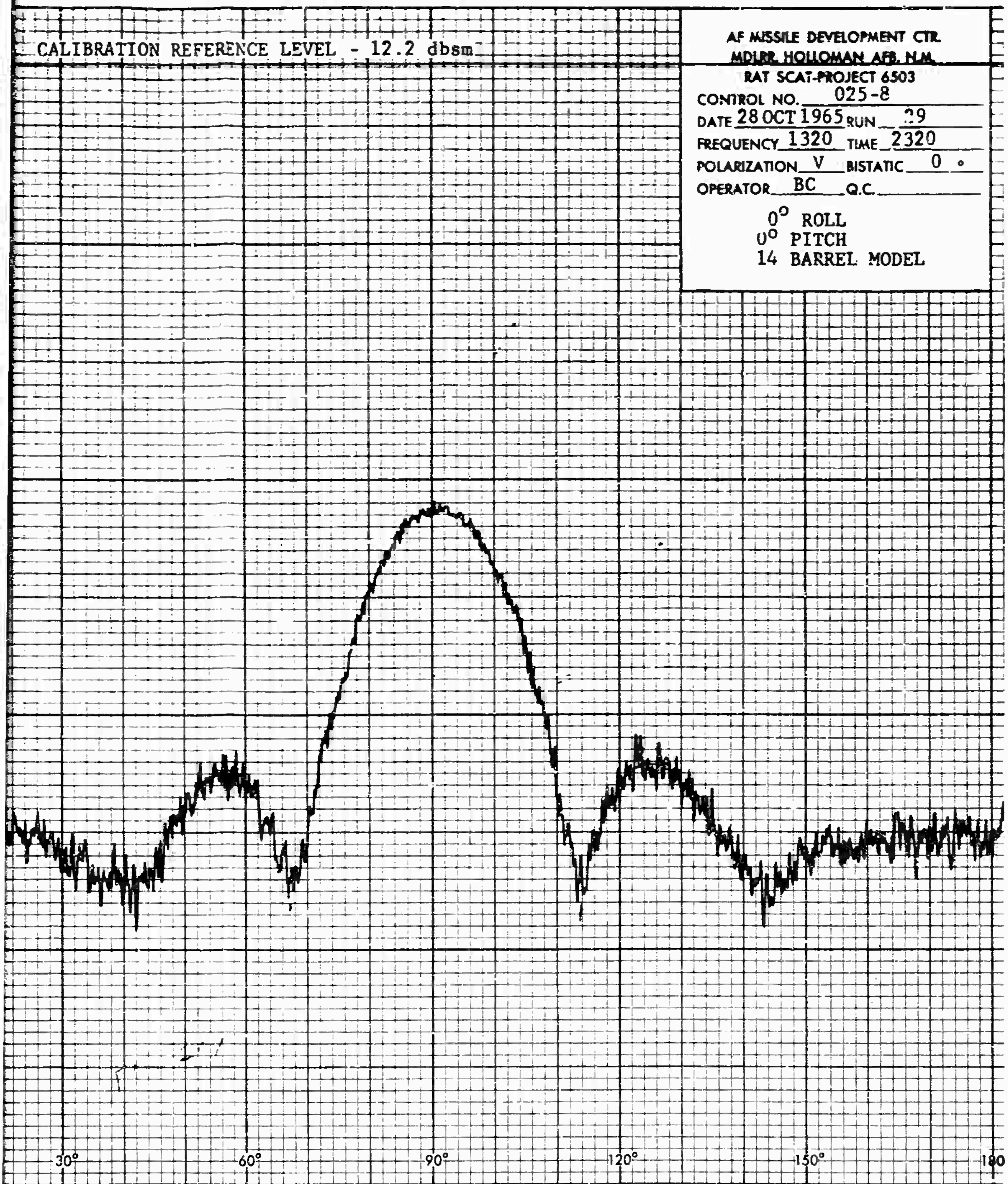

Fig. 109 SCALED MODEL CROSS SECTION CORRESPONDING TO 30 MHz FULL SCALE (VERTICAL POLARIZATION)

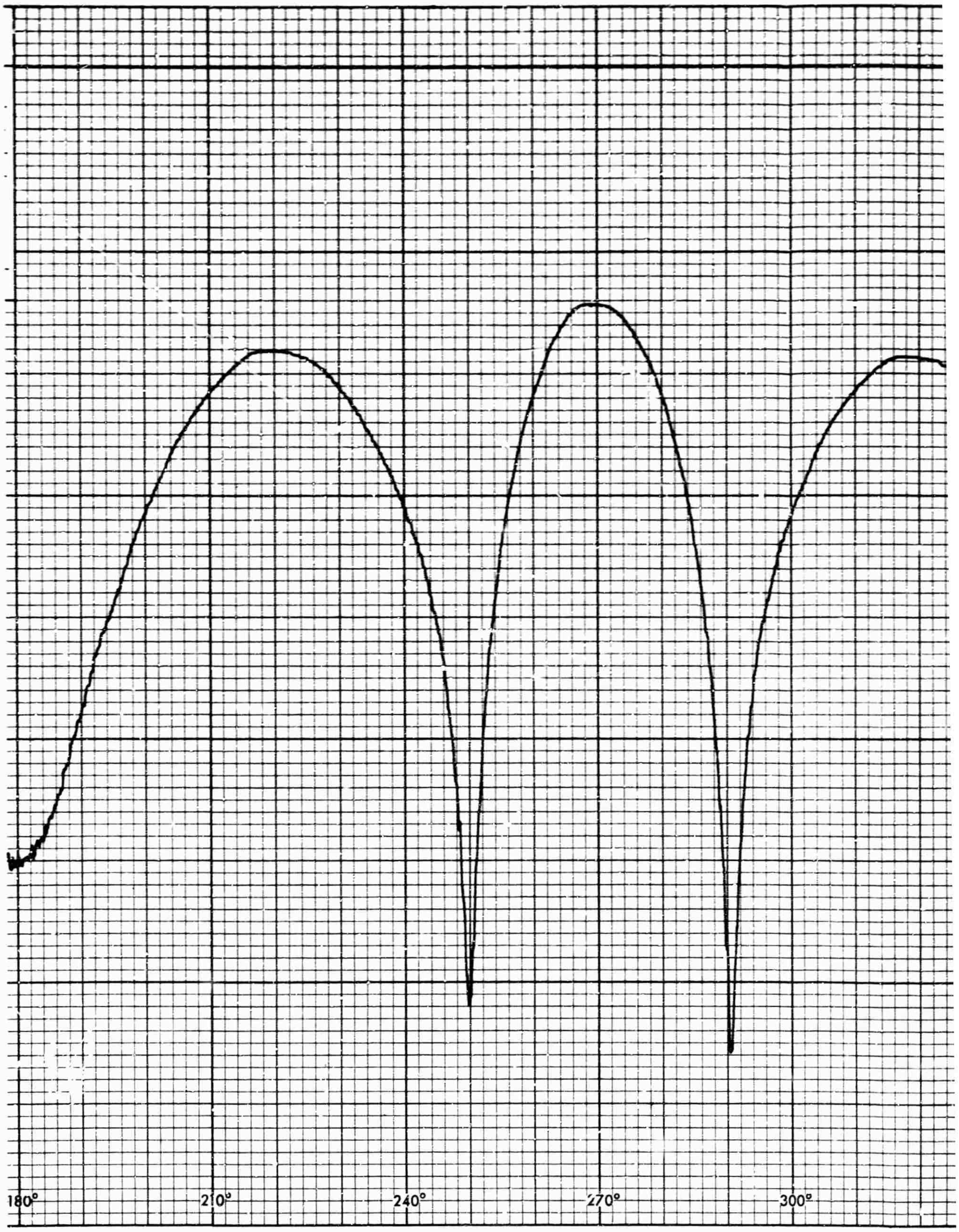

180°
210°
240°
270°
300°

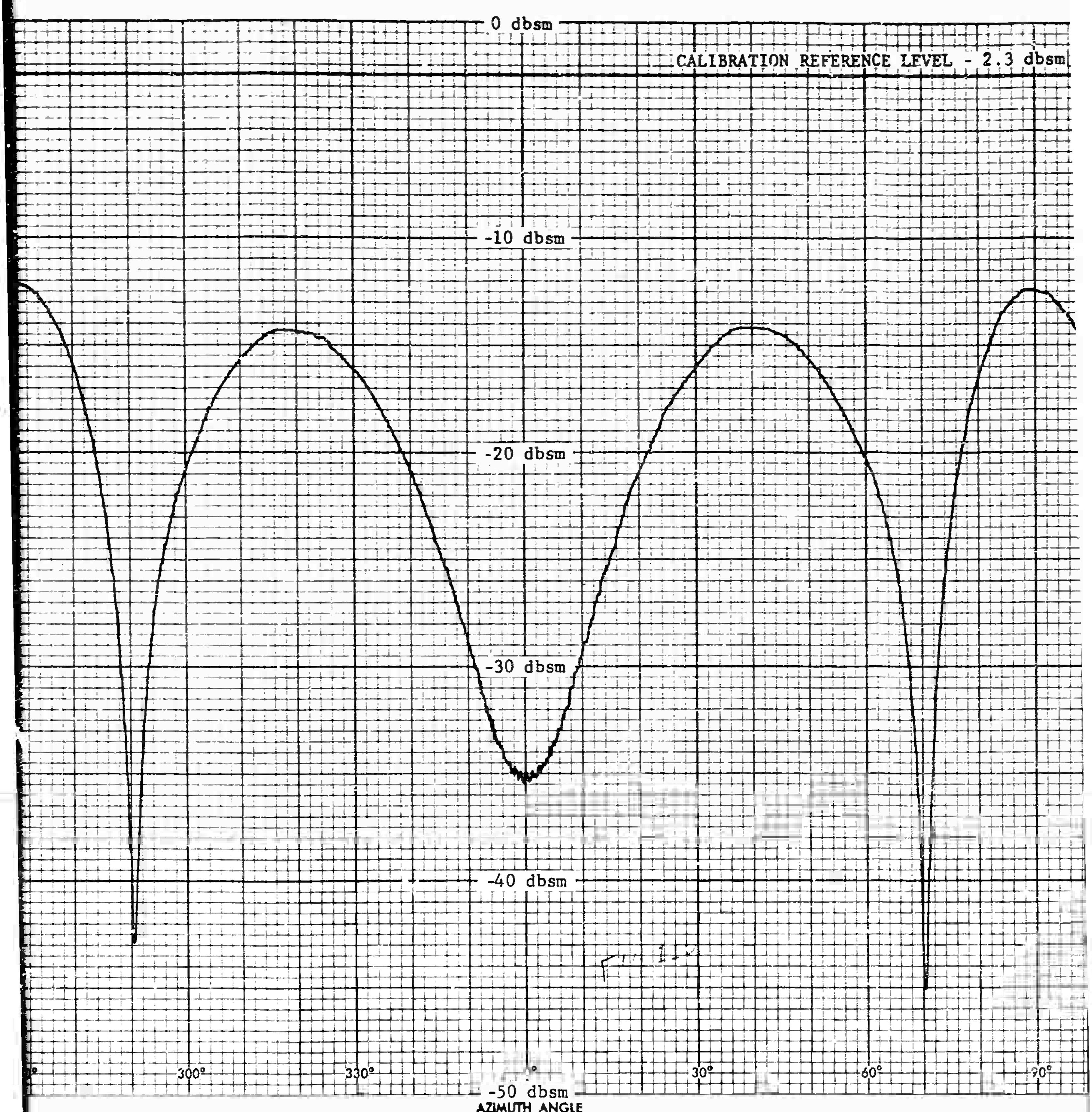

2

Fig. 110 SCAL
60 M

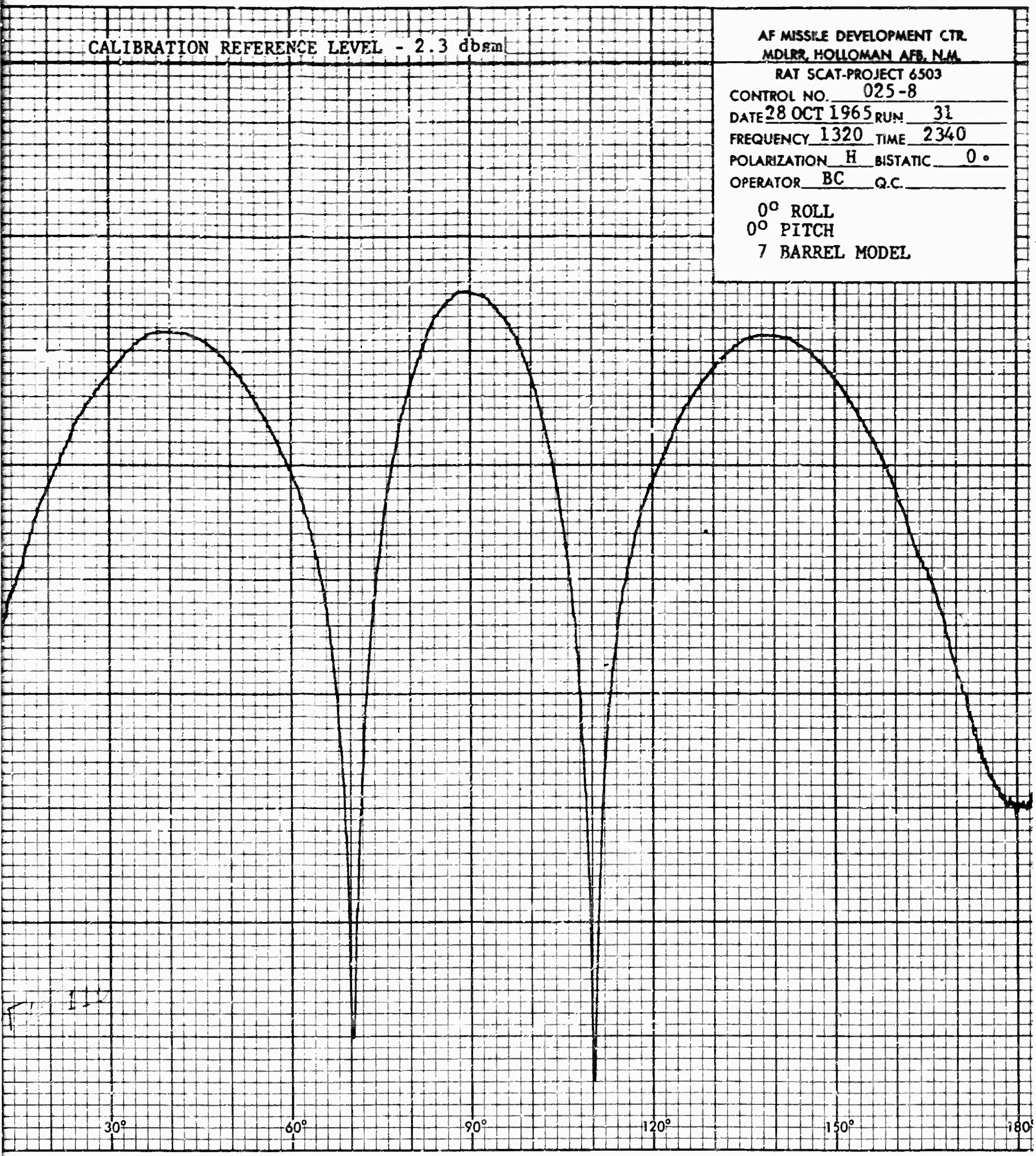

Fig. 110 SCALED MODEL CROSS SECTION CORRESPONDING TO 60 MHz FULL SCALE (HORIZONTAL POLARIZATION)

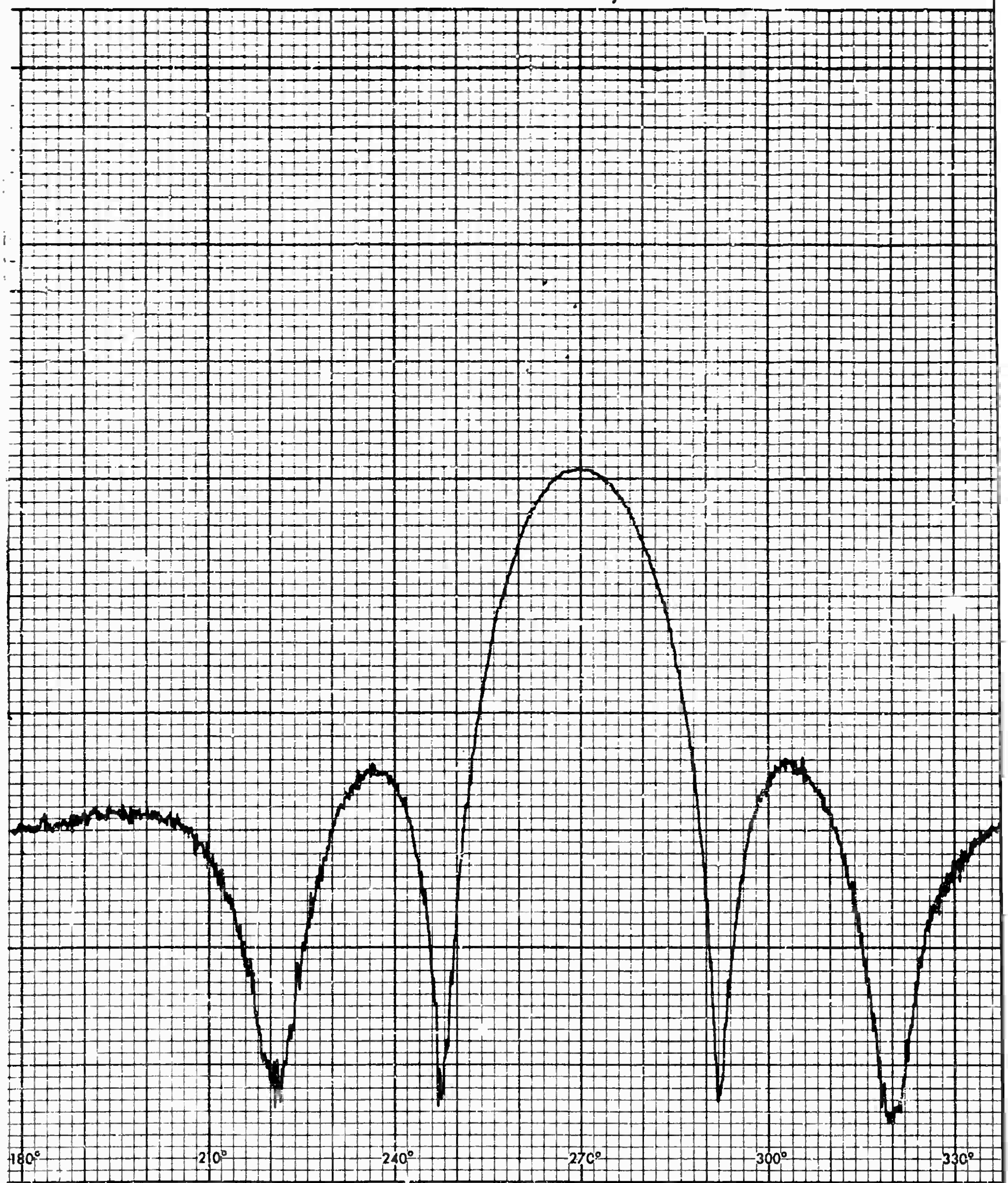

180°
210°
240°
270°
300°
330°

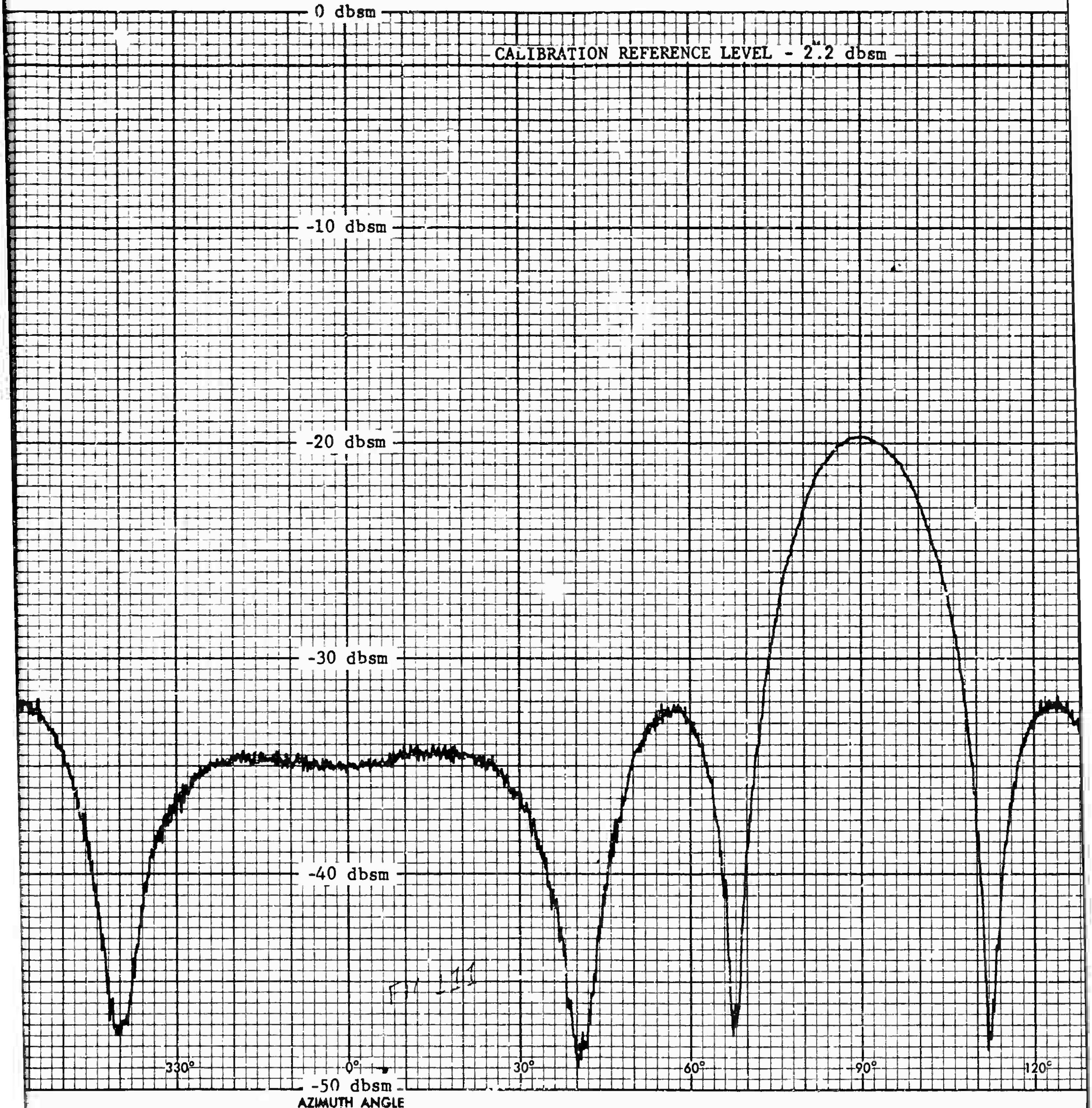

Fig. 111 SCALED MODEL CROSS SE
60 MHz FULL SCALE (VE

2

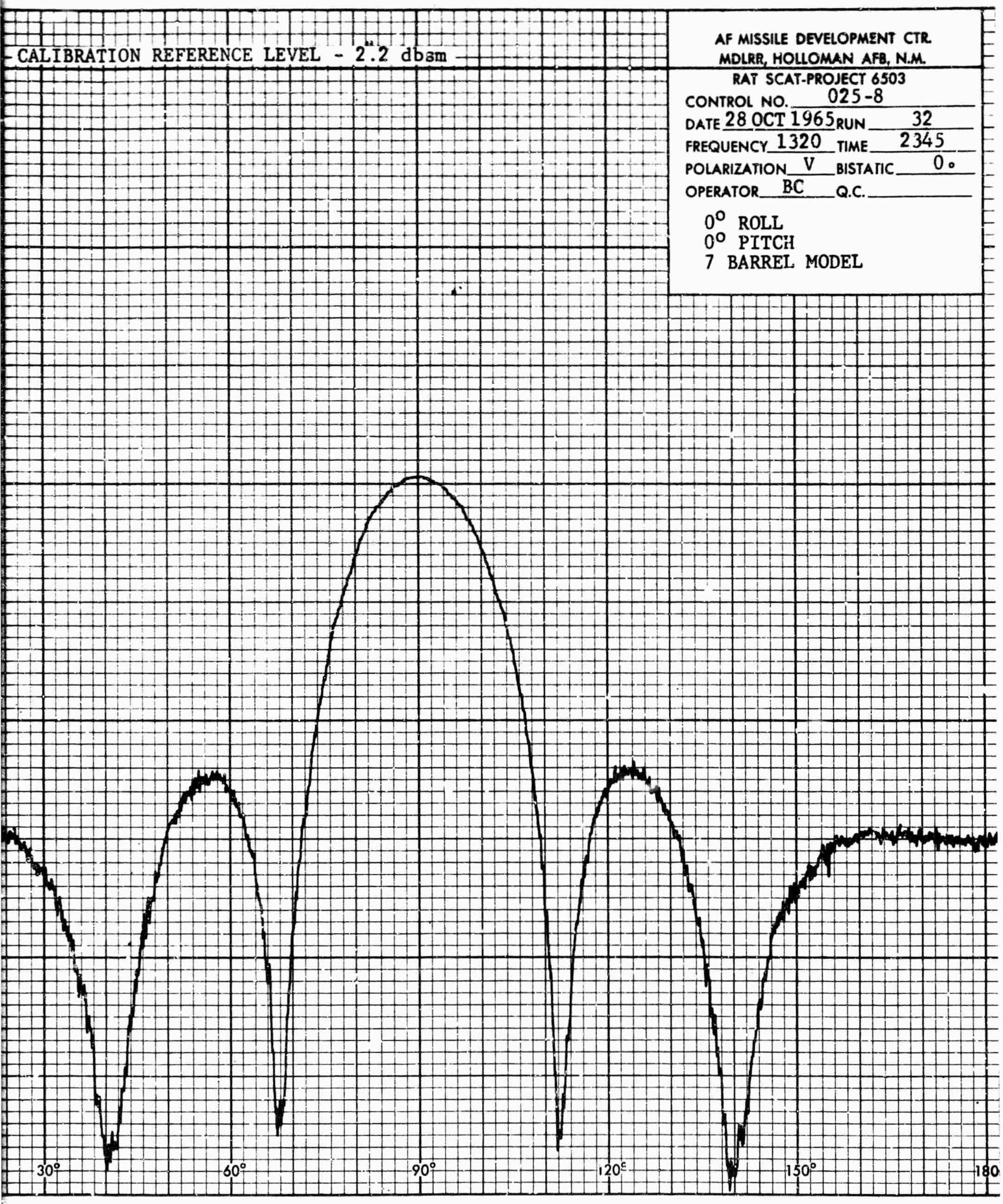

Fig. 111 SCALED MODEL CROSS SECTION CORRESPONDING TO 60 MHz FULL SCALE (VERTICAL POLARIZATION)

3

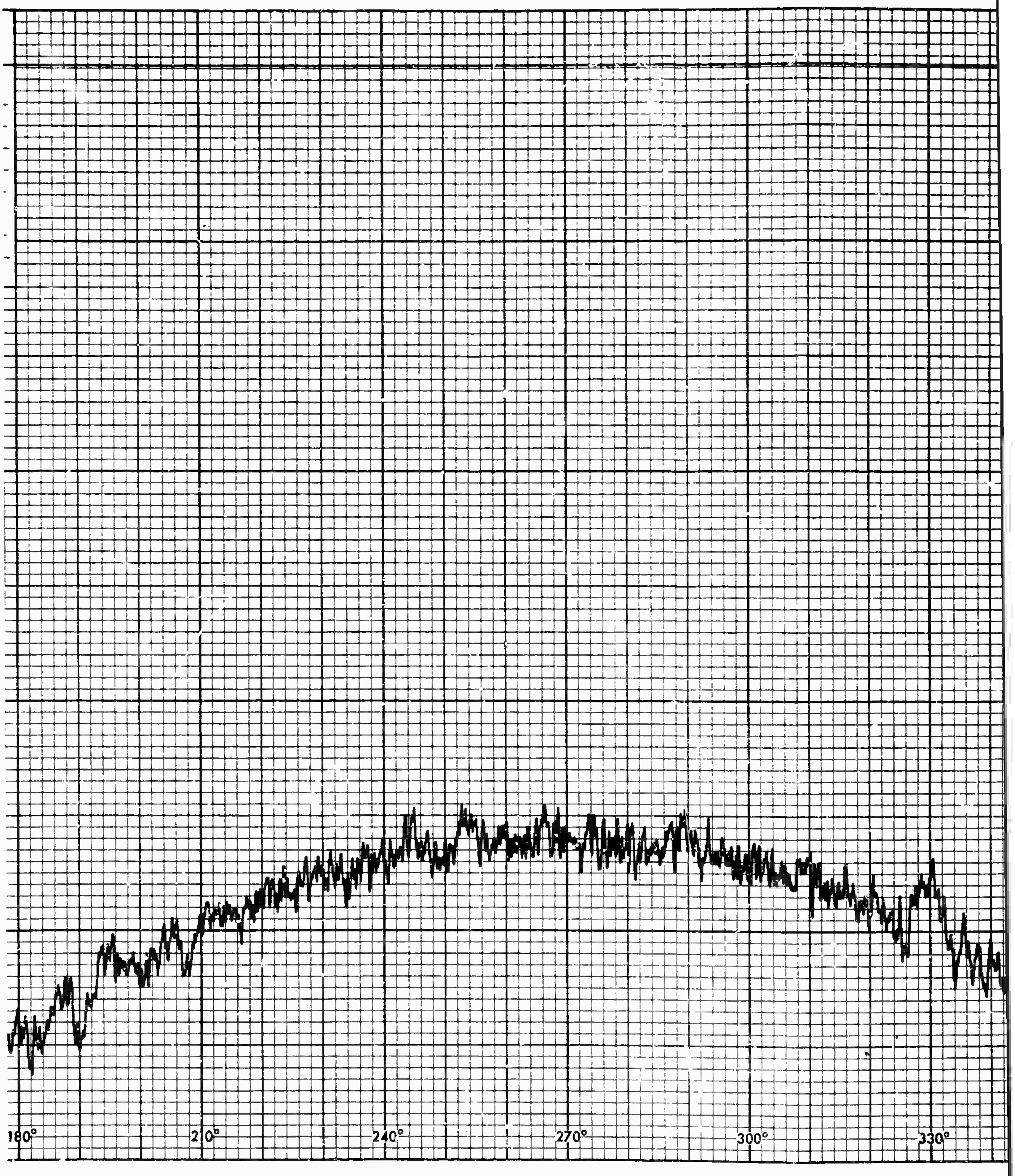

180°
210°
240°
270°
300°
330°

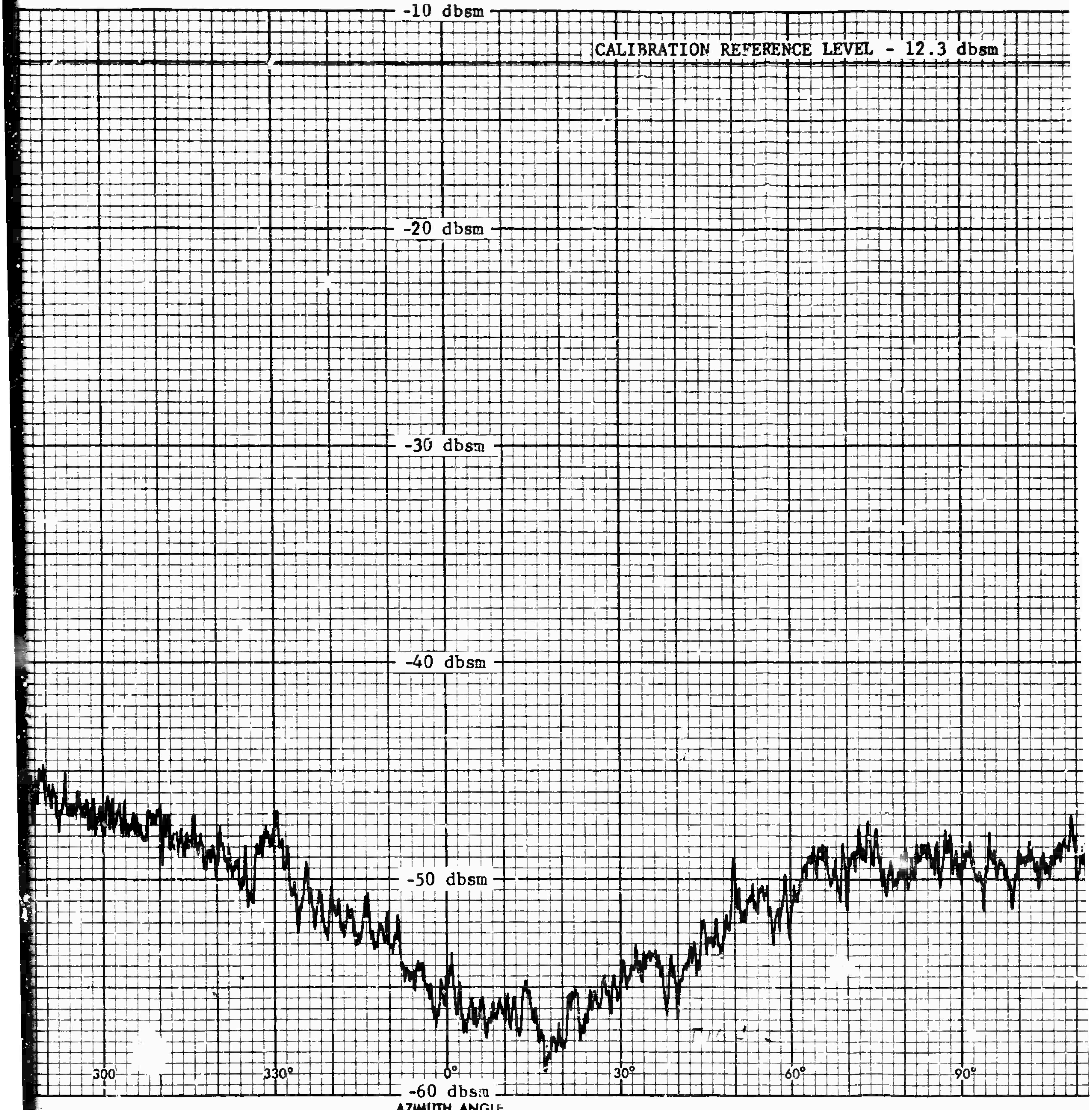

Fig. 112 SCALED MODE
POLARIZATIO

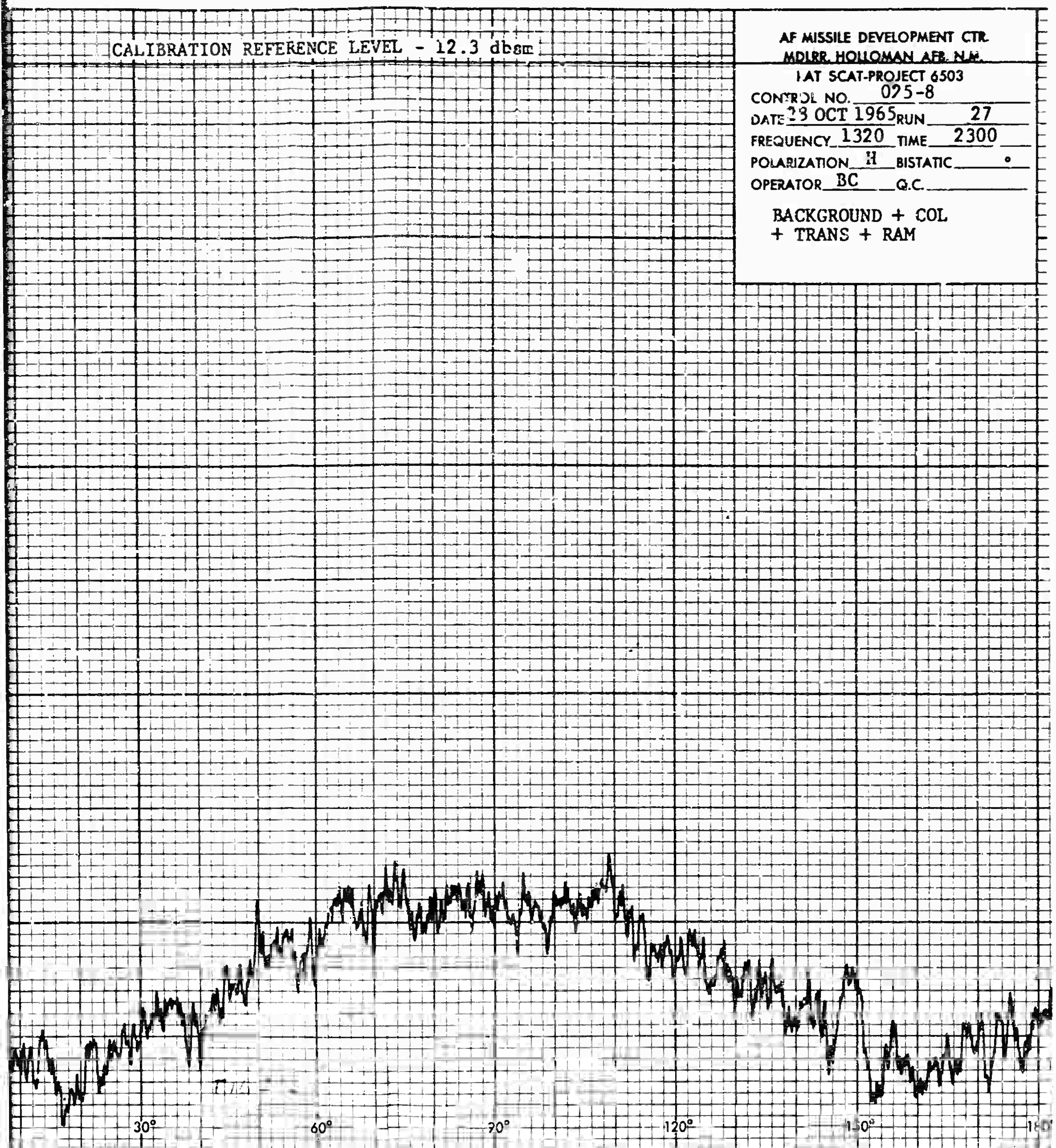

Fig. 112 SCALED MODEL BACKGROUND DATA (HORIZONTAL POLARIZATION)

3

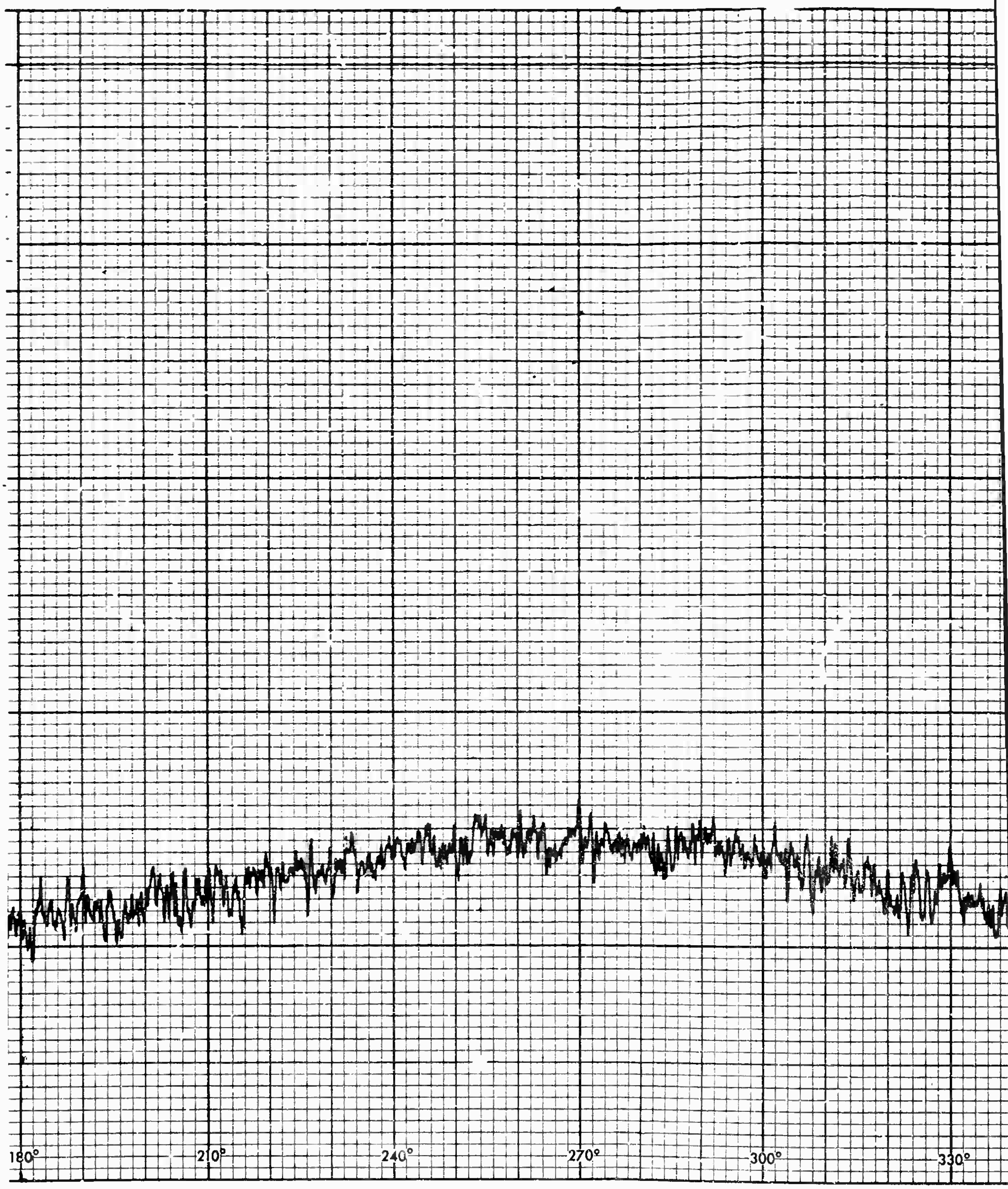
180°
210°
240°
270°
300°
330°

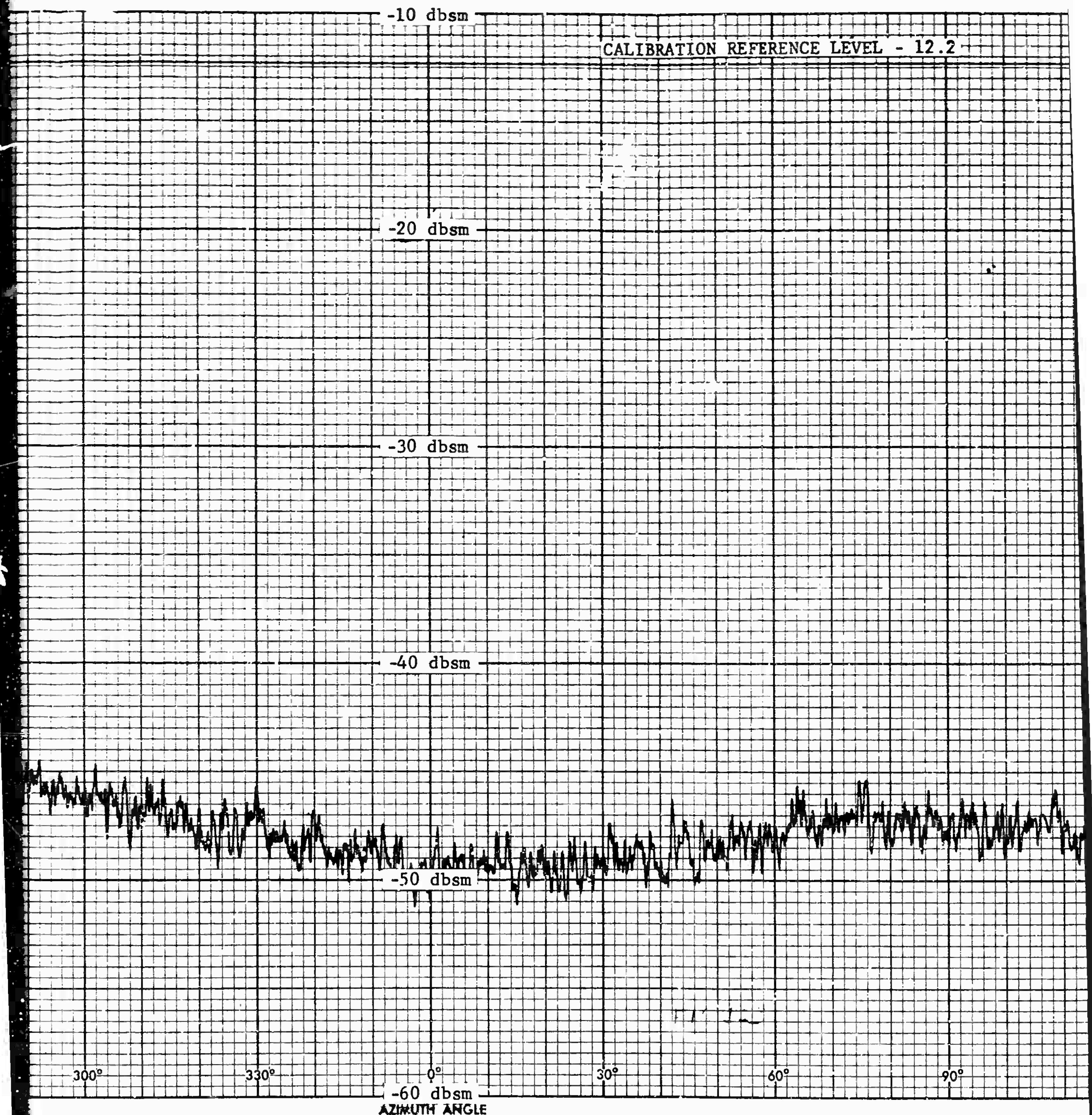

Fig. 113 SCALED MO
POLARIZAT

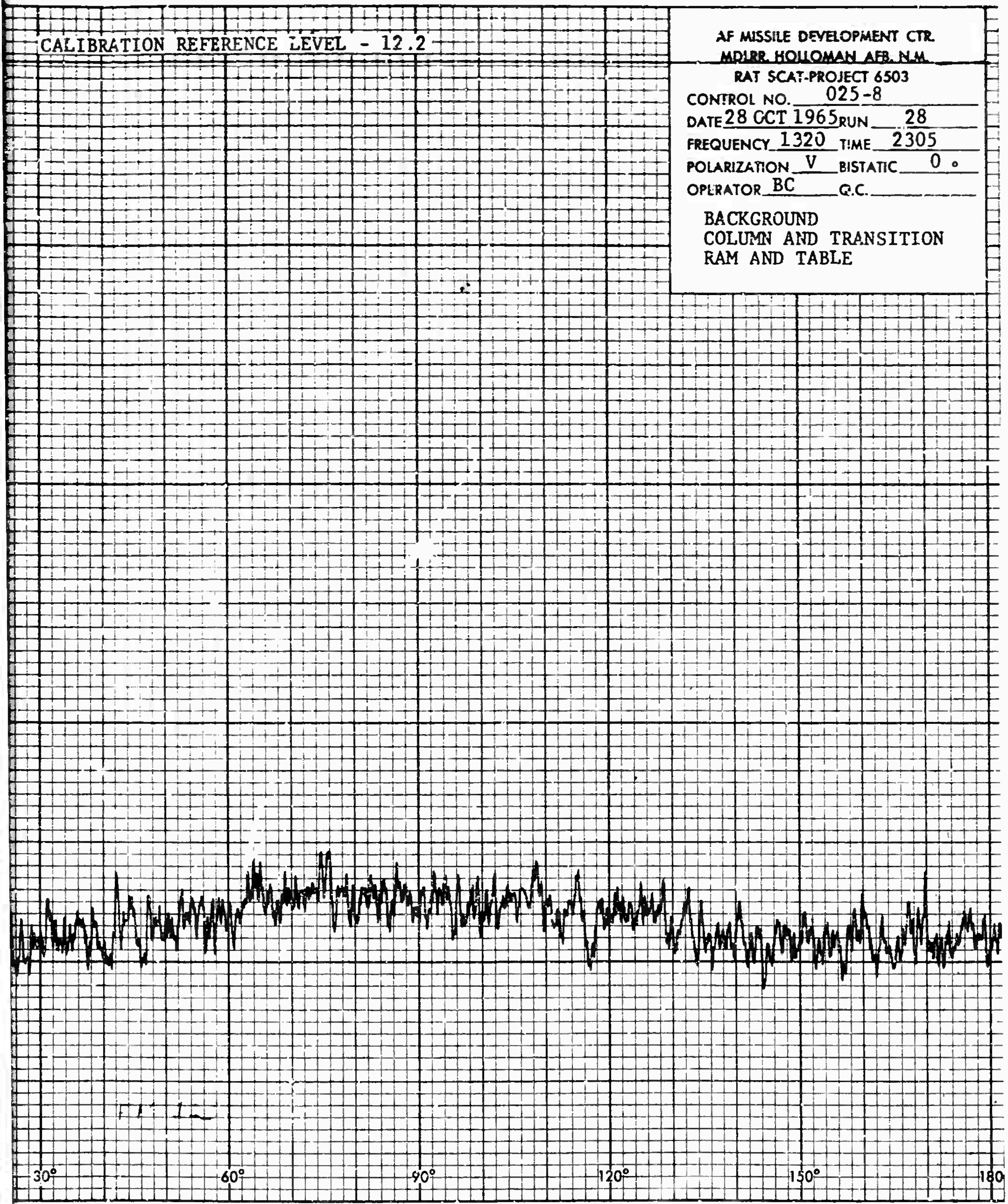

Fig. 113 SCALED MODEL BACKGROUND DATA (VERTICAL POLARIZATION)

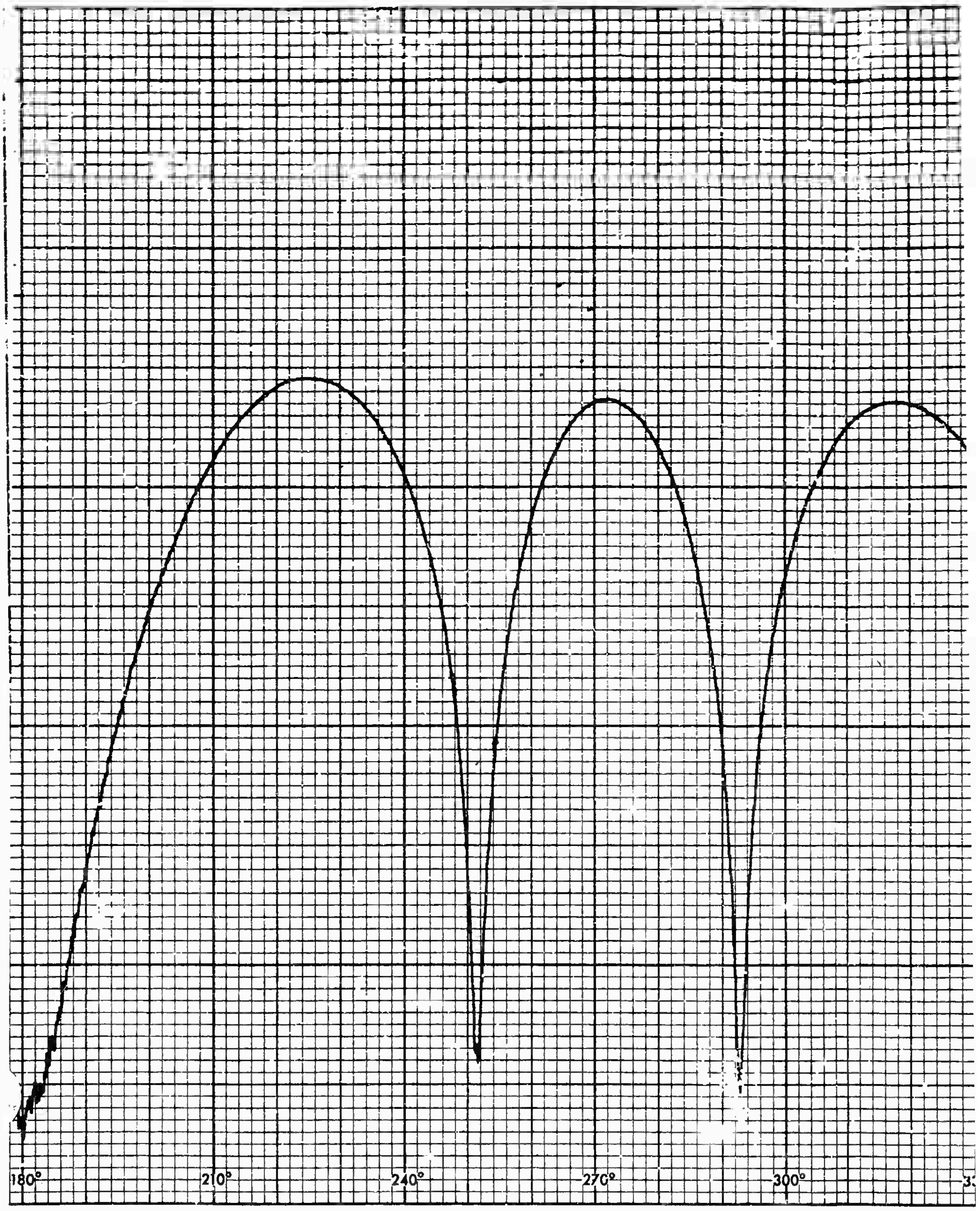

180°
210°
240°
270°
300°

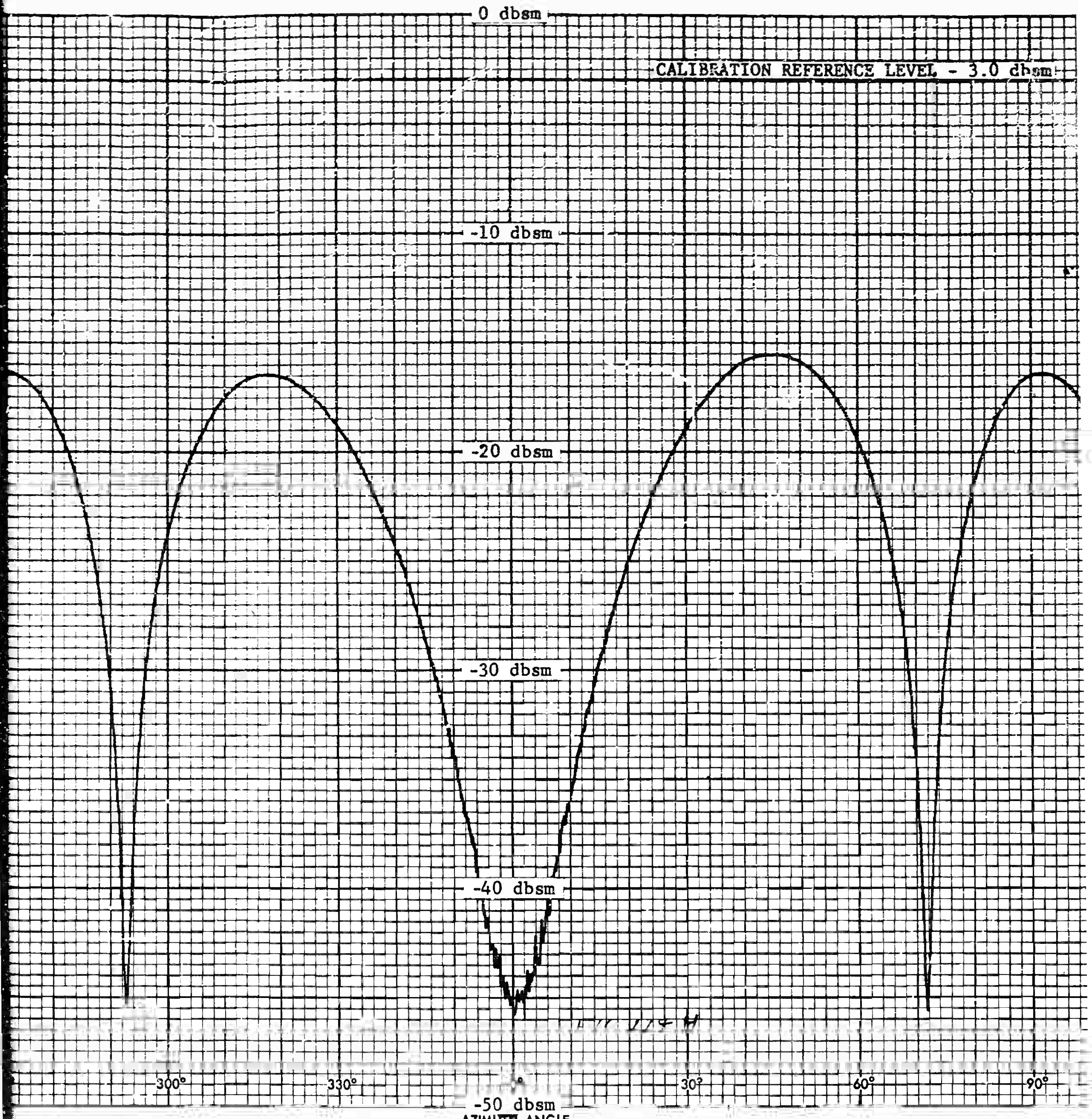

1

Fig. 114H SCALED M
AT 11° T

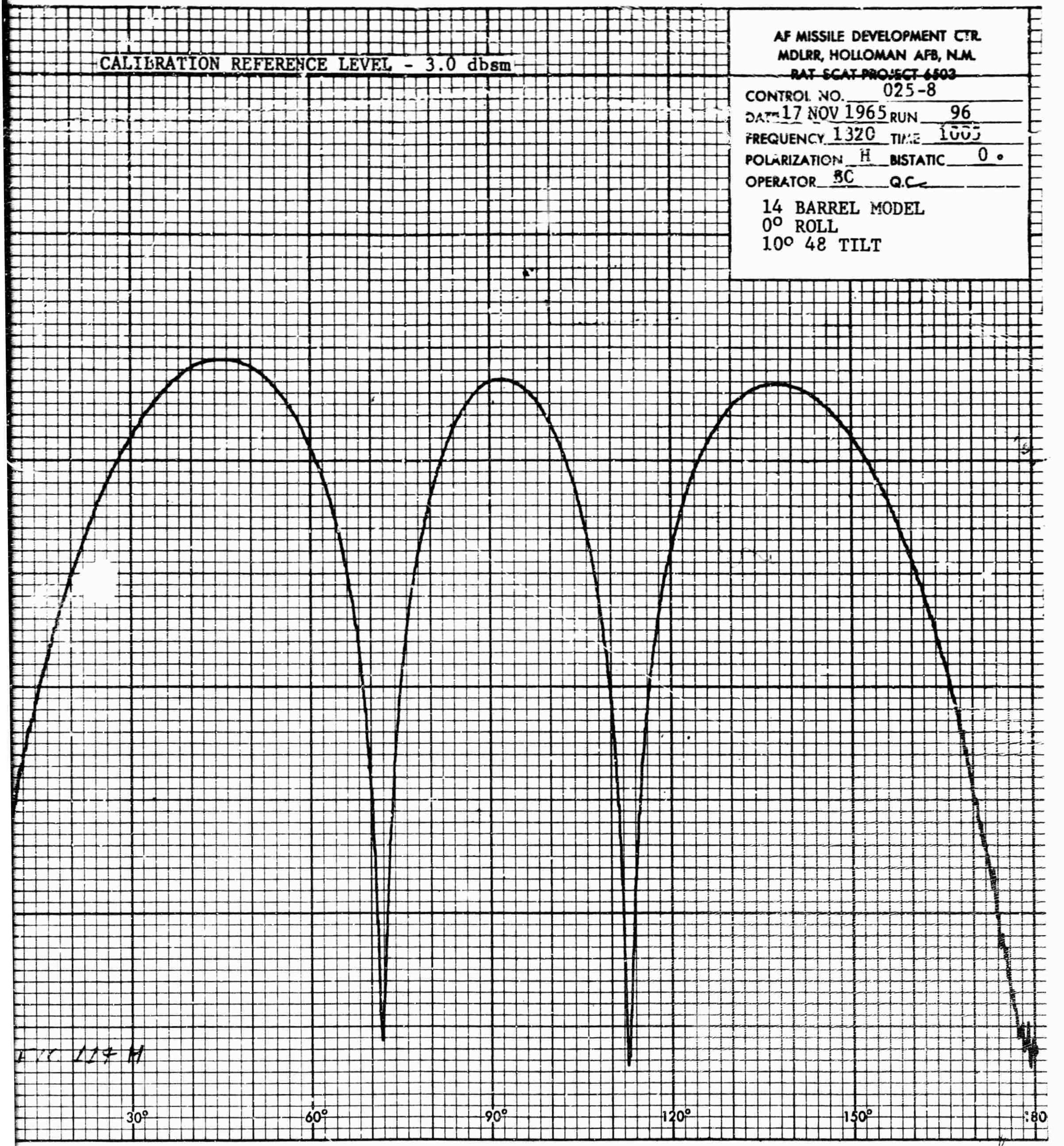

Fig. 114H SCALED MODEL OF 14 BARREL TARGET MEASURED AT 11° TILT ANGLE (HORIZONTAL POLARIZATION)

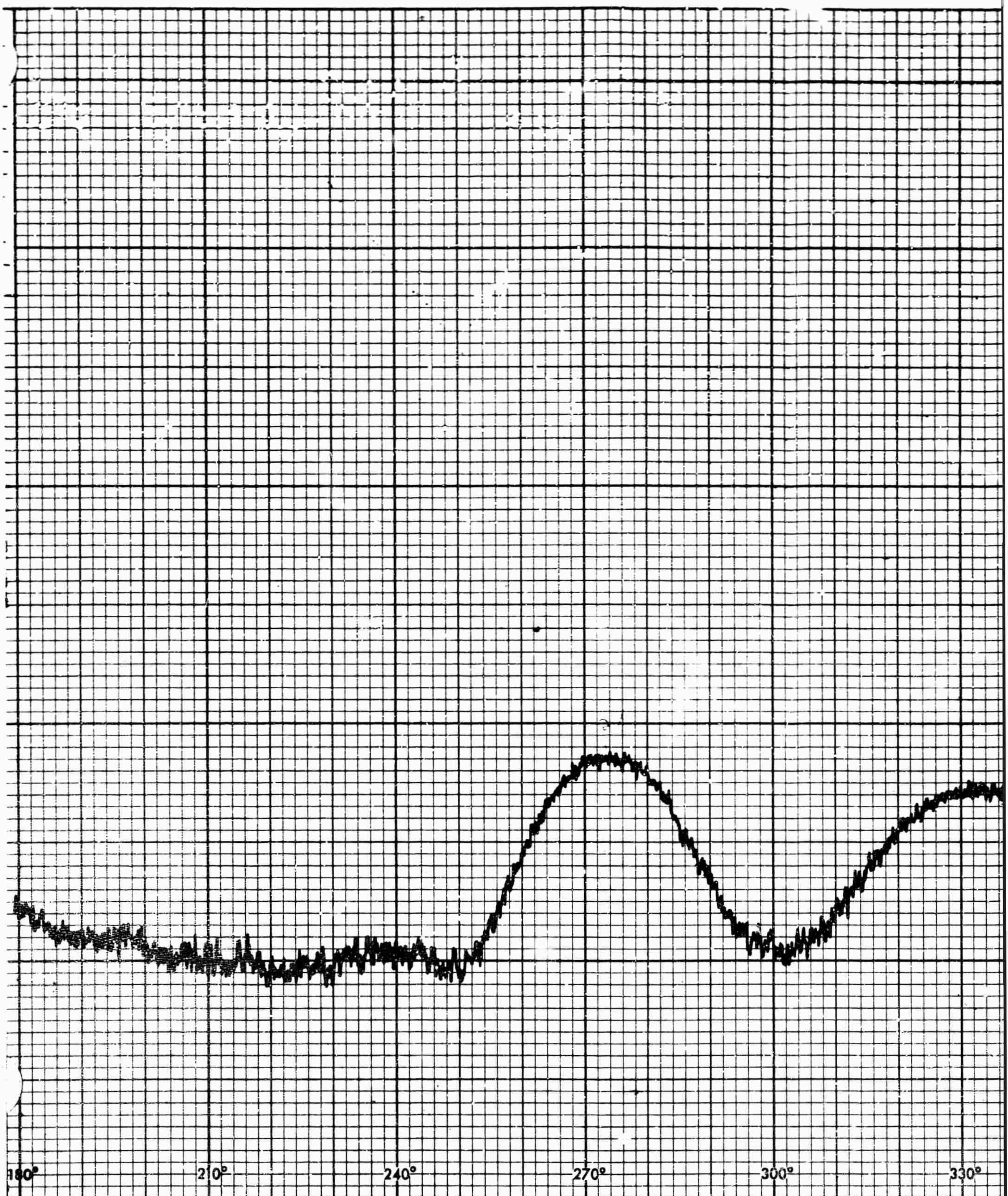
180°
210°
240°
270°
300°
330°

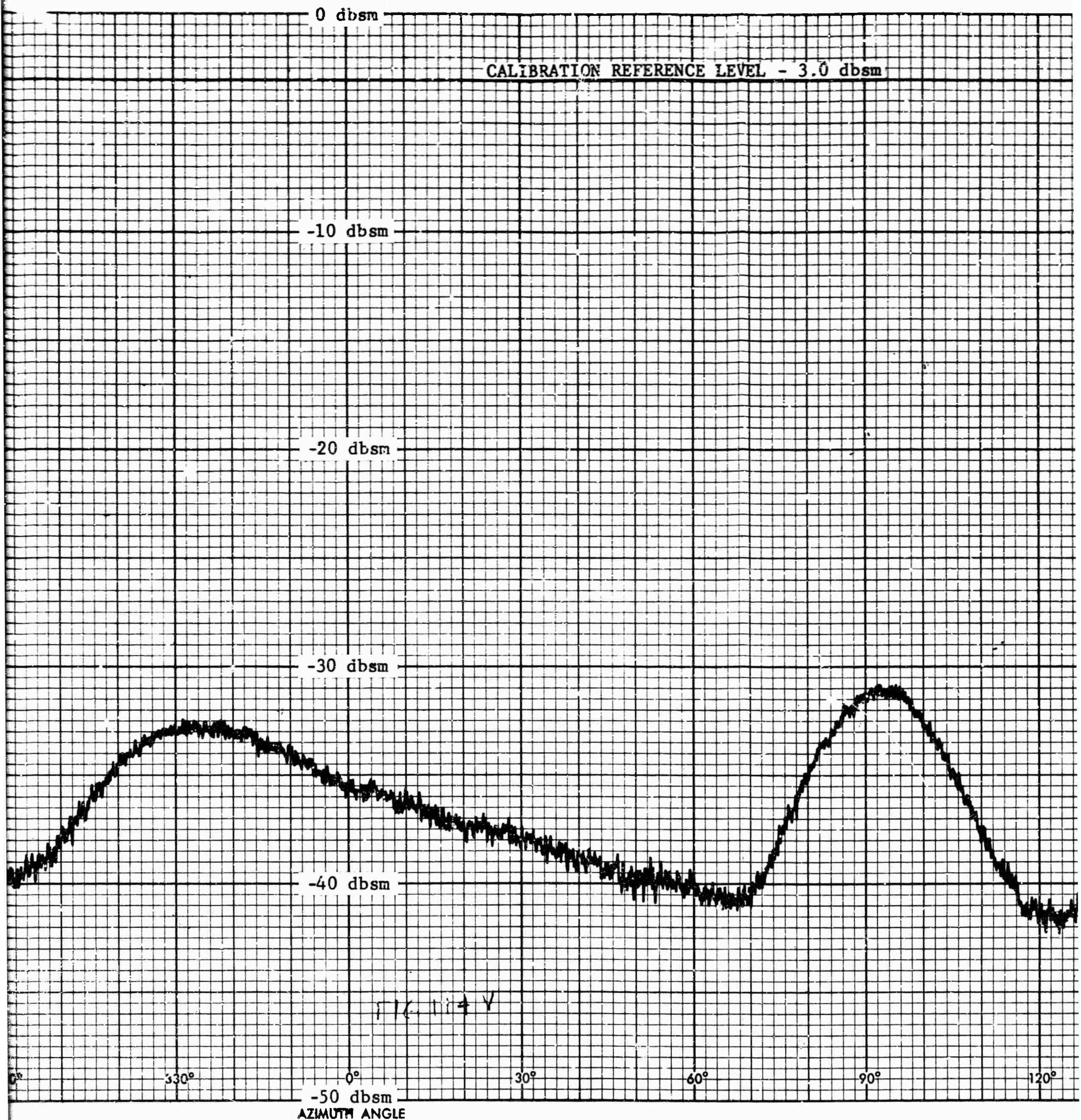

2

Fig. 114V SCALED MODEL AT 14
AT 5° TILT ANGLE (

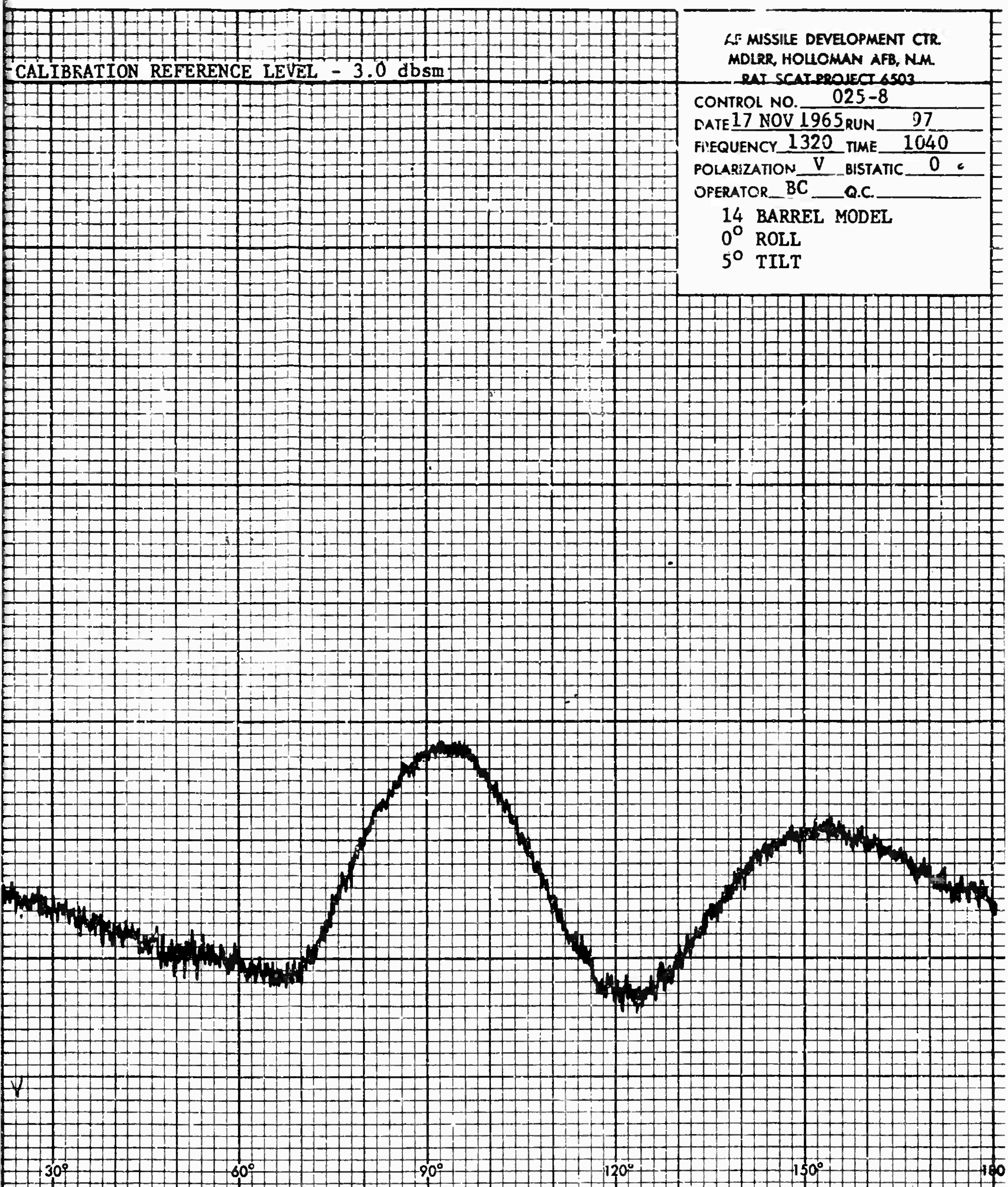

Fig. 114V SCALED MODEL AT 14 BARREL TARGET MEASURED AT 5° TILT ANGLE (VERTICAL POLARIZATION)

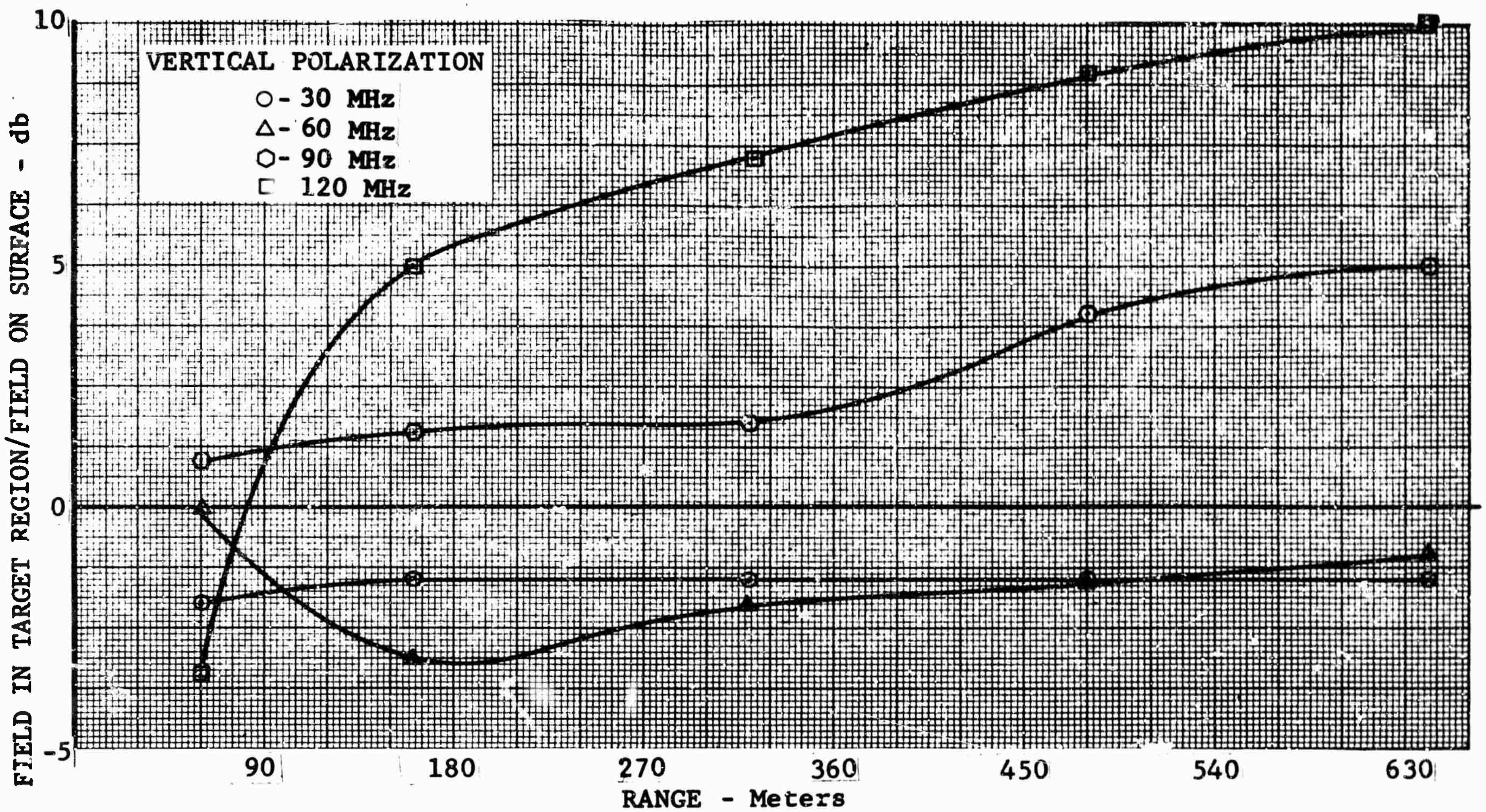

Fig. 115 FIELD IN TARGET REGION VS SURFACE FIELD AS A FUNCTION OF RANGE AND FREQUENCY

RANGE-1050 FEET
ANTENNA HEIGHT-33 FE

15% MOISTUR

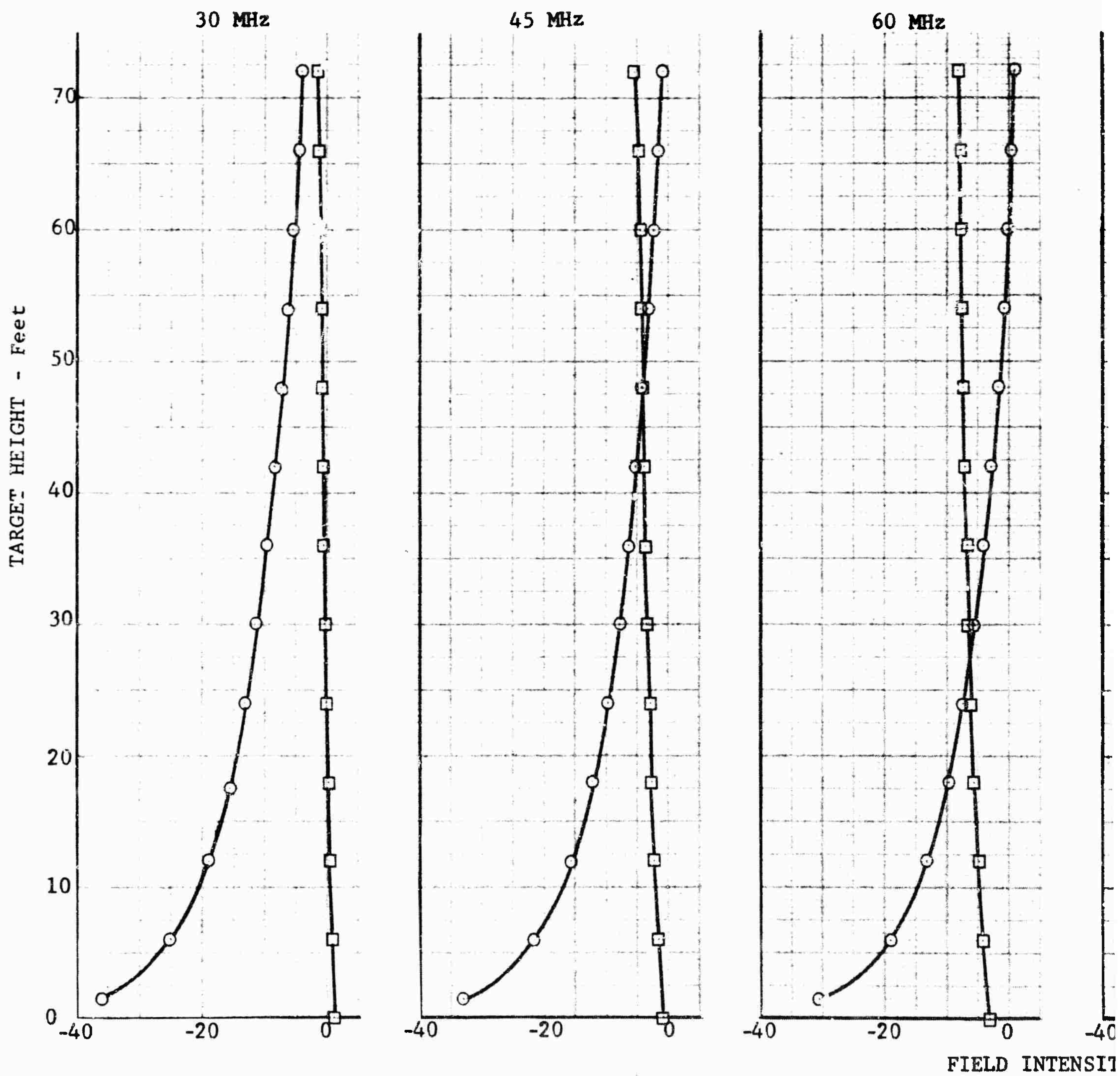

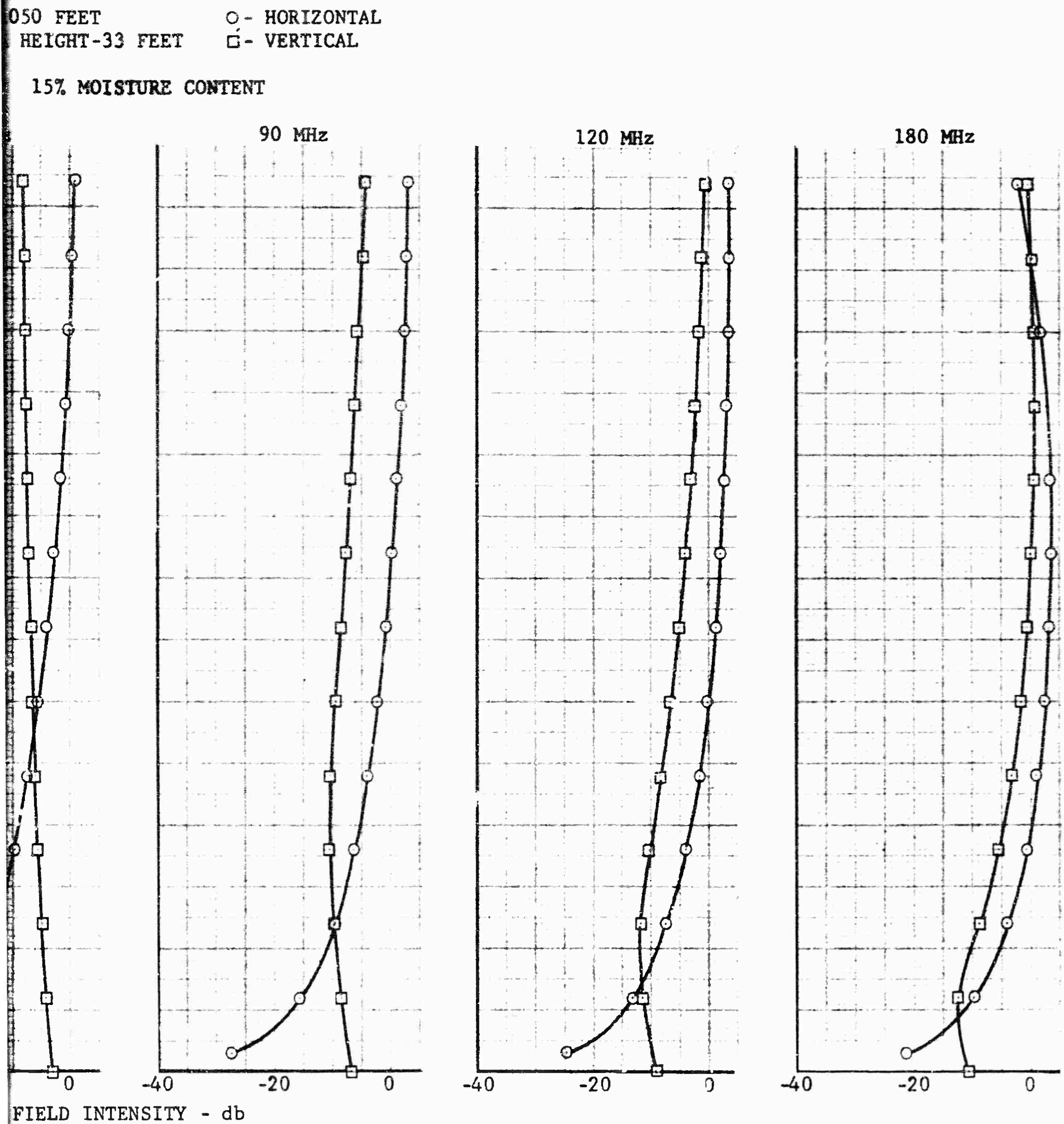

Fig. 116 FIELDS AT 1049 FOOT RANGE (33 FOOT ANTENNA HEIGHT, 15 PERCENT MOISTURE)

2

RANGE-1050 FEET
ANTENNA HEIGHT- 33 FEET

20% MOISTURE C

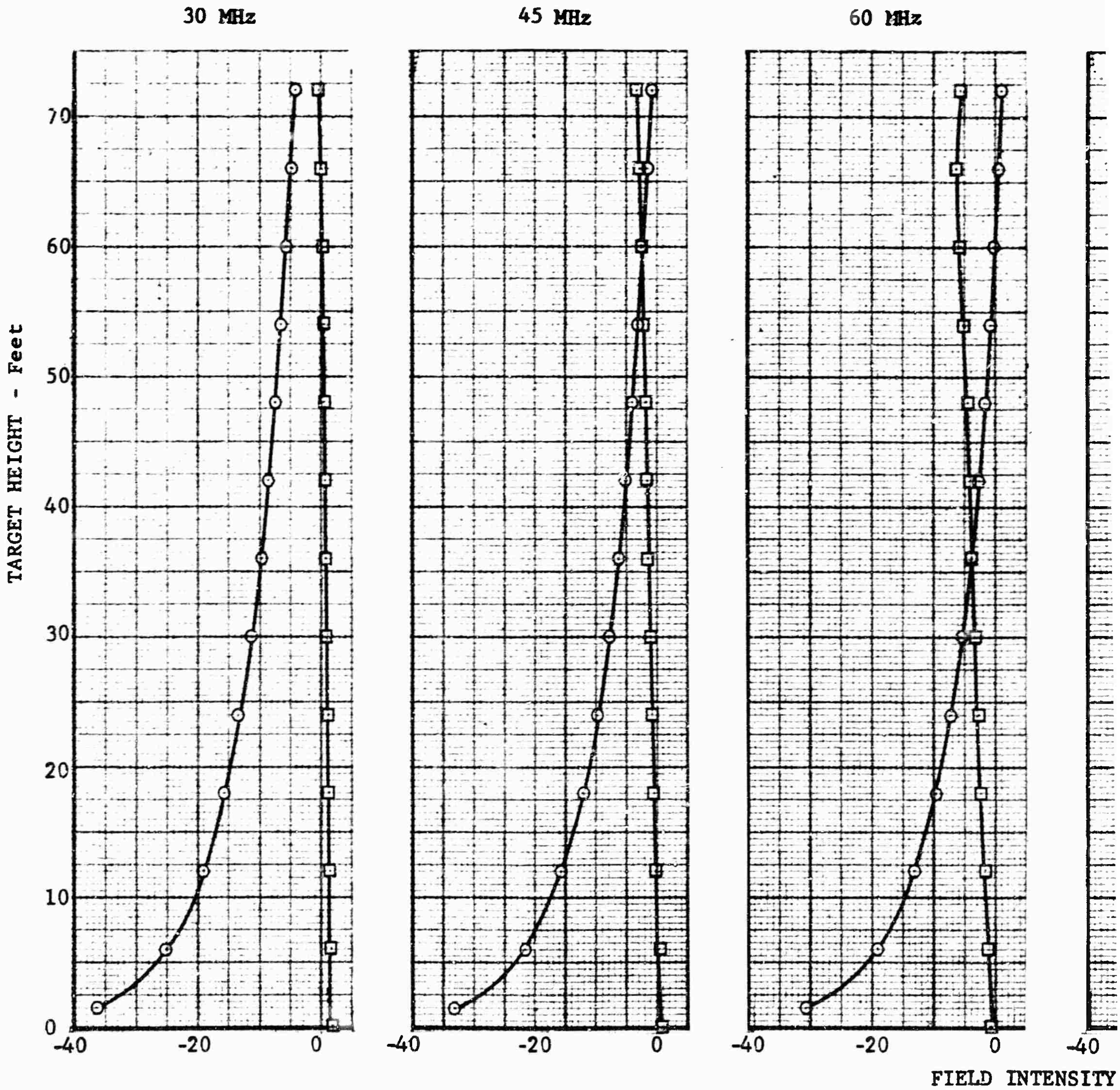

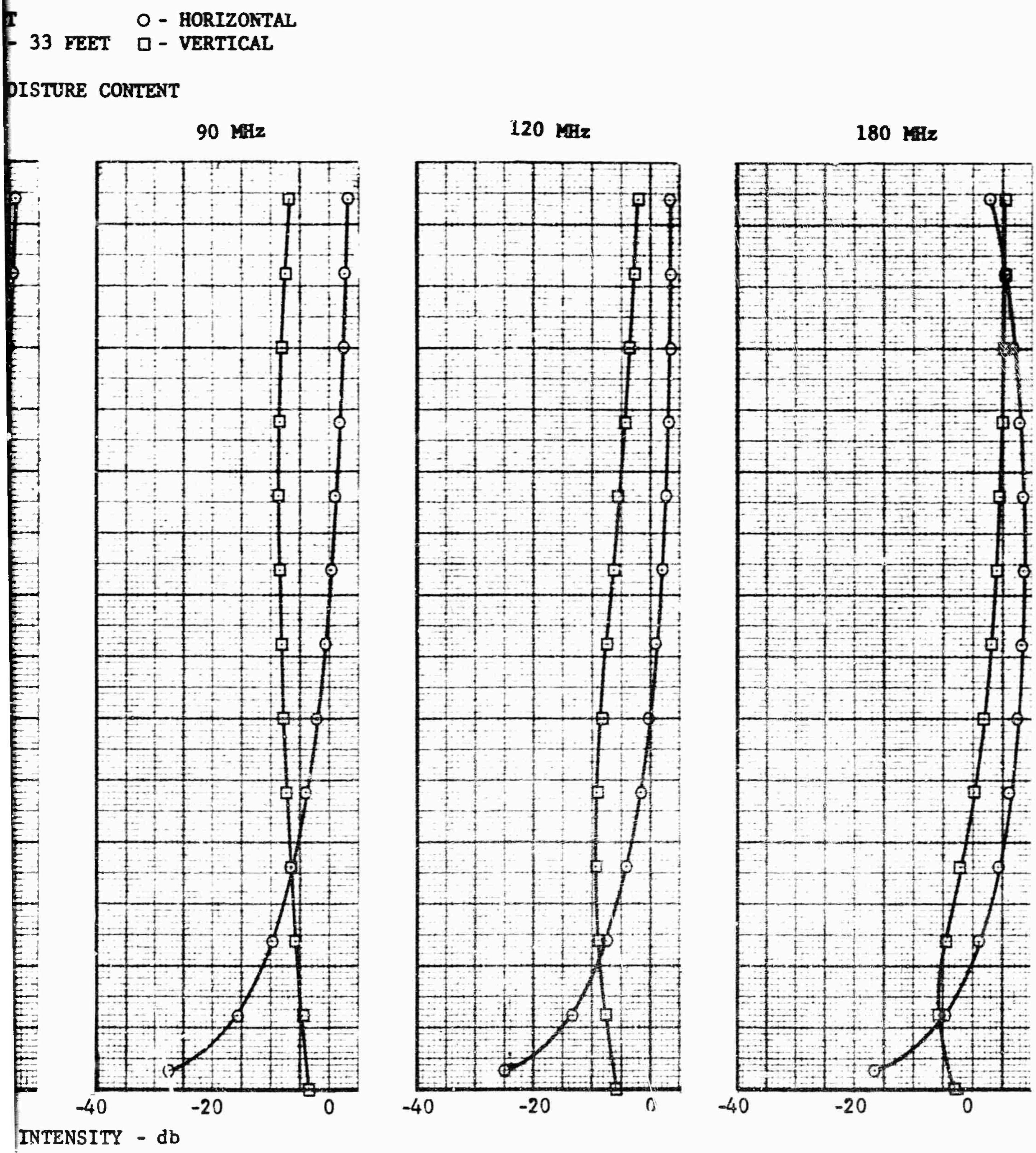

Fig. 117 FIELDS AT 1049 FOOT RANGE
(33 FOOT ANTENNA HEIGHT, 20 PERCENT MOISTURE)

2

RANGE: 1049'
ANTENNA HEIGHT: 49'
15% MOISTURE CON

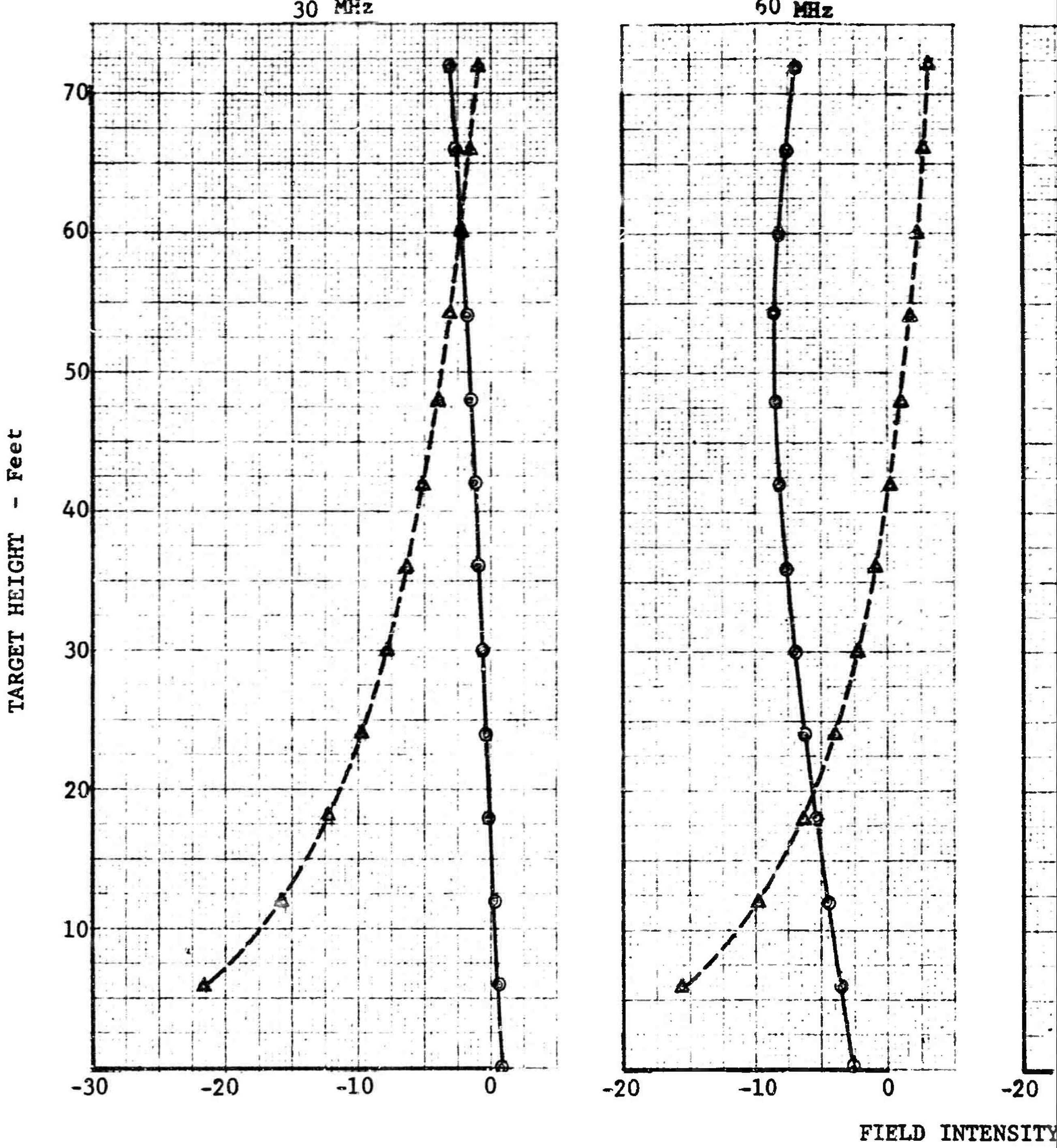

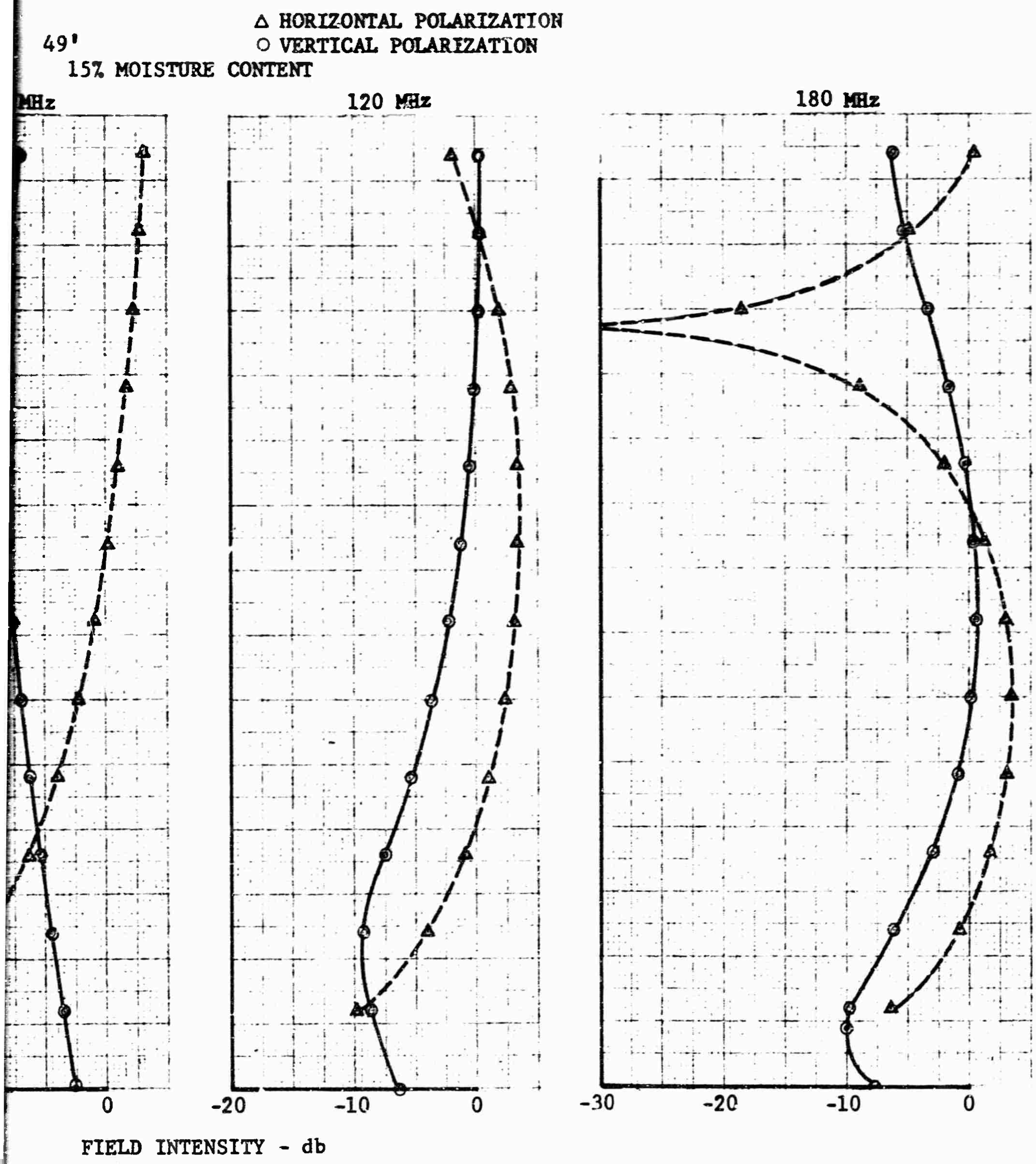

Fig. 118 FIELDS AT 1049 FOOT RANGE
(49 FOOT ANTENNA HEIGHT, 15 PERCENT MOISTURE)

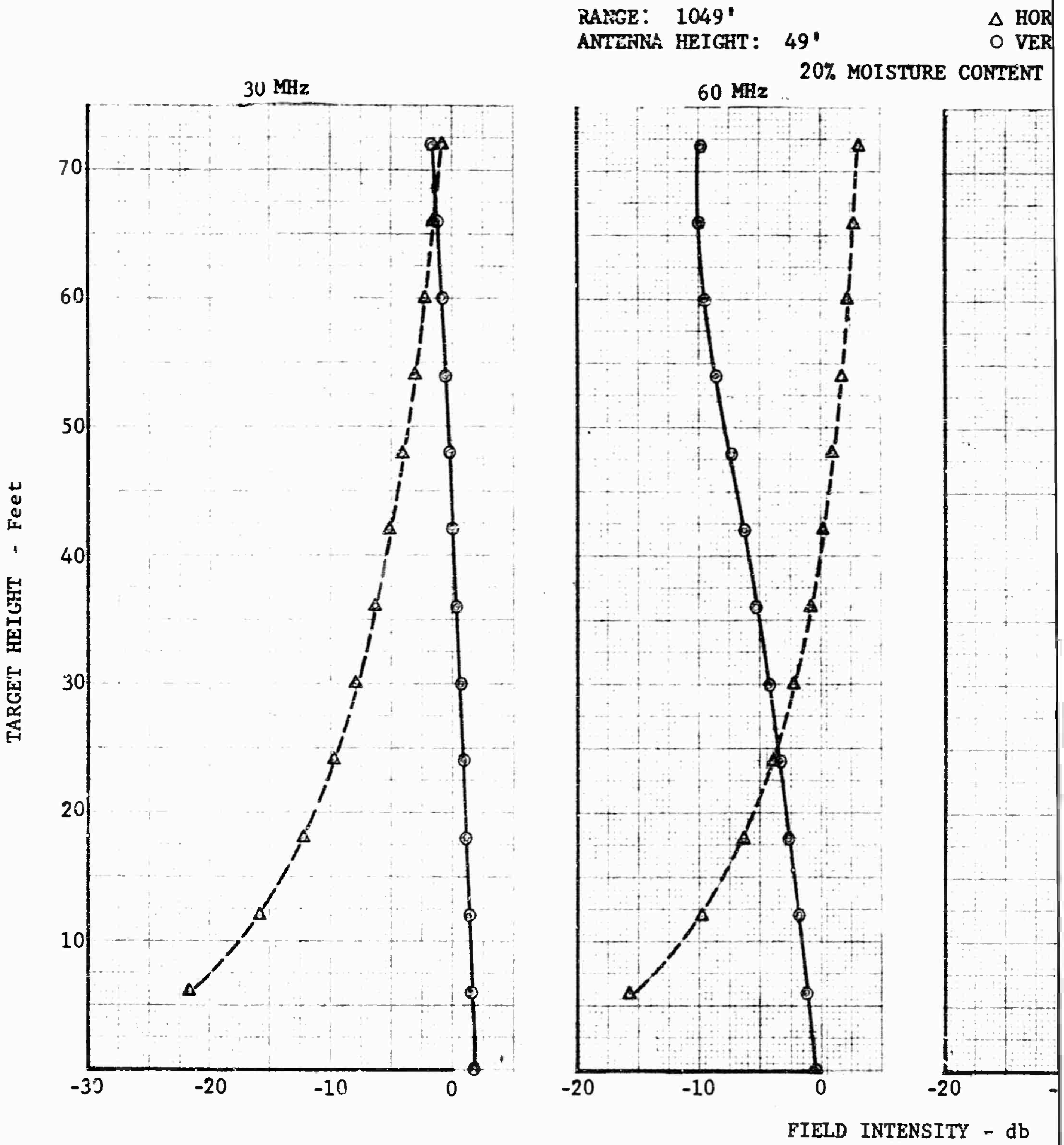
RANGE: 1049'
ANTENNA HEIGHT: 49'
△ HOR
○ VER
20% MOISTURE CONTENT
30 MHz
60 MHz
TARGET HEIGHT - Feet
70
60
50
40
30
20
10
-30
-20
-10
0
-20
-10
0
-20
FIELD INTENSITY - db

(4

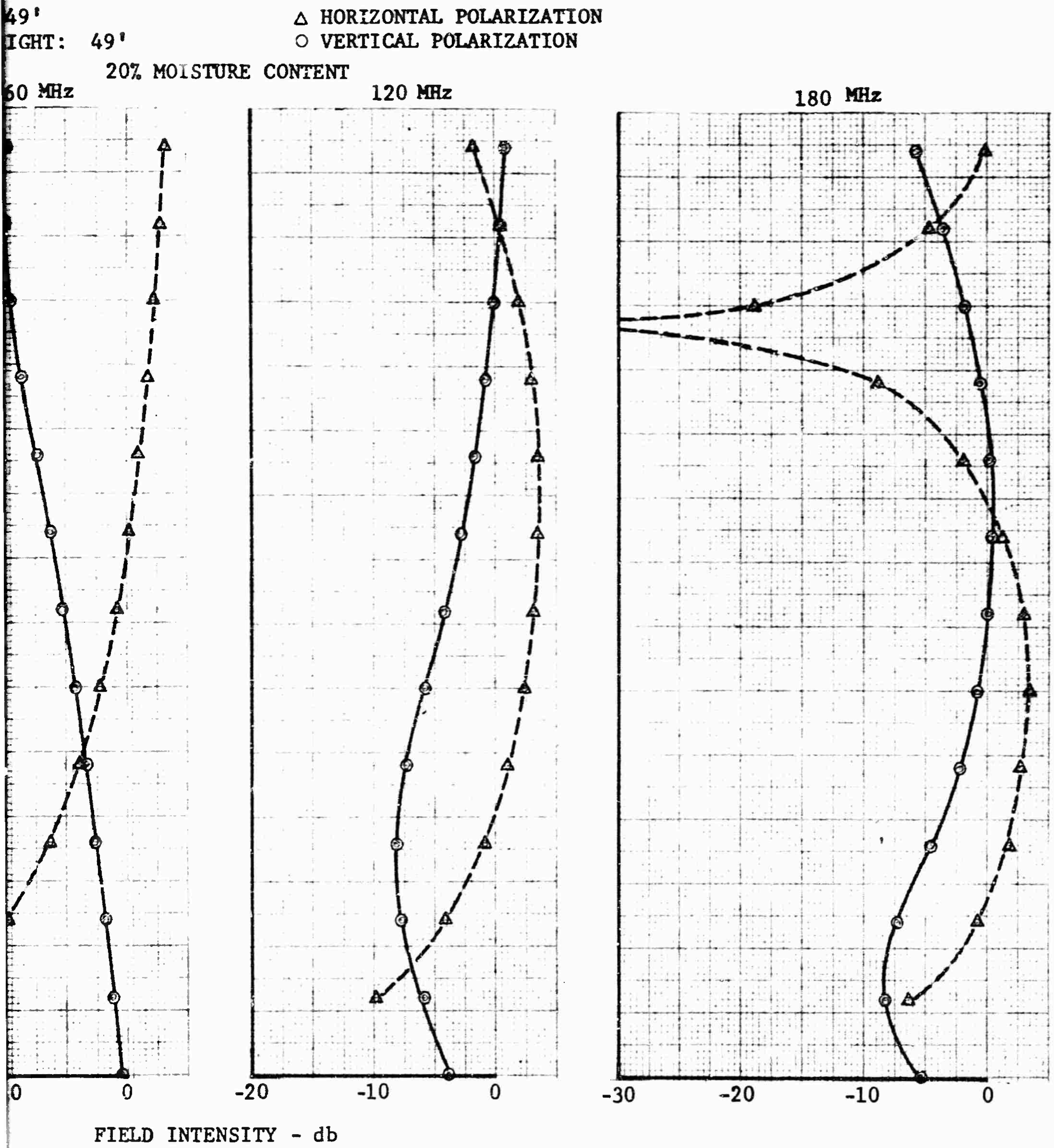

Fig. 119 FIELDS AT 1049 FOOT RANGE
(49 FOOT ANTENNA HEIGHT, 20 PERCENT MOISTURE)

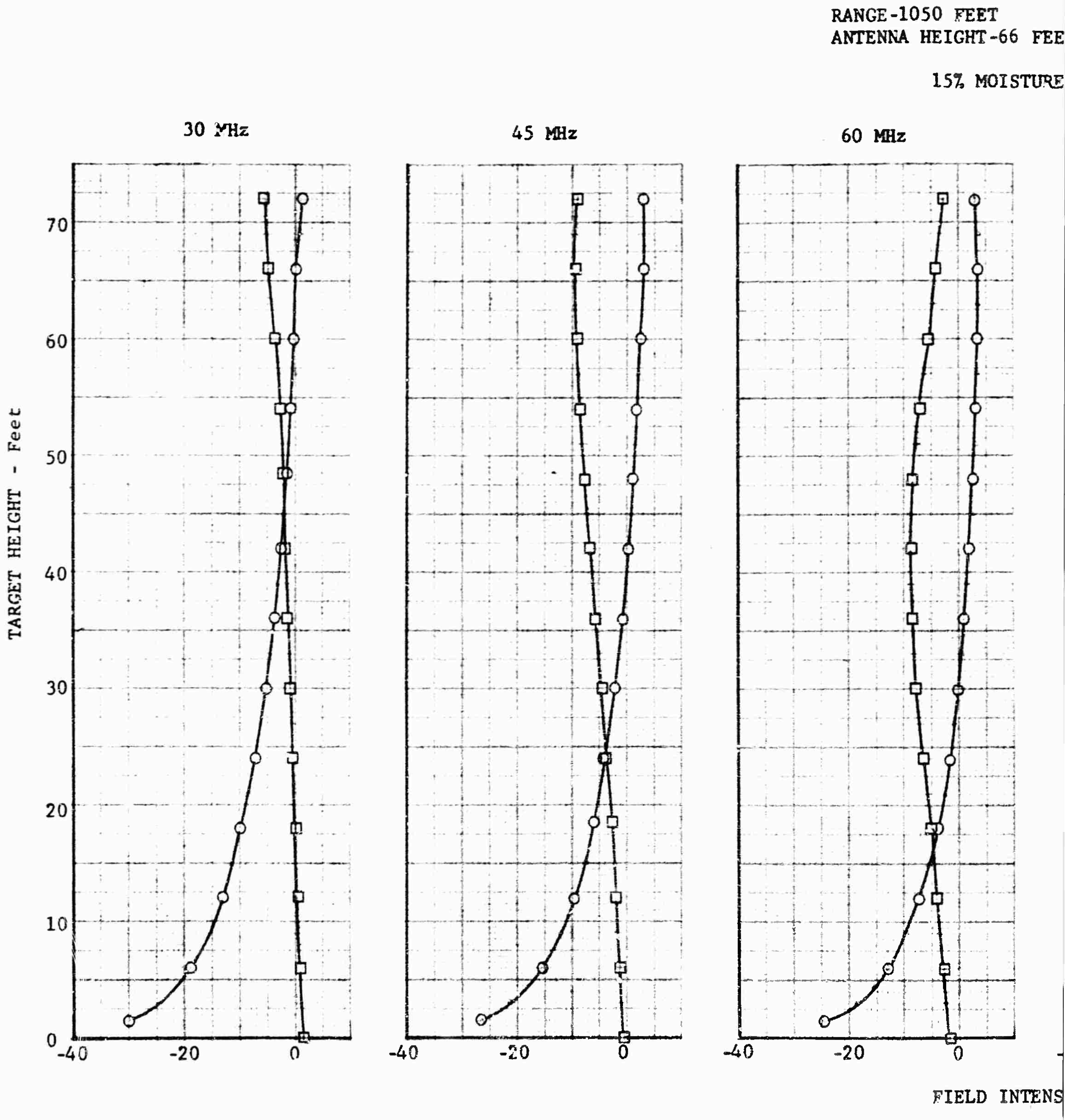
RANGE-1050 FEET
ANTENNA HEIGHT-66 FEE
15% MOISTURE
30 MHz
45 MHz
60 MHz
TARGET HEIGHT - Feet
0
10
20
30
40
50
60
70
-40
-20
0
FIELD INTENS

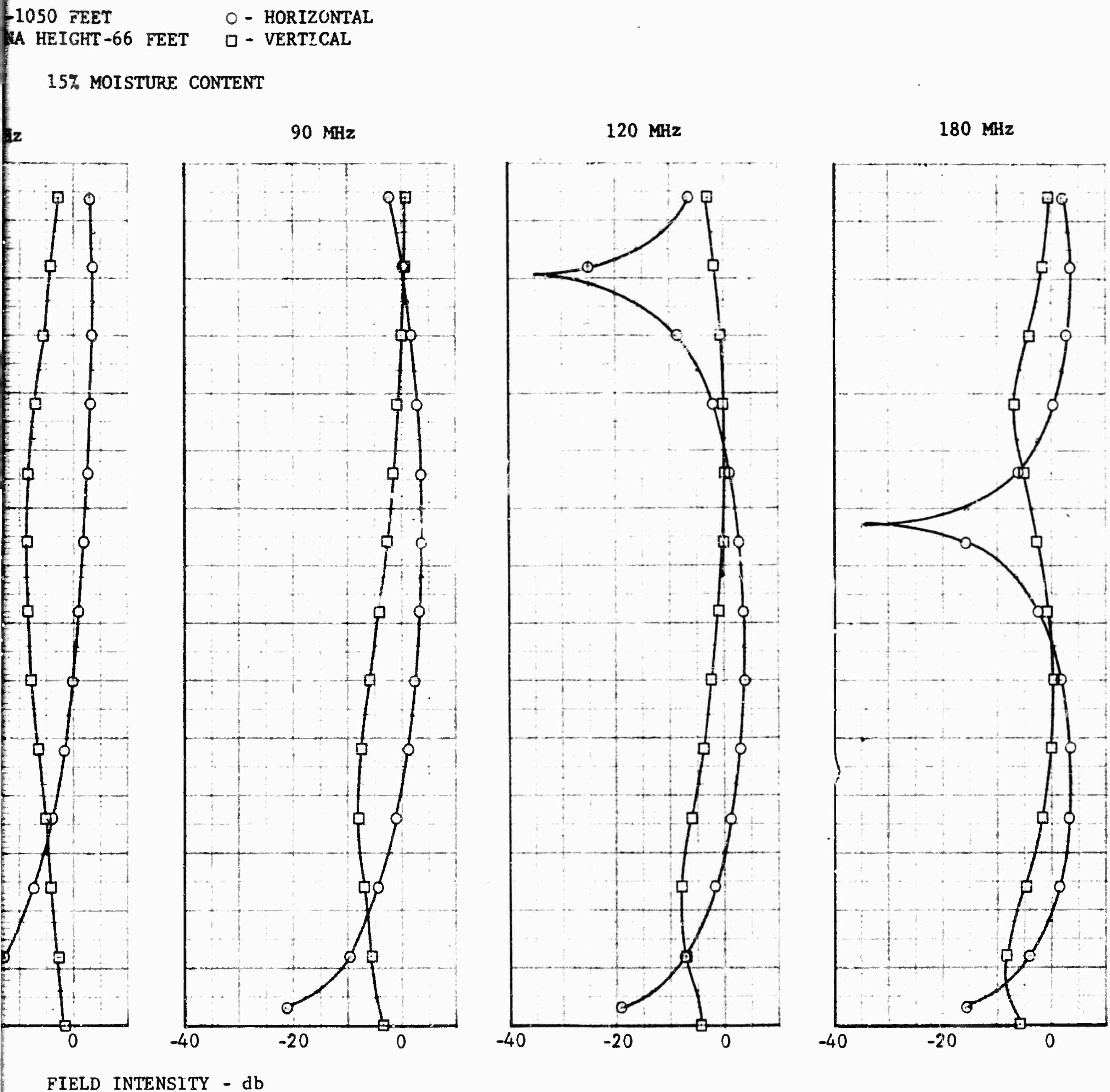

Fig. 120 FIELDS AT 1049 FOOT RANGE
(66 FOOT ANTENNA HEIGHT, 15 PERCENT MOISTURE)

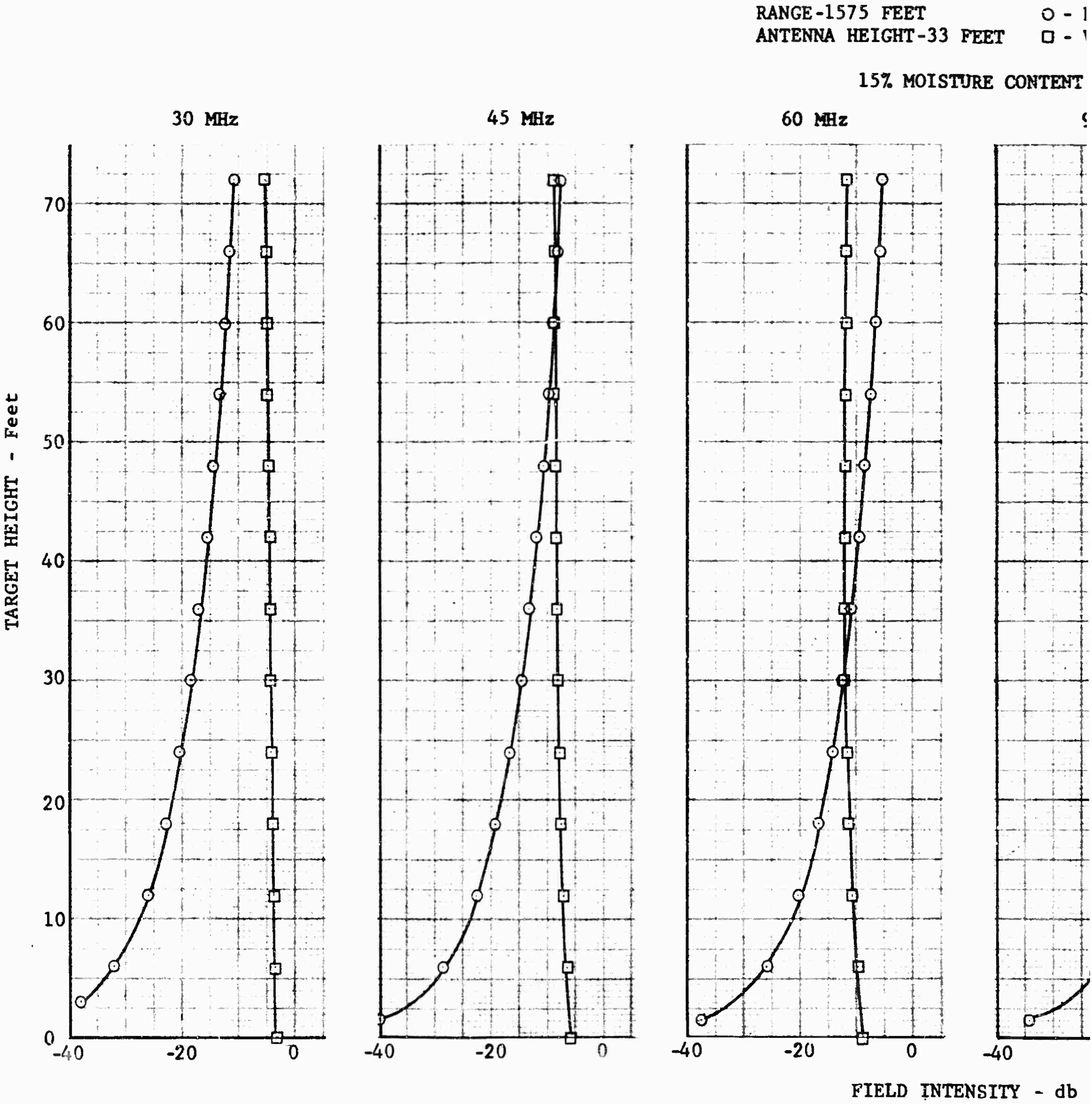
RANGE-1575 FEET
ANTENNA HEIGHT-33 FEET
15% MOISTURE CONTENT
30 MHz
45 MHz
60 MHz
TARGET HEIGHT - Feet
70
60
50
40
30
20
10
0
-40
-20
0
FIELD INTENSITY - db

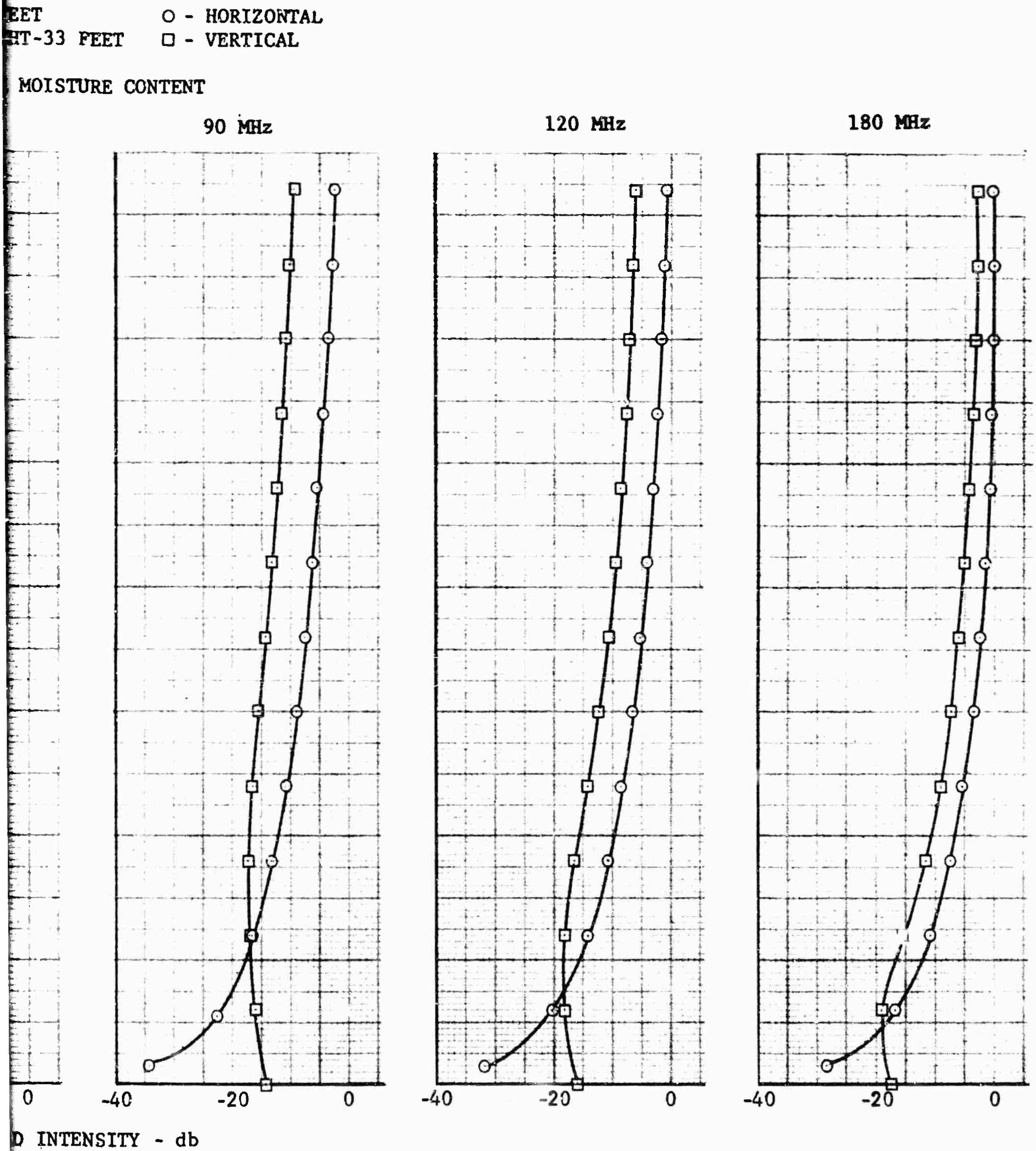

Fig. 121 FIELDS AT 1575 FOOT RANGE
(33 FOOT ANTENNA HEIGHT, 15 PERCENT MOISTURE)

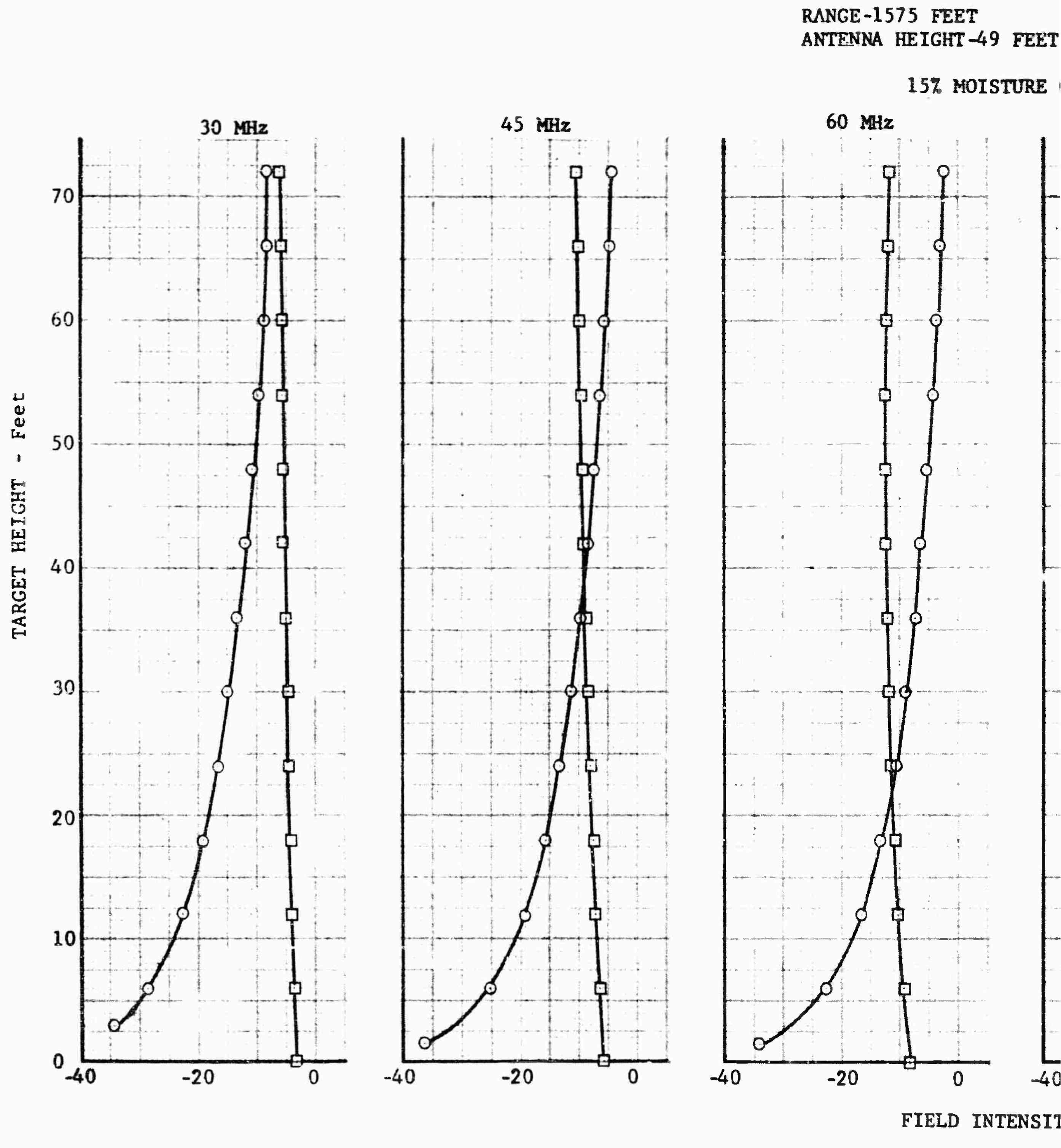

RANGE-1575 FEET
ANTENNA HEIGHT-49 FEET
15% MOISTURE
30 MHz
45 MHz
60 MHz
TARGET HEIGHT - Feet
0
10
20
30
40
50
60
70
-40
-20
0
FIELD INTENSIT

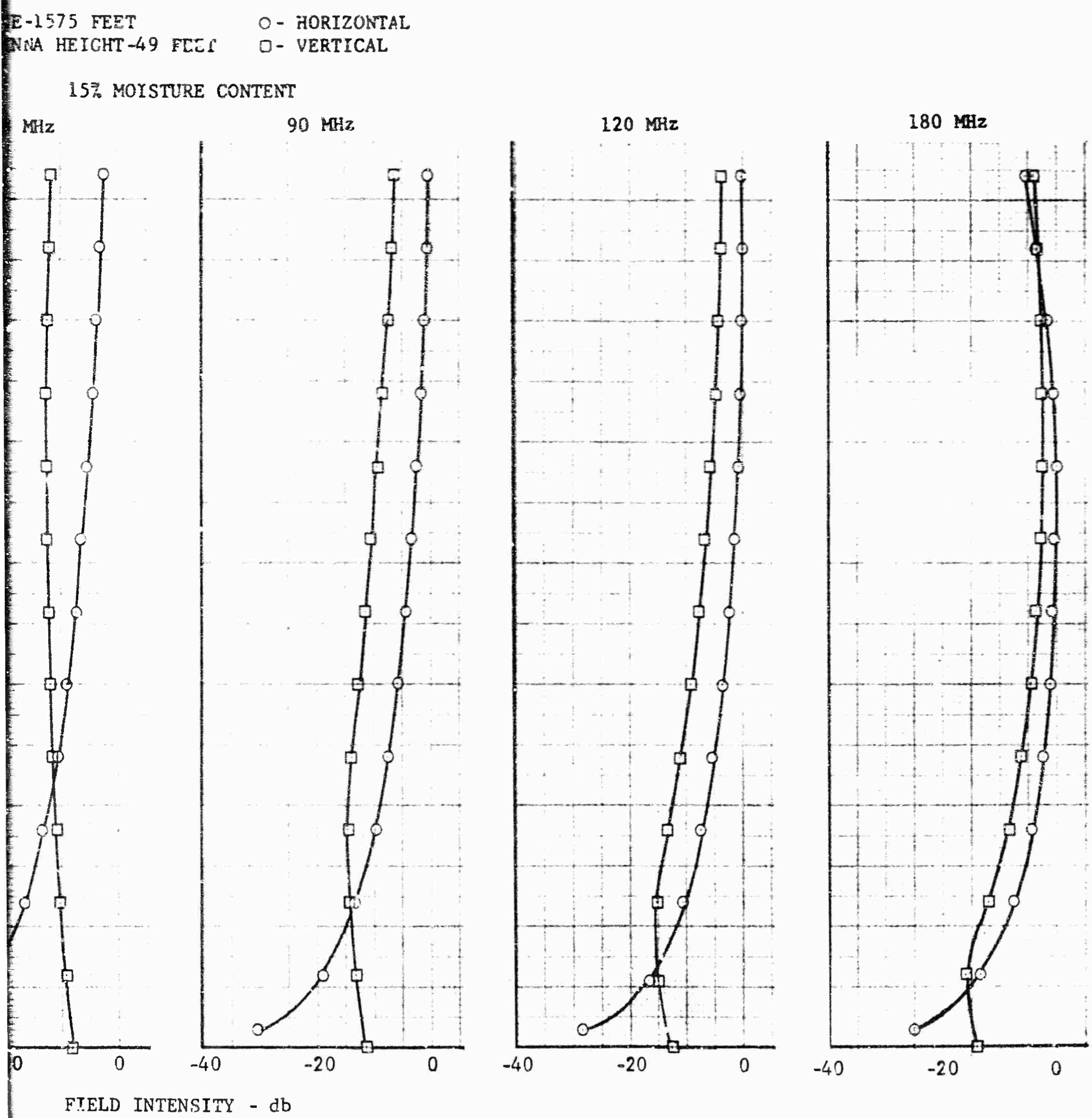

Fig. 122 FIELDS AT 1575 FOOT RANGE
(49 FOOT ANTENNA HEIGHT, 15 PERCENT MOISTURE)

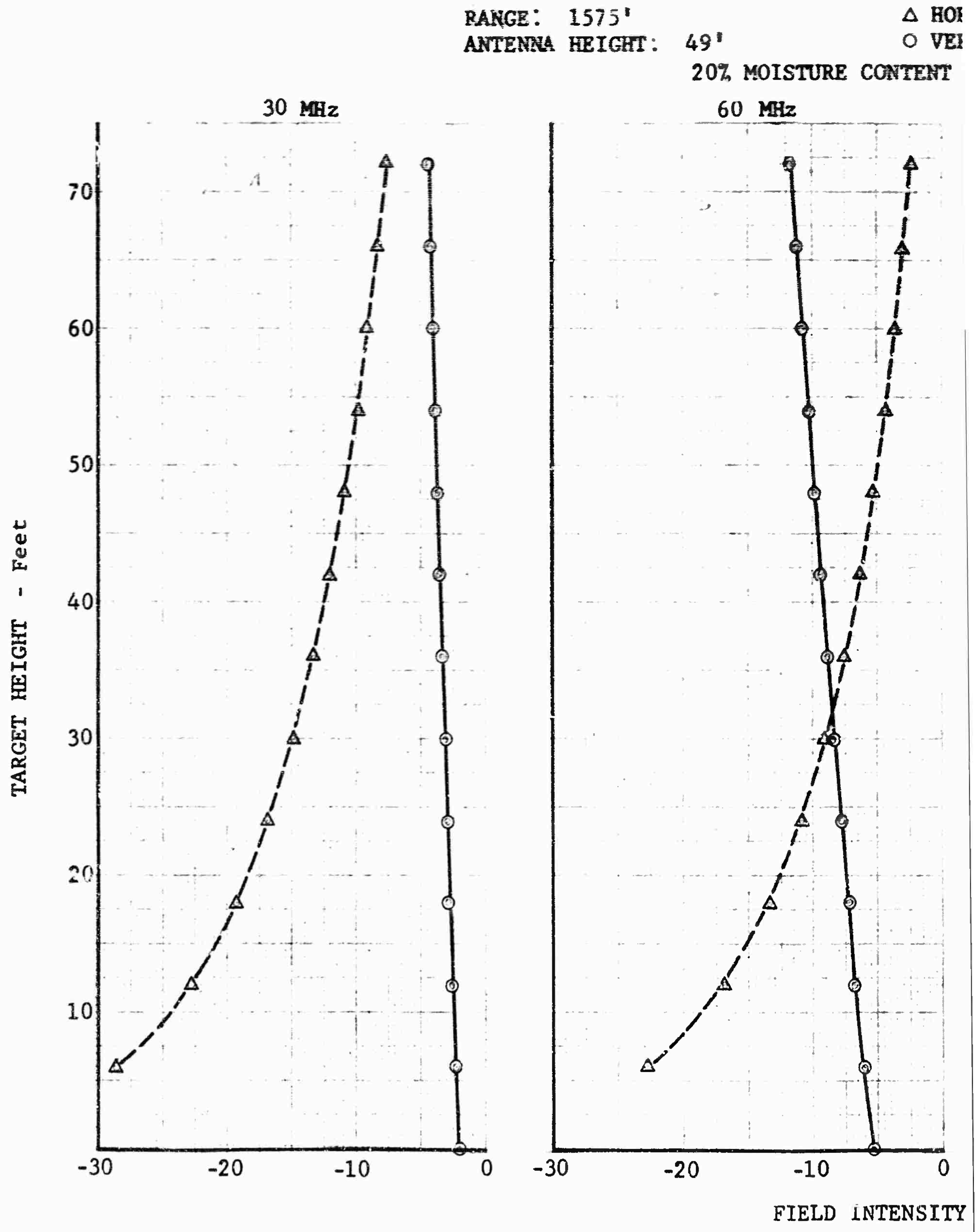

RANGE: 1575'
ANTENNA HEIGHT: 49'
Δ HOR
O VER
20% MOISTURE CONTENT
30 MHz
60 MHz
TARGET HEIGHT - Feet
70
60
50
40
30
20
10
-30
-20
-10
0
FIELD INTENSITY

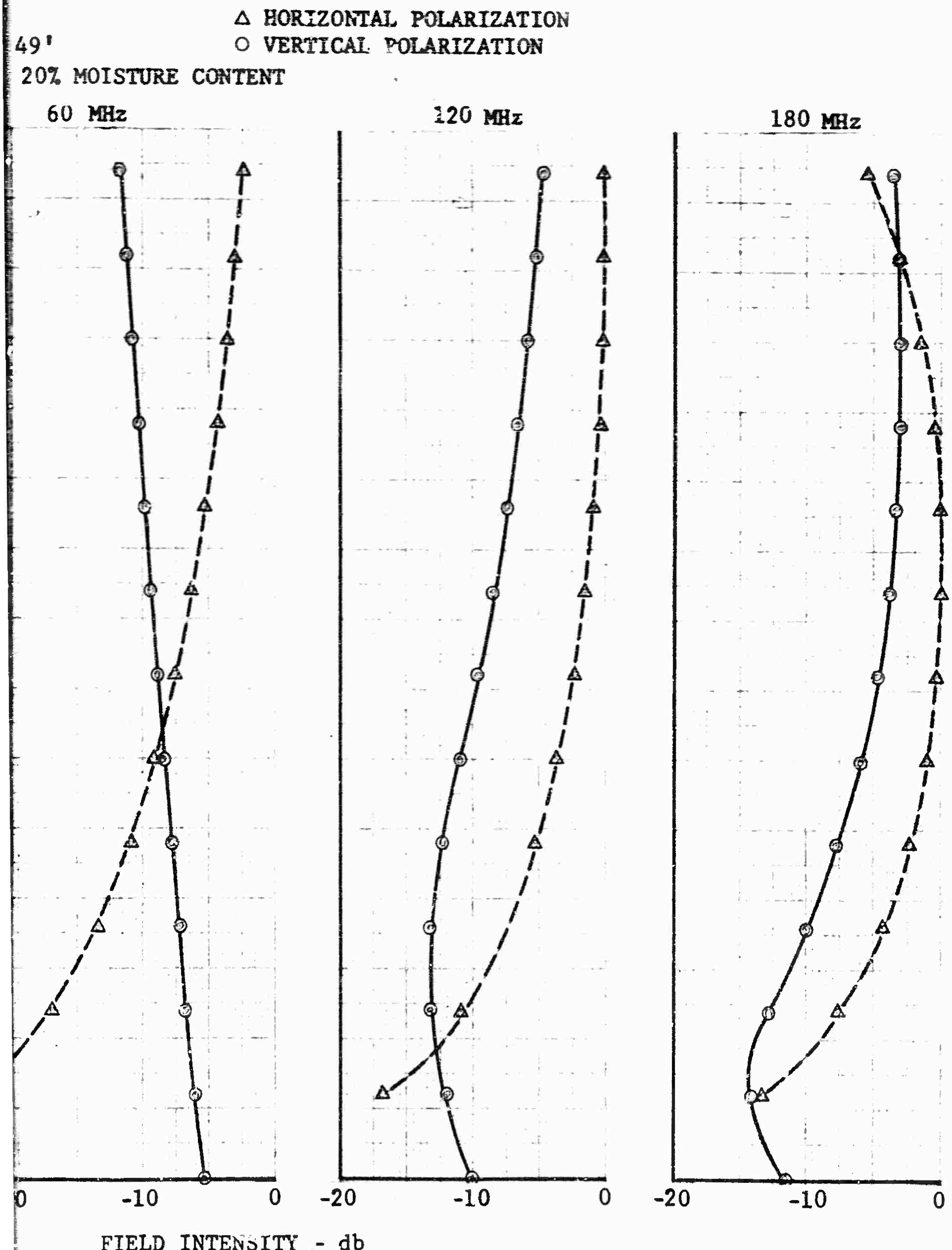

Fig. 123 FIELDS AT 1575 FOOT RANGE
(49 FOOT ANTENNA HEIGHT, 20 PERCENT MOISTURE)

2

RANGE-1575 FEET
ANTENNA HEIGHT-66 FEET

15% MOISTURE CONTENT

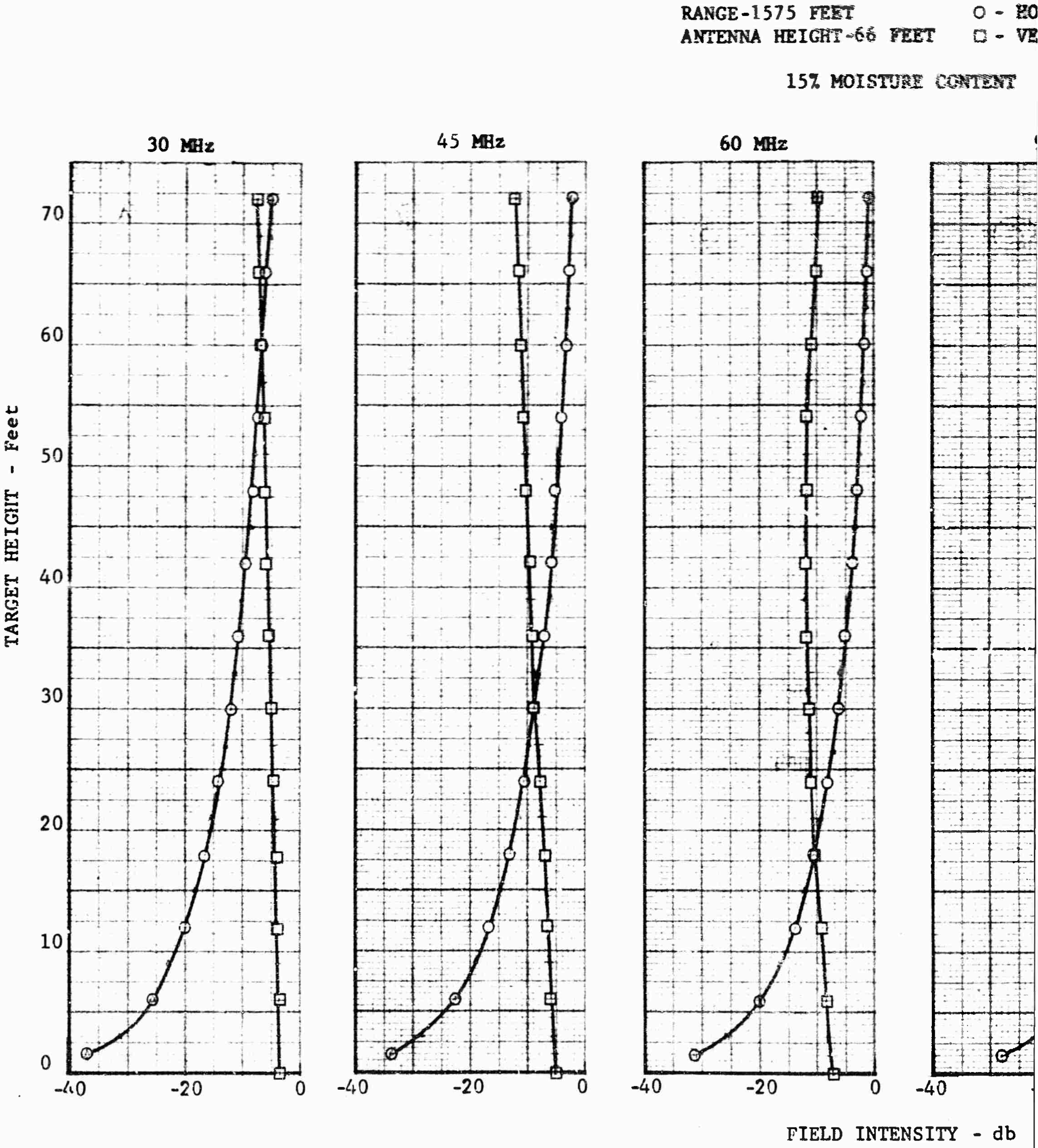

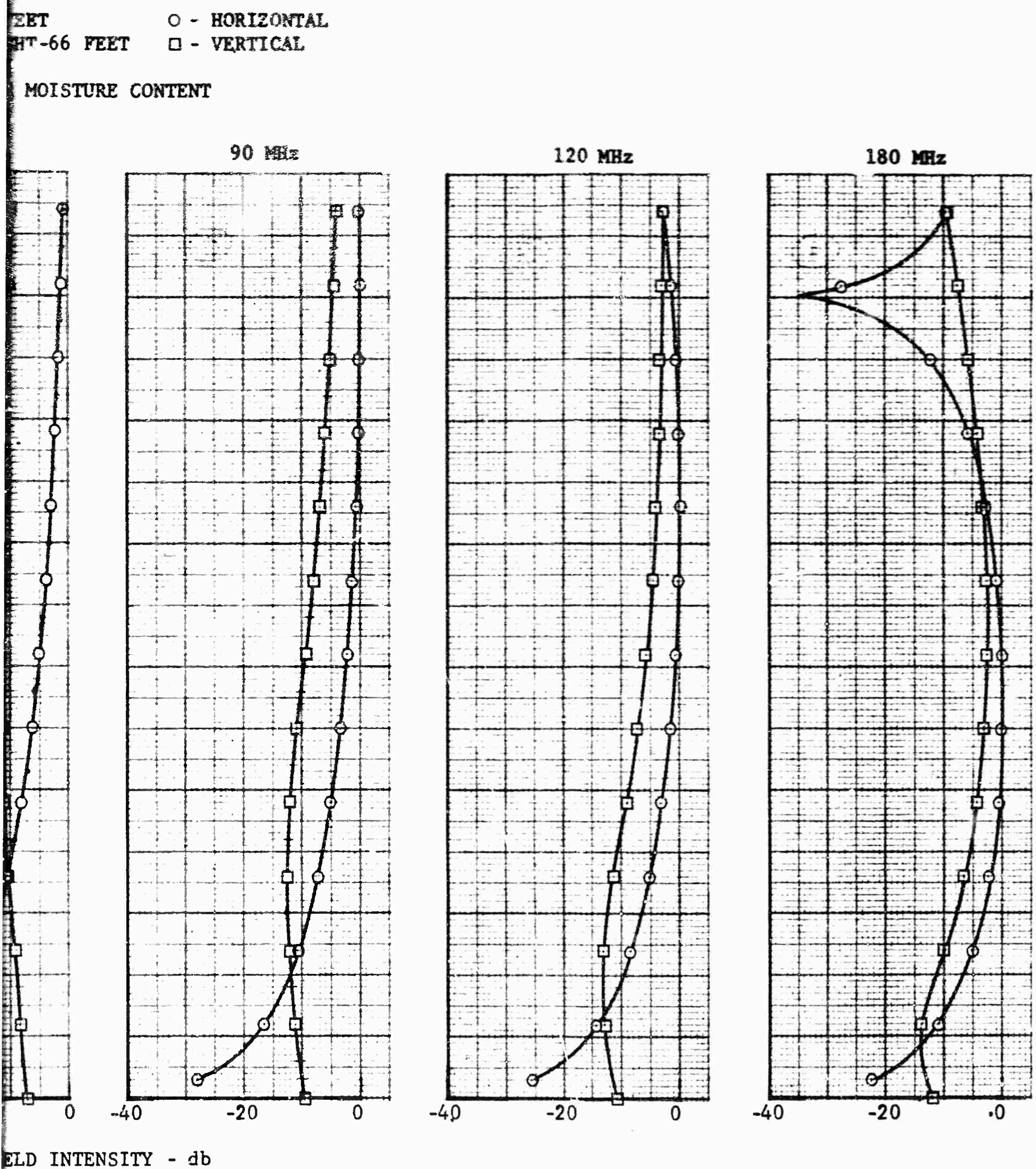

Fig. 124 FIELDS AT 1575 FOOT RANGE
(66 FOOT ANTENNA HEIGHT, 15 PERCENT MOISTURE)

RANGE-1575 FEET
ANTENNA HEIGHT-85 FEET

15% MOISTURE CO

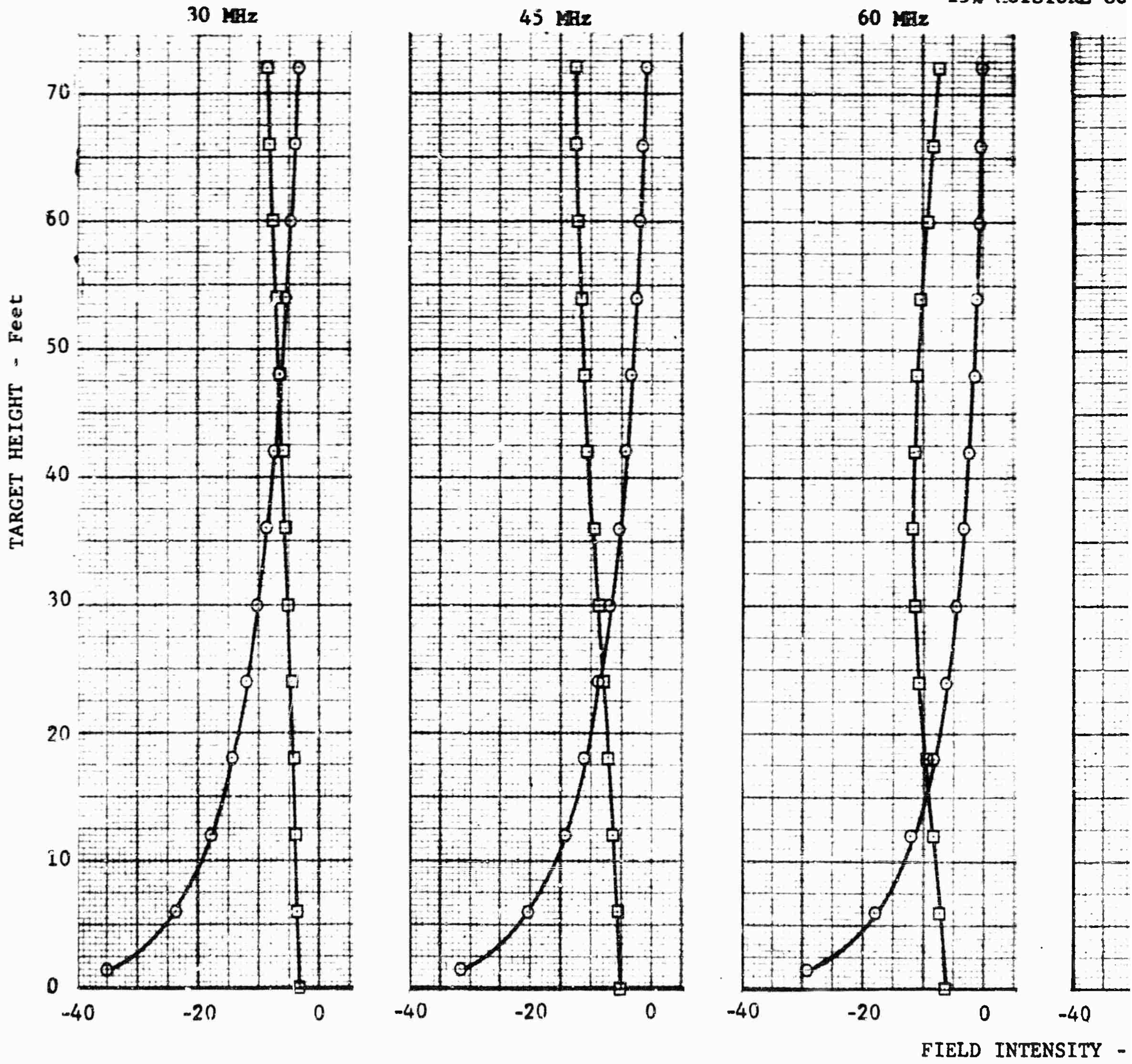

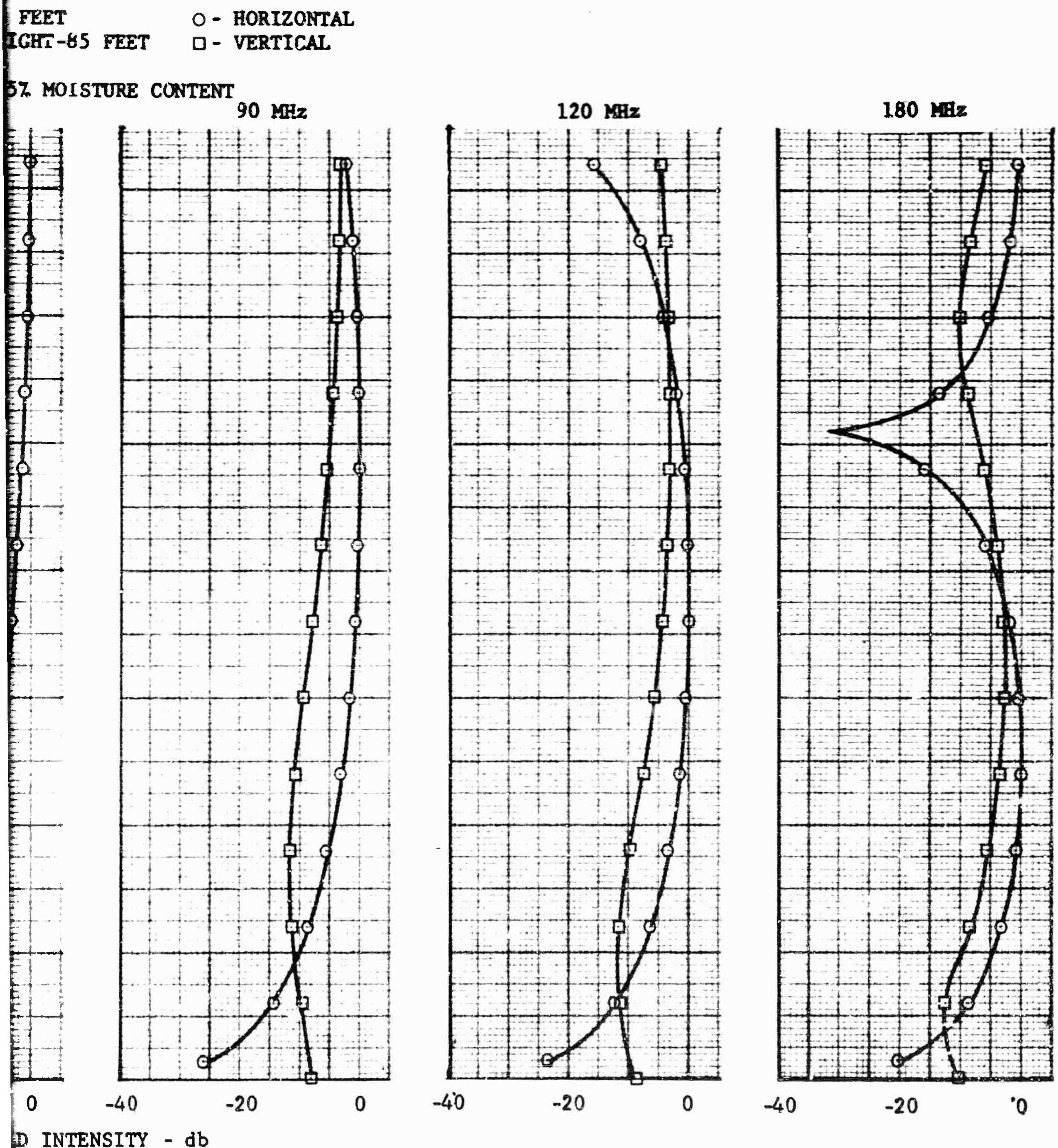

Fig. 125 FIELDS AT 1575 FOOT RANGE
(85 FOOT ANTENNA HEIGHT, 15 PERCENT MOISTURE)

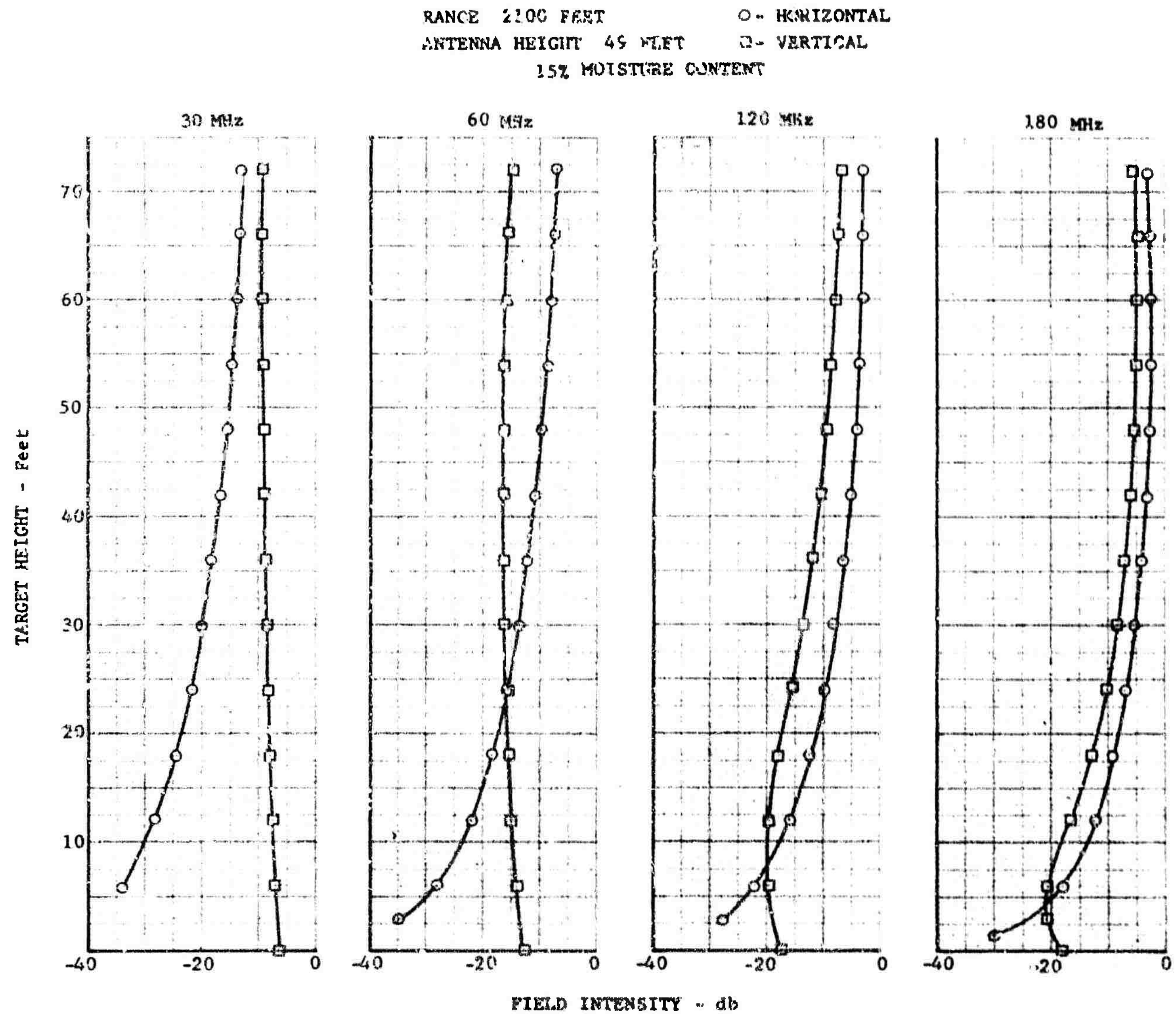

Fig. 126 FIELDS AT 2100 FOOT RANGE (49 FOOT ANTENNA HEIGHT, 15 PERCENT MOISTURE)

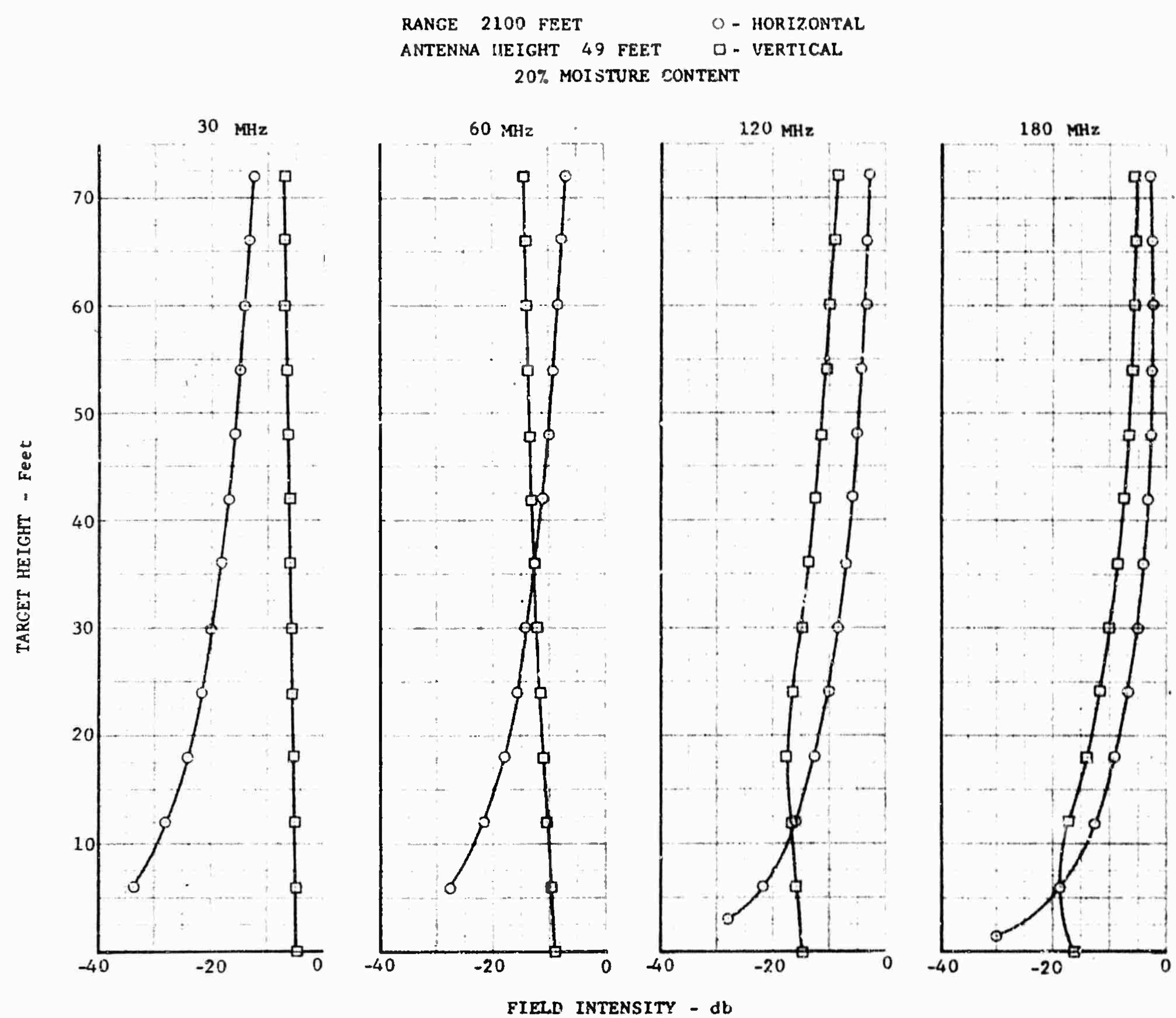

Fig. 127 FIELDS AT 2100 FOOT RANGE (49 FOOT ANTENNA HEIGHT, 20 PERCENT MOISTURE)

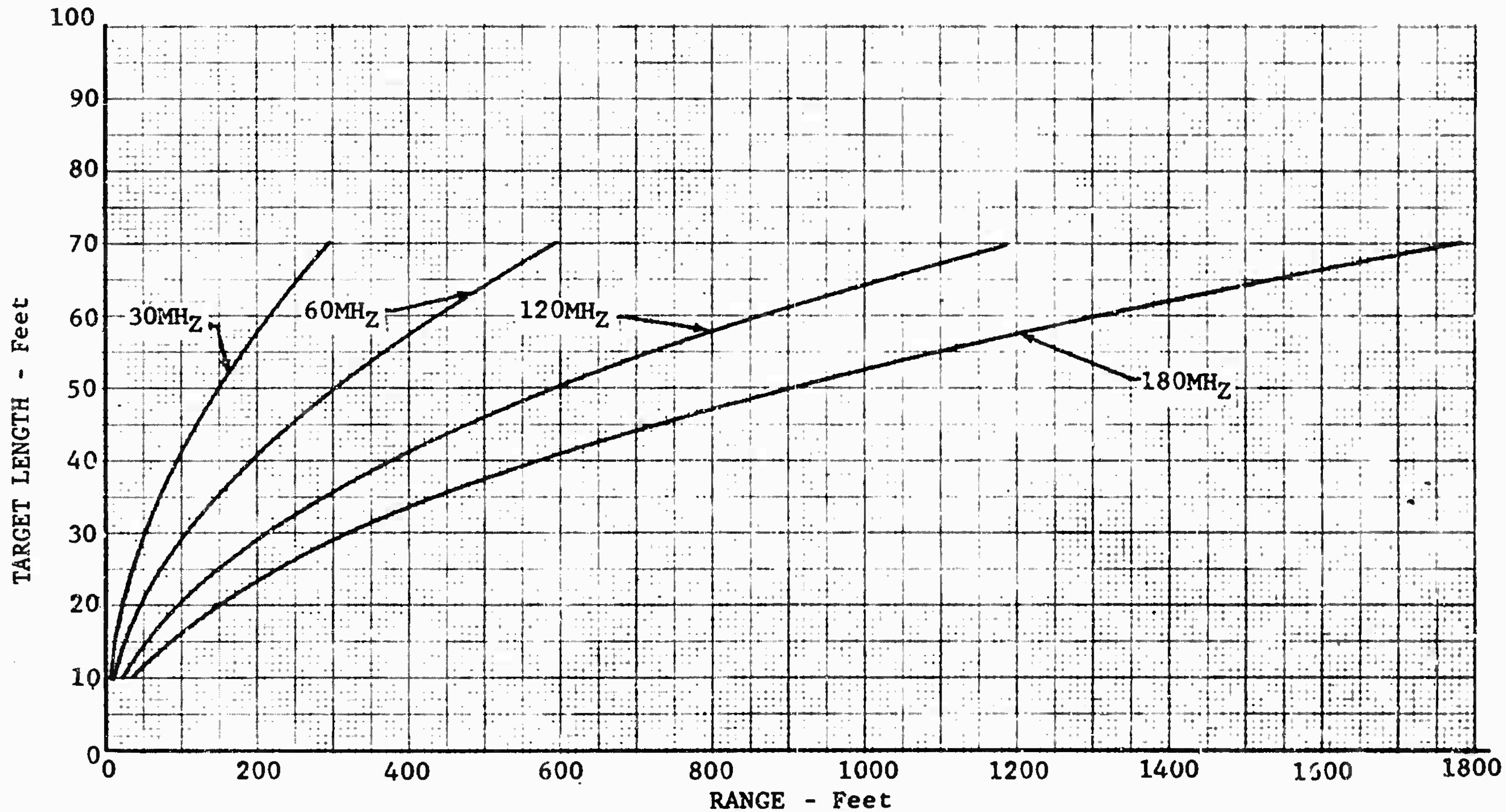

Fig. 130 TARGET SIZE AND RANGE LIMITATIONS DUE TO $2D^2/\lambda$ CRITERION

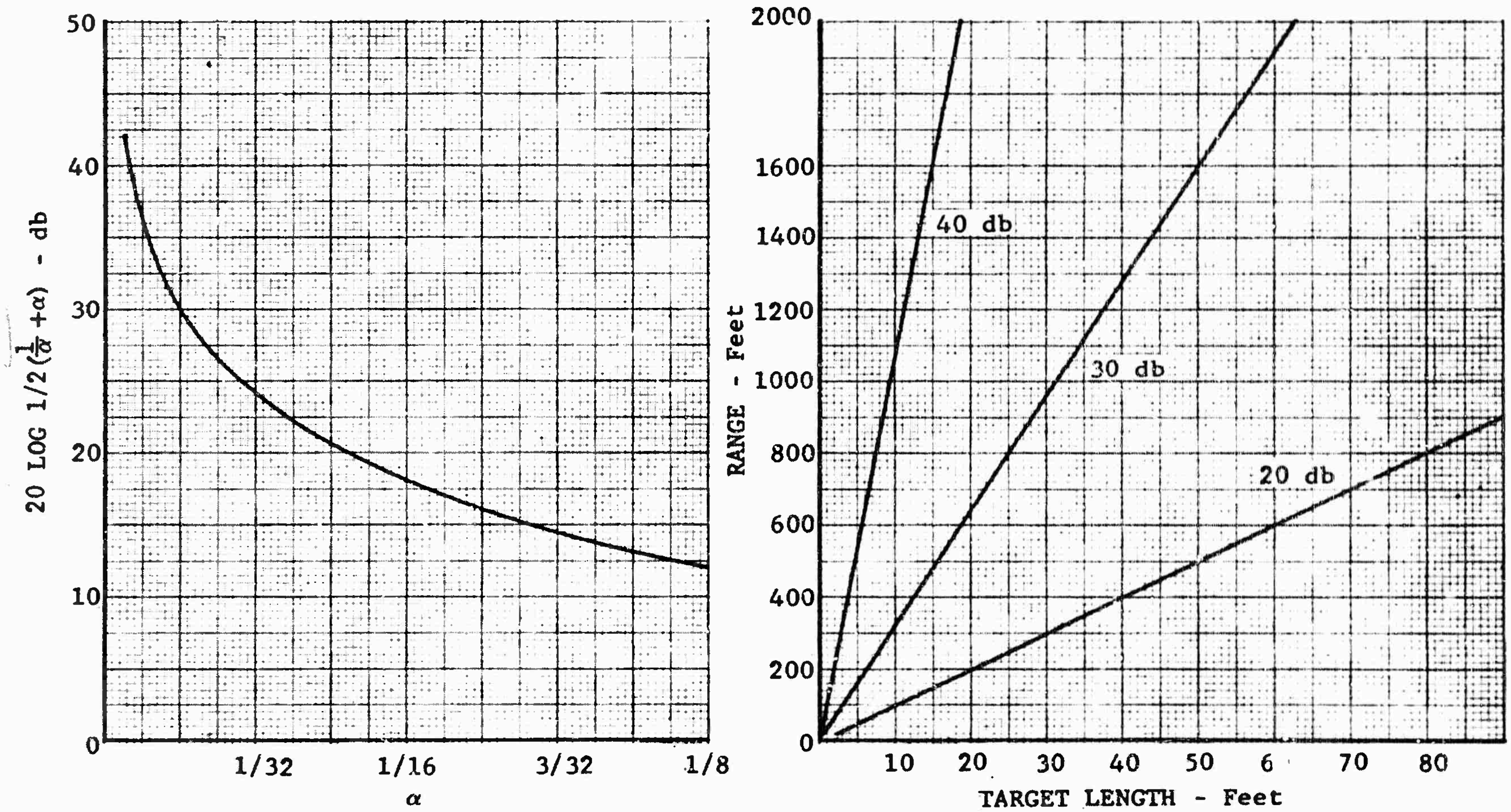

Fig. 131 NEAR FIELD ERROR CAUSED BY 1/R FIELD INTENSITY DECAY

APPENDIX A

A.1 Electrical Constants

To obtain the soil electrical constants ϵ_r, $\tan\delta$, and σ, the measured input admittance of a circular waveguide filled with the soil may be related to the desired quantities through the use of transmission line equations. With reference to Figure 4 the measured input admittance, denoted by Ym, is determined by the length of line between the point of measurement and the soil sample (Le), the characteristic admittance of this line (Yo), the characteristic admittance of the section of line containing the soil sample (Yos), the length of the soil test sample (Ls), and the test section terminating admittance (Yl). The parameters are related as shown in Equation A-1.

$$Ym = Yo \left[\frac{Ys + jYo\tan KoLe}{Yo + jYs\tan KoLe}\right] \qquad \text{(A-1)}$$

where

$$Ys = Yos \left[\frac{Yl + Yos\tanh \gamma sLs}{Yos + Yl\tanh \gamma sLs}\right]$$

$$Ko = 2\pi/\lambda$$

$$\gamma s = jKo\left[\epsilon r\mu r\left(1 - \tan\delta_\epsilon \tan\delta_\mu - j(\tan\delta_\epsilon + \tan\delta_\mu)\right)\right]^{\frac{1}{2}}$$

$\tan\delta_\epsilon$ = dielectric loss tangent

$\tan\delta_\mu$ = magnetic loss tangent

ϵr = relative dielectric constant

μr = relative permeability

$$Yos = Yo\left[\frac{\epsilon r}{\mu r}\right]^{\frac{1}{2}} \left[\frac{1 - j\tan\delta_\epsilon}{1 - j\tan\delta_\mu}\right]^{\frac{1}{2}}$$

In the following discussion, it will be assumed that the soil is nonmagnetic, in which case $\mu_r = 1$ and $\tan\delta_\mu = 0$. Also, it should be noted that in Equation A-1, the air-filled guide of length Le is assumed to be lossless.

By expressing the measured admittance Ym as Gm+jBm, Equation A-1 may be used to obtain Ys = Gs+jBs in terms of measured values as shown in Equations A-2 and A-3.

$$Gs = \frac{Yo^2 \left[1+\tan^2 KoLe\right]}{(Bm\tan KoLe+Yo)^2 + (Gm\tan KoLe)^2} \qquad \text{(A-2)}$$

$$Bs = \frac{(Bm\tan KoLe+Yo)\;(Bm-Yo\tan KoLe) + Gm^2\tan KoLe}{(Bm\tan KoLe+Yo)^2 + (Gm\tan KoLe)^2} \qquad \text{(A-3)}$$

Placing a short circuit at the input plane of the test section and measuring the short-circuit admittance $Yme = -jBme = -jYo/\tan KoLe$ will eliminate $\tan KoLe$ from Equations A-2 and A-3. The relationships then may be written as given in Equations A-4 and A-5.

$$Gs = \frac{Gm\left[1+\left(\frac{Yo}{Bme}\right)^2\right]}{\left[1-\frac{Bm}{Bme}\right]^2 + \left[\frac{Gm}{Bme}\right]^2} \qquad \text{(A-4)}$$

$$Bs = \frac{Yo\left[(1-Bm/Bme)\;(Bm/Yo + Yo/Bme) - \frac{(Gm)^2}{YoBme}\right]}{\left[1-\frac{Bm}{Bme}\right]^2 + \left[\frac{Gm}{Bme}\right]^2} \qquad \text{(A-5)}$$

To relate Gs and Bs to the material constants, consideration is given to the two possible situations which may occur when the terminating admittance Yl is varied. The first is that in which Yl has no effect on the value of Ym; in this case the line appears to be infinitely long, and Ys is equal to the characteristic admittance of the soil, Yos. If the load admittance is found to affect Ym, the load may be adjusted to give either $Yl = 0$ (i.e., an open circuit), or $Yl = \infty$ (i.e., a short circuit). By letting Y_s^o denote the open circuit case and Y_s^s denote the short-circuit case, Ys may be expressed as shown in Equations A-6 and A-7.

$$Y_s^o = G_s^o + jB_s^o = Yos\tanh \gamma sLs \qquad \text{(A-6)}$$

$$Y_s^s = G_s^s + jB_s^s = Yos/\tanh \gamma sLs \qquad \text{(A-7)}$$

The sample length, Ls, may be eliminated by taking the product of Y_s^o and Y_s^s to give

$$Y_s^o Y_s^s = Yo_s^2 = G_s^o G_s^s - B_s^o B_s^s + j(G_s^o B_s^s + G_s^s B_s^o) \qquad \text{(A-8)}$$

The definition of Yos, along with Equations A-2, A-3, and A-8, may then be used to relate the material constants ϵ_r, $\tan\delta_\epsilon$, and σ to the measured quantities G_m^o, B_m^o, G_m^s, B_m^s, and Bme.

$$\epsilon_r = \frac{G_m^o G_m^s \left[1 + (Y_o/B_{me})^2\right]^2 - NY_o^2}{DY_o^2} \quad \text{(A-9)}$$

$$\tan\delta_\epsilon = \frac{-Y_o \left[1 + (Y_o/B_{me})^2\right] \left[G_m^s K + G_m^o L\right]}{G_m^o G_m^s \left[1 + (Y_o/B_{me})^2\right]^2 - NY_o^2} \quad \text{(A-10)}$$

where $D = \left[(1-B_m^o/B_{me})^2 + (G_m^o/B_{me})^2\right] \left[(1-B_m^s/B_{me})^2 + (G_m^s/B_{me})^2\right]$

$N = LK$

$L - (1 - B_m^s/B_{me}) (B_m^s/Y_o + Y_o/B_{me}) - \frac{(G_m^s)^2}{Y_o B_{me}}$

$K = (1 - B_m^o/B_{me}) (B_m^o/Y_o + Y_o/B_{me}) - \frac{(G_m^o)^2}{Y_o B_{me}}$

The conductivity, σ, is obtained by using the relationship between σ, ϵ_r, $\tan\delta_\epsilon$, and λ as shown below.

$$\sigma = \frac{\epsilon_r \tan\delta_\epsilon}{60\lambda} \quad \text{(A-11)}$$

For the case in which Y1 has not effect on the value of Ym, a single measurement $Y_m = G_m + jB_m$ is used, and ϵ_r and $\tan\delta_\epsilon$ are given as

$$\epsilon_r = \frac{G_m^2 \left[1 + (Y_o/B_{me})^2\right]^2 - (N'Y_o)^2}{D'Y_o^2} \quad \text{(A-12)}$$

$$\tan\delta_\epsilon = \frac{-2Y_o \left[1 + (Y_o/B_{me})^2\right] N'G_m}{G_m^2 \left[1 + (Y_o/B_{me})^2\right]^2 - (N'Y_o)^2} \quad \text{(A-13)}$$

where

$D' = \left[(1 - B_m/B_{me})^2 + (G_m/B_{me})^2\right]^2$

$N' = (1 - B_m/B_{me}) (B_m/Y_o + Y_o/B_{me}) - \frac{(G_m)^2}{Y_o B_{me}}$

The conductivity, σ, is determined by use of Equation A-11.

A.2 Meter Corrections

The two most important sources of system error were found to be the mutual couplings between the different branches of the admittance bridge and the inductance of the sections of line between the junction of the bridge arms and the center of the measuring coils. Corrections for the errors produced by cross-coupling were made by using Equations A-14 and A-15 (Reference 1):

$$Gc = \frac{Gm + 0.0085\ Bm + .17}{D} \qquad \text{(A-14)}$$

$$Bc = \frac{Bm - (0.0085\ Gm + .17)}{D} \qquad \text{(A-15)}$$

where $D = 1 + 0.00042\ (Gm - Bm)$ and Gm and Bm are the measured conductance and susceptance before correction.

To correct for the junction inductance error, Equations A-16 and A-17 were used (Reference 1):

$$Gx = Gc/A \qquad \text{(A-16)}$$

$$Bx = \frac{Bc\left[1 + Bc/B1 - 2(GcYo)/(B1)^2\right] + Gc/B1\ (Gc - Yo)}{A} \qquad \text{(A-17)}$$

where $\quad A = (1 + Bc/B1)^2 + (Gc/B1)^2$

$$B1 = \frac{1 \times 10^{12}}{(2\pi f)(1.19)}$$

Gc and Bc are the values obtained from the cross-coupling corrections.

In the earliest phase of the measurement program, it was found that the form of the equations used to relate measured quantities to the desired electrical properties (Equations A-9 - A-13) placed a strict limit on measurement tolerances. Specifically, the computations tended to square any error present in measured data. To avoid this amplification of error, an attempt was made to restrict the magnitude of the measured conductance and susceptance to a region in which the maximum measurement accuracy could be obtained. This objective was attained by adjusting the length of the soil test sample as a function of the moisture content, the frequency, and the temperature at which a given measurement was to be made. The resulting lengths of the test sections were found to be short enough, in most cases, to allow simplifications to be made in the computations. A further virtue of using the shorter lengths was that the describing equations contained fewer terms which exaggerated small errors. To show the effect of these simplifications, Equation A-1 is first written with the full expression for Ys:

$$Ym = Yo \left[\frac{Yos \left[\frac{Yl + Yos \tanh \gamma s\, Ls}{Yos + Yl \tanh \gamma sLs} \right] + jYotanKoLe}{Yo + jYos \left[\frac{Yl + Yos \tanh \gamma sLs}{Yos + Yl \tanh \gamma sLs} \right] tanKoLe} \right] \qquad \text{(A-18)}$$

In the first attempts to obtain Y_L^o (open-circuit load admittance), it was noted that the measured admittance was slightly larger than it should have been, in correspondence to the physical inability to obtain a perfect open circuit. In addition to the imperfect open-circuit termination, the amount of soil used for a given measurement was often insufficient to completely fill a standard length of air guide. For these cases, another "load" term was necessary to completely describe the system. The above mentioned relationships are illustrated in Figure 5 where

Ls = length of test section

lo = length of remaining air filled guide and dielectric bead

l'o = effective length necessary to describe imperfect open-circuit

If the open-circuit load is assumed to be very small, but not zero, Equation A-18 is reduced to

$$Y_m^o = Yo \left[\frac{(Y_L^o + Yos \tanh \gamma sLs) + jYotan\, KoLe}{Yo + j(Y_L^o + Yos \tanh \gamma sLs)\, tanKoLe} \right] \qquad \text{(A-19)}$$

where Y_L^o is the total open-circuit load admittance.

If the lengths Le and Ls are assumed to be sufficiently short to allow the approximations tanx = x and tanhx = x, and the definitions for Yos and γs are used, Equation A-19 becomes

$$y_m^o = \frac{Ertan\,\delta_\epsilon + j(Er + bme + b_L^o)}{(1 - bmeb_L^o - Erbme) + j\, Ertan\,\delta_\epsilon\, bme} = g_m^o + jb_m^o \qquad \text{(A-20)}$$

where

$$bme = \frac{2\pi Le}{\lambda}$$

$$b_L^o = \frac{2\pi Lo}{\lambda} = -jY_L^o/Yo$$

$$Er = \frac{2\pi Ls}{\lambda}\epsilon_r$$

In Equation A-20, Y_m^o, G_m^o, B_m^o, and B_L^o have been normalized to Yo.

Equating the real and imaginary parts of Equation A-20 gives

$$Er = \frac{(g_m^o)^2 bme(1-bme\,b_L^o) + (1+b_m^o bme)\left[b_m^o - bme - b_L^o(1+b_m^o bme)\right]}{(1+b_m^o bme)^2 + (g_m^o bme)^2} \quad \text{(A-21)}$$

$$\tan\delta_\epsilon = \frac{g_m^o\left[1-bme(Er+b_L^o)\right]}{Er(1+b_L^o bme)^2} \quad \text{(A-22)}$$

For the case of the short-circuit measurements on sections in which Ls and Le are very small, Equation A-18 is reduced to

$$ym = \frac{\left[\dfrac{Y_L^s}{1+jY_L^s KoLs}\right] + jYoKoLe}{Yo+jKoLe\left[\dfrac{Y_L^s}{1+jY_L^s KoLs}\right]} \quad \text{(A-23)}$$

Note that Equation A-23 gives no added information on the soil parameters when very short test sections are used.

A.3 Statistical Analysis

To obtain a representative description of the soil electrical parameters at a fixed temperature and moisture content, it was found necessary to repeat measurements by using different lengths of test section so that a statistical average could be found. This was necessary even though any set of data could be reproduced to within ± 5 percent of the first set obtained under similar "environmental" conditions. Also noted was an increase in the standard deviation of ϵ_r, σ, and $\tan\delta_\epsilon$ as the moisture content was increased; consequently, it was highly desirable to obtain a larger volume of measured data at the higher moisture contents. The standard deviation of ϵ_r as a function of moisture content is illustrative of this increase (Figure 25) as well as the standard deviation of the subsurface conductivity as a function of moisture content (Figure 26).

To relate the statistical variation of the results with measurement errors and "environment" fluctuation, small changes in the temperature, moisture content, soil test section length (Ls), and recorded values of Gm and Bm were analytically introduced to simulate the effect of combined system error. The specific errors assumed were $\pm 2^{o}$F in the temperature, ± 1 percent in the moisture content, ± 5 percent in the ability to define the test section length, Ls, and ± 5 percent in the measured input admittance, Ym.

From the above investigation, the error which contributed most to the variations in ϵr was found to be the inherent error in the admittance meter (i.e., ± 5 percent in Ym). The effect of such an error may be visualized from Equation A-21. Since the normalized conductance (g_m^2) in the numerator is squared, any error in the recorded conductance is also squared. This increase essentially amplifies a 5-percent error to almost 30 percent, the total effect depending upon the error associated with b_m^2. Although squared terms also exist in the denominator, cancellation of error was negligible as a result of the product formed with $(bme)^2$. In Figure 25, the maximum expected deviation resulting from the above mentioned variations in temperature, moisture content, etc., is shown. When this deviation is compared with the actual standard deviation also shown, it is noted that, for all practical purposes, the standard deviation is bounded by the calculated error limits.

To describe the variations of the conductivity in terms of system errors, two cases must be considered in terms of measurements at the prescribed frequencies. The first case is that in which measurements are based on the assumption that the soil is not disturbed between measurements, i.e., the density of the soil in the test section is the same for each measurement. The second case arises when the reproduction of measurements is attempted. In other words, when the soil is emptied from the test section and then repacked, the unavoidable difference in "packing density" limits the reproducibility of measurements to approximately 95 percent.

For the first case, the calculated total error and the actual variations encountered are in good agreement, each indicating a deviation of approximately 10 percent.

To investigate the expected change in the conductivity caused by a change in packing density, the empirical expression describing the conductivity is used to obtain the partial derivative of σ with respect to ϵr.

$$\frac{\delta\sigma}{\delta\epsilon_r} = 2\epsilon r\,\sigma o\left|.1+5(\%)\right|\left|1+8(\%)^2\right| e^{(.041)T} = \frac{2\sigma}{\epsilon_r} \qquad \text{(A-25)}$$

The percent change in σ caused by a given percent change in ϵr may then be written as

$$\%\text{ change in }\sigma = \frac{\delta\sigma}{\sigma\,\delta\epsilon r}\,\Delta\epsilon r(100) = 2\ (\%\text{ change in }\epsilon r)$$

Although the above change in σ is not shown directly as a function of density, use of the expression containing a variation in ϵr produces the same effect. In other words, given two samples of different packing densities, the sample with the lowest density will exhibit the lowest relative dielectric constant. To define, realistically, what the total effect is, the tolerances on reproducibility must be used; unfortunately, these tolerances are exaggerated in Equation A-21.

As a result of the error amplification, a considerable effort was made to define, as accurately as possible, the soil electrical properties under the most likely conditions to be met at the proposed VHF location. Specifically included was concentration at 10-, 15-, 20- and 25-percent moisture content. (See Figure 2.)

At 25 percent, however, the loss tangent, and thus the conductivity did not increase to the values predicted on the basis of the lower moisture content results. On the basis of the mean value of ϵr obtained for 25 percent, which was in very good agreement with that expected from theory, and the empirical expression for the conductivity, an expected value for the loss tangent at 25-percent moisture content was calculated. To justify this calculation, it is noted that, if the measurement system were to distinguish the loss tangent at 20 percent moisture content from that expected at 25-percent moisture content, it must be able to separate $(1+j70)^{\frac{1}{2}}$ from $(1+j90)^{\frac{1}{2}}$. In terms of measured input admittances, this operation would require separating 1+j35 from 1+j45. When the effect of small system errors is considered, the problem becomes apparent. To obtain the accuracy needed at 25 percent, it is felt that the system would have to have been operated with these specific measurements in mind rather than the wide range of conditions encountered when all moisture contents are considered.

DOCUMENT CONTROL DATA - R&D

(Security classification of title, body of abstract and indexing annotation must be entered when the overall report is classified)

1. ORIGINATING ACTIVITY (Corporate author)
General Dynamics
Fort Worth, Texas

2a. REPORT SECURITY CLASSIFICATION
UNCLASSIFIED

2b. GROUP

3. REPORT TITLE
RADAR TARGET SCATTER SITE (RAT SCAT)
VHF MEASUREMENT FEASIBILITY INVESTIGATION

4. DESCRIPTIVE NOTES (Type of report and inclusive dates)
INTERIM (PHASE I - INVESTIGATION)

5. AUTHOR(S) (Last name, first name, initial)
FREENY, C.C.
CISCO, D.O.

6. REPORT DATE
August 1966

7a. TOTAL NO. OF PAGES
254

7b. NO. OF REFS
L

8a. CONTRACT OR GRANT NO.
AF30(602)-3815

b. PROJECT NO.
6503

c. Task 650301

d.

9a. ORIGINATOR'S REPORT NUMBER(S)
FZE-528

9b. OTHER REPORT NO(S) (Any other numbers that may be assigned this report)
RADC-TR-66-215

10. AVAILABILITY/LIMITATION NOTICES
This document is subject to special export controls and each transmittal to foreign governments or foreign nationals may be made only with prior approval of RADC (EMLI) GAFB, N.Y. 13440.

11. SUPPLEMENTARY NOTES

12. SPONSORING MILITARY ACTIVITY
Rome Air Development Center (EMASP)
Griffiss AFB, N.Y. 13440

13. ABSTRACT

ABSTRACT

The material presented in this report is a result of an investigation of the feasibility of making radar cross section measurements in the VHF region at the Radar Target Scatter Site, White Sands Missile Range (RAT SCAT). Included [redacted] are the results of an experimental and analytical investigation which was conducted in the 30-to 80-megahertz region for the purpose of (1) determining the feasibility of making measurements at RAT SCAT and (2) defining the range condition(s) and measurement technique(s) for use in a feasibility demonstration program to be conducted at RAT SCAT.

A study was made of the properties of RAT SCAT soil since a ground plane cross section measurement technique was under consideration. The electrical properties of the soil, in terms of the complex permittivity and associated loss tangent, were measured as a function of moisture, temperature, and sample location. The results of the soil investigation were used in conjunction with a ground plane model programmed on a CDC 1604 to investigate the RF field patterns to be expected at RAT SCAT. These fields were studied as a function of frequency, range, soil conditions, antenna height, and target height. A VHF radar system from the Fort Worth Division of General Dynamics was taken to RAT SCAT to obtain information with which to validate the results of the computer study and obtain additional information on the feasibility of operating VHF equipment at the RAT SCAT site. The results of the study and measurements are analyzed and a dual range and measurement technique are described; this technique is considered a feasibile approach to measuring targets up to 70 feet in length.

UNCLASSIFIED
Security Classification

14 KEY WORDS	LINK A ROLE	LINK A WT	LINK B ROLE	LINK B WT	LINK C ROLE	LINK C WT
Electromagnetic Fields						
Field Theory						
Radar Echo Areas (Radar Reflections)						
Radar Reflections (Electromagnetic wave reflections)						
Very High Frequency (limited to 30 - 100 megahertzians)						

This is an interim reporting of an experimental investigation and theoretical analysis which has established confidence that dual polarization amplitude and phase measurements are possible on a ground plane radar cross section range in the 30 to 100 megahertzian band. The results of this phase of the VHF measurement investigation established the basis of the design for a hardware feasibility demonstration model to be implemented at the RAT SCAT facility during May 1966. Final feasibility demonstration tests are then to be conducted during June 1966.

INSTRUCTIONS

1. ORIGINATING ACTIVITY: Enter the name and address of the contractor, subcontractor, grantee, Department of Defense activity or other organization (*corporate author*) issuing the report.

2*a*. REPORT SECURITY CLASSIFICATION: Enter the overall security classification of the report. Indicate whether "Restricted Data" is included. Marking is to be in accordance with appropriate security regulations.

2*b*. GROUP: Automatic downgrading is specified in DoD Directive 5200.10 and Armed Forces Industrial Manual. Enter the group number. Also, when applicable, show that optional markings have been used for Group 3 and Group 4 as authorized.

3. REPORT TITLE: Enter the complete report title in all capital letters. Titles in all cases should be unclassified. If a meaningful title cannot be selected without classification, show title classification in all capitals in parenthesis immediately following the title.

4. DESCRIPTIVE NOTES: If appropriate, enter the type of report, e.g., interim, progress, summary, annual, or final. Give the inclusive dates when a specific reporting period is covered.

5. AUTHOR(S): Enter the name(s) of author(s) as shown on or in the report. Enter last name, first name, middle initial. If military, show rank and branch of service. The name of the principal author is an absolute minimum requirement.

6. REPORT DATE: Enter the date of the report as day, month, year; or month, year. If more than one date appears on the report, use date of publication.

7*a*. TOTAL NUMBER OF PAGES: The total page count should follow normal pagination procedures, i.e., enter the number of pages containing information.

7*b*. NUMBER OF REFERENCES: Enter the total number of references cited in the report.

8*a*. CONTRACT OR GRANT NUMBER: If appropriate, enter the applicable number of the contract or grant under which the report was written.

8*b*, 8*c*, & 8*d*. PROJECT NUMBER: Enter the appropriate military department identification, such as project number, subproject number, system numbers, task number, etc.

9*a*. ORIGINATOR'S REPORT NUMBER(S): Enter the official report number by which the document will be identified and controlled by the originating activity. This number must be unique to this report.

9*b*. OTHER REPORT NUMBER(S): If the report has been assigned any other report numbers (*either by the originator or by the sponsor*), also enter this number(s).

10. AVAILABILITY/LIMITATION NOTICES: Enter any limitations on further dissemination of the report, other than those imposed by security classification, using standard statements such as:

(1) "Qualified requesters may obtain copies of this report from DDC."

(2) "Foreign announcement and dissemination of this report by DDC is not authorized."

(3) "U. S. Government agencies may obtain copies of this report directly from DDC. Other qualified DDC users shall request through ______."

(4) "U. S. military agencies may obtain copies of this report directly from DDC. Other qualified users shall request through ______."

(5) "All distribution of this report is controlled. Qualified DDC users shall request through ______."

If the report has been furnished to the Office of Technical Services, Department of Commerce, for sale to the public, indicate this fact and enter the price, if known.

11. SUPPLEMENTARY NOTES: Use for additional explanatory notes.

12. SPONSORING MILITARY ACTIVITY: Enter the name of the departmental project office or laboratory sponsoring (*paying for*) the research and development. Include address.

13. ABSTRACT: Enter an abstract giving a brief and factual summary of the document indicative of the report, even though it may also appear elsewhere in the body of the technical report. If additional space is required, a continuation sheet shall be attached.

It is highly desirable that the abstract of classified reports be unclassified. Each paragraph of the abstract shall end with an indication of the military security classification of the information in the paragraph, represented as *(TS)*, *(S)*, *(C)*, or *(U)*.

There is no limitation on the length of the abstract. However, the suggested length is from 150 to 225 words.

14. KEY WORDS: Key words are technically meaningful terms or short phrases that characterize a report and may be used as index entries for cataloging the report. Key words must be selected so that no security classification is required. Identifiers, such as equipment model designation, trade name, military project code name, geographic location, may be used as key words but will be followed by an indication of technical context. The assignment of links, rules, and weights is optional.

UNCLASSIFIED
Security Classification